Golder Associates
CONSULTING GEOTECHNICAL AND MINING ENGINEERS

REPORT TO
CANMET

DEVELOPMENT OF AN OUTBURST MODEL FOR THE SYDNEY COALFIELD

CAPE BRETON, NOVA SCOTIA

DSS Contract No. 23440-6-9025

CONTRACT SERIAL NO. 69025-01-SQ
REQUISITION NO. 6-9025
CONTRACTOR: Golder Associates

Distribution:

15 copies - CANMET
(Cape Breton Research Laboratory)
Sydney, Nova Scotia

2 copies - Golder Associates
Mississauga, Ontario

253 pp + figures

MICROMEDIA

March 1987

861-1290

GOLDER ASSOCIATES (EASTERN CANADA) LTD. • 3151 WHARTON WAY, MISSISSAUGA, ONTARIO, CANADA L4X 2B6 • TELEPHONE (416) 625-0094 • TELEX 06-961136

OFFICES IN CANADA • UNITED STATES • UNITED KINGDOM • AUSTRALIA

ABSTRACT

A research study has been undertaken to develop a mechanistic model for the initiation of rock - gas outbursts experienced in no. 26 colliery of the Sydney Coalfield. The research program included a worldwide review of similar phenomenon and of the published case histories and mechanistic models for the occurrences of outbursts; a review of the outburst data and experiences from the Sydney Coalfield; a field program to measure the dynamic effects of blasting and analyses of selected outburst events using numerical modelling techniques to develop the most probable mechanism for the outburst initiation.

The various hypotheses put forward to explain the outburst events conformed to a trend: initiation of event was thought to be brought about by a change from triaxial to biaxial stress conditions, and the gas present played a major role in their initiation and subsequent manifestation of the event (violent expulsion of the failed material).

The results of the review of 37 rock-gas outburst events in the Sydney Coalfield revealed that all of them occurred where a sandstone erosion channel was present within 2.7 m of the top of the coal seam. All but one of the events were initiated by blasting, and all but three of them happened in development headings. There was no correlation between the direction of drivage and their occurrence, but there did appear to be correlation between depth and intensity. Other parameters included in the review were the pattern and sequence of blasting used to develop the roadway and the sequence of excavation in relation to the surrounding longwall coal extraction. From this aspect of the analysis it was discovered that it appeared possible to prevent outbursts by driving development roadways (e.g. 13N Airway) alongside previously extracted panels.

An experimental blast monitoring program was undertaken in a development heading in the Lingan Mine to monitor the dynamic and static stress changes during typical shotfiring rounds in roadway development. The results indicated that the dynamic effect of the shotfiring event is significant. An attentuation equation for the dynamic stress was derived from the test results. Tensile stresses normal to the bedding of the roof strata could be induced due to wave reflection at the free surface of the rock mass to be excavated.

A series of elastic stress analyses were carried out to study the effects of location and thickness of the outburst-prone sandstone layer; the in situ stresses; the

relative rock mass stiffnesses of the sandstone and the adjacent siltstone and the position of the extracted longwall panel. The combined effects of static stresses, pore gas pressure and blast induced dynamic stresses were studied by considering the effective principal stresses and Griffith's criterion of fracture initiation.

It was noted that based on the range of estimated gas pressures, the stress conditions in the sandstone for all the outburst events are such that fracture initiation would take place based on Griffith's failure criterion. The probability of outburst in 13N airway, however, is substantially lower. It appears that the stress concept and the mode of failure proposed in the model is consistent with the observed events in no. 26 colliery.

Predictive measures for outburst events would include delineation of outburst-prone strata by drilling investigation; noting zones of core discing and defining in situ stress condition.

Preventative methods considered to be applicable to the Sydney Coalfield would include developing roadway within a stress relief zone, slotting around the excavation and presupport of the roof strata ahead of the face.

RESUME

Une étude a été entreprise pour développer un modèle du mécanisme de formation des coups de charge et de grisou ressentis à la mine de charbon No. 26 du bassin houiller de Sydney. Ce programme d'étude comprend les points suivants; une révision bibliographique au niveau mondiale des phénomènes similaires à l'aide des études de cas publiés et des modèles déjà développés, la révision des données des coups de charge ressentis dans la houillère de Sydney, un programme de mesure sur le terrain des effets dynamiques des sautages ainsi que l'analyse de certains coups de charge et de grisou à l'aide de modélisations numériques afin de développer un modèle du mécanisme qui provoque l'initiation des coups de charge et de grisou.

La tendance principale des diverses hypothèses utilisées pour expliquer l'initiation des coups de grisou et de toit se résume de la façon suivante; l'initiation des coups de charge et de grisou est possiblement reliée au changement d'état des contraintes dans la roche lorsque celle-ci devient chargée biaxialement alors qu'elle était chargée triaxialement ainsi qu'à la présence de gas jouant un rôle majeur lors de l'initiation et du déroulement subséquent de l'évènement (explosion violente de matériel fracturé).

Les résultats de la révision de 37 cas de coup de charge et de grisou dans la houillère de Sydney montrent que ceux-ci se sont tous produits dans un intervalle de 2.7 m au-dessus de la couche de charbon où le grès était érodé. Tout sauf un de ces évènements furent provoqués par un sautage. De plus, à l'exception de trois d'entre eux ces évènements se sont tous produits lors du développement de départ. Aucune corrélation a été trouvée entre la direction du développment et la possibilité de coup de charge ou de grisou, mais il semble y avoir une relation entre la profondeur et l'intensité des évènements. Les autres paramètres qui sont inclus dans la révision sont les suivants; le patron et la séquence de sautage utilisés pour le développement des galeries ainsi que la séquence d'excavation des panneaux de longue taille. A partir de cette analyse, il est apparut possible de prévenir les coups de charge et de grisou en développement les galeries d'accès (C.A.D. 13N Airway) le long des panneaux de longue taille déjà exploités.

Un programme de mesure des vibrations de sautage a été entrepris lors du développement de tête à la mine Lingan afin de mesurer les changements dynamiques et statiques des contraintes dans la roche lors du sautage d'une volée

typique dans les galeries de développement. Les résultats ont indiqués que l'effet dynamique des sautage est significatif. Une équation d'atténuation de la contrainte dynamique a été dérivée à partir de ces essais. Les contraintes de tension normales aux roches stratifiées composant le toit peuvent être produites par la réflection de l'onde de choc sur la face libre inférieure du massif sauté.

Une série d'analyse des contraintes élastiques a été faite afin d'étudier les points suivants; l'influence de la position et de l'épaisseur de la couche de grès sujette à des coups de grisou, les contraintes in-situ, la rigidité relative du grès ainsi que celle de la couche de "siltstone" adjacente et enfin l'influence de la position du panneau de charbon exploité par longue taille. Les effets combinés des contraintes statiques, de la pression des gas et des contraintes dynamiques induites par le sautage ont été étudiés en considérant les contraintes principales effectives ainsi que le critère de fracturation de Griffith.

En se basant sur l'estimation de l'intervalle des pressions des gas, l'état de contrainte du grès lors des coups de charge et de grisou est assez élevé pour provoquer la fracturation de la roche selon le critère de Griffith. Pour ce qui est de la galerie 13N, la probabilité de coup de grisou est considérée comme faible. Il semble que le concept du changement d'état de contrainte ainsi que le mode de fracturation proposé dans cette étude correspond bien avec les événements observés à la mine de chabon No. 26.

Les mesures permettant de déterminer les zones potentiellement sujette à des coups de grisou devraient inclure une investigation du massif à l'aide de forage afin de noter les régions où il y a du litage ainsi que pour connaître les différents états de contrainte.

De plus, les méthodes préventives suivantes devraient être appliquées au bassin houiller de Sydney; développement des galeries d'accès dans une zone où les contraintes sont relâchées, création d'une ouverture autour de la zone qui sera sautée et mise en place de soutènement au toit au dessus de la volée.

TABLE OF CONTENTS

Page No.

ABSTRACT i

1. INTRODUCTION 1-1

2. REVIEW OF ROCK AND GAS OUTBURST PHENOMENA IN THE SYDNEY COALFIELD 2-1

- 2.1 Introduction 2-1
- 2.2 Geological and Geotechnical Data 2-2
  - 2.2.1 Regional and Local Geology 2-2
  - 2.2.2 Sandstone Paleo-River Channels 2-2
- 2.3 Regional Stress Distribution in the Sydney Coalfield 2-4
- 2.4 Rock Properties and Characteristics 2-5
  - 2.4.1 Strength and Deformation Properties 2-5
  - 2.4.2 Petrographic Data of Outburst Sandstone 2-6
- 2.5 Strata Gas Pressure 2-7
  - 2.5.1 Gas Pressure Calculation from Cored and Grab Samples 2-8
  - 2.5.2 In situ Gas Pressure Measurement 2-8
  - 2.5.3 Evaluation of In situ Gas Pressure based on Outburst Data 2-9
  - 2.5.4 Gas Pressure Determination from Reservoir Engineering Estimates 2-12
  - 2.5.5 Summary 2-12
- 2.6 Core Discing Phenomenon at No. 26 Colliery 2-12
- 2.7 Mining Method 2-15
- 2.8 Rock and Gas Outburst Events at No. 26 Colliery 2-16

3. REVIEW OF ROCK AND GAS OUTBURST CASE HISTORIES 3-1

- 3.1 Case Histories of Rock and Gas Outbursts in Coal Mines 3-2
  - 3.1.1 Horonai Coal Mine, Japan 3-2
  - 3.1.2 Dombass (Donetz) Basin, USSR 3-2
  - 3.1.3 Soko Basin, Yugoslavia 3-3
  - 3.1.4 Nowa Ruda Mine, Polant 3-3
  - 3.1.5 Merlebach Colliery, France 3-4
  - 3.1.6 Ibbenburen Colliery, West Germany 3-5
- 3.2 Case Histories of Rock and Gas bursts in Salt and Potash Mines 3-7
  - 3.2.1 Louisiana Salt Mines, USA 3-7
  - 3.2.2 Werra Potash Mines, GDR 3-7
  - 3.2.3 Sudharz Potash Field, GDR 3-8
- 3.3 Other Case Histories of Rock and Gas Outbursts 3-9
  - 3.3.1 Sangerhausen and Mansfeld Copper-Slate Mining District, GDR 3-9
  - 3.3.2 Other Case Histories 3-9

TABLE OF CONTENTS (cont'd)

Page No.

3.4 Summary and Discussion 3-11

4. REVIEW OF OUTBURST MODELS 4-1

4.1 An Overview of Coal Outburst Theories 4-1
4.2 An Overview of Physical Mechanisms in Rock and Gas Outbursts 4-2
4.3 Review of Existing Rock and Gas Outburst Models and Other Dynamic Phenomena 4-3
4.3.1 Outbursts in Salt and Potash Mines 4-3
4.3.1.1 Outbursts in Louisiana Salt Mines 4-3
4.3.1.2 Outbursts in German Potash Mines 4-5
4.3.2 Coal and Gas Outburst Models 4-5
4.3.2.1 Coal and Gas Outbursts (Khristianovich and Salganik, 1983 4-5
4.3.2.2 Coal and Gas Outbursts (Kidybinski, 1981) 4-6
4.3.2.3 Coal and Gas Outbursts (Litwiniszyn, 1985) 4-8
4.3.2.4 Coal and Gas Outbursts (Paterson, 1986) 4-9
4.3.2.5 Coal and Gas Outbursts (Barron, 1972) 4-9
4.3.2.6 Coal and Gas Outbursts (Hiramatsu, 1983) 4-10
4.3.2.7 Coal and Gas Outbursts (Gray, 1980) 4-12
4.3.2.8 Coal and Gas Outbursts (Farmer and Pooley, 1967) 4-16
4.3.2.9 Coal and Gas Outbursts Associated with Geological Structures (Shepherd et al, 1984) 4-17
4.3.3 Sandstone and Gas Outbursts 4-19
4.3.3.1 Sandstone and Gas Outbursts (Jovanovic et al, 1979) 4-19
4.3.3.2 Rockbursts (Petukhov, 1983) 4-20
4.3.3.3 Rock and Gas Outbursts (Karogodin et al, 1983) 4-22
4.3.3.4 Rock or Coal Outbursts (Ujihira et al, 1985) 4-23
4.3.3.5 Rock and Gas Outbursts (Sevelev, 1979) 4-24
4.3.3.6 Sandstone and Gas Outbursts (Revalor et al, 1985) 4-29
4.3.3.7 Bursting of Sandstone Layer Above Working (Zorin et al, 1981) 4-30

TABLE OF CONTENTS (cont'd)

Page No.

4.3.4 Other Relevant Rock Outburst Models 4-30
4.3.4.1 Dynamic Rock Failure (Hueckel, 1981) 4-30
4.3.4.2 Rockbursts in Tunnel Headings (Dikunov, 1971) 4-31
4.4 Discussion 4-32
4.4.1 Initiation Mechanisms 4-32
4.4.2 Effect of Blasting and Mining Method 4-33
4.4.3 Energy Available and Consumed 4-34
4.4.4 Cavity Shape and Fish Scale Fracturing 4-34
4.4.5 End of an Outburst Event 4-35

5. FACTORS AFFECTING THE OCCURRENCE OF OUTBURSTS 5-1

5.1 Introduction 5-1
5.2 Stresses in Rock Mass 5-2
5.2.1 In situ Stresses 5-2
5.2.2 Stresses Around Mine Openings 5-3
5.3 Mechanical Properties of Rock 5-6
5.3.1 Stress-Strain Relationships 5-6
5.3.2 Extension Fracture in Brittle Rock 5-7
5.3.2.1 Effective Tensile Stresses 5-7
5.3.2.2 Extension Strain Criterion for Fracture Initiation 5-8
5.3.2.3 Mechanism of Rock Fracturing Close to a Free Face 5-9
5.3.3 Core Discing 5-11
5.3.4 Effect of Rock Mass Properties on the Blasting Process 5-13
5.4 Hydraulic Properties of Rock 5-15
5.4.1 Porosity 5-15
5.4.2 Permeability 5-16
5.5 Lithology 5-17
5.6 Variation in Rock Properties in a Changing Stress Regime 5-17
5.6.1 Effect of Confining Pressure on Rock Failure 5-17
5.6.2 Effects of Loading Rate 5-18
5.6.3 Effect of Stress Changes on Rock Properties 5-19
5.6.4 Rock Behaviour Under High Rate of Stress Change 5-20
5.7 Gas Effects 5-24
5.8 Blasting Effects on Surrounding Rock Mass 5-26

TABLE OF CONTENTS (cont'd)

Page No.

5.8.1 Theoretical Considerations of the Dynamic Stresses caused by Shotfiring 5-26
5.8.2 Theoretical Considerations of Blast Induced Damages to Rock Masses 5-35

6. EXPERIMENTAL PROGRAM 6-1

6.1 Blast Monitoring Program 6-1
6.1.1 Introduction 6-1
6.1.2 Field Program and Procedures 6-2
6.1.3 Review of Current Blasting Practices at Lingan Mine 6-4
6.1.4 Results of Stress Monitoring 6-5
6.1.5 Evaluation of Effects of Current Blasting Practices on Rock Fracturing in the Lingan Mine 6-8
6.1.6 Summary 6-10
6.2 Laboratory Testing Program 6-11
6.2.1 Introduction 6-11
6.2.2 Axial Unloading under Constant Confining Stresses in a Closed Pore Gas System 6-12
6.2.3 Drag Effect of Gas Flowing Through a Sample 6-14
6.2.4 Strength under Biaxial Loading 6-14
6.2.5 Discussion 6-15

7. DEVELOPMENT OF AN OUTBURST MODEL 7-1

7.1 Introduction 7-1
7.2 Proposed Rock and Gas Outburst Model 7-2
7.3 Stress Analysis of a Development Roadway in No. 26 Colliery 7-9
7.3.1 Effects of the Location and Thickness of Sandstone in Relation to the Development Roadway 7-10
7.3.2 Effect of In Situ Stresses 7-13
7.3.3 Effect of Relative Rock Mass Stiffness 7-14
7.3.4 Analysis of the 13N Airway 7-15
7.3.5 Effects of Blast Damage 7-16
7.3.6 Effects of Blast Induced Stresses 7-17
7.3.7 Combined Effects of Pore Gas Pressure and Stresses 7-19

8. COAL MINING UNDER OUTBURST PRONE CONDITIONS 8-1

8.1 Outburst Risk Assessment 8-1

TABLE OF CONTENTS (cont'd)

Page No.

8.2 Prediction of Outburst Hazards 8-3
8.3 Prevention of Outbursts 8-5
8.3.1 Gas Drainage 8-6
8.3.2 Destressing of the Rock Mass 8-6
8.3.3 Modification of the Blasting Parameters 8-8
8.3.4 Use of Mechanical Excavation Equipment 8-9
8.3.5 Isolation of the Volume of Rock to be Excavated 8-10
8.3.6 Pre-support Ahead of the Face 8-10
8.3.7 Safety Measures 8-11
8.3.8 Summary 8-12

9. CONCLUSIONS 9-1

10. RECOMMENDATIONS FOR FURTHER RESEARCH 10-1

11. ACKNOWLEDGEMENTS 11-1

LIST OF TABLES x

LIST OF FIGURES xi

LIST OF APPENDICES xiii

APPENDIX A - Borehole Log B162, B163 D164

APPENDIX B - Evaluation of Effects of Current Blasting Practices on Rock Fracturing in the Lingan Mine

LIST OF TABLES

Table 2.1 Stresses Measured at Different Mines in the Sydney Coalfield
Table 2.2 Summary of Rock Properties of the Siltstone and Outburst Prone Sandstone From No. 26 Colliery
Table 2.3 Summary of Rock Properties in the Sydney Coalfield
Table 2.4 Summary of Core Discing Phenomenon in Sydney Coalfield, Borehole 162, Borehole B164
Table 2.5 Correlation Between Blasting Pattern and Rock and Gas Outburst at No. 26 Colliery
Table 2.6 Description of All The Outburst Occurrences Recorded at No. 26 Colliery, Sydney Coalfield, Nova Scotia
Table 3.1 Summary Description of Geologic Features Associated with Rock and Gas Outbursts in Louisiana Salt Mines
Table 3.2 Brief Summary of Case Histories
Table 4.1 Typical Rock and Gas Parameters and Energy Calculations Based on Rockburst Events in Russian Coal Mines
Table 5.1 Factors Relevant to Outburst Phenomenon
Table 5.2 Critical Values of Extension Strain - (Based on Testing of Core Sample)
Table 6.1 Summary of Dynamic Stress Measurements and Evaluations, Lingan Mine No. 3 Deep
Table 6.2 Summary of Measured Changes in Static Stresses, Lingan Mine No. 3 Deep
Table 7.1 Cases for Finite Element Analyses of Typical Roadway Development
Table 7.2 Dynamic Stresses Generated From Reference Blast Patterns Used in No. 26 Colliery
Table 7.3 Stress Condition at the Roof of the Roadway in No. 26 Colliery
Table 8.1 Method of Risk Assessment for Outburst Prone Sandstone Used in USSR

LIST OF FIGURES

Figure 2.1 Regional Geology of the Sydney Coalfield
Figure 2.2 Schematic Reconstruction of Paleo-Topography At Time of Sandstone Channel Formation and Characteristic of Paleo-River Channel
Figure 2.3 Location of Sandstone Channel in Roof Strata, Sydney Coalfield
Figure 2.4 Principal Stress Directions Measured in Sydney Coalfield
Figure 2.5 Stress Components Measured at Different Mines in the Sydney Coalfield
Figure 2.6 Strength Characteristics of Sandstone From No. 26 Colliery
Figure 2.7 Strength Characteristics of Different Rock Types From Lingan Mine
Figure 2.8 Strength Characteristics of Different Rock Types From Prince Mine
Figure 2.9 Methane Content of Return Airway After Outburst No. 37
Figure 2.10 Profile of Outburst Cavities After Events No. 36 and 37 in No. 26 Colliery, Sydney Coalfield
Figure 2.11 Plan of No. 26 Colliery and Locations of Investigation Boreholes
Figure 2.12 Blast Patterns Used at No. 26 Colliery
Figure 2.13 Locations of Outburst Events in No. 26 Colliery
Figure 2.14 Volume of Material Ejected and Arches Damaged During Rock and Gas Outbursts in No. 26 Colliery
Figure 2.15 Extent of Development & Mining Activities at the Time of Driving 13N Airway Through Channel Sandstone
Figure 2.16 Extent of Development & Mining Activities at The Time of Driving 14N Airway Through Channel Sandstone
Figure 3.1 Idealized Seismo Acoustic Recording of a Sudden Three-Phase Gas Outburst
Figure 4.1 Criterion for Penny Shaped Crack Containing High Pressure Gas
Figure 4.2 Failing Disc in Relation to its Initial Surrounding Stress State
Figure 4.3 The Processes of Secondary Failure of Flaked Pieces and the Creation of a Conical Shape Cavity
Figure 4.4 Model of Rock and Gas Outburst
Figure 4.5 Status of Equilibrium in the Stress-Strain Relationship

LIST OF FIGURES (cont'd)

Figure 5.1 Distribution of Vertical Stress Produced by Longwall Extraction Showing Front and Flank Abutment Zones
Figure 5.2 Permeability Reduction Due to Rock Stress
Figure 5.3 Permeability Curves for Increasing Confining Pressure
Figure 5.4 Variation in Rock Properties for Three Sandstones with Increasing Confining Pressure
Figure 5.5 Profile of Detonation in an Incompressible and a Readily Compressible Medium
Figure 5.6 Typical Composite Attenuation Plots Across Layers of Sandstone/Shale/Coal
Figure 6.1 Location of Blast Monitoring Tests in Lingan Mine
Figure 6.2 Typical Blast Patterns in Coal and Sandstone Used in Lingan Mine
Figure 6.3 Plot of Dynamic Stress with Scaled Distance
Figure 6.4 Suggested Modifications to Blast Design for Lingan Mine
Figure 7.1 Principal Stresses at the Roof of a Typical Roadway in No. 26 Colliery for Various Positions of Sandstone Layer
Figure 7.2 Principal Stresses at the Roof of a Typical Roadway in No. 26 Colliery for Various Thickness of Sandstone Layer
Figure 7.3 Variations of Principal Stresses with Distance of Sandstone/Siltstone Contact from Crown of Roadway - Reference Case
Figure 7.4 Variations of Principal Stresses with Distance of Sandstone/Siltsone Contact from Crown of Roadway for Various In situ Stress Conditions
Figure 7.5 Variations of Principal Stresses with Distance of Sandstone/Siltstone Contact from Crown of Roadway from Various Stiffnesses of Sandstone
Figure 7.6 Principal Stresses at the Roof of a Typical Roadway and 13N Airway in No. 26 Colliery
Figure 7.7 Principal Stresses at the Roof of a Typical Roadway in No. 26 Colliery with the Presence of a Blast Damaged Zone

LIST OF APPENDICES

APPENDIX A - Borehole Log B162, B163, D164
APPENDIX B - Evaluation of Effects of Current Blasting Practices on Rock Fracturing in the Lingan Mine

1. INTRODUCTION

The No. 26 Colliery in Glace Bay, Nova Scotia was in operation until April 1984 when a fire caused the closure of the mine. Development headings in virgin coal, using drilling and blasting were subject to violent dynamic phenomena (described as rock and gas outbursts) whenever sandstone erosion channels were located within 2.7 m of the top of the coal seam. Workings in other operating mines in the Sydney Coalfield could encounter similar conditions before the end of the decade as they reach greater depths in their mining operations. For this reason a long term research program has been implemented by the Coal Research Laboratory of the Canada Centre for Mineral and Energy Technology (CANMET) to study the problem.

Golder Associates was awarded a research contract under the auspices of CANMET through the Department of Supply and Services (DSS contract no. 23440-6-9025/01-SR) to develop a mechanistic model for the initiation of rock and gas outbursts experienced in No. 26 Colliery. The work involved in this study included:

a. a review of the rock and gas outburst phenomena and the associated data collected by the Coal Research Laboratory of CANMET and the Cape Breton Development Corporation (CBDC).

b. a review of the published rock and gas outburst case histories relevant to the outburst phenomena experienced in the Sydney Coalfield.

c. a review of the published mechanistic models for the occurrences of outbursts in other countries.

d. a discussion and summary of the factors affecting the initiation and propagation of outbursts including the effects of rock properties, blasting practices and gas pressure within the rock strata.

e. a field program to measure the (during shotfiring) dynamic effects of blasting on the rock mass and the in situ parameters for use in the analysis of the underground development.

f. a laboratory program in which samples of a reference sandstone were tested to study the general behaviour of the rock mass under the effect of internal gas pressure in a closed system.

g. analyses of selected outburst events using numerical modelling techniques to develop the most probable mechanism for the outburst initiation in the Sydney Coalfield.

h. a discussion of the possible predictive measures and working methods under outburst prone conditions.

This report presents the findings of the study and identifies areas where further research efforts are required.

2. REVIEW OF ROCK AND GAS OUTBURST PHENOMENA IN THE SYDNEY COALFIELD

2.1 Introduction

Between 1977 and April 1984, 37 events described as rock and gas outbursts occurred in No. 26 Colliery of the Sydney Coalfield. All the outbursts occurred between 703 m and 790 m in depth (below sea level). The frequency and intensity of the events increased with depth. In the earlier events (prior to June 1983), gas was neither detected,tested nor recorded after the outbursts. In the latter events, however, a substantial volume of gas was detected after each outburst.

All outbursts occurred almost exclusively in development roadways regardless of their orientation. Bursting generally occurred upon creation of the opening, excavated by drill and blast methods. The failure surfaces exposed within the outburst cavities were typical of surfaces resulting from shear failure.

The bursting formations were invariably sandstones, sometimes with interbeds of siltstone. Outbursts only took place when the sandstone unit was located within 2.7 m (above) of the coal seam. The failed material was generally pulverized or consisted of small flakes.

Over the past five years, the outburst problem in the Sydney Coalfield has been a subject of considerable practical and research interest. Field and laboratory data relating to the outburst events has been compiled by both the Cape Breton Development Corporation and CANMET. A review of this data is presented in the following sections.

2.2 Geological and Geotechnical Data

2.2.1 Regional and Local Geology

The productive measures of the Sydney Coalfield lies within a 2200 m sequence of strata known as the Pictou Group (Figure 2.1), the most extensive and youngest coal deposits of Nova Scotia occur within this group. Eleven major coal seams (six of them are of economic importance) are present, ranging in thickness between 1.0 to 4.5 m. The coal is classified as high volatile "A" bituminous coal. The strata between the coal seams are sandstones, siltstones, mudstones, minor shales and non-marine limestones, which are considered to be of fluvial origin.

There is no major faulting in the coalfield. The major structural features are the northeast trending folds forming the Sydney Synclinorium. No major tectonic activity has perturbed the area. The coal seams dip north 4 to 10 degrees while the gradient on the flanks of the folds rarely exceeds 15 degrees.

2.2.2 Sandstone Paleo-River Channels

Sandstone intrusions (channel sandstone) replacing the normal roof sequence of the coal are observed within the seam or in close proximity (Figure 2.2).

The following is a description of the geological features of the channel sandstone as given by Forgeron et al (1986):

> "Mapping has shown that the paleo-sandstone channels are linear in nature and may move down from, or up into the roof strata, in a manner which is presently unpredictable. Because of their coarser grained texture, the composition of constituent grains

> (subangular quartz, mica and feldspar), the inclusion of lithic fragments within their mass, their downward concave base, their cross-bedded structure and tendency to cut out underlying strata, it is believed that they are, in reality, in-filled paleo-river channels which eroded and migrated across the alluvial plain sometime shortly after the deposition of peat."

Some of the observed effects (Forgeron, 1986) of the sandstone channels on mining operation that are of geotechnical importance for this study are summarized below:

- the rock immediately adjacent to rapid sandstone pinch out zones tends to be weak. Rock falls as high as 2 m have been reported in the mine where such a unit occurred in the roof.

- the sandstone-mudstone contacts always constitute planes of weakness along which rock immediately separates when coal is removed.

- the channels reduce or completely destroy the natural beaming strength of the roof strata.

- outbursts generally originate from such sandstone overbank deposits above the seam. Five of these sandstone channels were identified in No. 26 Colliery and outbursts were recorded at each of these locations.

- the sandstone channels are limited in width and their geometric shapes are difficult to delineate in three dimensions using borehole data. Figure 2.3 shows the known distribution of sandstone channels in the Sydney Coalfield.

2.3 Regional Stress Distribution in the Sydney Coalfield

In situ stress measurements have been carried out at four sites in the Sydney Coalfield; including the Donkin Mine, No. 26 Colliery, and the Prince and Lingan Mines. The scope of the stress measurement program at each site differed because of different project requirements. Results of the stress determinations at Donkin Mine and No. 26 Colliery have been published in Golder Associates reports No. 831-6014(1985) and 831-1296(1984) respectively. Results of the measurements at Prince and Lingan Mines were reported in Golder Associates Report No. 851-6025(1986).

In each test program, the stresses measured have been resolved in components in the N-S, E-W and vertical directions and the stress tensors were evaluated for No. 26 Colliery, the Prince and Lingan Mines by the method of least squares. As the in situ stress data is an important parameter for the study of the rock and gas outburst problems, the available data from these four sites is summarized and discussed below.

Table 2.1 presents a summary of the stresses measured at the four mines in the Sydney Coalfield. Figure 2.4 shows the directions of the principal stresses measured at the No. 26 Colliery, Prince and Lingan Mines. In general the major principal stress (σ_1) is trending E-W and the intermediate principal stress (σ_2) is oriented N-S. These two principal stresses are close to or slightly off horizontal. The minor principal stress (σ_3) is close to or slightly off vertical. In No. 26 colliery, the stress system is fairly isotropic; the principal stress directions vary from the general trend.

A plot of the stress components in the E-W, N-S and vertical directions is presented in Figure 2.5. The general trend is a gradual increase in stress with depth. The vertical stress components measured at the four sites are generally consistent with the overburden stress. The horizontal stress components (E-W and N-S) at Donkin Mine, Prince Mine and No. 26 Colliery differ only slightly resulting in a fairly isotropic horizontal stress system. At Lingan Mine however, σ_{E-W} is significantly higher than σ_{N-S}. This may have resulted from the influence of the monocline which trends in the E-W orientation across the mine. (Golder Associates Report No. 851-6025 (1986)).

The stresses determined from the hydrofracture tests are also plotted in Figure 2.5. The measured vertical stresses are generally consistent with the overburden stresses, but the measured maximum horizontal stresses at Prince Mine are considerably higher than those obtained from the overcoring tests.

Of particular interest in this study are the in situ stresses at No. 26 Colliery. Measurements were made mostly in the siltstone. The stresses are fairly isotropic with very low shear stresses. The major principal stress is 26.3 MPa, oriented in the E-W direction at an inclination of 64°. The ratio of the major and minor principal stresses is about 1.1. The average vertical stress component measured at the test site (14 South Main Level) is about 15 % higher than the static vertical stress.

2.4 Rock Properties and Characteristics

2.4.1 Strength and Deformation Properties

Information relating to the properties of the sandstones at No. 26 Colliery is abundant. Table 2.2 presents the data available from previous work by Golder Associates and from other sources. Figure 2.6 shows the results of triaxial testing performed on sandstone samples obtained from No. 26 Colliery.

Results of laboratory tests on other rock types from the Sydney Coalfield are summarized in Table 2.3. The triaxial strengths of different rock types from Prince and Lingan Mines are presented in Figures 2.7 and 2.8. The results indicate that the Lingan sandstone is marginally stronger than the No. 26 Colliery sandstone.

2.4.2 Petrographic Data of Outburst Sandstone

A study of outburst prone material from No. 26 Colliery based on thin sections and x-ray diffraction analyses was performed by Corelab-Canada Ltd.(1986). The material was described as follows:

> "... very fine and fine grained moderately to well sorted, well cemented, well lithified sandstones with very poor porosity and very poor pore communication. Quartz is the predominant framework grain and composes 49 to 71 percent of the sample. Authigenic or regenerated quartz varies from 5 to 11 percent of these samples. Detrital clays occur in only minor amounts (trace to 4%) in these relatively clean sandstones. The most abundant grain contacts found in these sandstones are curved grain contacts. Porosity of all samples examined is very poor to poor. Intergranular porosity, microporosity and occasionally dissolution porosity is present in these samples. Minor amounts of microporosity is associated with the presence of authigenic kaolinite and the detrital clay lining and filling pores. Dissolution porosity occurs as a result of partial dissolution of chert and feldspar grains."

In addition to the petrographic analysis described above, the pore diameter of the burst prone sandstone was determined by Gorski(1984) and was reported to range from 0.08 to 0.35μ. The average grain size ranged from 0.13 mm to 0.19 mm.

Comparison of petrographic data from the burst-prone sandstone from No. 26 Colliery and the sandstone from the Lingan mine has not reveals no major variations.

2.5 Strata Gas Pressure

The determination of strata reservoir pressure is a difficult task principally because of the very low permeability of the sandstone. The Coal Research Laboratory of CANMET have carried out a number of studies(Aston, 1985; Gallant and Aston, 1985) relating to the determination of strata gas pressure in the Sydney Coalfield. These included:

- determination of gas content from cored and grab samples from outburst cavities,
- in situ gas pressure measurement,
- back calculation of gas pressure from rock and gas volumes ejected during the last two outburst events.

In addition, raw gas from the underground coal mines was analysed and the results are as follows:

Gas	Percentage
Methane	75 - 80%
Nitrogen	≃ 10%
Ethane	5 - 10%
Other hydrocarbons and CO_2	2 - 5%

The results obtained from CANMET's gas pressure studies are summarized and discussed in the following sections.

2.5.1 Gas Pressure Calculation from Cored and Grab Samples

Sandstone samples obtained from an outburst site at No. 26 Colliery were ground to minus 2 mm in a sealed ball mill under inert nitrogen atmosphere. The reported total gas released from the four different samples is summarized below:

Sandstone Sample	Weight (g)	Gas Released (mL)	(mL/1000g)
1. Ejected Material	1390	426	306.0
2. Ejected Material*	5886	351	59.6
3. Intact Core	1083	160	147.7
4. Intact Core	1714	259	151.1

*sample consisted of silstone and mudstone bands

Sample No. 2 in the above table was diluted with siltstone/mudstone and was therefore not representative of the outburst prone sandstone. The intact core samples showed more consistent results. However, the measured gas release was likely to be representative of the gas remaining in the samples at the time of testing rather than that of the original reservoir condition.

2.5.2 In situ Gas Pressure Measurement

In situ gas pressure measurements were undertaken by CANMET in the vicinity of the main deeps on the 14 South Coal Road in No. 26 Colliery. The testing procedure was described in detail by Aston and Gallant(1985).

A double packer arrangement was installed in a borehole drilled into a sandstone erosion channel and the gas pressure within the section sealed by the packers was monitored. After 5 days, no pressure increase was noted. The borehole cavity was then pressurized to 3.5 MPa. An equilibrium pressure of 2.8 MPa was obtained after 45 days.

Some leakage through the packer system was detected during a laboratory calibration test. A certain amount of leakage was anticipated under field conditions. The measured equilibrium pressure of 2.8 MPa might therefore have been the steady state pressure within the sealed section of the borehole rather than the in situ reservoir pressure in the sandstone unit.

2.5.3 Evaluation of In Situ Gas Pressure Based on Outburst Data

The methane content of air in the return airway in No. 26 Colliery in which outburst No. 36 and 37 took place was monitored by CBDC. The volume of rock ejected during these two events were also determined from surveys undertaken subsequent to the outbursts.

The measured volumes of gas and rock ejected are as follows:

Outburst Event No.	Volume of Gas measured (m^3)	Volume of Rock Ejected (m^3)
36	753	316
37	3171	145

The maximum methane content measured during event No. 37 was 1% (Figure 2.9) which was the limit of the reading set for the gas monitoring equipment installed in the vicinity of the outburst area. It may be noted from this Figure that the calculated gas volumes are very sensitive to the way the extrapolation was made and could therefore lead to misleading interpretations.

On the basis of the measured rock and gas volumes and the porosity of the sandstone, the gas pressure were back calculated from outbursts No. 36 and 37 by CANMET(1985). Strata gas pressure was reported to be 4.6 and 39.1 MPa respectively for events No. 36 and 37.

Discussion

In view of the large volume of gas measured during event No. 37, it is highly improbable that the gas released in the event would have been contained within the recovered broken sandstone. The surveyed cavity profiles (shown in Figure 2.10) resulting from the two adjacent outbursts (outbursts No. 36 and 37) do not reveal a cone-shaped cavity which is typical of the geometric shape of outburst cavities (see Sections 3 and 4) noted in other outbursts in the Sydney Coalfield and in other countries. However, it was noted that the final clean-up of the area was not fully completed at the time the cavity profile survey was carried out. In fact, CBDC personnel involved in the clean-up operation confirmed that the face of outburst No. 37 as shown in Figure 2.10 was still heavily broken. On this basis, it may be inferred that the cavity was not cleaned up to the limit of the outburst area. The rock volume measured may have been underestimated.

The lightly dotted profile shown in Figure 2.10 represents the inferred boundary of the outburst cavity ahead of the exposed face. If the volume of this cavity were included, the volume of rock affected in outburst No. 37 becomes approximately 250 m^3.

In addition, based on discussion with the mining engineer in charge of the re-habilitation works, it is understood that a coal bench was exposed after event No. 37. Although the coal did not burst, some crushing and grinding along the top edge of the coal/sandstone contact was noted. The surface area of the exposed coal was estimated, from the plan and cross-section of the outburst zone, to be at least 24 m^2. If one assumes that all the gas from this 2 m thick seam was rapidly desorbed by the passage of the seismic wave through the coal during the rarefaction phase of the wave, as proposed by Litwiniszyn (1985), the gas volume given out by the volume of coal alone could range from approximately 670 m^3 to 1500 m^3.

From the above discussion, it is apparent that a number of factors which could have significant influence on the gas volume assessment have not been considered in the previous back calculations of the reservoir gas pressure. In addition, there are uncertainties regarding the extrapolation of the gas percentage from the recorded data. It is also likely that the volume of rock contributing to gas emission was substantially higher than that measured from the cavity volume. Because of the potential desorption of the exposed coal surfaces, the total contribution of gas release from the rock may be much lower than what was indicated from the calculations. Accordingly, the amount of gas emitted per unit volume of rock during event No. 37 may be lower than that calculated.

In view of the need to invoke various assumptions to arrive at the input parameters, the calculations of the strata gas pressure measured for the last event are therefore very subjective.

2.5.4 Gas Pressure Determination from Reservoir Engineering Estimates

Paterson (1986) estimated initial gas pressure from natural gas reservoir formation pressure using a relationship of 23 kPa per meter of depth below surface. Accordingly, the gas pressure at a depth of 790 m at No. 26 Colliery would be approximately 18.0 MPa.

Aston and Cain (1985), on the other hand, derived a gas pressure value using the hydrostatic water column, a reservoir engineering "rule of thumb". For a depth of 790 m, the gas pressure would be about 7.9 MPa.

Based on a discussion with officials of the Nova Scotia Department of Mines and Energy, gas pressure measurements made during offshore drilling ventures in the vicinity of the Sydney Coalfield, to a depth of 4500 m, appear to correlate with "rule of thumb" of 10.74 kPa per meter of depth. That is, at 790 m, the gas pressure would be approximately 8.5 MPa.

2.5.5 Summary

Based on the discussions presented above, it is apparent that the reservoir gas pressure at the outburst areas in No. 26 Colliery cannot be uniquely defined from back calculations based on the available data. The use of empirical expressions for estimating gas pressure only provides a general range of values for the gas reservoir pressure. By assimilating the field data and the back calculations and empirical values, the best estimate of the gas pressure is between 2.8 and 8.0 MPa.

2.6 Core Discing Phenomenon at No. 26 Colliery

Core discing is a phenomenon associated with the formation of closely spaced fracture surfaces normal to the axis of the rock cores. This is characterized by thin discs of cores of generally uniform thickness. The surface of the fractured discs are similar to those created by a tension failure or shear failure under minimal normal stress. Obert and Stephenson (1965) have demonstrated experimentally that by coring into a triaxially loaded specimen, core discing could take place under proper loading conditions. A series of such phenomena was also noted under field conditions in the Sydney Coalfield.

In the Sydney Coalfield, however, core discing was observed in the erosion channel sandstone layers (refer to discussion in Section 2.1.2.) as wet as in coal intersected by drill holes collared at elevations below -640 m (640 m below mean sea level). A summary of the observed conditions is presented below.

In connection with the investigations of the coal seams and stratigraphy between the Harbour seam and the Gardiner seam, two boreholes (B162 and B163) were put down by the Cape Breton Development Corporation along the gate road on the north side of the 12N longwall panel in No. 26 Colliery. In addition, an upwardly inclined (42.5° to horizontal) borehole (D164) was also drilled at the gate road on the north side of the 13N longwall panel, close to the main deeps. The locations of these boreholes are shown in Figure 2.11.

At the time of drilling B162 and B163 (between September and October 1980), the 12N longwall panel had been completely developed and the 13N longwall panel had been developed to about 1070 m (3500 ft.) from the main deeps. Borehole D164, however, was drilled in relatively undisturbed ground since development work in longwall panels 14S and 15S has not started at the time of drilling.

The borehole logs compiled by the Geological Department of CBDC are presented in Appendix A of the report. It should be noted that at the time the boreholes were logged, the phenomenon of core discing was noted but was not specifically recorded in all the logs.

Core discing occurrences were subsequently recorded in detail for Boreholes B162 and D164 but not for B163.

A summary of the core discing phenomena observed in B162 and D164 boreholes are presented in Table 2.4. The following observations were noted from the borehole data:

- Core discing only occurred in the sandstone layers. There were no indications of discing in the siltstone and mudstone layers. The sandstone layers considered herein (ie. B162, B163 and D164) are located below elevation -645 m.

- Sandstone layers located close to the borehole collar (e.g. in boreholes B162 and D164) did not exhibit core discing.

- In general, core discing was not noted in relatively massive (bedded) sandstone and silty sandstone or interbedded siltstone and sandstone. (For example, sandstone layers 2, 3, 5, 7, 10 and 11 in B162). On the other hand, core discing occurred consistently in cross-bedded sandstone layers which were referred to as paleo-sandstone river channels (Forgeron et al, 1986).

- The core discing occurrences appear to be independent of the orientation of the boreholes. Discing was observed in the upwardly inclined hole (D164) as well as in the vertical downholes.

- The depths at which core discing was noted in the boreholes correlate very well with the depths at which outburst events were encountered. A summary of all the outburst events and the correlatable factors is presented in Section 2.8.

On the basis of the above observations from the borehole data and their correlation with the outburst events, it appears that core discing could be used as an indicator of potential outburst hazards.

2.7 Mining Method

No. 26 Colliery produced 890,000 tonnes of coal in 1983 from two advancing longwall faces. The longwall faces were 210 m in width and extended along strike from the main development entries or "deeps". Inter-panel pillars are 90 to 100 m wide.

The development headings were drilled and blasted to typical dimensions of 4.57 m (15 ft) width and 3.66 m (12 ft.) high. Generally, the coal was shot and mucked prior to blasting the stone (sandstone or siltstone). Roof support was provided by steel arches at 0.9 m intervals, strutted and lagged with timber. The springline (the point where the straight leg of the arch begins) of the arches were at 1.83 m (6 ft.) above the invert. The rock and gas outbursts consistently occurred in the development headings at depths greater than 700 m (below sea level).

All the outburst events occurred often shotfiring (except one, just prior to shotfiring). However, the shotfiring practice at Colliery No. 26 was quite variable. The patterns used were determined by the type of heading being advanced and the rock conditions expected. Figure

2.12 summarizes three typical blast patterns used at No. 26 Colliery (provided by CBDC). Table 2.5 presents a correlation between the blast patterns and rock and gas outbursts at No. 26 Colliery.

2.8 Rock and Gas Outburst Events at No. 26 Colliery

The data compiled by the engineering staff of CDBC on all the rock and gas outburst occurrences at No. 26 Colliery is summarized in Table 2.6 and Figure 2.13.

The salient points from these records are presented below:

- Outbursts occurred in development headings driven into virgin ground with the exception of events No. 10, 11 and 12. Events 10 and 11 had caused minimal damage; no noticeable outburst cavities were recorded (Table 2.6).

- Similar rock conditions encountered in gate roads driven with the advancing longwall faces were not conducive to significant outbursts.

- All bursts but one (No. 24) were associated with shotfiring. In the case of even no. 24, sudden rupture of the sandstone "beam" across the face may have triggered the outburst.

- Number of events, volume expelled and the degree of damage to the steel arches associated with the outburst events tended to increase with depth as illustrated by the correlation shown on Figure 2.14 (Aston and Cain, 1985).

- Sandstone erosion channels located within 2.7 m of the coal seam were prone to bursting.

- The outburst events generally terminated when the events choked themselves or when the outburst cavity reached the siltstone strata above the sandstone channel (e.g. events No. 36-37).

- No outburst occurred during the drivage of 13N Airway although it intersected the same sandstone channel that caused events no. 10 to 12. It was noted that the 13N longwall face has advanced over 550 m (1800 ft.) away from its starting location at the time when the airway heading (located only about 60 m (200 ft.) from the initial longwall face location) crossed the sandstone channel. This situation can be compared with the drivage of the 14N Airway which took place before the advance of the 14N Longwall panel. It has produced events No. 28 and 31 as it crossed a sandstone channel. Figures 2.15 and 2.16 show the status of the development at the time of driving the 13N and 14N Airways respectively.

- Outbursts are not correlatable with the direction of drivage, which is probably due to the relatively isotropic in situ stress field.

TABLE 2.1

STRESSES MEASURED AT DIFFERENT MINES IN THE SYDNEY COALFIELD

Mine Site	Depth of[(1)] Test Site (m)	Method of Stress Measurement	Principal Stresses[(2)] (MPa) (Azimuth/Dip) (Degrees)			Stress Components[(3)] (MPa)			Overburden Stress (MPa)
			σ_1	σ_2	σ_3	σ_{E-W}	σ_{N-S}	σ_v	
Donkin Mine	165 (12)	overcoring	-	-	-	9.04	7.93	4.90	4.2
No. 26 Colliery	762 (90)	overcoring	26.3 (278/64)	24.05 (9/13)	23.2 (270/-25)	23.31	24.98	25.27	21.7
Prince	222 (20)	overcoring	11.8 (263/14)	9.54 (-7.8/5)	5.1 (64/-75)	10.76	9.51	6.00	5.5
		hydrofracturing	17.8-25.4 (274/0)	12.8-14.1 (6/0)	5.4-5.9 (-)	-	-	-	-
Lingan	593 (70)	overcoring	33.84 (88/4.0)	14.49 (4/-55)	12.21 (355/35)	33.73	13.76	13.05	14.3
		hydrofracturing	-	-	7.8/15.4 (-)	-	-	-	-

Notes:

(1) Depth below sea level, Figure in ( ) indicates depth of water.

(2) σ_1, σ_2, σ_3: Major, intermediate and minor principal stresses.

(3) σ_{E-W}, σ_{N-S}, σ_v: Stress components in E-W, N-S and vertical directions.

TABLE 2.2

Summary of Rock Properties of the Siltstone and Outburst Prone Sandstone from No. 26 Colliery

Rock Type (Data Source)	Rock Properties								Remarks
	σ_c (MPa)	σ_t (MPa)	E (GPa)	E_d (GPA)	ν	γ (Mg/m^3)	η (%)	K(g) (md)	
SANDSTONE (CANMET)	59.3	7.7 - 8.0	16.5	N.A.	0.09	N.A.	0.8	0.01	Samples from BH D-164
SANDSTONE (Golder Associates Report No. 841-1287 and 831-1296)	49.0	N.A.	13.1 - 17.5	35.0	0.2	2.6	2		
SANDSTONE (Aston and Cain, 1985)	60 - 100	2.6 - 8.0	12.0 20.0	-	0.09 - 0.28	-	4.5 - 5.5	0.02 (vertical) 0.05 - 0.0005 (horizontal)	
SILTSTONE (CANMET))	82.3	-	25.8	-	-	2.7	-	-	

NOTE:

σ_c = Uniaxial compressive strength
σ_t = Tensile strength
E = Young's Modulus
E_d = Dynamic Young's Modulus

ν = Poisson's Ratio
γ = Bulk Density
η = Porosity
K(g) = Gas permeability

TABLE 2.3

SUMMARY OF ROCK PROPERTIES IN THE SYDNEY COALFIELD

(a) PROPERTIES OF COAL (Ref: Aston et al, 1984)

Mine Site	Direction of Loading Relative to Bedding	Point Load Index Strength Is_{54} (MPa)	Calculated Uniaxial Compressive Strength (MPa)	Calculated Tensile Strength (MPa)
No. 26	Parallel	0.32	9.3	0.89
	Perpendicular	0.46	13.5	1.28
Lingan	Parallel	0.58	16.9	1.60
	Perpendicular	1.23	35.8	3.41
Lingan	Parallel	0.58	16.9	1.61
	Perpendicular	1.22	35.7	3.39
Prince	Parallel	0.75	22.0	2.10
	Perpendicular	0.41	12.0	1.14
NOVACO	Parallel	0.26	7.6	0.72
Point Aconi	Perpendicular	0.18	5.2	0.50

Density of coal in situ: 1.3 - 1.5 Mg/m3

(b) ROCK PROPERTIES AT LINGAN MINE (Ref: Golder Associates Report 841-1287)

Medium Grained Sandstone

Bulk density (Mg/m^3)	2.45
Porosity (%)	6
Gas permeability (cm/s)	2.93×10^{-6} (at 7.1 MPa)

σ_c (MPa)	73.4
σ_t (MPa)	3.9 - 9.2
Young's Modulus (GPa)	11.57
Dynamic Modulus (GPa)	19.4

TABLE 2.3 (cont'd)

(c) ROCK PROPERTIES AT LINGAN MINE (Ref: Golder Associates Report No. 851-6025)

	Siltstone	Sandstone	Mudstone
σ_c (MPa)	48.6	80.0	59.4
σ_t (MPa)	7.0	6.9	7.0
E (GPa)	36.8	30.4	15.5
ν	0.21	0.18	0.11

Note: See Figure 2.7 for triaxial strength characteristics

(d) ROCK PROPERTIES AT PRINCE MINE (Ref: Golder Associates Report No. 851-6025)

	Medium Grained Sandstone	Fine Grained Sandstone	Siltstone	Mudstone
σ_c (MPa)	46.4-56.2	142.8-153.0	63.5-82.1	67.0-89.3
σ_t (MPa)	4.4	10.0	5.6	8.0
E (GPa)	16.2	38.8	15.8	20.4
ν	0.21	0.17	0.16	0.12

Note: See Figure 2.8 for triaxial strength characteristics

TABLE 2.4

SUMMARY OF CORE DISCING PHENOMENON IN SYDNEY COALFIELD
BOREHOLE 162

SANDSTONE LAYER	DEPTH FROM BOREHOLE COLLAR (m)	ELEVATION (m)	DESCRIPTION OF SANDSTONE	CORE DISCING OBSERVED
1	0 to 5.88	-646.57 to -652.48	light grey, medium grained, locally fine grained, bedding planes contain micaceous bands and trace amounts of carbonaceous material.	no core discing noted
2	12.62 to 13.96	-659.19 to -160.33	light grey, fine to medium grained, very massive and comptent; cross-bedding common localized silty phases.	no core discing noted
3	14.87 to 17.65	-661.44 to -664.22	light grey, fine grained, ironstone blebs very common, massively bedded but with localized bedding and cross bedding as at 16.64 m. Dip 10_{o} - 20_{o}.	no discing noted
4	17.92 to 20.06	-664.49 to -666.63	light grey, fine to medium grained micaceous, cross-bedding common unit is hard and competent	core discing between 18.74 m - 18.94 m 18.99 m - 19.06 m Calcareous cement in disced locations.
5	22.37 to 24.11	-668.94 to -670.68	light grey, fine grained, locally calcareous; top portion contains calcareous iron stone nodules (approx. 1 mm) interbedded siltstone and some mudstone present.	no discing noted

NOTES: 1. Refer to Figure 2.11 for borehole location.
2. Refer to Appendix A for detailed borehole logs.

TABLE 2.4 (cont'd)

SUMMARY OF CORE DISCING PHENOMENON IN SYDNEY COALFIELD
BOREHOLE 162

SANDSTONE LAYER	DEPTH FROM BOREHOLE COLLAR (m)	ELEVATION (m)	DESCRIPTION OF SANDSTONE	CORE DISCING OBSERVED
6	34.96 to 36.18	-681.53 to -682.75	white, looks bleached, medium grained, breaks easily as in box along bedding perpendicular to core axis and crumbles; Moderately calcareous.	possibly core discing
7	36.30 to 39.20	-682.87 to -685.77	light grey, silty to very fine grained cross bedding extremely pervalent due to a carbonaceous material along bedding planes. Less turbulent at base.	no discing noted
8	40.37 to 44.81	-687.14 to -691.38	light grey, fine to medium grained, carbonaceous material along bedding planes, cross bedding becomes common. 44.25 - 44.47 m Calcareous zone 44.71 - 44.80 m LAG: reminants of erosional features (mudstone)	core discing noted between 43.74 - 44.86 m 44.00 - 44.29 m 44.38 - 44.60 m 44.68 - 44.78 m
9	45.72 to 47.55	-692.29 to -694.12	light grey, fine grained, locally cross-bedded, typically micaceous on ends. Gradational contact from above over 100 mm. Unit ends as a LAG consisting of a mixture of mudstone clasts on the bottom contact. Oxidized ironstone nodules and zonations common on bottom 100 mm.	core discing noted between 46.33 - 47.56 m

NOTES: 1. Refer to Figure 2.11 for borehole location.
2. Refer to Appendix A for detailed borehole logs.

TABLE 2.4 (cont'd)

SUMMARY OF CORE DISCING PHENOMENON IN SYDNEY COALFIELD
BOREHOLE 162

SANDSTONE LAYER	DEPTH FROM BOREHOLE COLLAR (m)	ELEVATION (m)	DESCRIPTION OF SANDSTONE	CORE DISCING OBSERVED
10	47.55 to 48.46	-694.12 to -695.03	fine to medium grained, zones of finer and darker siltstone within unit. Ironstone clasts present, dip approx. 20°.	no core discing noted
11	48.46 to 50.75	-695.03 to -697.32	grey, medium to coarse grained, generally massive bedding. Progressively coarser towards base, numerous claystone fragments and many oxidized fragments; coaly fossil remains present with locally large 1 mm muscovite micas present. Claystone seems to form the matrix as it encompasses the grains; pebbles up to 1 cm common on unit.	no core discing noted
12	51.15 to 52.28	-697.72 to -698.85	light grey, fine grained, cross-bedded and whispy in nature; a 40% constituent of silt becomes common in the cross-bedding.	core discing noted between 51.25 - 51.71 m 51.51 - 52.24 m
13	71.20 to 71.68	-717.77 to -718.25	light grey, fine grained	core discing noted core broke into 25 mm pieces

NOTES: 1. Refer to Figure 2.11 for borehole location.
2. Refer to Appendix A for detailed borehole logs.

TABLE 2.4 (cont'd)

SUMMARY OF CORE DISCING PHENOMENON IN SYDNEY COALFIELD
BOREHOLE 162

SANDSTONE LAYER	DEPTH FROM BOREHOLE COLLAR (m)	ELEVATION (m)	DESCRIPTION OF SANDSTONE	CORE DISCING OBSERVED
14	76.34 to 77.90	-722.91 to -724.47	light grey, interbedded sandstone, cross-bedded easily breaks along bedding planes; gradation into siltstone.	core discing noted between 76.35 - 77.11 m 77.64 - 77.77 m
15	89.73 to 91.62	-736.30 to -738.19	light grey, fine grained, not competent.	Intense discing noted between 89.91 - 90.22 m
16	99.13 99.55	-745.70 to -746.12	light grey, fine to medium grained.	core discing noted core broke into thin discs
17	105.53 to 107.67	-752.10 to -754.24	light grey, fine grained ground pieces, micaceous. Lost core 105.76 - 107.89 m only 0.46 m removed.	possibly core discing in section of core loss
18	110.41 to 120.23	-756.98 to -766.80	light grey, fine to medium grained generally broken into 100 mm pieces or less; generally massive bedding with cross-bedding carbonaceous material (60 mm) at 177.95 m; tendency to become coarser towards base and generally more massive.	Entire unit disced with the exception of bottom 0.38 m (119.77 - 120.15 m)
19	121.76 to 128.17	-768.33 to -775.34	light grey, fine to medium grained, carbonaceous material whispy along bedding; unit appears to have been deposited under varying energies in coarser sandstone, feldspar present.	Entire unit disced. Average thickness of disc is 7 m

NOTES: 1. Refer to Figure 2.11 for borehole location.
2. Refer to Appendix A for detailed borehole logs.

TABLE 2.4 (cont'd)

SUMMARY OF CORE DISCING PHENOMENON IN SYDNEY COALFIELD
BOREHOLE B163

SANDSTONE LAYER	DEPTH FROM BOREHOLE COLLAR (m)	ELEVATION (m)	DESCRIPTION OF SANDSTONE	CORE DISCING OBSERVED
1	0 - 6.55	-685.28 to -691.83	light grey; very fine - fine grained, highly micaceous; contains an abaundance of plant fossils; unit is covered by a calcareous coating, but is not calcareous; first 2.74 m is highly ground up, contains much more carbonaceous matter than the remainder; abundance of coal shards between 4.42 - 4.88 m; highly broken up in core box; direction of bedding is not apparent; lower contact is very sharp; generally competent.	To be supplied by CBDC
2	15.39 to 15.91	-700.67 to -701.19	light grey; fine grained; highly micaceous; slightly calcareous; slightly cross-bedded; contains a few mudstone fragments (60 mm); abrupt lower contact; competent.	
3	18.56 to 20.76	-703.84 to -706.04	light grey; fine-medium grained; contains numerous interbeds of coarse grained siltstone throughout unit; cross-bedded; slightly micaceous; calcareous; mudstone fragments throughout; erosive lower contact; bedding not apparent; competent.	
4	25.05 to 27.16	-710.33 to -712.44	medium-dark grey; sandstone - fine grained; siltstone - coarse grained; highly micaceous; slightly calcareous; ironstone nodules throughout; plant fossils absent; gradational lower contact; competent.	

NOTES: 1. Refer to Figure 2.11 for borehole location.
2. Refer to Appendix A for detailed borehole logs.

TABLE 2.4 (cont'd)

SUMMARY OF CORE DISCING PHENOMENON IN SYDNEY COALFIELD
BOREHOLE B163

SANDSTONE LAYER	DEPTH FROM BOREHOLE COLLAR (m)	ELEVATION (m)	DESCRIPTION OF SANDSTONE	CORE DISCING OBSERVED
5	27.16 to 53.89	-712.44 to -739.19	light-medium grey; fine to medium grained; highly micaceous; slightly calcareous; massive; plant fossils noted; lower contact - abrupt; competent.	To be supplied by CBDC
6	75.59 to 77.27	-760.87 to -762.55	light grey, fine grained; massive; slightly calcareous; micaceous; slightly cross-bedded; contains numerous interbeds of siltstone and mudstone from 76.35 - 76.93; abrupt lower contact; competent.	
7	103.48 to 108.36	-788.76 to -793.64	light grey; fine grained; massive and structureless; slightly calcareous; micaceous; plant fossils absent; abrupt lower contact; competent.	
8	116.13 to 128.17	-801.41 to -813.45	light grey; fine grained; highly calcareous; massive; abundance of plant fossils; bedding not apparent; slightly cross-bedded in sections; ironstone nodules throughout unit; conglomeritic sandstone from -810.40 to -810.55; gradational lower contact; competent.	

NOTES:
1. Refer to Figure 2.11 for borehole location.
2. Refer to Appendix A for detailed borehole logs.

TABLE 2.4 (cont'd)

SUMMARY OF CORE DISCING PHENOMENON IN SYDNEY COALFIELD
BOREHOLE B163

SANDSTONE LAYER	DEPTH FROM BOREHOLE COLLAR (m)	ELEVATION (m)	DESCRIPTION OF SANDSTONE	CORE DISCING OBSERVED
1	0 - 6.55	-685.28 to -691.83	light grey; very fine - fine grained, highly micaceous; contains an abundance of plant fossils; unit is covered by a calcareous coating, but is not calcareous; first 2.74 m is highly ground up, contains much more carbonaceous matter than the remainder; abundance of coal shards between 4.42 - 4.88 m; highly broken up in core box; direction of bedding is not apparent; lower contact is very sharp; generally competent.	
2	15.39 to 15.91	-700.67 to -701.19	light grey; fine grained; highly micaceous; slightly calcareous; slightly cross-bedded; contains a few mudstone fragments (60 mm); abrupt lower contact; competent.	
3	18.56 to 20.76	-703.84 to -706.04	light grey; fine-medium grained; contains numerous interbeds of coarse grained siltstone throughout unit; cross-bedded; slightly micaceous; calcareous; mudstone fragments throughout; erosive lower contact; bedding not apparent; competent.	
4	25.05 to 27.16	-710.33 to -712.44	medium-dark grey; sandstone - fine grained; siltstone - coarse grained; highly micaceous; slightly calcareous; ironstone nodules throughout; plant fossils absent; gradational lower contact; competent.	

NOTES: 1. Refer to Figure 2.11 for borehole location.
2. Refer to Appendix A for detailed borehole logs.

TABLE 2.4 (cont'd)

SUMMARY OF CORE DISCING PHENOMENON IN SYDNEY COALFIELD
BOREHOLE B163

SANDSTONE LAYER	DEPTH FROM BOREHOLE COLLAR (m)	ELEVATION (m)	DESCRIPTION OF SANDSTONE	CORE DISCING OBSERVED
5	27.16 to 53.89	-712.44 to -739.19	light-medium grey; fine to medium grained; highly micaceous; slightly calcareous; massive; plant fossils noted; lower contact - abrupt; competent.	
6	75.59 to 77.27	-760.87 to -762.55	light grey, fine grained; massive; slightly calcareous; micaceous; slightly cross-bedded; contains numerous interbeds of siltstone and mudstone from 76.35 - 76.93; abrupt lower contact; competent.	
7	103.48 to 108.36	-788.76 to -793.64	light grey; fine grained; massive and structureless; slightly calcareous; micaceous; plant fossils absent; abrupt lower contact; competent.	
8	116.13 to 128.17	-801.41 to -813.45	light grey; fine grained; highly calcareous; massive; abundance of plant fossils; bedding not apparent; slightly cross-bedded in sections; ironstone nodules throughout unit; conglomeritic sandstone from -810.40 to -810.55; gradational lower contact; competent.	

NOTES: 1. Refer to Figure 2.11 for borehole location.
2. Refer to Appendix A for detailed borehole logs.

TABLE 2.4 (cont'd)

SUMMARY OF CORE DISCING PHENOMENON IN SYDNEY COALFIELD
BOREHOLE D164

SANDSTONE LAYER	DEPTH FROM BOREHOLE COLLAR (m)	ELEVATION (m)	DESCRIPTION OF SANDSTONE	CORE DISCING OBSERVED
1	3.38 to 3.51	-758.62 to -758.49	fine medium grained well laminated	no core discing noted
2	3.63 to 4.52	-758.37 to -757.48	medium fine grained thinly laminated silty inclusions	no core discing noted
3	4.88 to 5.64	-757.12 to -756.36	thinly laminated small subrounded silty inclusions near top of section	no core discing noted
4	6.25 to 7.74	-755.75 to -754.26	well laminated becoming slightly laminated towards top of section; wispy silty fragments	core discing noted
5	7.92 to 8.15	-754.00 to -753.85	sandstone massive at base of section becoming progressively laminated towards top	no core discing noted
6	8.32 to 8.59	-753.68 to -753.41	sandstone carbonaceous material along bedding	core discing noted
7	8.89 to 9.22	-753.11 to -752.78	laminate 10% sand, 30% silt	core discing noted

NOTES:
1. Refer to Figure 2.11 for borehole location.
2. Refer to Appendix A for detailed borehole logs.
3. Borehole D164 was drilled upwards at an inclination of 42.5° to the horizontal.

TABLE 2.5

CORRELATION BETWEEN BLASTING PATTERN AND ROCK AND GAS OUTBURSTS AT NO. 26 COLLIERY

Rock and Gas Outbursts Reference No.	Location	Associated Blast Pattern* Reference No.
15 to 24, 26-27, 29-30, 32	14N Coal Road	1
10 to 12	13N Brushing Face in Sandstone	2

The blasting pattern used for the headings in which the remaining events took place were not available. Consequently, the events were correlated with available blasting patterns from similar types of headings.

Rock and Gas Outbursts Reference No.	Location	Associated Blast Pattern* Reference No.
5 to 9	13S Top Level	1
2 to 4	13N Coal Road	1
1	13N Top Level	1
25	13N Airway	1
28, 31	14N Airway	1
13-14, 33 to 37	Main Deeps	1

*Refer to Figure 2.12 for reference blast patterns

REGIONAL GEOLOGY OF THE SYDNEY COALFIELD (AFTER CALDER, 1985)

FIGURE 2.1

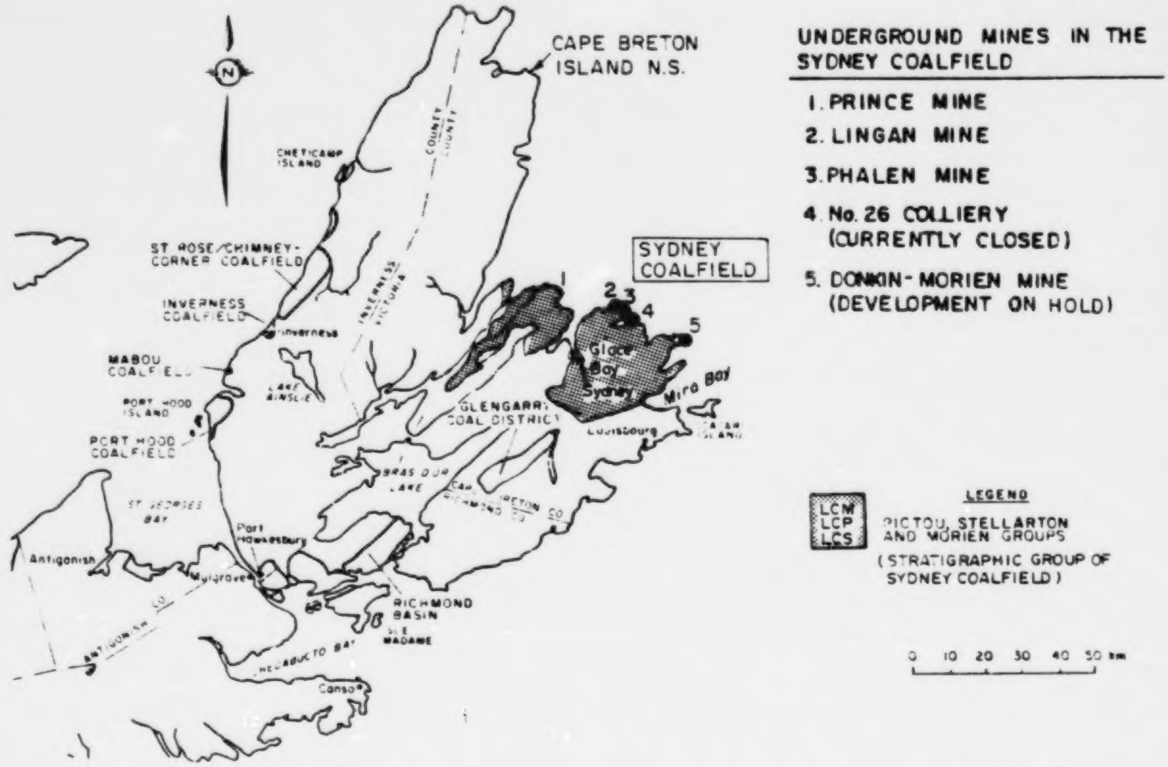
CAPE BRETON ISLAND N.S.
N
CHETICAMP ISLAND
ST ROSE/CHIMNEY-CORNER COALFIELD
INVERNESS COALFIELD
Inverness
MABOU COALFIELD
PORT HOOD ISLAND
PORT HOOD COALFIELD
LAKE AINSLIE
INVERNESS
VICTORIA
COUNTY
COUNTY
SYDNEY COALFIELD
1
2
3
4
5
Glace Bay
Sydney
Mira Bay
GLENGARRY COAL DISTRICT
Louisbourg
SCATARI ISLAND
BRAS D'OR LAKE
CAPE BRETON CO
RICHMOND CO
ST GEORGES BAY
Antigonish
Port Hawkesbury
Mulgrave
ANTIGONISH CO
RICHMOND BASIN
ISLE MADAME
CHEDABUCTO BAY
Canso
UNDERGROUND MINES IN THE SYDNEY COALFIELD
1. PRINCE MINE
2. LINGAN MINE
3. PHALEN MINE
4. No. 26 COLLIERY (CURRENTLY CLOSED)
5. DONKIN-MORIEN MINE (DEVELOPMENT ON HOLD)
LEGEND
LCM LCP LCS
PICTOU, STELLARTON AND MORIEN GROUPS
(STRATIGRAPHIC GROUP OF SYDNEY COALFIELD)
0 10 20 30 40 50 km

LOCATION MAP OF SYDNEY COALFIELD, NOVA SCOTIA

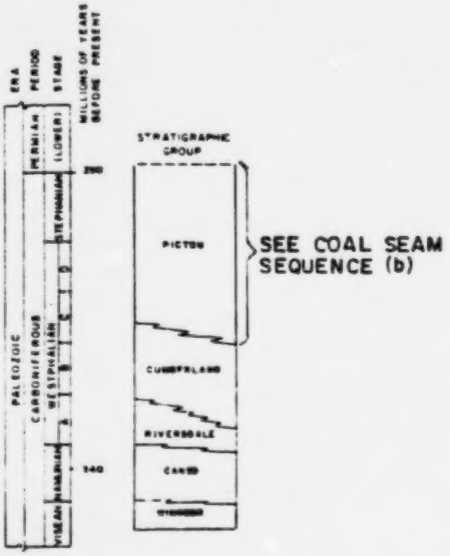
ERA
PERIOD
STAGE
MILLIONS OF YEARS BEFORE PRESENT
PALEOZOIC
PERMIAN
CARBONIFEROUS
(LOWER)
STEPHANIAN
WESTPHALIAN
NAMURIAN
VISEAN
290
340
STRATIGRAPHIC GROUP
PICTOU
CUMBERLAND
RIVERSDALE
CANSO
WINDSOR
SEE COAL SEAM SEQUENCE (b)

a) GEOLOGICAL GROUPS OF THE CARBONIFEROUS PERIOD IN NOVA SCOTIA

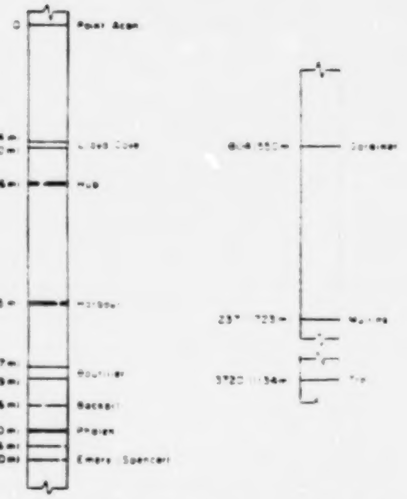
0
Point Aconi
376 (116 m)
394 (120 m)
Lloyd Cove
512 (156 m)
Hub
902 (275 m)
Harbour
1105 (337 m)
1145 (349 m)
Bouthillier
1233 (376 m)
Backpit
1312 (400 m)
Phalen
1364 (416 m)
1410 (430 m)
Emery (Spencer)
Gardiner
Mullins
Tracy

b) IDEALIZED STRATIGRAPHIC COLUMN OF THE SYDNEY COALFIELD SHOWING MAJOR COAL SEAMS

(AFTER CALDER, (1985))

NOT DRAWN TO SCALE

Date MARCH, 1987

Project 861 - 1290

Golder Associates

Drawn D. M.

Chkd

SCHEMATIC RECONSTRUCTION OF PALEO-TOPOGRAPHY AT TIME OF SANDSTONE CHANNEL FORMATION AND CHARACTERISTICS OF PALEO-RIVER CHANNEL

FIGURE 2.2

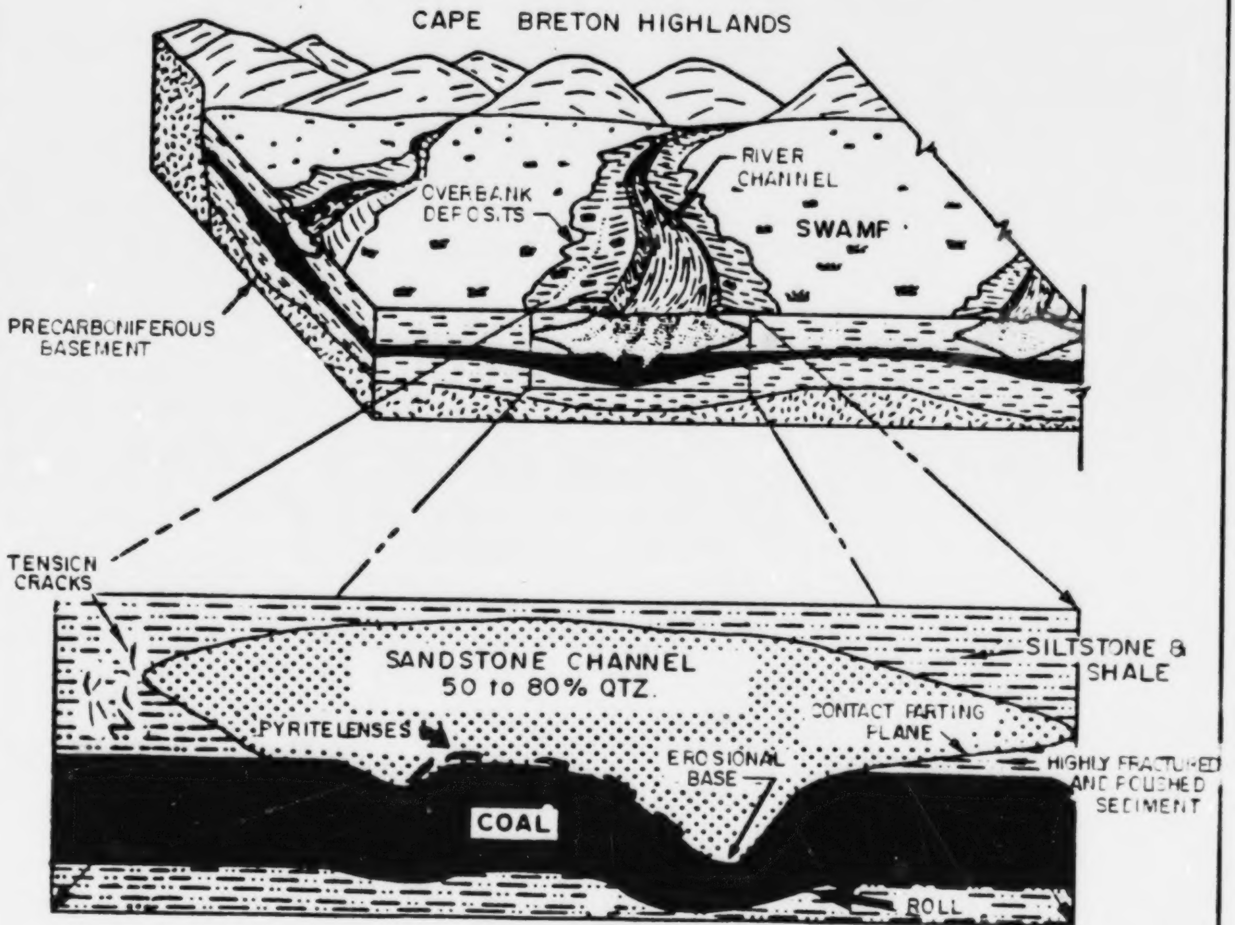
CAPE BRETON HIGHLANDS
RIVER CHANNEL
OVERBANK DEPOSITS
SWAMP
PRECARBONIFEROUS BASEMENT
TENSION CRACKS
SANDSTONE CHANNEL 50 to 80% QTZ.
SILTSTONE & SHALE
PYRITE LENSES
CONTACT PARTING PLANE
EROSIONAL BASE
HIGHLY FRACTURED AND POLISHED SEDIMENT
COAL
ROLL

(AFTER FORGERON et al, (1986))

NOT DRAWN TO SCALE

Date MARCH, 1987
Project 861-1290

Golder Associates

Drawn D.M.
Chkd

B61 - 1290 FIG 2.3 LOCATION OF SANDSTONE CHANNEL

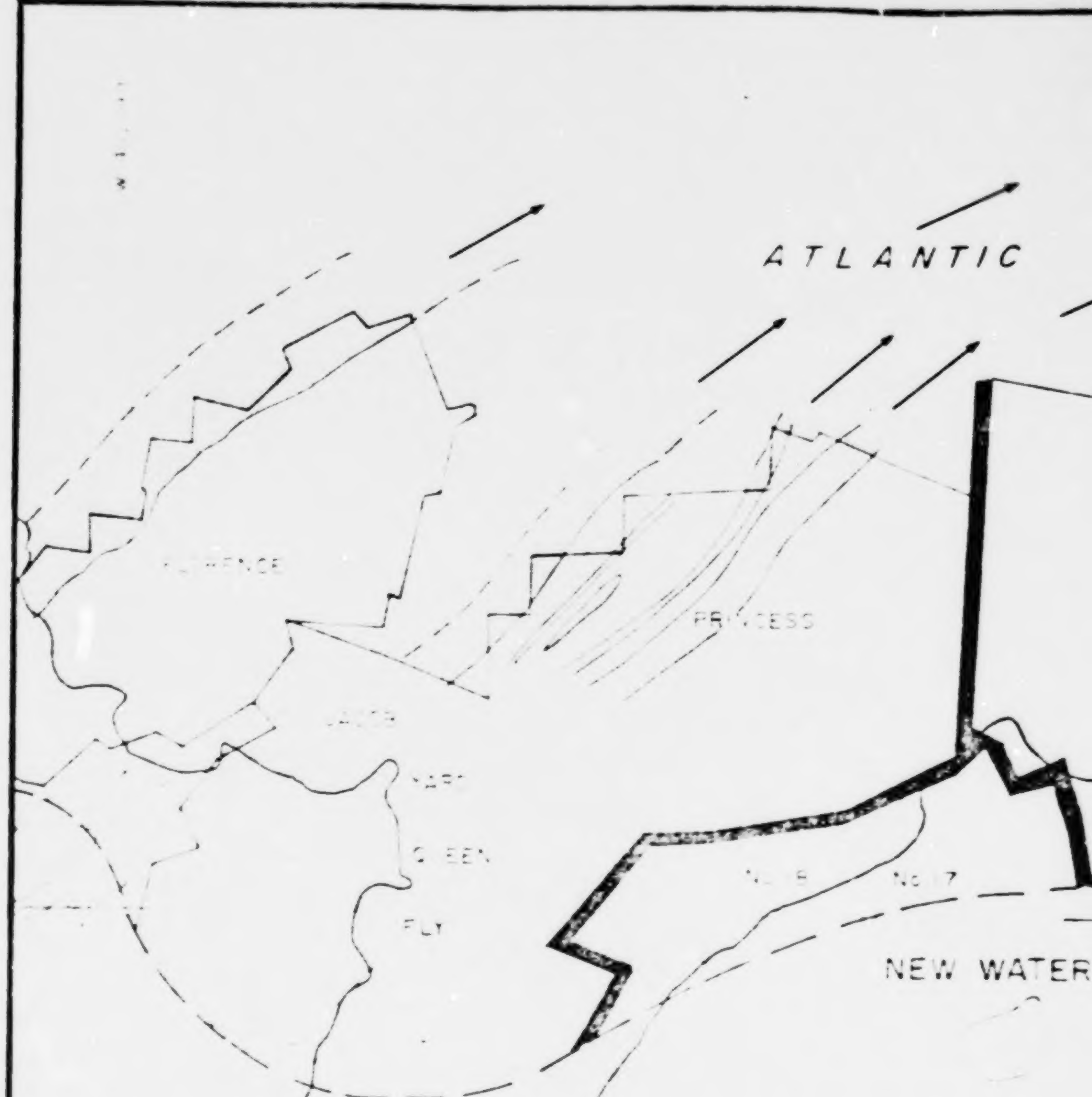
ATLANTIC
FLORENCE
PRINCESS
JACOB
HARD
GREEN
FLY
No 18
No 17
NEW WATER
SYDNEY
HARBOUR

LOCATION OF SANDSTONE CHANNEL IN ROOF STRATA, SYDNEY COALFIELD

FIGURE 2.3

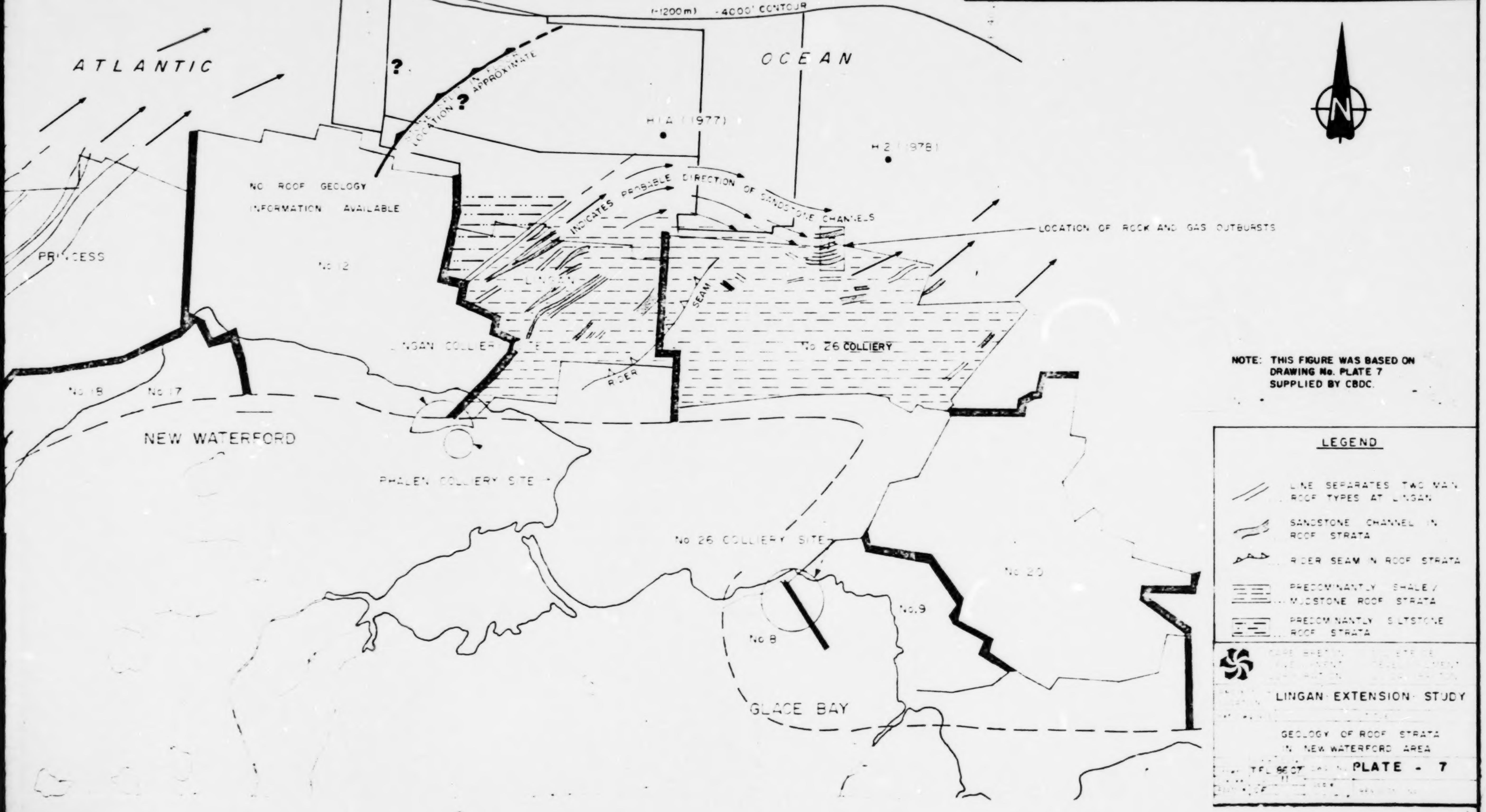
(-1200m) -4000' CONTOUR
ATLANTIC
OCEAN
?
?
LOCATION APPROXIMATE
H1A (1977)
H2 (1978)
NO ROOF GEOLOGY INFORMATION AVAILABLE
INDICATES PROBABLE DIRECTION OF SANDSTONE CHANNELS
LOCATION OF ROCK AND GAS OUTBURSTS
PRINCESS
No 12
LINGAN
SEAM
RIDER
LINGAN COLLIERY
No 26 COLLIERY
No 18
No 17
NEW WATERFORD
PHALEN COLLIERY SITE
No 26 COLLIERY SITE
No 20
No 9
No 8
GLACE BAY
N
NOTE: THIS FIGURE WAS BASED ON DRAWING No. PLATE 7 SUPPLIED BY CBDC.
LEGEND
LINE SEPARATES TWO MAIN ROOF TYPES AT LINGAN
SANDSTONE CHANNEL IN ROOF STRATA
RIDER SEAM IN ROOF STRATA
PREDOMINANTLY SHALE / MUDSTONE ROOF STRATA
PREDOMINANTLY SILTSTONE ROOF STRATA
CAPE BRETON DEVELOPMENT CORPORATION
LINGAN EXTENSION STUDY
GEOLOGY OF ROOF STRATA IN NEW WATERFORD AREA
PLATE - 7

Date MARCH, 1987
Project 861-1290

Golder Associates

Drawn DM
Chk'd

PRINCIPAL STRESS DIRECTIONS MEASURED IN SYDNEY COALFIELD

FIGURE 2.4

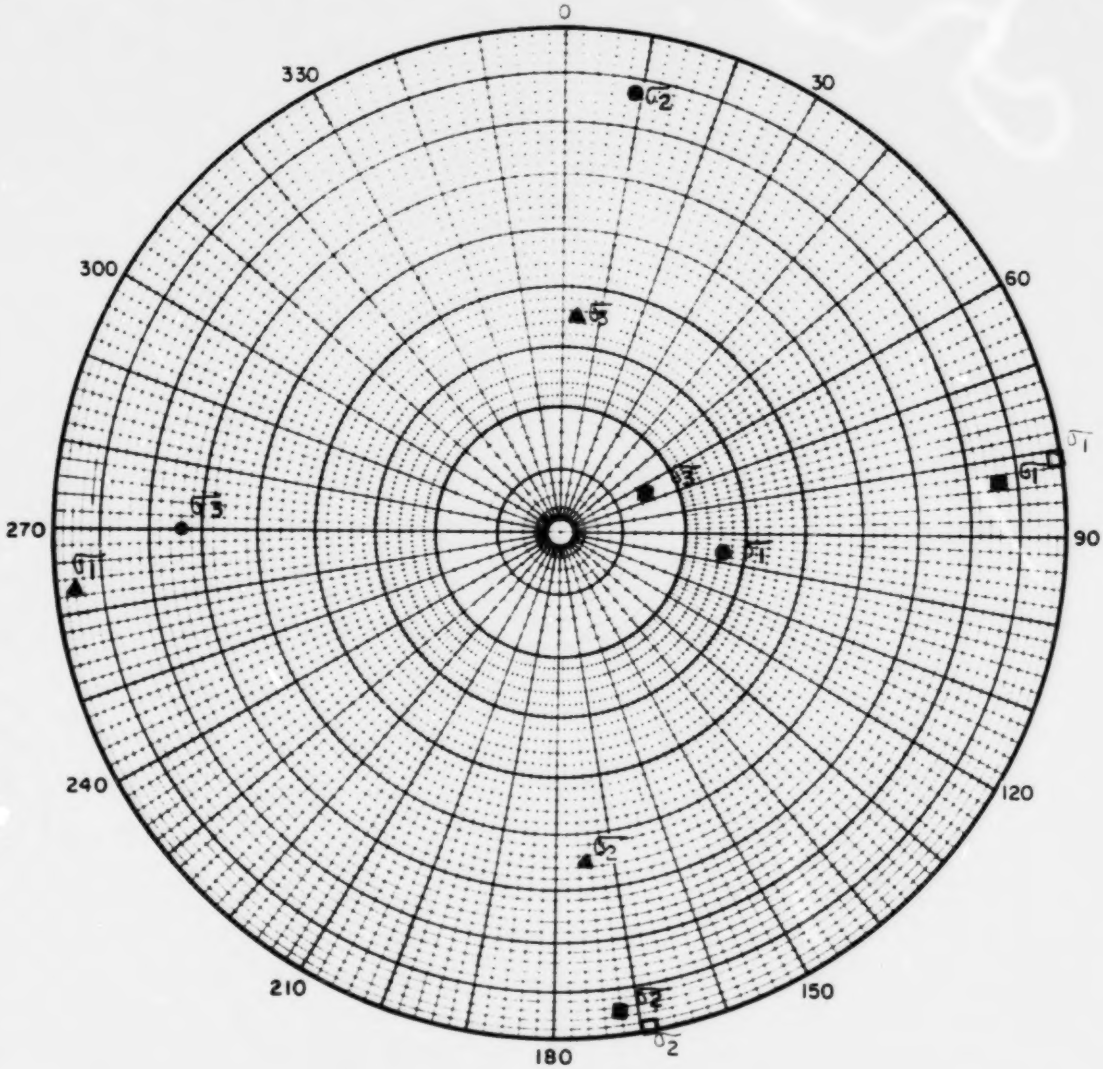

POLAR EQUAL AREA STEREONET
LOWER HEMISPHERE PROJECTION

(AFTER GOLDER ASSOCIATES REPORT 851-6025, (1986))

NOTES

1) σ_1, σ_2, σ_3 = MAJOR, INTERMEDIATE AND MINOR PRINCIPAL STRESSES RESPECTIVELY

2) ● DATA FROM No. 26 COLLIERY
■ DATA FROM PRINCE MINE
▲ DATA FROM LINGAN MINE
} OBTAINED FROM OVERCORING TESTS USING USBM GAUGE

□ DATA FROM PRINCE MINE - OBTAINED FROM HYDROFRACTURE TEST

Date FEB. 6, 1987
Project No. 861-1290

Golder Associates

Drawn D. M
Chkd [illegible]

STRESS COMPONENTS MEASURED AT DIFFERENT MINES IN THE SYDNEY COALFIELD

FIGURE 2.5

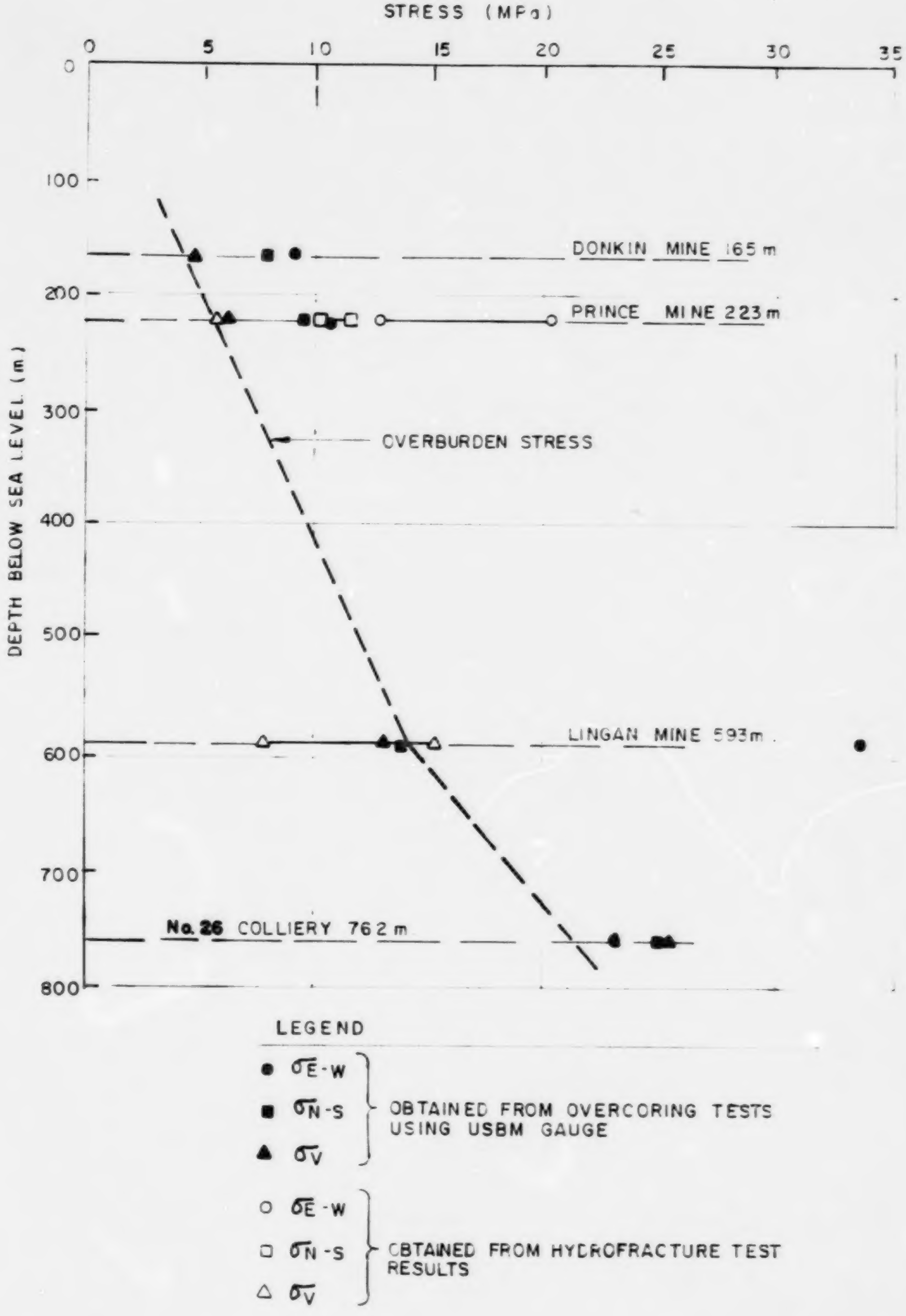

NOTE

OVERBURDEN STRESS WAS CALCULATED FROM WEIGHT OF ROCK AND WATER ABOVE TEST SITE.
(AFTER GOLDER ASSOCIATES REPORT No. 851-6025,(1986))

Date FEB. 9, 1987
Project 861-1290

Golder Associates

Drawn C M
Chkd

STRENGTH CHARACTERISTICS OF SANDSTONE FROM No. 26 COLLIERY

FIGURE 2.6

DESCRIPTION OF SANDSTONE TESTED

Alternate beddings of sandstone and siltstone/mudstone. The beddings are inclined with respect to the core axis at an angle of approximately 10°. The width of the sandstone bands varies between 1.0 to 3.0 mm whereas it is between 0.1 to 1.0 mm [illegible] the siltstone/mudstone bands. In some samples, the sandstone band was up to [illegible] mm in thickness.

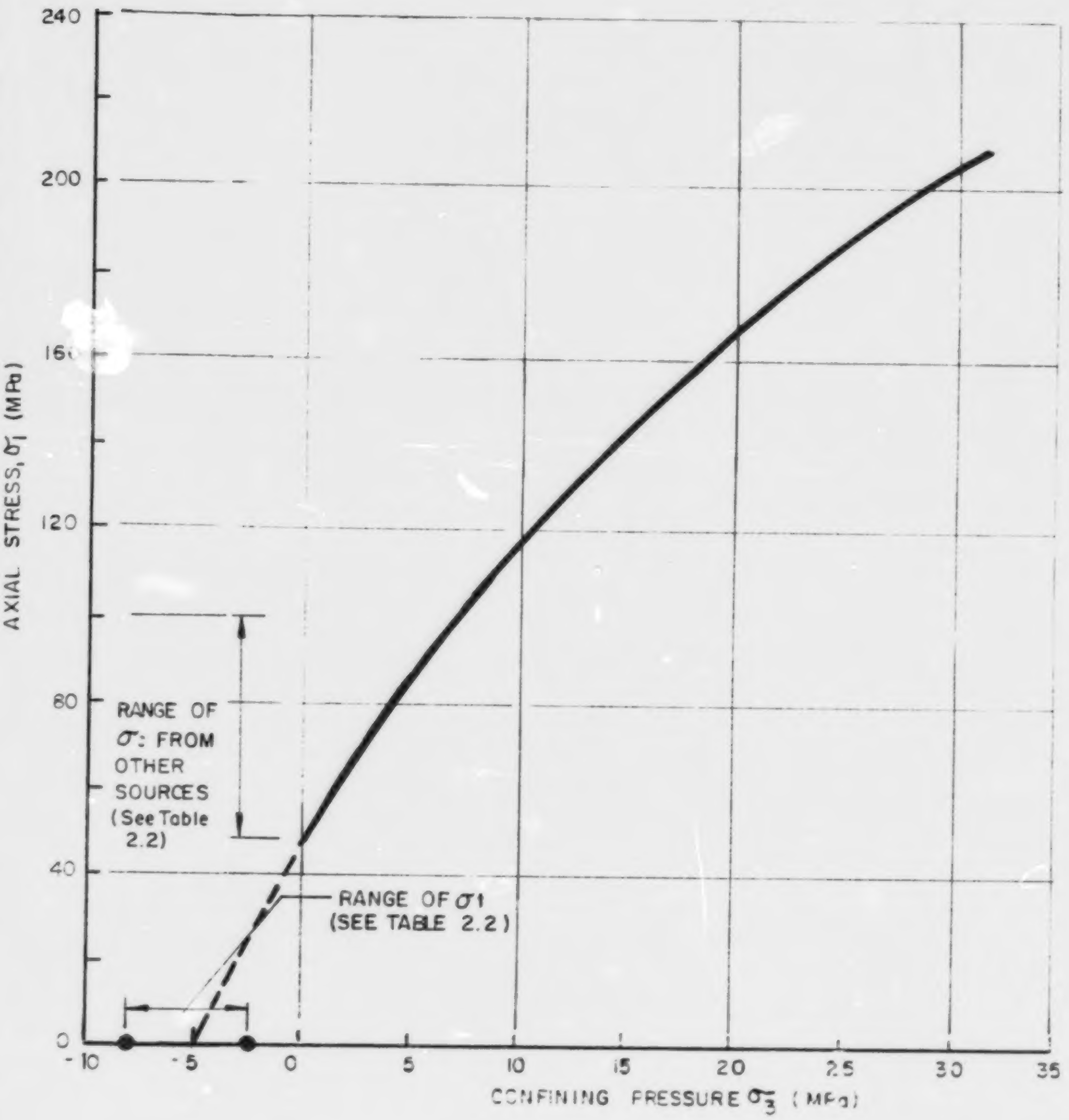

(AFTER GOLDER ASSOCIATES REPORT No. 841-1287-2 (1985))

Date FEB 6, 1987

Project 861-1290

Golder Associates

Drawn D M

Chkd

STRENGTH CHARACTERISTICS OF DIFFERENT ROCK TYPES FROM LINGAN MINE

FIGURE 2.7

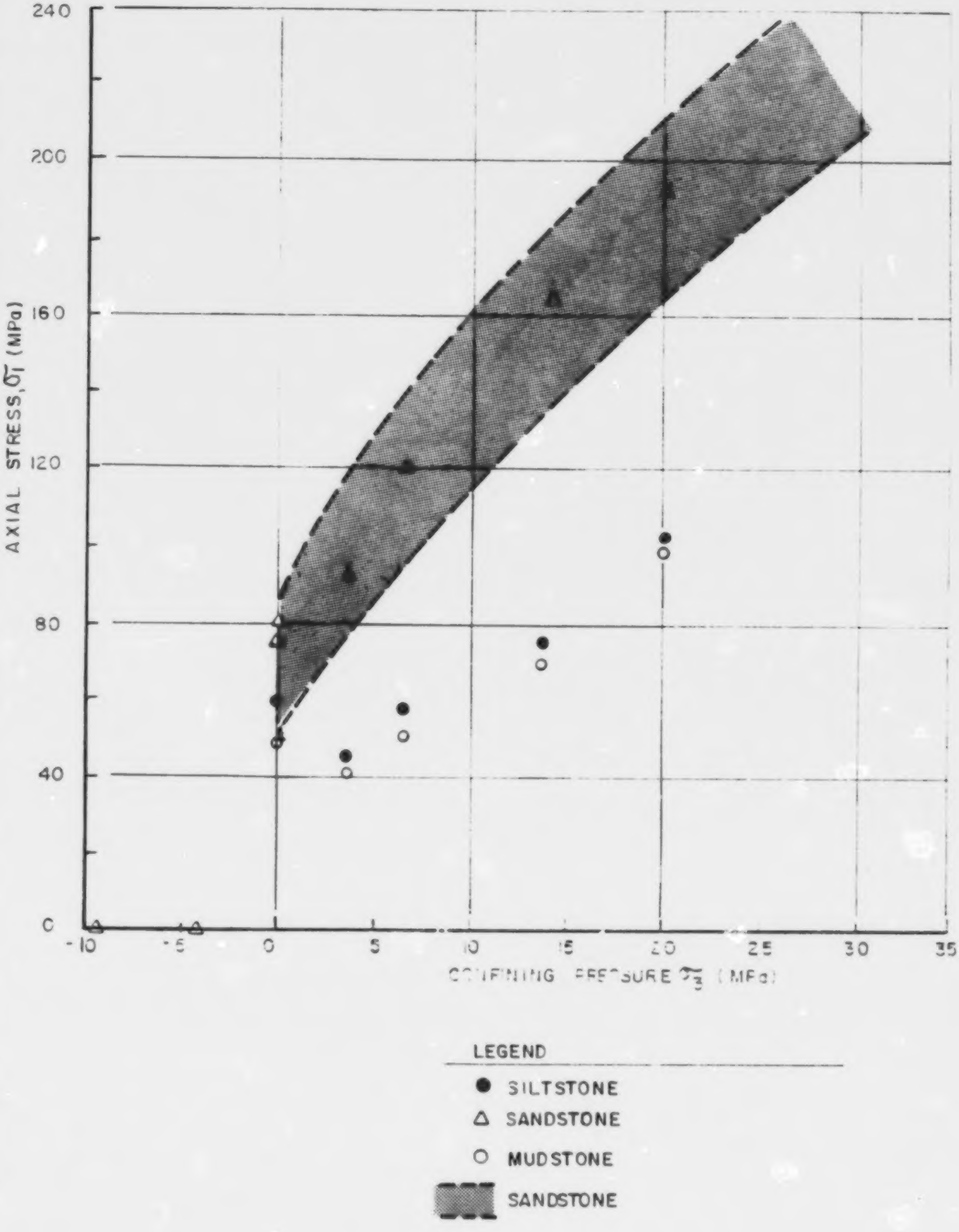

(AFTER GOLDER ASSOCIATES, 851-6025, 841-1287-2, (1985))

Date MARCH, 1987

Project 861-1290

Golder Associates

Drawn D. M.

Chkd

STRENGTH CHARACTERISTICS OF DIFFERENT ROCK TYPES FROM PRINCE MINE

FIGURE **2.8**

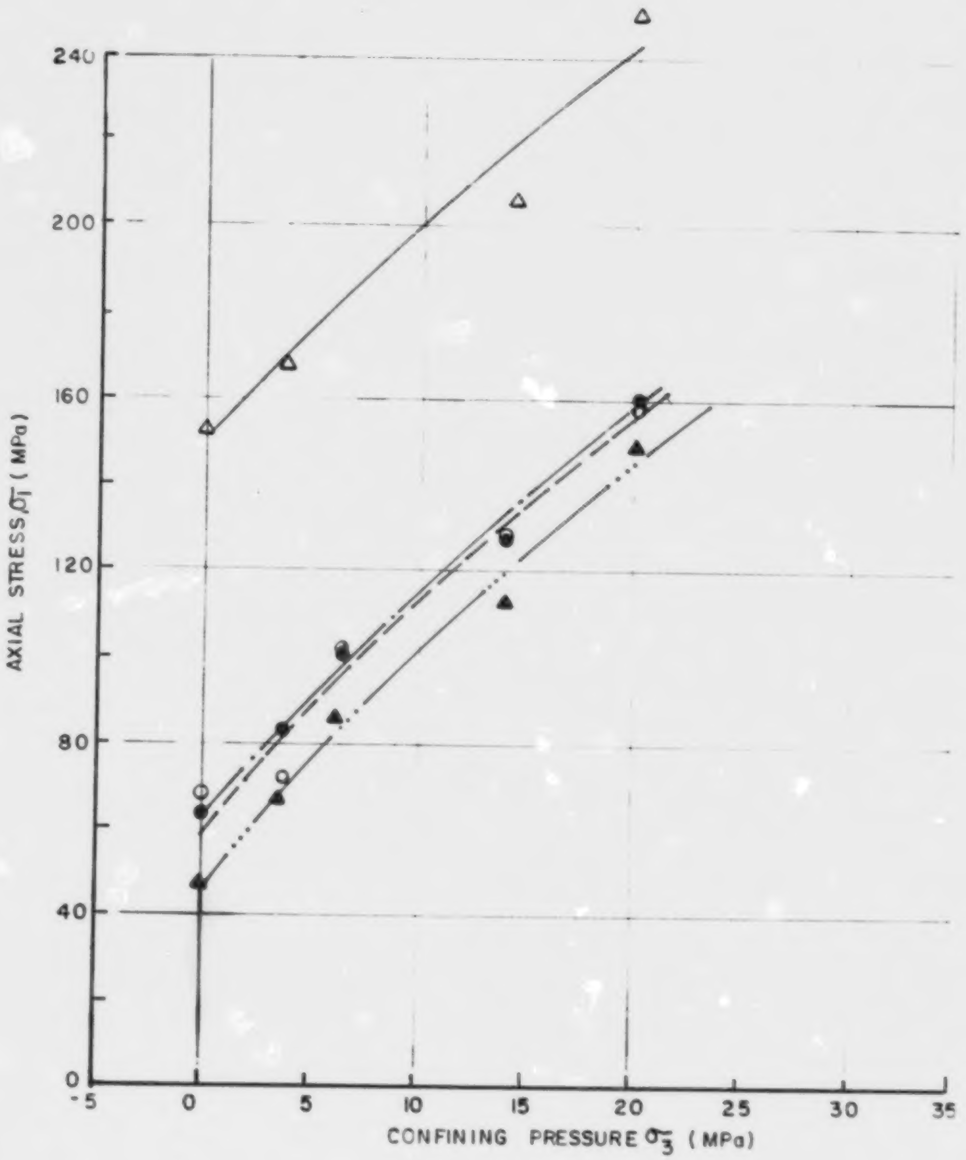

NOTE

LINES THROUGH DATA POINTS INDICATE APPROXIMATE TRENDS ONLY.

LEGEND

- – –○– SILTSTONE
- –·–○– MUDSTONE
- ——△— FINE GRAINED SANDSTONE
- —···△— MEDIUM GRAINED SANDSTONE

(AFTER GOLDER ASSOCIATES 851-6025, (1986))

Date FEB. 6, 1987
Project 861-1290

Golder Associates

Drawn D M
Chkd

METHANE CONTENT OF RETURN AIRWAY AFTER OUTBURST No. 37

FIGURE 2.9

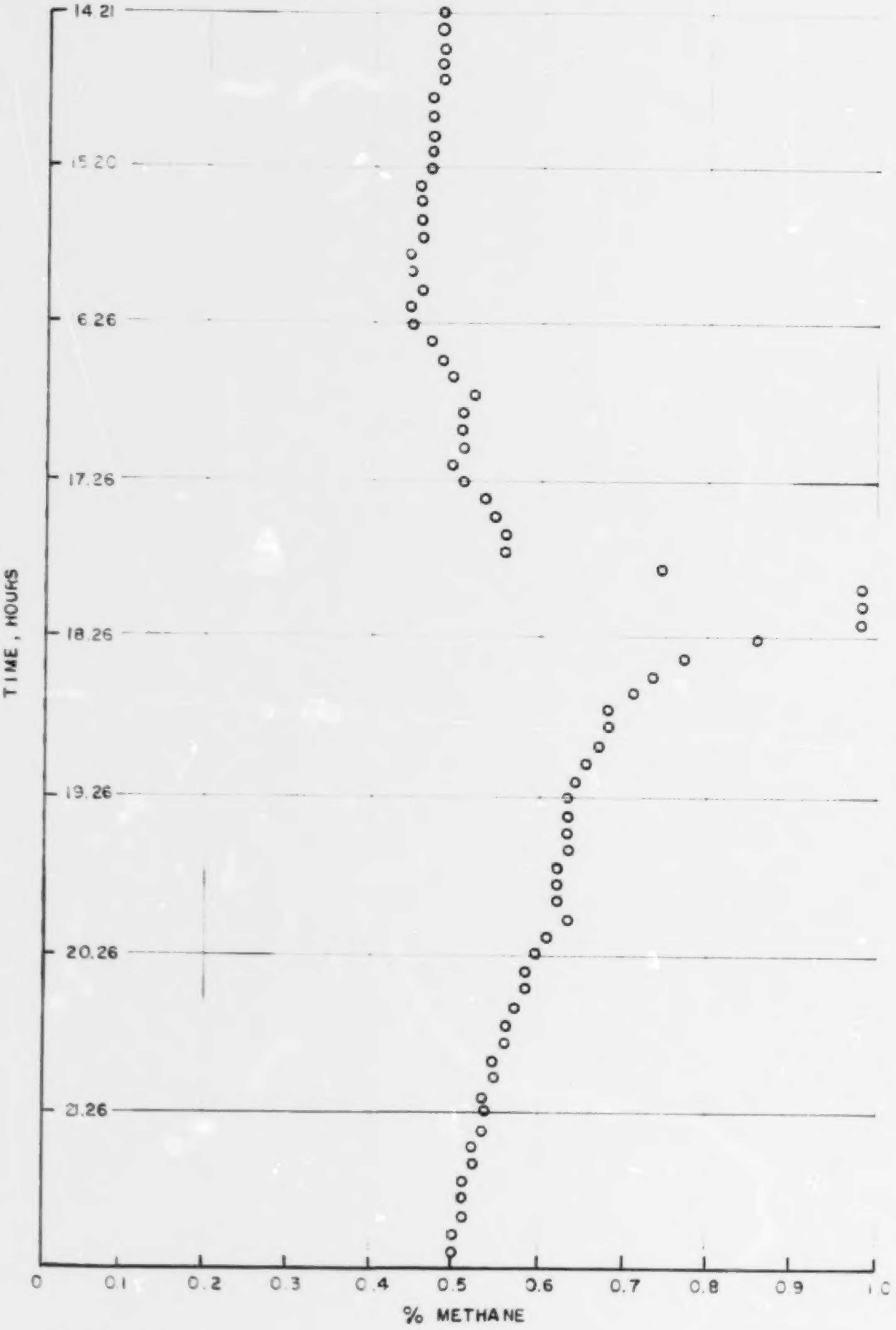

Date MARCH 30, 1987
Project 861-1290

Golder Associates

Drawn D. M.
Chkd

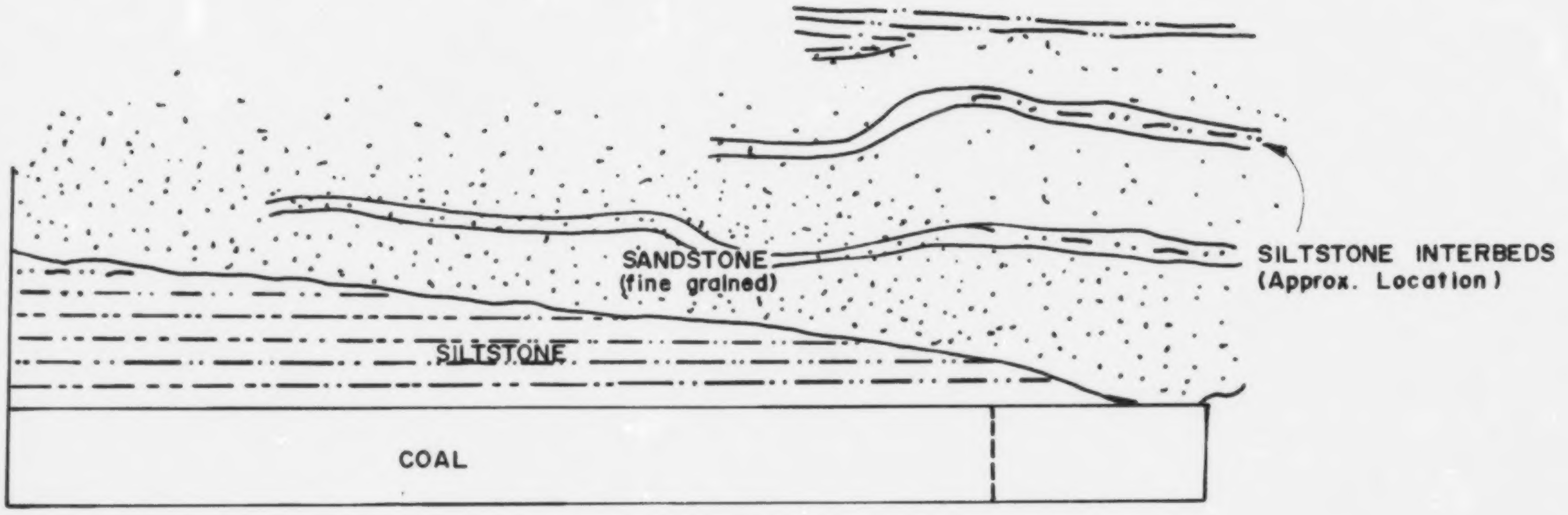
SANDSTONE
(fine grained)
SILTSTONE INTERBEDS
(Approx. Location)
SILTSTONE
COAL

GEOLOGICAL CROSS SECTION ALONG A-B

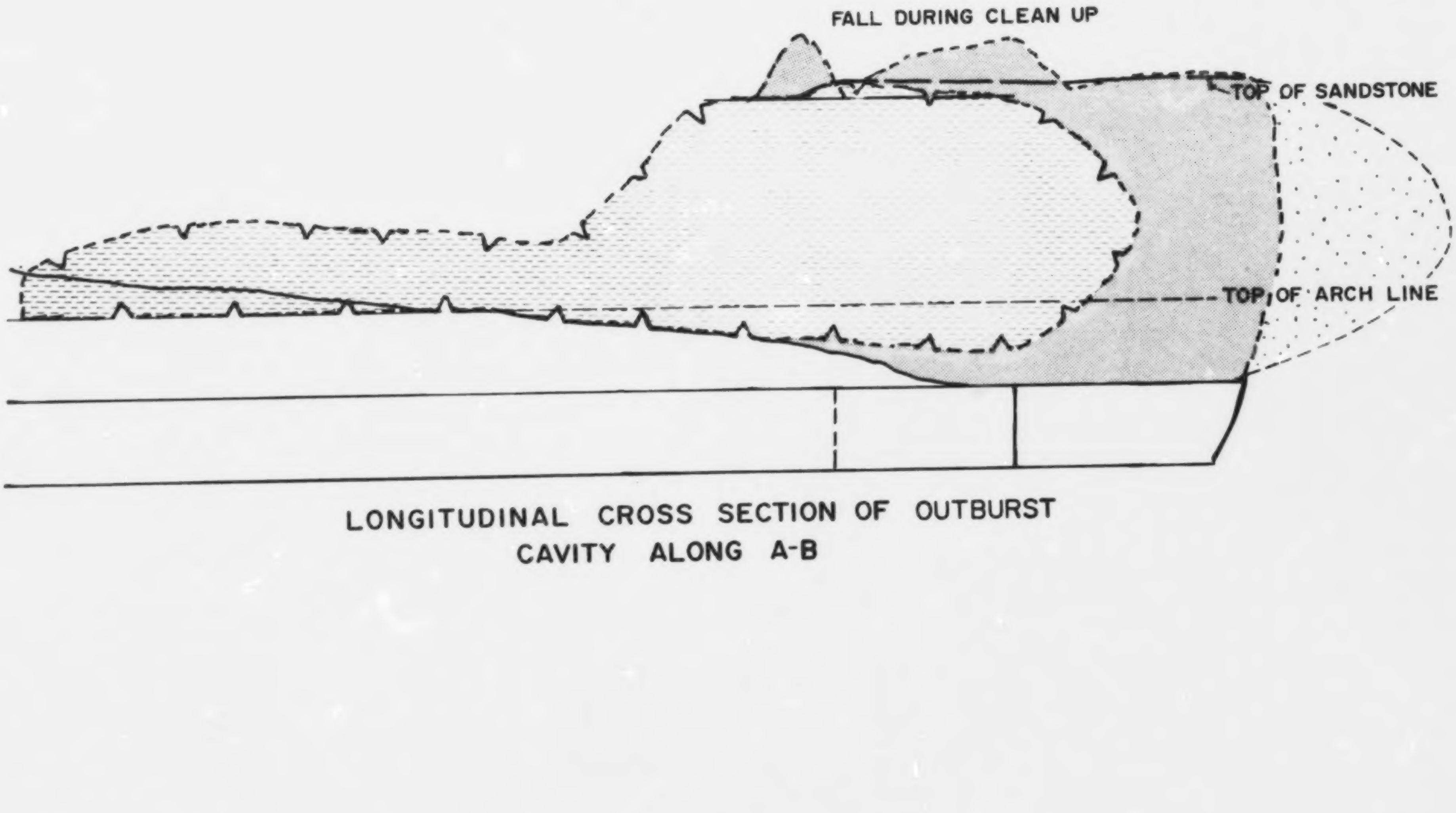
FALL DURING CLEAN UP
TOP OF SANDSTONE
TOP OF ARCH LINE

LONGITUDINAL CROSS SECTION OF OUTBURST CAVITY ALONG A-B

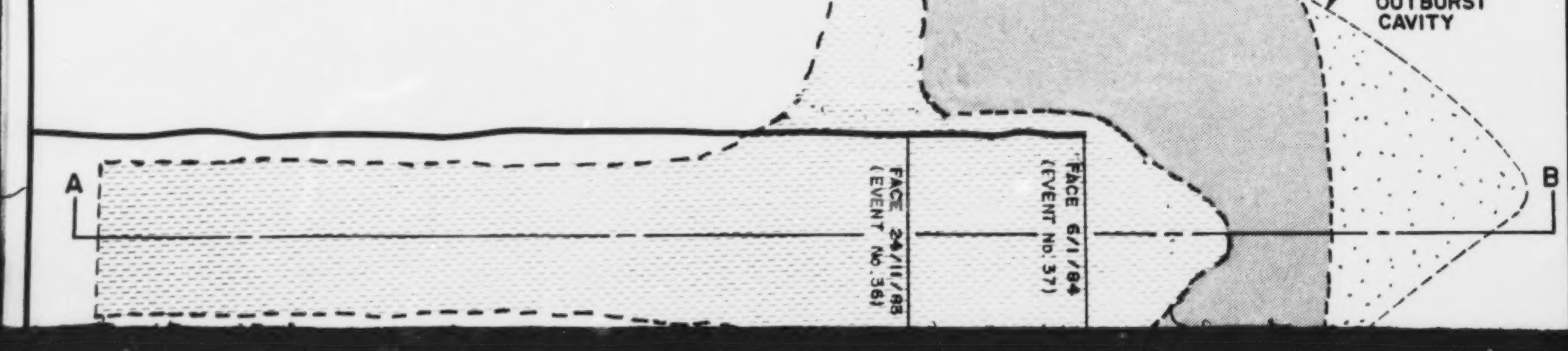
INFERRED
OUTLINE OF
OUTBURST
CAVITY
A
B
FACE 24/11/83
(EVENT No.36)
FACE 6/1/84
(EVENT No.37)

PROFILE OF OUTBURST CAVITIES AFTER EVENTS No. 36 AND 37, IN No. 26 COLLIERY SYDNEY COALFIELD

FIGURE 2.10

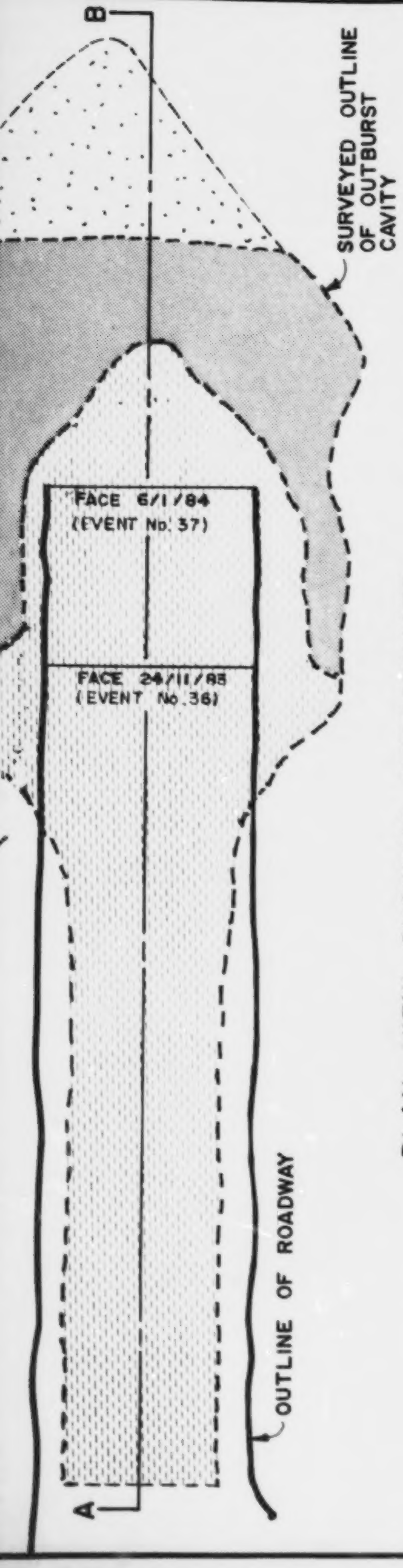
B
SURVEYED OUTLINE OF OUTBURST CAVITY
FACE 6/1/84 (EVENT No. 37)
FACE 24/11/83 (EVENT No. 36)
OUTLINE OF ROADWAY
A

PLAN VIEW SHOWING APPROXIMATE OUTLINE OF OUTBURST CAVITY

LEGEND

☐ CAVITY RESULTING FROM EVENT No. 36

☐ CAVITY RESULTING FROM EVENT No. 37

▨ INFERRED FRACTURE ZONE BEYOND FACE OF OUTBURST CAVITY

NOTE

THIS FIGURE IS BASED ON SURVEYED CROSS SECTIONS PROVIDED BY C.B.D.C. (PREPARED IN IMPERIAL SCALE)

SCALE : 1 INCH TO 10 FEET

Date: FEB. 24, 1987
Project: 861-1290

Golder Associates

Drawn: TMG
Chkd: -

831 - 1216 FIG 2.11 INVESTIGATIONS BOREHOLES

REFERENCE

CAPE BRETON DEVELOPMENT CORPORATION No. 26 COLLIERY PLAN SHOWING ABANDONMENT OF No. 26 COLLIERY AND PORTIONS OF RETURN AIRWAY 1-B. DRAWING No. 240-Q.

NOTE

1) BOREHOLES B162, B163 AND D164 WERE INVESTIGATION BOREHOLES DRILLED BY CBDC.
2) INSITU MEASUREMENT WAS CARRIED OUT BY GOLDER ASSOCIATES (REF. GOLDER ASSOCIATES REPORT No. 831-1216)

PLAN OF No. 26 COLLIERY AND LOCATIONS OF INVESTIGATION BOREHOLES

FIGURE 2.11

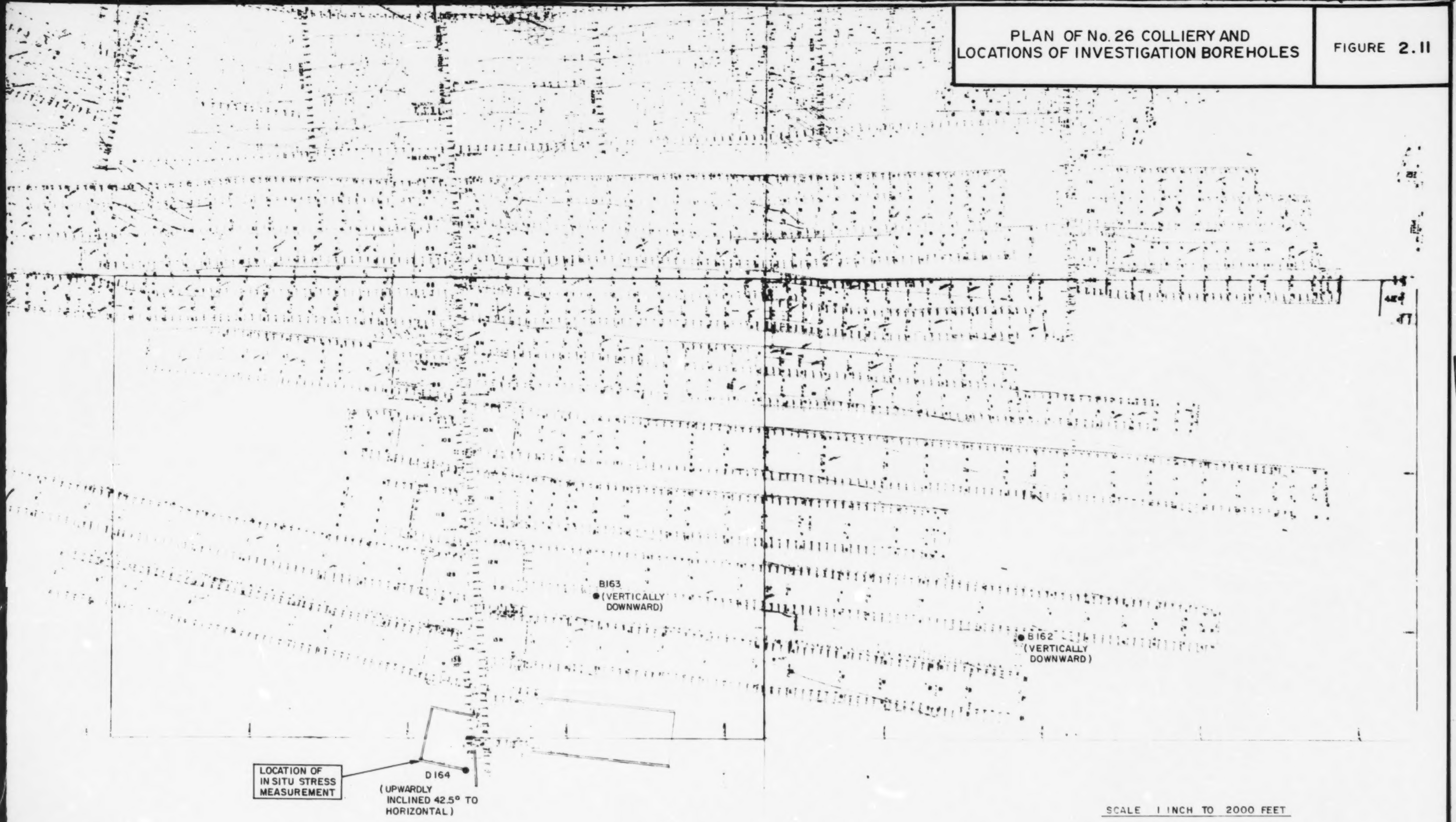
B163
(VERTICALLY DOWNWARD)
B162
(VERTICALLY DOWNWARD)
LOCATION OF IN SITU STRESS MEASUREMENT
D164
(UPWARDLY INCLINED 42.5° TO HORIZONTAL)

SCALE 1 INCH TO 2000 FEET

Date MARCH 30, 1987
Project 861-1290

Golder Associates

Drawn D. M.
Chkd

No. 26 COLLIERY
14 NORTH COAL ROAD

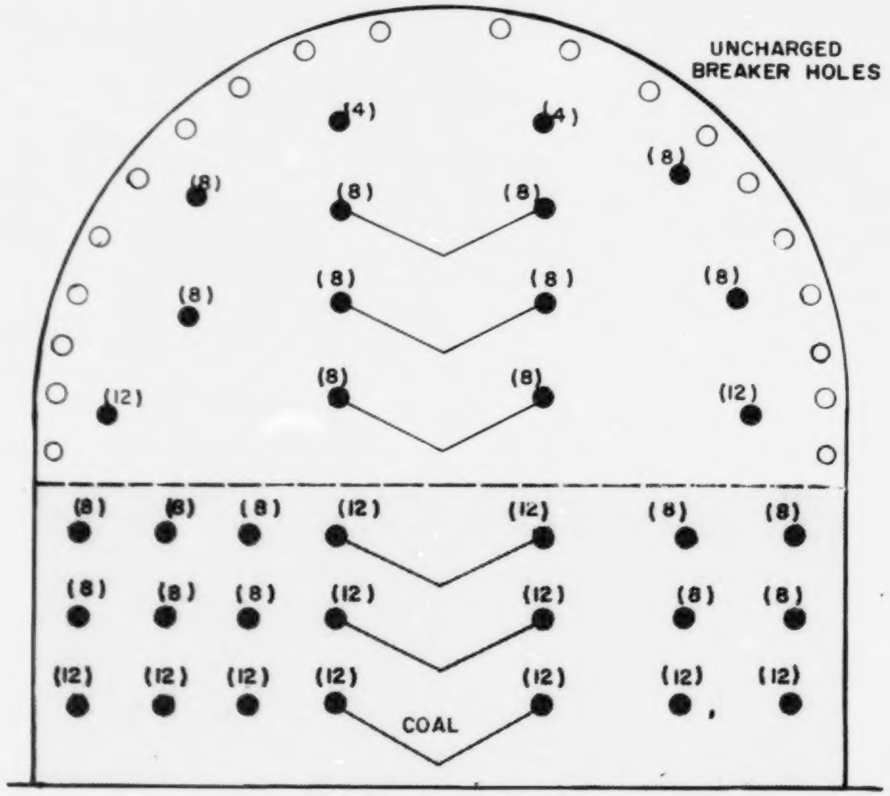
UNCHARGED BREAKER HOLES
(4)
(4)
(8)
(8)
(8)
(8)
(8)
(8)
(8)
(8)
(12)
(8)
(8)
(12)
(8)
(8)
(8)
(12)
(12)
(8)
(8)
(8)
(8)
(8)
(12)
(12)
(8)
(8)
(12)
(12)
(12)
(12)
(12)
(12)
(12)
COAL

(NOT DRAWN TO SCALE)

BLAST PATTERN REFERENCE No. 1

NOTES

o BORE BREAKER HOLES IN TOP BRUSHING.

o BORE COAL. SHOOT 'X' IN COAL FIRST. [illegible] SHOOT [illegible] COAL SEPARATE. (THIS CAN BE DONE DURING REGULAR SHIFT.

o BORE 'Y' IN STONE. THIS CAN ALSO BE SHOT DURING THE REGULAR SHIFT.

o BOTH WINGS IN STONE TO BE SHOT SEPARATELY BETWEEN SHIFTS.

No. 26 COLLIERY
13 NORTH BRUSHING FACE IN SANDSTONE

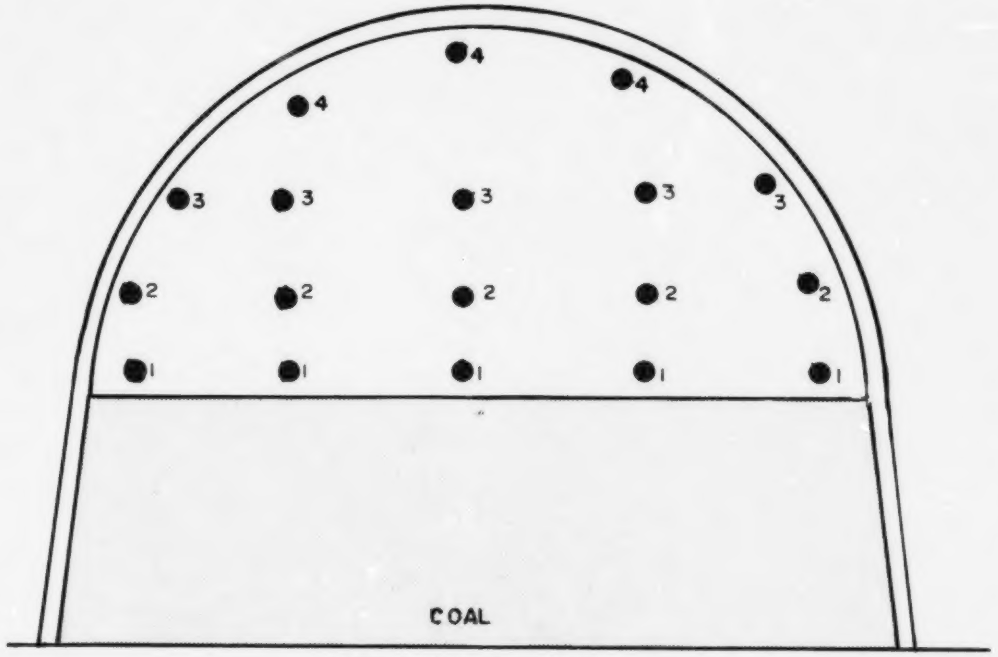
4
4
4
3
3
3
3
3
2
2
2
2
2
1
1
1
1
1
COAL

(NOT DRAWN TO SCALE)

BLAST PATTERN REFERENCE No. 2

NOTES

o HOLE LENGTH: 6 FT.

o HOLE SPACING: APPROX. 2 FT. HORIZONTAL
APPROX. 1.5 FT. VERTICAL

o AMOUNT OF EXPLOSIVE PER HOLE: 24 oz. OF MONOBEL S-1
(32 mm x 200 mm, 8 oz. CARTRIDGE)

o HOLES TO BE STEMMED 4 FT. WITH NON-COMBUSTIBLE MATERIAL
(DAMP CLAY)

No. 26
13 SOU

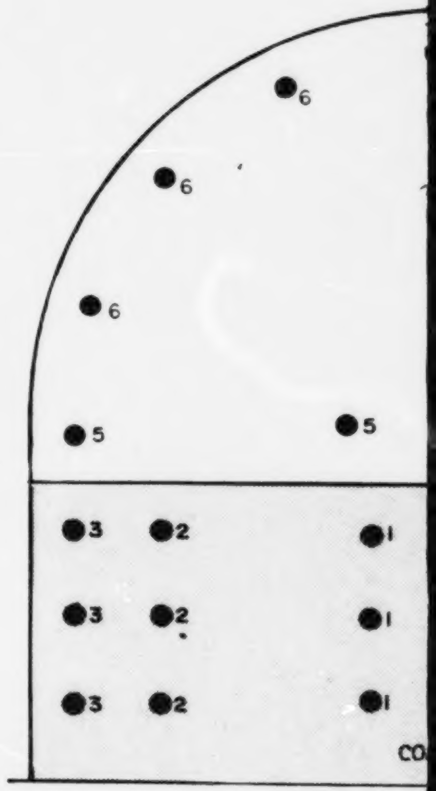
6
6
6
5
5
3
2
1
3
2
1
3
2
1
CO

(NOT DRAWN

BLAST PATTERN

NOTES

o HOLE LENGTH: IN C
IN S

o HOLE SPACING: IN C
IN S

o AMOUNT OF EXPLOSIVE

BLAST PATTERNS USED AT No.26 COLLIERY

FIGURE 2.12

LEGEND

●^{3} CHARGED HOLE AND DELAY NUMBER

●$^{(8)}$ CHARGED HOLE AND AMOUNT OF EXPLOSIVE IN OUNCES

REFERENCE

REFERENCE BLAST PATTERNS WERE PROVIDED BY CBDC

No.26 COLLIERY
13 NORTH BRUSHING FACE
IN SANDSTONE

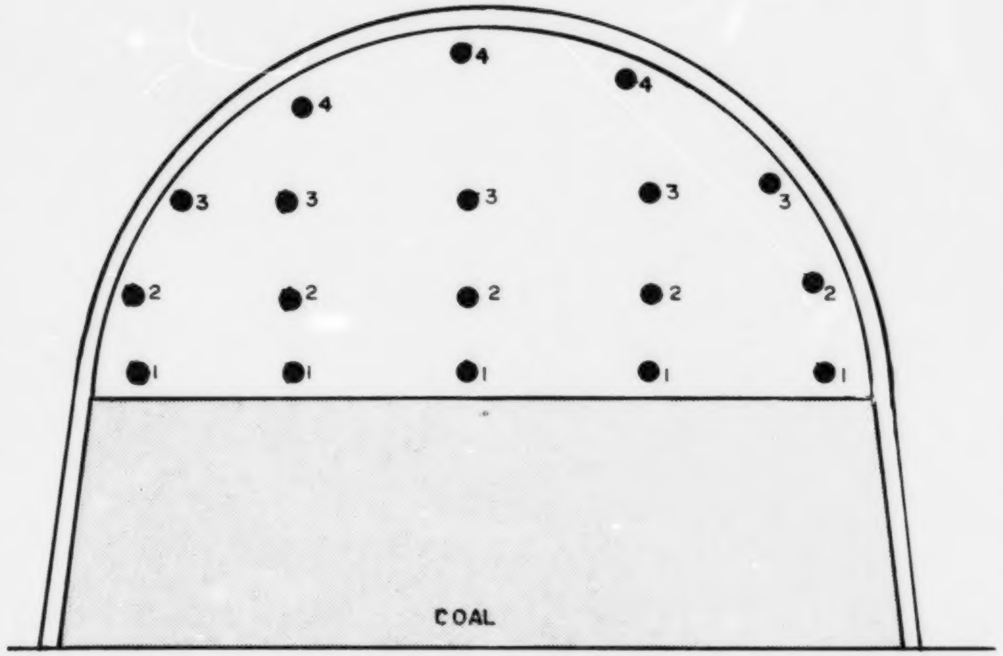

(NOT DRAWN TO SCALE)

BLAST PATTERN REFERENCE No. 2

NOTES

- HOLE LENGTH: 6 FT.
- HOLE SPACING: APPROX. 2 FT. HORIZONTAL
  APPROX. 1.5 FT. VERTICAL
- AMOUNT OF EXPLOSIVE PER HOLE: 24 oz. OF MONOBEL S-1
  (32 mm x 200 mm, 8 oz. CARTRIDGE)
- HOLES TO BE STEMMED 4 FT. WITH NON-COMBUSTIBLE MATERIAL
  (DAMP CLAY)

No. 26 COLLIERY
13 SOUTH AIRWAY

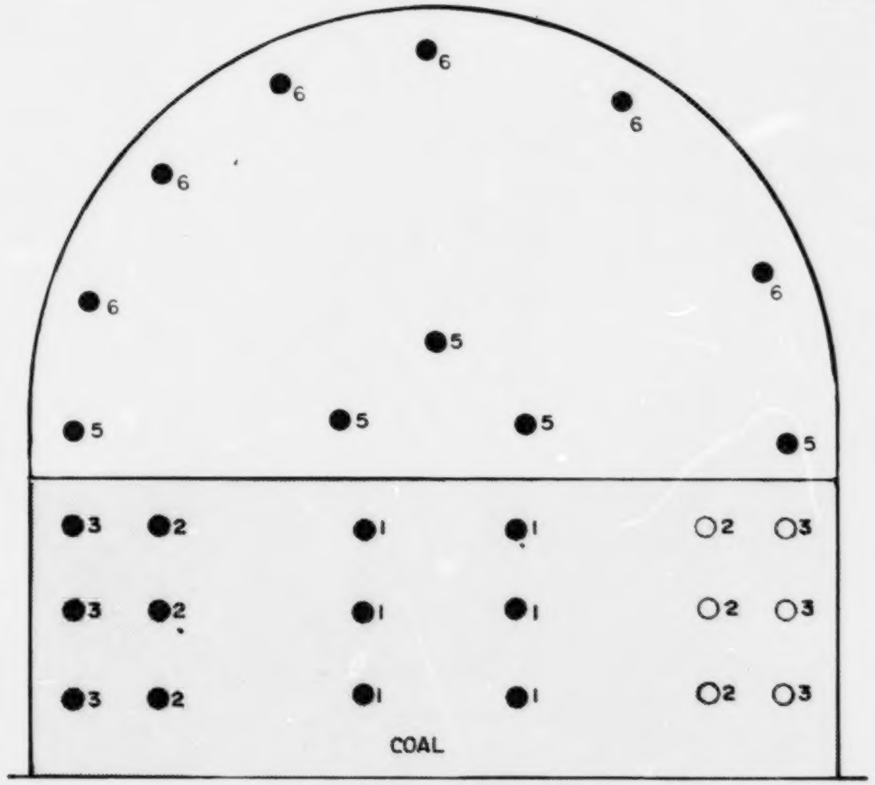

(NOT DRAWN TO SCALE)

BLAST PATTERN REFERENCE No. 3

NOTES

- HOLE LENGTH: IN COAL 4.5 FT.
  IN STONE 4.0 FT.
- HOLE SPACING: IN COAL 2 FT. (6' FROM RIB)
  IN STONE 2 FT. (8' FROM RIB)
- AMOUNT OF EXPLOSIVE PER HOLE: 16 oz. OF MONOBEL S-1

Date FEB. 23, 1987
Project 861-1290

Golder Associates

Drawn TMG
Chkd

VOLUME OF MATERIAL EJECTED AND ARCHES DAMAGED DURING ROCK AND GAS OUTBURSTS IN No.26 COLLIERY

(AFTER ASTON AND CAIN, (1985))

FIGURE 2.14

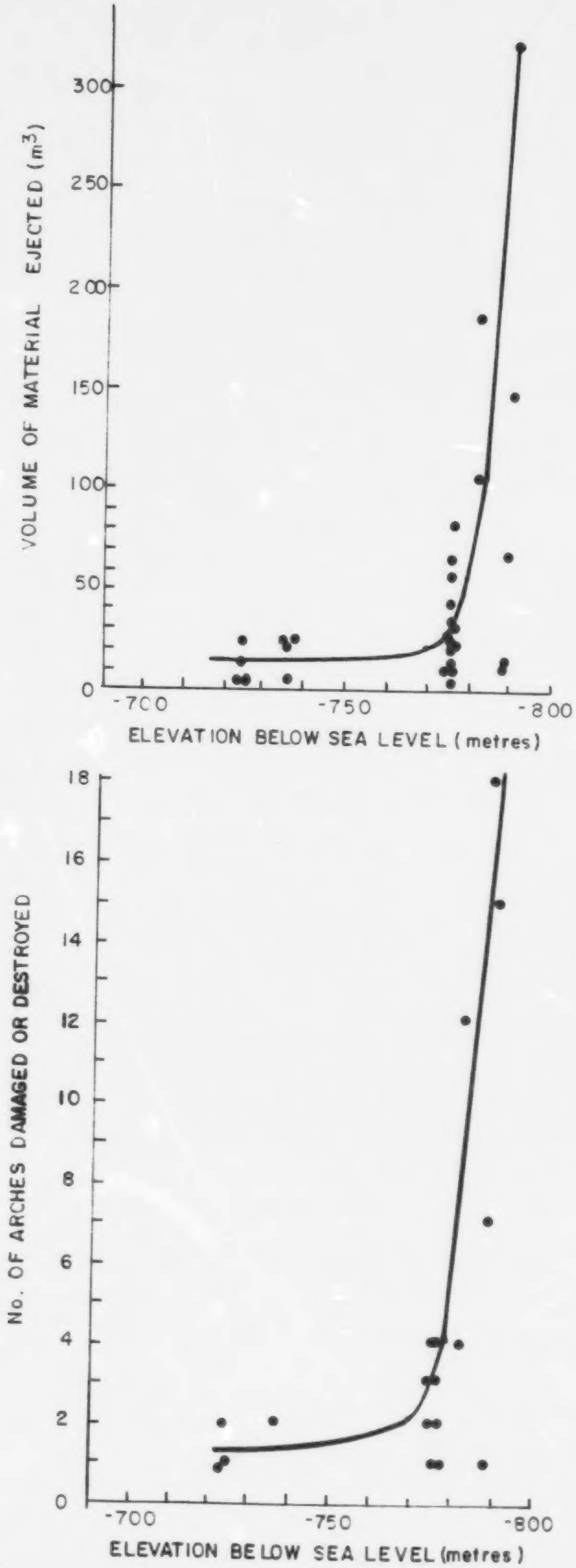

Date FEB 3,1987

Project 861-1290

Golder Associates

Drawn C. M

Chkd

EXTENT OF DEVELOPMENT AND MINING ACTIVITIES AT THE TIME OF DRIVING 13 N. AIRWAY THROUGH CHANNEL SANDSTONE

FIGURE 2.15

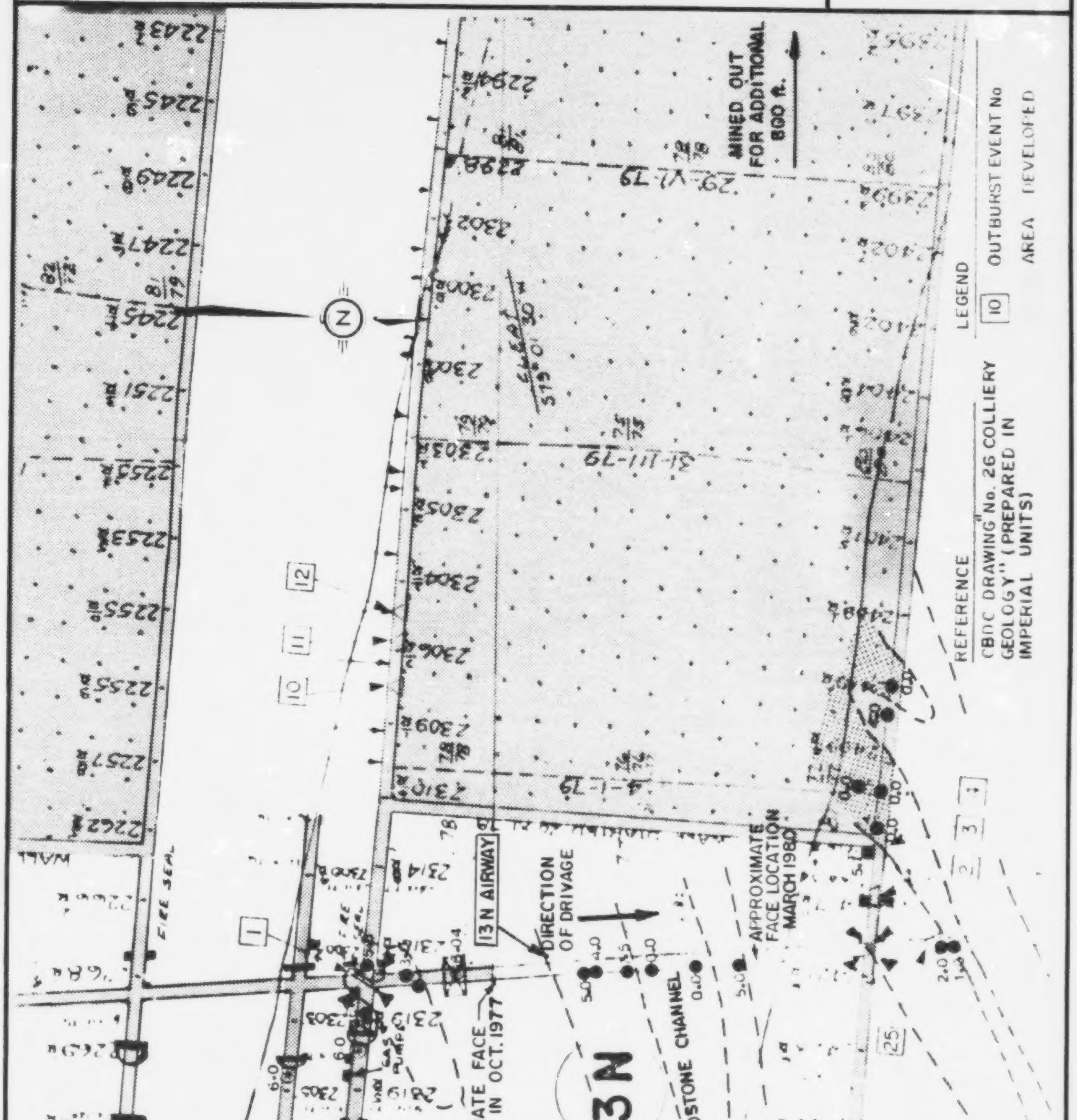
MINED OUT FOR ADDITIONAL 800 ft.
29-VI-79
31-III-79
4-I-79
N
12
11
10
1
25
2
3
4
FIRE SEAL
13 N AIRWAY
DIRECTION OF DRIVAGE
APPROXIMATE FACE LOCATION IN OCT. 1977
APPROXIMATE FACE LOCATION MARCH 1980
SANDSTONE CHANNEL
13 N
GAS PUMP
LEGEND
10 OUTBURST EVENT No
AREA DEVELOPED
REFERENCE
"CBDC DRAWING No. 26 COLLIERY GEOLOGY" (PREPARED IN IMPERIAL UNITS)

Date MARCH 31, 1987
Project 861-1290

Golder Associates

Drawn D. M.
Chkd

Form GA-D-4m (metric)
FORM PRODUCED JUNE 1986

EXTENT OF DEVELOPMENT AND MINING ACTIVITIES AT THE TIME OF DRIVING 14N AIRWAY THROUGH CHANNEL SANDSTONE

FIGURE 2.16

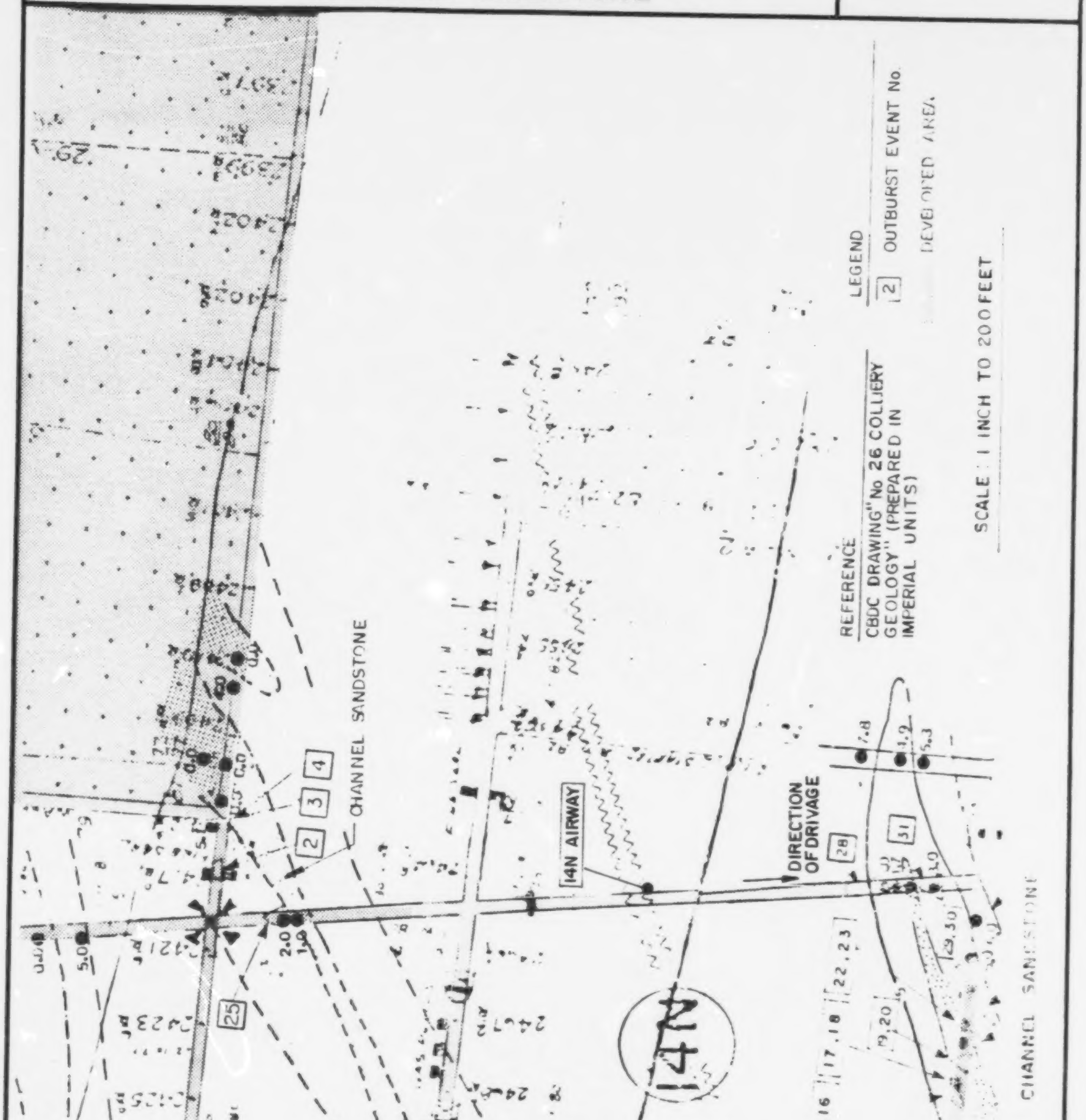
LEGEND
[2] OUTBURST EVENT No.
DEVELOPED AREA
REFERENCE
CBDC DRAWING" No 26 COLLIERY GEOLOGY" (PREPARED IN IMPERIAL UNITS)
SCALE: 1 INCH TO 200 FEET
CHANNEL SANDSTONE
14N AIRWAY
DIRECTION OF DRIVAGE
14N
2
3
4
25
28
31
17,18
22,23
15,16
9,20
29,30
CHANNEL SANDSTONE

Date MARCH 30,1987

Project 861-1290

Golder Associates

Drawn D M.

Chkd

3. REVIEW OF ROCK AND GAS OUTBURST CASE HISTORIES

Dynamic events occurring in the course of underground mining can be classified according to the following definitions:

- Seismic events: sudden movement resulting from a release of strain energy in the earth.
- Rock Burst: seismic events that cause damage in underground workings. The associated rock failure results from overstressing. The seismic energy released from the rock burst is sufficiently large to cause violent expulsion of the surrounding rock mass. These events, which generally occur in hard rock environment are not associated with gas emission.
- Outburst of coal and gas: spontaneous ejection of coal and large quantities of gas (gases) from the solid coal where the ejected material is finely communited and pneumatically transported.
- Rock and gas outbursts: sudden ejection of rock and gas generally associated with shotfiring and often characterized by the emission of a large quantity of gas, the fine communition of the ejected material and the pneumatic transport of fragments; this type of outbursts often occur in coal and salt mines when mining has reached some critical depth.

There are pronounced similarities between coal and gas and rock and gas outbursts, in particular with respect to the conditions leading to the events and the mechanisms of material fracturing and ejection. This section presents a review of the case histories of outbursts of rock and gas(es) documented in the literature worldwide including a wide spectrum of events in various rock types and the observed characteristics in each case. The purpose of the review is to identify the characteristics common to these events.

3.1 Case Histories of Rock and Gas Outbursts in Coal Mines

3.1.1 Horonai Coal Mine, Japan

REF: Watanabe, et al, (1981)

Since 1975, when a gas explosion followed a rock and gas outburst, the phenomenon has become a serious problem in this Japanese Colliery. Generally, these events occurred immediately after blasting in a particular sandstone seam.

The seam dips at 25° and overlies a 0.8 m thick coarse-grained sandstone and a 2.0 m thick medium-grained sandstone. Above the seam is a sandy shale bed while the lower sandstone is underlain by a shale strata. The uniaxial compressive strength and porosity of the coarse-grained sandstone are 77 MPa and 5% while those of the medium-grained sandstone are 108 MPa and 2% respectively. The overall gas pressure, back-calculated from gas and rock volume measurements in events involving both seams simultaneously, was approximately 6.5 MPa. The gas involved was methane.

3.1.2 Dombass (Donetz) Basin, USSR

REF: Karagodin et al, (1983)
Belin, J., (1981)

This area has experienced rock and gas outbursts since 1950. The events started when the depth of the coal workings reached 700 m. Each event was initiated by blasting. Rock ejections (220 tonnes/ ejection on average but up to 3500 tonnes) accompanied by large quantities of gas (CH_4) were numerous. The resulting cavities ranged between 10 to 15 m in height.

As of January 1983, over 3400 rock and gas outbursts have occurred in 22 mines, in which 174 outburst-prone sandstone strata were delineated, mainly by core discing.

The rock most frequently found to present an outburst hazard are alluvial sandstone, sandstones from underwater river drifts and off-shore sandstones.

3.1.3 Soko Basin, Yugoslavia

REF: Jovanovic et al, (1979)

This coal mine experienced both coal outbursts and rock and gas outbursts. The coal outbursts occurred in the faulted zones of the coal seam. The sandstone and gas outbursts occurred in development roadways for a new production zone. The events were associated with blasting and the gases involved were methane, carbon dioxide and nitrogen. Gas pressure was determined to be approximately 17 MPa with a sandstone strength and porosity of 100 MPa and 4.4% respectively.

3.1.4 Nowa Ruda Mine, Poland

REF: Kozlowski and Kalisz, (1981)

As of 1981, there had been only 2 outbursts of rock and carbon dioxide in Poland, but they were very powerful.

The events took place at a depth of 550 m in an exploratory cross-cut driven toward an old mined-out field. Gas pressure measured in boreholes drilled along the axis of the heading to a depth of about 20 m showed a gas pressure of 3.9 MPa. While blasting the face there was an outburst of sandstone and gas (1840 tonnes of rock with 20000 m^3 of carbon dioxide). Arched supports were destroyed along more than 80m of the roadway from the face. When the drivage resumed, a second outburst (1300 tonnes of rock and 13000 m^3 of CO_2) took place after an additional 11 m of advance.

The outbursts occurred in sandstone which was an arkosic light grey rock with feldspar, psammitic structure (grain size up to 2 mm). The strength of sandstone was in the low to medium range but the porosity and gasiness were high.

3.1.5 Merlebach Colliery, France

REF: Revalor et al, (1985)
Josien et al, (1982)

Six sandstone and gas outbursts occurred in this colliery at a depth of 1250 m during the drivage of an accessway in virgin ground. Two more outbursts occurred in 1986. These bursts were predicted by core discing from advance drilling. The onset of the phenomena were found to be initiated by blasting. Seismo-acoustic recordings have shown that the events were coincidental with the last delay and died away in 1 to 3 seconds. In each event, a total volume of rock ranging between 1500 to 3000 m^3 was broken (as opposed to 60 - 80 m^3 for regular blasts) and as much as 500 m^3 was ejected as far as 50 m away from the face. The fragmentation of the sandstone was intergranular, resulting in small platy pieces of several centimeters in thickness. The gas emitted was methane in volumes ranging from 6000 to 8000 m^3. Gas pressure was estimated to lie between 3 and 10 MPa.

The sandstone strata intersected by the access way dipped 60° although in the area where the events took place it shows substantial variability. The uniaxial compressive strength and elastic modulus of the sandstone were 89 MPa and 20.7 GPa respectively. In situ stress measurements indicated horizontal stresses of 34.5 MPa normal to the axis of drivage, 17.5 MPa in the direction of advance and a vertical stress of 27.5 MPa. There was correlation between the angle of incidence of the major horizontal stress, the direction of drivage and the occurrence of outbursts.

3.1.6 Ibbenburen Colliery, West Germany

REF: Paul (1983)

In West Germany, sandstone-methane bursts were limited to the Ibbenburen colliery where anthracite coal is mined.

The No. 2 seam in the mine is overlain by a layer of argillaceous shale 1.6 m in thickness which is in turn overlain by a bed of sandstone 13.5 m thick. The first outburst incident in the mine was initiated by blasting. A dome-like cavity of elliptical cross-section (dia. 0.5-3.0 m) of several meters in height broke out of the roof, primarily under the influence of gravity. The walls of the cavity were smooth. Small amounts of methane were released.

A series of major events took place subsequently. On one occasion, 530 tonnes of rock was ejected along with 1400 m^3 of methane. The cavity ran into the rock perpendicular to the stratification. The walls exhibited clear evidence of pressure relief exfoliation. The rock was expelled into the heading and was reduced in size of less than 10 mm. Six meters further into the heading, a second outburst took place ejecting about 400 tonnes of rock and 1100 m^3 of methane.

Outbursts of sandstone and gas also occurred in other sandstone beds in the mine.

On one occasion, a 6 m dia. shaft was advanced through a bed of sandstone already identified as prone to outbursts. Although drilling was undertaken through a pilot hole 1.4 m in diameter, eight small outbursts took place over a period of 1 month in the 10 m section of the sandstone bed, 150 tonnes of rock was ejected with gas volume ranging between 50 to 1000 m^3. It was believed that the weight of the drilling equipment prevented the ejection of larger quantity of rock.

All cores drilled from holes ranging from 48 to 200 mm diameter exhibited clear pressure relief exfoliation of the cores in the area of burst-prone sandstone zones. The cores broke up into discs of 5 to 50 mm thick with the convex surfaces of the discs facing in the direction of drilling.

3.2 Case Histories of Rock and Gas Outbursts in Salt and Potash Mines

3.2.1 Louisiana Salt Mines, USA

REF: Mahtab (1982)

Outbursts of salt rock and gas have accompanied routine blasting in some areas of the mines producing cavities up to 30 m in diameter and up to 50 m in length (height). The gas ejected was methane.

As many as five salt mines in Louisiana have experienced this phenomenon. It generally occurred between 200 and 400 m depth and at the top corners and faces of rooms or in the roof. The cavities were elliptical to circular with conspicuous scale-like fissures at the periphery.

Geological investigations have shown that there was good correlation between shear zones containing pressurized gas and the occurrence of rock and gas outbursts (Table 3.1).

3.2.2 Werra Potash Mines, GDR

REF: Gimm et al, (1976)
Gimm and Pforr, (1964)

In the potash mining district of Werra more than 10,000 outbursts of rock and gas have occurred, threatening the very existence of the mines.

Outbursts of salt and gas were initiated by the blasting process. There were 10 ejections of more than 10,000 tonnes of salt (100,000 tonnes in one occasion). The gas involved was carbon dioxide in sylvinite rock although nitrogen was present in carnalite rocks.

Research studies have shown that 90% of all bursts occurred within a radius of 70 m of the fault zones. The outbursts were limited to eruption-prone horizons where CO_2 concentration ranges between 7 to 8 m^3 per tonnes of salt (gas pressure up to 0.4 MPa). However, it was noted from the records that in order to initiate an event, a relatively large free surface of the horizon must be exposed at a sufficiently rapid rate by mining. The fracturing process took place along curved surfaces at the edge of the cavity. The broken salt could be projected up to several hundred meters. The outbursts generally choked themselves and a thin de-gassed protective layer was then formed along the edges of the cavity.

To bring into perspective the energy involved during these events, the following incident is very illustrative:

It occurred on February 9, 1975, at the Marx-Engels Mine, while a 280 mm diameter hole was being drilled using a drill jumbo, an outburst was initiated, ejecting about 8000 tonnes of salt into the heading. The drill jumbo, weighing 11.3 tonnes, was displaced 145 m.

Discing was observed in the core obtained from drillholes within the zone where outbursts occurred during subsquent mining. The discs were curved and the curve was always symmetrical about the drill hole axis with the centre of the curve on the collar end of the drillhole.

3.2.3 Sudharz Potash Field, GDR
REF: World Mining, (1967)

Outburst of salt and rocks were known in this area since 1950 although they were much smaller in magnitude than those in the Werra district. Most of the outbursts were in the potash beds and the gases were CH_4, N_2 and CO_2.

3.3 Other Case Histories of Rock and Gas Outbursts

3.3.1 Sangerhausen and Mansfeld copper-slate mining district, GDR

REF: World Mining, (1967)

In both districts, outbursts of sandstone and gas were experienced. There were up to 20 ejections of over 100 tonnes of rock resulting in many fatalities. The largest one involved about 1500 tonnes of material. The outbursts were confined to certain sandstone horizons and took place during blasting. The gas involved was nitrogen. In both districts, there has been a correlation between the occurrence of the events and marked zones of tectonic deformation.

3.3.2 Other Case Histories

The cases presented below are based on the work of Belin (1981).

a) An ejection occurred at a depth of 180 m in a pilot heading passing through two faults to penetrate a conglomerate sandstone during the construction of a hydroelectric project. Blasting was followed by the ejection of 400 m^3 of solid material, of remarkable fineness, and 120,000 m^3 of methane, of which 35,000 m^3 were given off in the first 2 hours. Gas continued to emit for some years from one of the fissures exposed.

b) In the Cevennes coalfield 1,656 tonnes of shale were expelled on May 10, 1969 at a depth of 650 m in the Destival mine after firing of a round of shots to negotiate 4 m of faulted rock at the mica schist/carboniferous contact.

The expulsion of about 1,650 tonnes of rock resulted in a chimney-like cavity with a cross-sectional area 1-2 sq.m, just as if a "pocket of fault rock" had emptied itself through this hole. The gas involved was CO_2.

c) In the same coalfield at the St. Martin mine, 6000 tonnes of rock together with CO_2 was ejected on August 17, 1931 when sinking of the Famel shaft reached a depth of 380 m, at a distance of 10 m from the mica schist. The shaft was entering a zone of contact rocks described as "friable shales and faulted stuff". Fine dust was projected as far as the surface.

d) A delayed ejection of rock and gas occurred in the same zone adjacent to the crystalline mica schist base.

On July 26, 1942, 832 tonnes of rock were ejected over 170 m of roadway. After the event had subsided, it was observed that the ejected material consisted of shales which were finely powdered in the first few metres at the toe of the pile and then became coarser and were mixed with blocks of increasing size as one moved nearer to the face.

Prior to the event, the drivage had been stopped for seven days because of poor ground. After resetting the supports, four shots were fired on the Saturday evening to widen the heading; the ejection described above took place on the Sunday.

3.4 Summary and Discussion

The relevant information gathered from most of these case histories, together with other published data on similar events are summarized in Table 3.2.

Several parameters common to the rock and gas outbursts have emerged from the review and they are discussed below.

a) At Merlebach, Horonai and No. 26 Collieries, there was marked variations in the intensity of the events in the same horizon; from none to a total outburst at only a few tens of meter away.

b) At Ibbenburen and Nova Ruda mines and No. 26 Colliery, a second outburst occurred just after resuming drivage following a major outburst of rock and gas.

c) Most of the events occurred in development headings (in virgin ground) excavated by drill and blast method. Outbursts in sandstone were generally triggered by shotfiring.

d) At Merlebach and Horonai Collieries and Werra Potash mines, seismo-acoustic emission monitoring showed that outbursts started during the shot firing itself or immediately afterwards. In the potash mines, it takes the form of a chain reaction in which a rise and fall in intensity can be observed (Figure 3.1). A typical event shows three phases in a period of 145 seconds. At Merlebach, it was found that the process lasted between 60 and 180 seconds. In Japan, acoustic emission monitoring has shown that in one instance the outburst started 150 milliseconds after blasting whereas in an other event, it triggered simultaneously with the last delay.

e) Based on the data reviewed, there is a general trend indicating that events involving carbon dioxide as outburst gas were more intense than the ones involving methane which in turn were more intense than the cases in which nitrogen was involved.

f) In Louisiana salt mines, a correlation exists between the proximity of shear zones and the occurrence of outbursts. In potash mines, 90% of all outbursts occurred within a radius of 70 m of fault zones. In the events reported by Belin (1981) fault zones or contacts were involved.

g) In sandstone and gas outbursts, a particular strata is generally involved with no correlation with structural features although in the Mansfeld and Sangerhausen districts, a correlation exists between events and zones of tectonic deformation.

In the Sydney Coalfield, the presence of slickensided surfaces at the interface of the sandstone channels and the siltstone are indicative of previous shear movements.

h) Outburst cavities were similar in shape, being in the form of a cone, and the presence of scale-like fracture surfaces over the outburst cavity was always noted. The expelled material was generally in flaky fragments and ejected to a considerable distance from the face.

TABLE 3.1

SUMMARY DESCRIPTION OF GEOLOGIC FEATURES ASSOCIATED WITH ROCK AND GAS OUTBURSTS IN LOUISIANA SALT MINES

(after Mahtab (1982))

Mine	Depth of Mining Levels	Inclusions	Anomalous (or shear) Zones	Depth of Outbursts	Remarks
Winnfeld (not operating)	Sublevel, at 190 m (620 ft.) flooded Main level 250 m (820 ft.)	Brine, CO_2 10% anhydrite	Not penetrated or recorded	200-240 m (650-790 ft.)	Five outbursts or "blowouts" all within 150 m of the edge of the dome
Jefferson Island (flooded, 1980)	Four levels, deepest at 450 m (1480 ft.)	Some sediment, brine, and gas	At edge and in centre of dome	350-400 m (1150-1300 ft.)	Several large outbursts near edge of shear zone
Avery Island	Three levels, deepest at 275 m (900 ft.)	Sandstone and brine	In centre of dome		No outbursts
Weeks Island	Two levels, at 150 m and 250 m (490 ft. and 820 ft.)	Sediments, some brine and oil, gas	At edge and in centre of dome	220-240 m (720-790 ft.)	Small to medium size outbursts in shear zones
Cote Blanche Island	One level, at 375 m (1230 ft.)	Sandstone, gas black clay	Not detected at edge or in centre, but two sediment-bearing, thin, and persistent zones	360-370 m (1180-1210 ft.	Medium size outbursts follow clay-bearing salt
Belle Isle	One level, at 425 m (1390 ft.)	Clay-lime sediment, brine, gas	At edge and in centre of dome	390-420 m (1280-1380 ft.	Several large outbursts associated with the central shear zone

MINE LOCATION AUTHORS, PAPER	TYPE OF MATERIAL	NUMBER OF EVENTS	DEPTH	MAXIMUM MAGNITUDE OF EVENT	TYPE OF OPENINGS	DIP	COAL MEASURES PROPERTIES	FAULTING, STRUCTURES AND STRESS	GAS PRESSURE, AND TYPE
1 Leichhardt Colliery Central Queensland (Australia) Moore, R.D.; Hanes, J. (1980)	COAL Gemini Seam 6 m	1974 - 1978 >200	400 m	3 large bursts displaced more than 300 tonnes of coal + stone	development headings, machine driven	3°	lithic sandstone, shale, siltstone } 15 m to 39 m most of sandstone=paleoriver channel	numerous faults with throw <10 m 2 faults with throw >10 m slickenside planes, cleating associated with cleat/induce fractures	16 m^3 methane/t. coal with ± 15% CO_2
2 Werra Potash Mines German Democratic Republic Gimm, W., Hafner, H.R., Marggraf, P. (1976)	POTASH	>10000		100000 tonnes ejected numerous > 10000 tonnes	in stopes + development headings, shotfiring		Carnallitite	90% of outburst at distance <70 m from faults	CO_2 7-8 m^3/t N_2
3 Nowa Ruda Mine Poland Kozlowski, B., Kalisz, E. (1982)	SANDSTONE	2	550 m	1840 tonnes with 20000 m^3 CO_2 1300 tonnes with 13000 m^3 CO_2	development heading; shotfiring		Burst material: arkosic light grey sandstone, grain size up to 2 mm, strength low-medium, porosity = 6.66% gassiness = high		CO_2 0.3 - 3.4 atm -(1) 6 atm - 40 atm -(2)
4 Ibbenburen Colliery Seam #2, FRG Paul, K. (1982)	SANDSTONE	Numerous	600 m and deeper	530t, 1400 m^3 CH_4 400t, 1100 m^3 CH_4 1570t. 400 m^3 CH_4	development headings drill & blast and machine shaft sinking		Low strength, porosity 10-14%, permeability=v.low sandstone 13 - 14 m above shale argillaceous shale 1.6 m above coal	burst occurred outside fault zones core discing occured in burst prone sandstone	CH_4 6 MPa
5 Horonai Coal Mine Hokkaido, Japan Watanabe, Y., et al (1981)	SANDSTONE (2 beds)	>20	1055 m	400 m^3 rock 1750 m^3 gas	headings 18.5 m^2 face drill & blast	25°	σ_c = 78 MPa porosity = 5% 0.8 m thick σ_c = 108 MPa porosity = 2% 2.0 m thick		Fire damp (CH_4)
6 Louisiana Salt Mines Louisiana, U.S.A. Mahtab, A. (1982)	SALT	Numerous	200 - 400 m	>10000 tonnes salt	drill & blast 63 ft. wide 22 ft. high rooms		impervious salt	associated with shear zones, edges of dome, etc.	CH_4
7 Australian Coal Mines Sidney & Bowen Basins Shepherd, J., et al (1984)	COAL	>372	350 - 500 m	Avg. 32 tonnes coal West Cliff Colliery	development headings			vicinity of faults, dykes roof rolls, etc.	CH_4 2.67 MPa CO_2
8 Merlebach Colliery Lorraine Collieries, France Revalor, R., et al (1985) Josien, et al (1982)	SANDSTONE	6	1250 m	1500-3000 tonnes 6-8000 m^3 CH_4	development headings, drill & blast	65° - 50°	sandstone σ_c = 89 MPa E = 20.7 GPa	highly anisotropic stresses	CH_4 3 - 10 MPa
9 Donets Coal Basin U.S.S.R. Airuni, A.T., et al (1976)	COAL & GAS AND SANDSTONE & GAS	3000 3000	500 - 700 m		development headings + stopes				
10 Donbass Coalfield U.S.S.R. Karagodin, L., et al (1983)	SANDSTONE 174 beds in 22 mines	>3400	>700 m	3500 tonnes	development headings, drill & blast and machine boring		sandstone porosity = 12.1%	core discing occurred in outburst prone sandstone	CH_4, CO_2, N_2 4.4 m^3/m^3 sandstone
11 Soko Coalfield Yugoslavia Jovanovic, G., et al (1979)	SANDSTONE	FEW		184 tonnes	development headings, drill & blast		sandstone U.C.S. = 100 MPa porosity = 4.4%	associated with fault zones in coal-gas outburst	

BRIEF SU

DIP	COAL MEASURES PROPERTIES	FAULTING, STRUCTURES AND STRESS	GAS PRESSURE, AND TYPE	DESCRIPTION OF CAVITY	SOLUTIONS	SEISMIC MONITORING
3°	lithic sandstone, shale, siltstone } 15 m to 39 m most of sandstone=paleoriver channel	numerous faults with throw <10 m 2 faults with throw >10 m slickenside planes, cleating associated with cleat/induce fractures	16 m^3 methane/t. coal with ± 15% CO_2	· mostly conical, intense cleavage · heavily fractured, bulged boundaries · when elliptical section developed, their short axis, in horizontal plane, is parallel to σ_1	development headings are now drilled and blasted	
	Carnallitite	90% of outburst at distance <70 m from faults	CO_2 7-8 m^3/t N_2	· triggered by blasting · one event initiated by boring 280 mm hole	· monitoring CO_2 · Regional Geology Pronostics · core drilling, gas pressure measurements	Yes
	Burst material: arkosic light grey sandstone, grain size up to 2 mm, strength low-medium, porosity = 6.66% gassiness = high		CO_2 0.3 - 3.4 atm -(1) 6 atm - 40 atm -(2)	· 80 m of arched supports destroyed · damage to pipes, ventilation and mining equipment · event occurred with shotfiring · cored sample from cavity: 480 microfissure/m	Provocative blasting charge = 130% remote drilling Protective barrier	
	Low strength, porosity 10-14%, permeability=v.low sandstone 13 - 14 m above shale argillaceous shale 1.6 m above coal	burst occurred outside fault zones core discing occured in burst prone sandstone	CH_4 6 MPa	· following blasting · dome like, elliptical = 0.5 - 3 m - height = several metres · size of fragment <10 mm · pressure relief ex-foliation	core discing drift in footwall, increase distance to sandstone	
25°	σ_c = 78 MPa porosity = 5% 0.8 m thick σ_c = 108 MPa porosity = 2% 2.0 m thick		Fire damp (CH_4)	· immediately after blasting	AE monitoring	Yes
	impervious salt	associated with shear zones, edges of dome, etc.	CH_4	· semi-ellipsoidal with axial length up to 50 m, diameter up to 30 m · thin bed separation, scale-like fissures · immediately after blasting		
		vicinity of faults, dykes roof rolls, etc.	CH_4 2.67 MPa CO_2	· conical cavities		
65° - 50°	sandstone σ_c = 89 MPa E = 20.7 GPa	highly anisotropic stresses	CH_4 3 - 10 MPa	· small platy pieces, flaky walls · intra-granular fractures · conical opening · immediately after shotfiring		Yes
				· in development heading 2 to 2.5 times more forceful than in exploitation headings · in sandstone at shotfiring	· shock-shooting · core discing · careful blast design (elliptical shape) · destressing	
	sandstone porosity = 12.1%	core discing occurred in outburst prone sandstone	CH_4, CO_2, N_2 4.4 m^3/m^3 sandstone	· initiated by shotfiring		
	sandstone U.C.S. = 100 MPa porosity = 4.4%	associated with fault zones in coal-gas outburst		· rock and gas outbursts initiated by shotfiring	Forecasting core discing working protective sames, destressing	

Date APRIL 14, 1987
Project 861- 1290

BRIEF SUMMARY OF CASE HISTORIES

TABLE 3.2

	SEISMIC MONITORING
s	Yes
andstone	
	Yes
	Yes

Date APRIL 14, 1987
Project 861- 1290

Golder Associates

Drawn RWR
Chkd

IDEALIZED SEISMOACOUSTIC RECORDING OF A SUDDEN THREE-PHASE GAS OUTBURST.

FIGURE 3.1

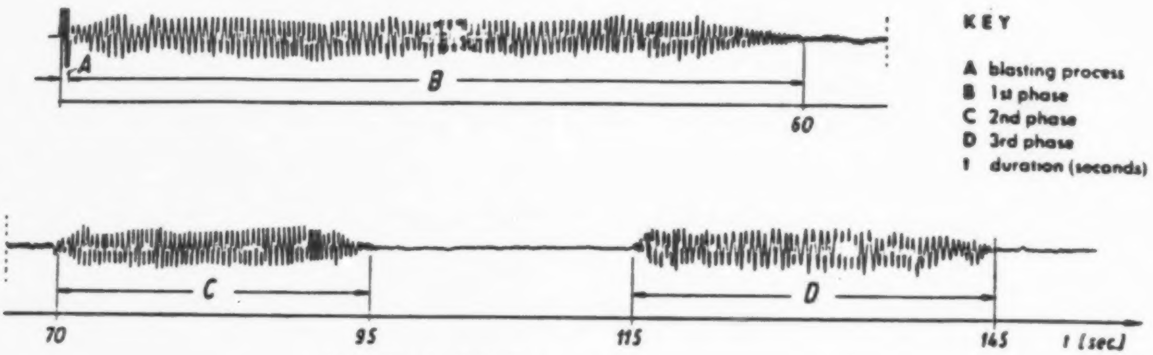
A
B
60
C
D
70
95
115
145
t (sec)
KEY
A blasting process
B 1st phase
C 2nd phase
D 3rd phase
t duration (seconds)

(AFTER GIMM AND PFORR)

Date FEB. 18, 1987.
Project 861-1290

Golder Associates

Drawn TMG
Chkd.

4. REVIEW OF OUTBURST MODELS

A number of authors have discussed the outburst mechanism. In general, the approaches used were varied mainly because some of the hypotheses put forth were based on limited information, most of which were obtained from the particular cases under their investigations with little review of work similar in nature. Recently, several review papers have been published (Belin 1981; Shepherd et al, 1981) and have provided broader analysis of the phenomenon. It may be noted from the literature that authors studying coal outbursts did not generally refer to work related to salt/potash outbursts or rock and gas outbursts. In the present research project, it was found necessary to review the state of knowledge in every aspect of dynamic rock fracturing with emphasis on phenomena involving gas(es). The following sections present a review of currently proposed outburst mechanisms, for coal and rock, together with discussions of other dynamic phenomena. Overviews of coal and gas, and rock and gas outburst theories are presented first. They are then followed by reviews and discussion of the concepts and mechanistic models of outbursts proposed by various researchers and practitioners.

4.1 An Overview of Coal Outburst Theories

(after Shepherd et al, 1981)

Coal outburst mechanisms have been studied for over 70 years and the theories, namely, the cavity, pocket and dynamic theories can be classified as those emphasizing the role of gas or stress.

The cavity theory pre-supposes the existence of open cavities containing pressurized gas within the coal seam.

The theory was discarded because of the lack of evidence regarding the presence of such cavities.

Then the pocket theory is based on the concept that crushed coal zones are present within the seam, in particular in the vicinity of faults. These act as a reservoir containing high pressure free gas ready to be released when the roadway approaches it. These soft coal pockets are usually associated with geological structures and surrounded by hard coal.

The dynamic theory is based on the dynamic failure behaviour of coal due to overstressing. Ahead of the advancing coal face, the presence of mining-induced fractures (due to overstressing) lowers the strength of the coal and permits rapid desorption of gas during failure.

4.2 An Overview of Physical Mechanisms in Rock and Gas Outbursts

(after Belin, 1981)

The current theories describing the outburst phenomenon can be grouped under two different concepts:

i) the outburst is a result of stress concentration and the gas plays a minor role,

ii) the outburst is a result of internal gas pressure and the stresses play a minor role.

Examples found in the literature are generally related to either of the above theories.

The "stress" concept pertains to the case in which drivages create local sharp local increases in compressive stress at the roadway perimeter causing rock failure by lateral extrusion (extension). The depth of the failure zone is a function of the direction and magnitude of the principal stresses. No gas is involved and this is considered a to be pure rockburst.

The "gas" concept relates to the case in which the rock is subjected to internal gas pressure. The reduction in effective stress would bring forward the failure condition expressed above. Gas pressure can develop in the fissures as they are created, facilitates the lateral extension, the ejection and transport of the material, and the propagation of the fissures into the rock mass.

4.3 Review of Existing Rock and Gas Outburst Models and Other Dynamic Phenomena

The initiating mechanisms of the outburst phenomenon proposed by various authors are summarized in the following sections. The effect of blasting on rock stresses and associated fracturing is also briefly reviewed.

4.3.1 Outbursts in Salt and Potash Mines

4.3.1.1 Outbursts in Louisiana Salt Mines
(Mahtab, 1982)

In these mines, it was shown that there was a correlation between the events and shear zones (faults). These zones were the sources of the gas and were termed pressure pockets. The proposed explanation was based on the following hypothesis:

- the outburst was initiated by biaxial compression,
- the cavity produced is enlarged by spalling of the walls (shear type of failure) and by further discing along the axis of the cavity,

- the progress of the outburst was halted by a combination of dilatancy hardening, increased stress in the rock mass and enlargement of the outburst cavity to the boundaries of the shear zone.

The initiation mechanism of the outburst was postulated as follows:

The impervious salt mass remaining between the pressure pocket and the free face acts as a dam. Although previous blasts and subsequent deformation might have initiated cracking of the salt mass, the confinement (confining pressure) is sufficient to restrict gas seepage and failure of the dam. Further blasting of the new face reduced the confinement below a critical value and fracturing of the dam mobilizes the pore pressure. Failure was then initiated by discing if the pore pressure is larger than the tensile strength of the salt. Subsequent enlargement of the cavity proceeds by shear failure under unconfined compression, governed by the Mohr-Coulomb criterion: induced fractures would be oriented along $45-\phi/2$ degree to the major principal stress.

A friction angle of 56° was reported for this salt mass and, on this basis, the fractures would make an angle of 17° to the tangent to the cavity perimeter. This mode of failure appeared to be consistent with the scale-like fissures observed around the exposed surface of the outburst cavity.

The shape of the outburst cavity was considered to be a function of the shape of the pressure pocket as well as the in situ stresses and material properties. In addition, it was proposed that the progress of the outburst would be stopped by dilatancy hardening if a critical stress loading rate is reached at the periphery of the cavity.

4.3.1.2 Outbursts in German Potash Mines

(Gimm and Pforr, 1964)

These authors suggested that rock and gas outbursts would take place when an opening (room, roadway or a large borehole) with a sufficiently large free area approaches close enough to a horizon in which the rock is susceptible to outbreak. Behind the free surface of the opening the triaxial stress field in the rock would change to a biaxial stress field, resulting in the destruction of the rock mass and the release of gas. Due to such changes in the loading conditions, a portion of the potential strain energy stored before the change in loading condition would be released resulting in destruction of the rock.

They recognized the complexity of the relationship between the rock strength properties, the gas content and the failure mechanics but considered the influence of the type of mining irrelevant to the process. Their research has also shown that the rock behaviour under changes in external loading conditions has a great significance in rockbursts, and rock and gas outbursts.

4.3.2 Coal and Gas Outburst Models

The coal and gas outburst models proposed by various researchers are discussed in the following section. The emphasis of the discussion is on the initiation mechanism of the outburst phenomenon.

4.3.2.1 Coal and Gas Outbursts

(Khristianovich and Salganik, 1983)

The authors' concept of coal (rock) and gas outburst phenomenon is one of hardrock mine rockburst greatly intensified by the energy of the gas. It is assumed that the gas exists in the rock formation as free gas in the isolated pores because of hydrostastic stress condition and low permeability.

Under uniaxial stress relief, the gas can only expand by rupturing the rock and thus forming a system of penny-shaped cracks growing in planes orthogonal to the direction of uniaxial stress relief. There is, however, a range of pore size in which this effect exists. Pores outside this range (smaller than a minimum radius and larger than a maximum one) will only change volume without initiating cracks. Within the range, pores will change volume at first and then initiate crack propagation.

Crack initiation will cause a change in the material deformation modulus, being lower near the free face and progressively increasing towards the intact state value at some distance inside the material. In addition the permeability of the material will also increase almost instantaneously in the plane orthogonal to the stress relief while remaining low in the direction of the stress relief. The pressure gradient near the free face, in the direction of the stress relief, is considerable and accounts for large outbursts.

The authors also pointed out that an outburst prone situation develops gradually during mining and that the outburst it-self is a dynamic process. A rapid dynamic stress relief in the form of a crushing wave concentrates the total gas pressure differential in a very thin near-surface layer. It causes layer-by-layer breaking away, crushing and liberation of the free gas.

4.3.2.2 Coal and Gas Outbursts
(Kidybinski, 1981)

This contribution presents three indices used in Poland to classify the potential of the coal to create bursts.

These indices are the Stored Strain Energy Index (Wet), the Bursting Efficiency Ratio (η) and the Rheologic Ratio (θ).

- Stored Strain Energy Index (Wet)

This is a simple indicator and it assumes that the energy released during bursting is proportional to the elastic strain energy accumulated in a unit volume of coal. The index is given by

$$Wet = \frac{\Phi_{sp}}{\Phi_{st}} \qquad (4.1)$$

where Φ_{sp} = available elastic strain energy
Φ_{st} = dissipated strain energy

Wet increases with the applied load since the non-elastic deformation due to the closure of pores and microcracks at the beginning of the loading represent a lesser percentage of the applied load. Therefore, Wet also increases with the number of loading cycles applied to the sample.

- Bursting Efficiency Ratio (η)

The value of the bursting efficiency ratio (expressed as a percentage) is given by the ratio of the total kinematic energy (ϕk) of fragments after failure of a specimen in uniaxial compression over the maximum elastic strain energy (ϕo) at failure.

$$\text{Thus } \eta = \frac{\phi k}{\phi o} \qquad (4.2)$$

- Rheologic Ratio (θ)

This index considers the energy release rate due to sudden failure of the coal. The energy release is a function of two parameters, the stress relaxation and the failure dynamics, both characterized by particular stress rate (Δ_σ/Δ_t).

The stress relaxation component is a function of the geometry, the stress concentration factor and the vertical load, the compressive strength of the coal and the extraction rate. The failure dynamics component has been based on the theoretical calculation of the impact power output sufficient to knock out hydraulic supports (mean load density of 400 kN/m) located at a distance of 1 m from the coal face. This component is a function of the elastic modulus, the dynamic compressive strength and the thickness of the extracted coal seam.

Each of the indices discussed above have been used by the author to rate the potential of coal outburst hazard in Polish Coal mines. However, these indices may not be directly applicable to conditions in the Sydney Coalfield.

4.3.2.3 Coal and Gas Outbursts

(Litwiniszyn, 1985)

The model describes the initial phase of the phenomenon of coal and gas outbursts with particular emphasis on hard coal. The medium (coal) is considered as a porous body with a system of capillaries filled with gas. It is hypothesized that the pores are sufficiently small that the gaseous substance undergoes capillary condensation, thereby creating a three-phase medium. The equation of state of such a medium enables a rarefaction shock wave to exist in the medium. (In a rarefaction shock wave, the value of the stress at the wave front is smaller than behind it). The propagation of such a wave permits a phase transformation from liquid to gas to occur in the medium, creating a stress gradient sufficiently large to crush the porous rock matrix. There was no reported experimental work associated with the development of this hypothesis.

4.3.2.4 Coal and Gas Outburst

(Paterson, 1986)

The proposed model attempts to quantify the descriptive research that has taken place worldwide on outbursts over many years. In particular, it considers such factors as the high rate of advance, coal permeability, strength and in situ stresses.

The principal assumption in this model is that an outburst is the structural failure of coal due to excess stress resulting from the body forces created by the gas released from the coal. The failure will predominantly be of tensile type. These body forces are induced by the pressure gradient of the flowing gas. The model includes components to account for the gas flow, the stresses and the failure behaviour. The gas flow through the coal is calculated and the pressure gradients or body forces (stress tensors) are determined. The in situ (induced) stress field is added to the stress components derived from pressure gradients and the new stress configuration is established. The incorporation of a failure criterion would determine the depth of the failure zone. It was considered that an outburst is predominantly a production of tensile failure. When a principal stress at some point reaches the specified tensile strength, cracks normal to that stress would occur and if crack growth is not arrested, an outburst could take place.

4.3.2.5 Coal and Gas Outbursts

(Barron, 1972)

The model assumes that outbursts of coal are gas induced failures. The model determines time-dependent, gas influenced fracture contours around a mine excavation. The major factors considered are the stress, permeability, gas pressure and failure criteria. With a set of given boundary loading conditions and excavation shape, stress distribution around the opening are determined. By assuming a permeability function of the coal dependent on the stress conditions, the permeability distribution around the excavation can be determined. Using the seam gas pressure and the permeability distribution, gas pressure distribution around the excavation can be defined for any time. The superposition of gas pressure and the static stress enables the effective stress distribution to be determined. A failure criterion is then applied to evaluate the extent of the failure zone.

4.3.2.6 Coal and Gas Outbursts

(Hiramatsu, 1983)

The proposed model postulates the outburst phenomenon as the mechanical fracture of coal by the combined effect of rock stress and gas pressure. The fracture criterion for coal containing high pressure gas is given by the analysis of the stress concentration around penny shaped cracks using the elastic theory.

By assuming the existence, in the coal seam, of a large number of penny shaped pores filled with gas at pressure Po, subjected to rock stress, the condition for the fracture of the coal, by concentrated tensile stress at the tips of the pores, is given by :

$$(1+b/a)(\sigma_3{}^*-\sigma_1{}^*)^2-2(b/a)^2(\sigma_3{}^*+\sigma_1{}^*-2p)^2T+ \\ 2b(\sigma_3{}^*+\sigma_1{}^*-2p)(1-(b/a)T)-4b = 0 \qquad (4.3)$$

in the region of compressive fractures

and by: $\sigma_3{}^* = 1+p$

in the region of tensile fractures. (4.4) with the tensile stress given by :

$$T = 1 - \sqrt{1 - \frac{a}{b}\left[\frac{(\sigma_3{}^* - \sigma_1{}^*)}{(\sigma_3{}^* + \sigma_1{}^* - 2p)}\right]^2} \qquad (4.5)$$

and with σ_t = tensile strength

σ_1 = major principal stress

σ_3 = minor principal stress

ν = Poisson's Ratio

$\sigma_1{}^* = \sigma_1/\sigma_t$

$\sigma_3{}^* = \sigma_3/\sigma_t$

$p = Po/\sigma_t$

Po = initial pore pressure

$a = \nu(\nu-3)(4-3\nu+\nu^2)$

$b = (1-\nu)^2(2-\nu)^2$

Figure 4.1 illustrates the conditions for the failure of coal ($\nu = 0.2$) under various gas pressure. The state of stress is plotted above the dash line and if the point falls on the right hand side of the curve representing the gas pressure condition, the coal is in a stable condition.

If the assumption is valid, the following features are easily understood:

- Geologically disturbed areas with associated weaker coal are more prone to outburst.
- Coal seam containing higher gas pressure are more prone to outburst.
- The finely crushed coal produced during an outburst is indicative of the role of gas contained in the coal structure.
- Pre-mining of overlying seam contributes to the reduction of stress concentrations.

This author also assumes that the change in gas pressure may be slower than the change in stress when the coal is blasted.

4.3.2.7 Coal and Gas Outbursts
(Gray, 1980)

This author considered that failure during a coal and gas outburst is dependent on stress and strength characteristics of the coal seam with the gas pressure acting as an operative stress. The cause of failure of the coal may therefore range from (a) overstressing where the coal strength is exceeded without any gas effect to (b) internal gas pressure exceeding the coal tensile strength. The actual mechanism may reside anywhere between this range.

The failure criterion proposed is the Mohr-Coulomb failure concept corrected for effective stresses.

Damage to the coal is related to the energy release. This energy originates from both the gas strain energy and the rock and coal strain energy. During the outbursts the potential energy is transformed into kinetic energy, accelerating coal, gas and the surrounding rock mass.

Of particular interest in the discussion is the demonstration that the gas strain energy is much larger than the coal/rock stored elastic strain energy. It was stated that:

"Instantly or near instantly released gas can be expected to expand and do work on itself and surrounding particles by accelerating them. If the expansion is fast enough it will approach the adiabatic case. On slower expansion heat will be absorbed from the coal and mine air with a resulting total greater gas energy release. The upper limit in the latter case will be the isothermal energy release. Some energy is probably absorbed from the gas as heat of sorption".

The energy released from expanding gas is given by:

adiabatic expansion: $$E = \frac{K}{1-\delta} (v)^{1-\delta} \Big|_{v_1}^{v_2} \qquad (4.6)$$

with $K = pv^{\delta}$
v = volume
v_1 = equivalent volume of gas in seam
v_2 = volume of V_1 at end of adiabatic expansion
δ = ratio of specific heat $C_p/C_v = 1.33$
C_p = specific heat at constant pressure
C_v = specific heat at constant volume

isothermal expansion: $$E = P_{at} V_{at} \ln \frac{(P_{seam})}{(P_{at})} \qquad (4.7)$$

with P_{at}, V_{at} = Pressure, Volume at atmospheric condition
P_{seam} = seam gas pressure

The strain energy released from cone shape cavities is obtained from the analysis of the loading concentrations on a disc part of an outburst cone as shown in Figure 4.2. During an outburst, the ejection of material in the x, y plane relieves the stress in z direction. Assuming elastic relaxation without contraction of the outburst cone, the associated strain is given by:

$$\epsilon_z = \frac{1}{E} \sigma_z \left\{1 - \frac{2\nu^2}{1-\nu}\right\} \qquad (4.8)$$

with ϵ_z = strain in z direction
E = Young's Modulus
ν = Poisson's Ratio
σ_z = stress in z direction

The strain energy associated with this stress relief is given by:

$$E_z = \int_v 1/2 \, \sigma_z \, \epsilon_z \, dv \qquad (4.9)$$

with v = volume of disc

Furthermore, as σ_z decreases under confined conditions, there is also a release of σ_x and σ_y existing within the disc. If $\sigma_x = \sigma_y$, the energy released from this elastic deformation of the cavity walls is given by:

$$E_r = \pi R \sigma_x U_r t \qquad (4.10)$$

where R = hole diameter
$U_r = 2R\sigma_x \frac{(1-\nu^2)}{(E)}$ = radial deformation
t = disc thickness

This analysis of energy release assumes that the cavity wall failure does not occur and that the shear strain energy is negligible.

During an outburst, energy is also consumed by the biaxial loading of the central disc. If the gas is ejecting the material away from the cavity, preventing it from acting as an energy absorber, the energy consumed by radial failure of a disc is given by:

$$E_c = \int_v 1/2 \, \Delta\epsilon_r \, \Delta\sigma_r \, dv \qquad (4.11)$$

with $\Delta\epsilon_r$ = the change in strain in the radial direction
$\Delta\sigma_r$ = the change in stress in the radial direction, $(\sigma_r=\sigma_x=\sigma_y)$

and with $\Delta\epsilon_r = \Delta\sigma_r \dfrac{(1-\nu u)}{(Eu)}$
νu = Poisson's Ratio in unloading (failure) phase
Eu = Elastic Modulus is unloading (failure) phase

Values of energy involved in coal outbursts (2 m diameter) were calculated from typical events which occurred in an Australian colliery.

The analysis revealed that:

1) for adiabatic expansion of seam gas pressure of only 1.5 to 2 MPa, the energy release is significantly greater than the energy released by the elastic strain energy of the coal mass.

2) the presence of a slight confinement away from the outburst face will greatly enhance the potential strain energy released of the outburst. This energy release however still remains lower than the gas energy.

4.3.2.8 Coal and Gas Outbursts
(Farmer and Pooley, 1967)

A hypothesis of the initiation mechanism of coal and gas outburst was proposed by considering four contributory factors: the in situ and induced stresses, the presence of geological, deformational and depositional structures, (e.g. folds, faults, rolls, slip etc) quantity and pressure of gas in the seam and the microstructure of outbursting coal.

It was considered that while stress conditions are an essential factor in the outburst process, they can only be responsible for outburst initiation in combination with other factors.

The presence of geological deformational structure would create local concentration of in situ stresses in the coal seam. The presence of the excavation would tend to alter the stress state from triaxial to biaxial or uniaxial and would lead to local failure depending on the strength and faiure characteristics of the coal and surrounding strata. The presence of pressurized gas in the coal would aggrevate the failure condition by violently expelling the failed material from the cavity.

It was reported that at the West Wales Collieries, in an average outburst of 50 tons (45 tonnes) of coal, a potential energy of the order of 10^8 kg-m (7.2×10^8 Joules) could be released from the gas absorbed into the structure of the coal at atmospheric pressures. If this amount of energy is relased instantaneously with the failure of the coal, it is sufficient to project the coal violently for a considerable distance.

4.3.2.9 Coal and Gas Outbursts Associated with Geological Structures

(Shepherd et al, 1984)

In and close to faults, sills, dykes and other geological structures, anomalous stress and gas conditions apparently exist. The proposed outburst mechanism is an energy balance hypothesis based on dynamic theory. It is postulates that for violent, uncontrolled failure to take place, there must be both sufficient stored energy in the coal and sufficient applied stress to cause the coal to fail. The stored energy in the coal comprises both the elastic strain energy and the gas energy. If sufficient stress is available to fail the coal but the stored energy is small, non-violent failure will occur.

When the energy available to cause unstable collapse is balanced by the maximum amount of strain energy that can be released by the volume of coal affected, the system would remain in equilibrium. When the maximum released energy is greater than the consumed energy, outbursts would be generated. At failure initiation,

$$W_r = W + W_i \qquad (4.12)$$

where W_r = released energy available from excavation

W = elastic strain energy per unit volume of coal

W_i = gas pressure energy (adiabatic expansion)

which are given by:

$$W_r = \sigma_{max} V$$

$$W = \frac{1}{2E}[(\sigma_1)^2+(\sigma_2)^2+(\sigma_3)^2-2\nu(\sigma_1\sigma_2+\sigma_2\sigma_3+\sigma_1\sigma_3)]$$

$$W_i = \frac{k}{1-\gamma} (v)^{1-\gamma} \Big|_{v_1}^{v_2}$$

with σ_{max} = maximum applied stress
V = coal block volume
k = $p_1(v_1)$ = $p_2(v_2)$ = constant
p_1, v_1 = gas pressure and volume in coal seam
p_2, v_2 = pressure and volume of expanded gas
γ = ratio of specific heats = C_p/C_v
C_p = specific heat at constant pressure
C_v = specific head at constant volume
E = Young's modulus
ν = Poisson's ratio
$\sigma_1, \sigma_2, \sigma_3$ = applied principal stresses

Knowing the width (w) and height (h) of the excavation in coal, it is possible to determine the depth of the outburst cavity by:

$$d = \frac{W + W_i}{\sigma_{max}(wh)} \qquad (4.13)$$

In practice, as the face approaches a fault or shear zone, the block of coal is subjected to biaxial compression. When the concentrated stresses overcome the strength of the coal, its cohesion breaks down and gas expansion to atmospheric pressure takes place, desintegrating and transporting the coal.

These authors also presented a model to explain the formation of cone shape cavities and pressure exfoliation fissures on cavity perimeter. It was considered that tunnel drivage perpendicular to the maximum principal stress creates an abutment pressure front (or stress concentration) that is sufficiently large to cause progressive stable failure (failed materials are still confined) ahead of the advancing face. The abutment pressures are then redistributed and gas is slowly released. If mining (stress) induced fractures are not extensive ahead of the face, the abutment pressure front would be close to the face and the pressure gradient near the face would generally be high.

When the coal strength is exceeded, closely spaced fractures would develop rapidly around the face area and excess elastic energy stored in the coal and surrounding roof and floor rocks is fed into the fractured coal. High gas pressure previously stored in the coal is then released in the fractured planes. The multilayer of coal buckles and a kink band is initiated near the face where σ_1/σ_3 ratio (σ_1 and σ_3 are major and minor principal stresses respectively) is large. The coal is easily comminuted and expelled from the cavity by a combination of the release of high pressure gas and excess elastic energy.

The model for the formation development of a cone-shaped outburst cavity is based on geological observations of mining-induced fracturing and general shapes of outburst cavities, and on the recognition that conically arranged mining-induced kink bands form a precursor to outbursting.

4.3.3 Sandstone and Gas Outbursts

4.3.3.1 Sandstone and Gas Outbursts
(Jovanovic et al,1979)

This study attempts to detail the role of free gas in the outburst process based on the coal mining experience in Yugoslavia. The outburst process is broken down in three phases and A_1, A_2 and A_3, are the corresponding work done during the phases:

- outburst and deformation of coal and rock (work done = A_1)
- heating of ejected material (work done = A_2)
- projection of the material over a certain distance (work done = A_3)

The total work involved, Atot, is given by the sum of the work performed in the three phases. Thus

$$A_{tot} = A_1 + A_2 + A_3 \qquad (4.14)$$

The energy available to the outburst process is assumed to originate from the free gas energy during isothermal (as opposed to adiabatic) gas expansion. By determining the porosity and the gas pressure in both rock and coal and the compressibility of the gas mixture , together with the emitted gas volume, the energy available from isothermal gas expansion is calculated.

Calculations based on data obtained from actual events have shown that the potential energy of the free gas involved is larger than the work performed during the outburst and thus is the dominating factor. As for the stress conditions in the rock mass and the physical characteristics of the mine openings, these are considered, by the authors, as factors that either amplify or reduce the outburst process.

4.3.3.2 Rockbursts

(Petukhov, 1983)

This theory of dynamic rock destruction takes into account rock mechanical behaviour, fracture and post-failure characteristics. Three conditions are necessary to generate a rockburst (dynamic failure), these are:

- limit load condition (I)
- instability condition (II)
- energy conditions (III)

The load applied to the rock element being fractured should reach a maximum critical value (I) while the rigidity of this element remain larger than the rigidity of the loading system, for example the surrounding rock mass (II). In addition, the level of released energy available should be high (III).

The rock mechanical properties to be consider include not only the elastic modulus and the strength envelope but also the post-failure behaviour, ie. the drop modulus and the dilatation coefficient as strain softening behaviour is prevalent. The geological features also play a significant role as they influence both the rock mechanical properties and the stress field. All those parameters are combined to define the stress-strain behaviour of the rock mass as the opening is being developed.

The stability of the rock mass is analysed in the light of the post-failure deformation, taking into account the possible dilatation and softening of fracture planes. The materials being fractured gain kinematic energy when its stability is lost. During the event, the material maintains its cohesion on one side of the fracture wave while on the other side the material is being fragmented. Fracture wave are analysed using laws of mass, impulse and energy conservation. The theory of energy balance characterises the dynamic phenomenon.

The event may also stop for different reasons; fracture wave entering an area where its propagation is difficult, rock inhomogeneity, reduction of rock mass volume ahead of the destruction front (in a pillar situation), or the formation of stable destruction boundaries.

The released energy is given by the sum of the stored strain energy in the material being destroyed and the energy released from the adjacent rock mass. The consumed energy is given by the sum of the work required to fracture the material, the kinetic energy of the fragments, the energy absorbed by the rock mass surrounding the failed area and the seismic oscillation of the surrounding zone.

Under energy equilibrium conditions this relation is given by :

$$W_m + (-\Delta W_S) = W_P + W_K + W_\sigma + W_C \qquad (4.15)$$

with W_m = energy contained in the material to be destroyed

$(-\Delta W_S)$ = energy released from adjacent rock mass

W_P = destruction of material

W_K = kinetic energy of fragments

W_σ = energy adsorbed by surrounding rock mass instead of destruction

W_C = seismic oscillation generated in rock mass

4.3.3.3 Rock and Gas Outbursts

(Karagodin et al, 1983)

This paper describes the energy aspect of rock and gas outbursts by considering the amount of stored strain energy released by the outburst and the work put into breaking the rock. It addresses such variables as the insitu state of stress, the elastic and rheological properties of the material and the time factor (rate of energy release).

It was found that with the rapid creation of a face (explosive breakage, t ⇒ o) within an elastic material, the energy of elastic deformation released will be at its maximum and is significantly higher than that resulting from slower extraction rate which permits relaxation of stresses within the rock mass.

4.3.3.4 Rock or Coal Outbursts
(Ujihira et al, 1985)

Through a very comprehensive series of physical models of outburst phenomenon and theoretical calculations, these researchers have shown that the fracture mechanism and outburst process can be explained by the gas pressure gradient developed within the surficial layer of outburst prone material as the confinement is suddenly released (through blasting). When the gas pressure is twice as large as the tensile strength of the tested material, the gas pressure gradient would induce tensile stresses that are sufficient to exceed the tensile strength of the material. Based on the model study, the flaking mechanism was also analysed as follows:

"When the peak (tensile) stress exceeds the (tensile) strength, the material is separated from the body by the first crack, this new crack plane should be considered as the next new surface. Beyond the new surface, almost the same changes of gas pressure and tensile stress distributions should occur. These are exemplified practically in Figure 4.3(A). Once the first flaked piece is separated from the material body, it will be pushed by the pressure difference $P_1(t)-P_0(t)$ between the front and back faces of the crack and may be sheared or bent to failure secondarily like Figure 4.3(B). In the same manner, separating and secondary failure might propagate the chain reaction toward the solid direction (away from the gas space). In this process, the secondary failing points move gradually to the center as shown in Figure 4.3(C), because a part of material left adhered to the interior walls of the apparatus (in the two dimensional model corresponding in practice to the roof and floor), disturbs the shearing or bending of the next pieces. Connecting these secondarily broken points, a parabolic envelope is created. This parabolic curve provides the conical type outburst cavity".

The effect of the in situ and induced stress concentrations, while not considered in this work, is said to favor crack propagation and therefore the effectiveness of the gas pressure action.

4.3.3.5 Rock and Gas Outbursts

(Sevelev, 1979)

This paper summarizes the research on rock and gas outbursts in USSR.

Preliminary studies have shown that the effect of gas pressure on sandstone strength was marked. Intact rock strength was reduced by the addition of pore gas pressure of 2 to 5 MPa (ie. σ_c = 100-120 MPa, σ_t = 7.5-13 MPa reduced to σ_c = 58-88 MPa, σ_t = 4-8 MPa). In addition, it was found that the law of effective stress (Skempton, 1961) does not apply in the sandstone tested. The following expression, however, was proposed for the effective stress:

$$\sigma^* = \sigma - [1-d(1-n)]P_g \qquad (4.16)$$

with σ = total stress

σ^* = effective stress

n = porosity (in decimal)

P_g = gas pressure

d = proportional constant reflecting grain contact area and size (d = 0.4 ± 0.15)

The outburst process was analysed by dividing the rock mass into four areas (I to IV on Figure 4.4(A)) and the proposed mechanism of the outburst process was as follows:

- In the undisturbed rock mass, the gas pressure is constrained by the stress field acting on the pores. (Area I)
- Near the surface of the newly created opening, deformation and fracturing caused by stress concentration and elastic recovery reduce the strength of the material. If the rock mass is overstressed, stresses would be redistributed according to the residual strength (uniaxial, biaxial, triaxial) of the material. In this area (II) the gas pressure starts acting on the rock material.

Figure 4.4(B) illustrates the interaction of the gas and rock mass within area II and its adjacent areas in more detail. The key processes postulated by the authors are summarized below.

i) in Zone A, the deformation of the rock mass are not disturbing the rock pore structure. Gas pressure effect in this zone could be evaluated by the static stress analysis described above (equation 4.16).

ii) in Zone B, normal and tangential stresses start influencing material deformation (extension type of strain) and the associated change in material strength (weakness increasing toward the cavity) starts to take place.

iii) Zone C is characterized by the appearance of fractures in which the kinetic energy of the gas increases. Gas is flowing from the pores to the fractures and although Ppores (gas pressure in the pores) decrease, Pfractures (gas pressures in the fractures) increases.

iv) in Zones D and E, the strength of the material is largely reduced because of its proximity to the free surface, and the area of influence of the gas pressure increases. Some of the strain and gas energies will be transformed into kinetic energy during the ejection of the rock fragment.

v) In zone E, the propagation of fracture systems towards the cavity boundary disturbs the gas dynamic balance of the system as the gas in the fracture is free to escape in the outburst area, zone F.

The gas energy consumed in Zones B to E was determined to be approximately 40% of the total gas energy available. Fragmentation of the material also takes place in area III (Zone F) where the fragments are reduced to smaller flakes by the same process and transported away from the cavity.

The gas dynamic balance was numerically modelled and typical results are shown on Figure 4.4(C) for Zones C to F. Curves 1 and 2 respectively show the gas pressure variation in the pores and fractures of the bursting material as a function of time.

At the beginning of crack initiation, in Zone C, the fracture volume rapidly changes from zero to a value larger than the total pore volume intersected by the fracture plane. The fracture gas pressure (curve 2), therefore, steeply decrease from the pore pressure to a much reduced value. Thereafter, the gas pressure in the fractures increases due to the volume of gas permeating from adjacent pore structure as they become connected by a growing network of microcracks. However, the maximum fracture gas pressure, reached at time t_P, will not equilibrate with the decreasing pore pressure (curve 1). After time t_P, the fracture volume increase at a rate that creates a drop in both the fracture and pore gas pressure. When the fracture breaks into the cavity, a fast change in the gas pressure characteristic of the system occurs. The times t'_H and t''_H shown on Figure 4.5C indicate two of the possible moments at which this may occur and the associated changes on the fracture and pore gas pressure (curves 1', 1", 2' and 2"). These changes are function of the boundary characteristics of the outburst.

Therefore, it is apparent that, within the rock mass disturbed by an outburst, each time interval during the event would be characterized by a complicated gas dynamic pressure.

The in situ stress data and typical calculations of the energy available during sandstone and gas outburst were also presented. In situ stress measurements indicated that the maximum compressive stress ranged between 40 to 70 MPa. Other relevant parameters and energy calculations are shown in Table 4.1.

The energy available during an outburst comprises the following components:

- potential energy of elastic deformation (based on effective stresses)

- internal energy of the compressed gas during adiabatic expansion

- energy consumed in volume change of the rock during the release of the stress (elastic recovery)

- the work consumed during the destruction process. It is proportional to the total surface area of the fragments produced as a consequence of bursting. Detailed investigation has shown that for 1 tonne of sandstone, the new surface area is of the order of 4200 m^2. Using a fracture energy of 2 kg-m/m^2(14.5 J/m^2), the fracturing work A is of the order of 8400 kg-m/tonne (60740 J/tonne).

Based on the calculations shown in Table 4.1, the author concluded that the compressed gas acts as an accumulator of potential energy which exceeds the elastic energy stored in the rock material. The initiation of a rock and gas outburst is a function of the mechanical properties of the material and the stress field acting on it. This would lead to the deformation of the rock material and associated fractures in which the potential energy of the gas is transformed into kinetic energy, further prolonging the destruction of the material and transporting the fragmented rock away from the cavity.

4.3.3.6 Sandstone and Gas Outbursts (Revalor et al, 1985)

The type of breakage observed after sandstone and gas outbursts, (ie. the flake-like fragments and the intense fissuration of the rock mass remaining in place) in French coal mines lead the authors to suggest that in situ mechanical stresses are the principal cause of outburst and that the gas is an aggravating factor which only decreases the strength of the rock.

In situ stress measurements in the outburst prone sandstone bed have shown that this rock unit was subjected to highly anisotropic stresses. The results were consistent with a structural analysis of the area.

A numerical analysis of the stress distribution around the perimeter and the face of a roadway driven in the sandstone was carried out. The results showed that a tensile stress (-3.5 MPa) is present at the face of the roadway when it is driven parallel to the major principal stress σ_1, but disappears when the drift makes an angle of 15° or more with σ_1. These results compare well with the observations that all the rock and gas outbursts took place in straight sections of the heading and disappeared when the drift changed direction.

Therefore, it was suggested that the events were caused by mechanical stresses (tensile stresses) in direct relation with the sudden removal of confinement at the face brought about by the blast. The presence of gas in the rock pore aggravated the stress regime and permitted the propagation of breakage. They also suggested that local conditions in the mines (i.e. high stresses or gas pressure, lower rock strength due to local heterogeneities of the rock mass) might have aggravated the situation.

4.3.3.7 Bursting of Sandstone Layer Above Working

(Zorin et al, 1981)

In a particular Russian mine, both development and extraction works were difficult when the distance between an overlying sandstone layer and the working was less than 5 m. These authors assume that during blasting in a tunnel heading, a dynamic stress field is superimposed over the in situ and induced stress conditions. The rapid fragmentation of the sandstone layer above the tunnel crown was believed to be caused by the rapid rate of elastic recovery following the passage of the stress wave.

4.3.4 Other Relevant Rock Outburst Models

4.3.4.1 Dynamic Rock Failure

(Hueckel, 1981)

This model covers the initiation of dynamic rock failures characterized by their capacity for self-inducement; ie, they occur without external dynamic loading. The following is a description of the initiation mechanism presented in the paper.

"A lowering of the stress level as the result of yielding in a particular region of the rock mass may be accompanied by elastic shedding of load in an adjacent, undisturbed region of the rock mass. When the elastic strain energy released during shedding of load in this region is greater than the energy used during the progressive yielding of the rock, an excess of energy accumulates causing an increase in the rate (acceleration) of deformation of the rock mass together with a rupture of brittle rock; this excess energy is transformed into kinetic energy".

This proposed concept was
a rock subjected to the str
pt. I, incremental increase in stress beyond this point will create a divergence (lack of equilibrium) between the applied stress and the stress that can be accommodated by the now failing material. As the rock material reaches pt. II, incremental increase in the strain to which the material is subjected will create a divergence (lack of geometric continuity) between the applied strain and the strain that can be accommodated by the rock material. However, for this displacement ϵ_{II}, (at pt. II), there exists a second state of equilibrium condition (pt. IV). To reach this new state, internal redistribution of stress and strain requires the system to liberate an excess of energy.

4.3.4.2 Rockbursts in Tunnel Headings
(Dikunov, 1971)

The author assumed that the main factor causing rock bursts is the overstressing of the rock mass ahead of the tunnel face, caused by its intrusion into a rock mass which is stressed in all directions.

During blasting, the displacement of the face of the heading and the concentration of stresses in the rock mass ahead of the face occur instantaneously (i.e. dynamic loading). The stresses are greater than if they were applied statically. The dynamic stress coefficient (kd) is in the order of 2. The total stress is given by the product of the in situ stress, the stress concentration factor and the dynamic coefficient. For a rockburst to occur, the total stress has to be greater than the strength of the rock under triaxial stress state.

when the rock strength is larger than the applied stress; that is, when the working assumes its natural equilibrium shape. The fish scale type of fracture on the boundary of the outburst cavity was considered to be caused by breakage along concentric layers.

4.4 Discussion

This section provides a brief discussion of the outburst models and mechanisms presented above. As anticipated, there is a wide variation in the qualitative and quantitative treatments of the phenomenon pertaining principally to the parameters considered and the degree of complexity of the analysis. While some papers specifically address the outburst phenomena in coal, the concepts are useful for the formulation of initiating mechanisms of rock and gas outbursts.

It is not within the scope of this study to assess the strength and weakness of the outburst models and mechanisms presented, or how they may contradict other theories or facts. However, by grouping the treatments of specific aspects of the phenomenon together, it may be possible to summarize the general trend of thinking.

4.4.1 Initiation Mechanisms

The change in the state of stress from a triaxial to a biaxial loading condition near the free face of the underground opening was considered by most researchers to be one of the likely causes for the initiation of rock failure in an outburst process. Induced tensile stresses at the free face resulting from such stress changes were at which the stress change occurred (resulting from blasting) was also observed by some Russian researchers to be one of the key contributory factors.

It is recognized by most researchers that gas plays a major role in the initiation of rock failure as well as in the subsequent manifestation of the event (violent expulsion of the failed material). There are, however, different opinions on the relative significance of the stress and gas effects.

4.4.2 Effect of Blasting and Mining Method

The first recognized effect of blasting is the rapid reduction of confinement of the burst-prone material. This, in turn, mobilizes the gas pressure gradient (Ujihira et al, 1985) as the change in stress during blasting is considered to be faster than the change in gas pressure (Hiramatsu et al, 1983). Furthermore, blasting also superimposes dynamic stresses over and above the static (redistributed) stresses brought about by the creation of the opening.

The creation of an opening by blasting also induces rapid (dynamic) elastic stress relief and associated extension strain rate. This process is believed to have led to the release of the maximum amount of strain energy (of elastic deformation) as compared to slower extraction methods. Boring rate using large diameter boring equipment was observed to correlate with the initiation of dynamic events. However, in the German potash mines, the type of mining is said to be irrelevant to the initiation of outbursts.

studied by many scientists and the energy sources and the work performed during an outburst are summarized below:

Energy Sources:

- Outburst rock and/or coal stored strain energy,
- Outburst compressed gas energy,
- Energy released from adjacent rock mass (can be both elastic or gas energy).
- Blasting energy

Energy Consumption:

- Vibration (oscillation) of adjacent rock mass,
- Acoustic energy,
- Creation of new surfaces in both outburst material and adjacent rock mass,
- Heat emission absorbed by rock fragments, the adjacent rock mass and mine air,
- Ejection of rock fragments (kinetic energy),
- Volume change of ejected material.

Of interest, is the treatment of the compressed gas energy. Adiabatic gas expansion is favoured over isothermal gas expansion.

4.4.4 Cavity Shape and Fish Scale Fracturing

The conical shape of the outburst cavity was noted by many researchers and was generally considered to be related to the configuration of the shear failure surfaces within the outburst cavity. Ujihira et al(1985) proposed that the conical shape of the cavity is a result of the secondary shear failure taking place during the breakage and expulsion of the thin layers of material.

The intense fracturing along the cavity perimeter is explained by various hypotheses. The main ones are (a) shear failure of Mohr-Coulomb type at $(45 - \phi/2)$ degrees to the principal stress trajectory, (b) the breakage along concentric layers of equal stress concentration due to the large abutment stress caused by the advancing face where the σ_1/σ_3 ratio is high, and (c) secondary shear failure planes.

4.4.5 End of an Outburst Event

There are more variations in the suggested factors which bring about the end of an outburst event.

In salt mines, the event generally stopped when the burst prone zone was emptied. This is specifically related to the geology of the sites as the outbursts are generally associated with the presence of shear zones or inclusions in the salt domes. Dilatancy hardening is also proposed.

The event could also be stopped by choking itself. The fragmented rock mass brings some confinement over the cavity perimeter and, therefore, creates more stable stress conditions. In particular, Ujihira et al, (1985) proposed that the cavity could attain a state of equilibrium due to the restraining effect of the sheared material remaining along the cavity perimeter.

Others assumed that the outburst stops when a new state of equilibrium is reached. This state of equilibrium can be related to the energy aspect of the event or simply to stress regime and rock strength parameters or to the shape of the cavity. The energy balance model of Shepherd et al, (1984) predicts that the event would end when the released energy from the event equals the sum of the gas pressure energy and the stored elastic energy of the outbursting volume.

TABLE 4.1

TYPICAL ROCK AND GAS PARAMETERS AND ENERGY CALCULATIONS BASED ON OUTBURST EVENTS IN RUSSIAN COAL MINES
(after Sevelev, 1979)

A) Rock and Gas Parameters

	Without Gas Pressure Influence	Under Gas Pressure of 5.0 MPa
Density, γ	2.4 tonnes/m^3	2.4 tonnes/m^3
Porosity, η	0.07	0.07
Compressive Strength, σ_c	110 MPa	80 MPa
Tensile Strength, σ_t	12 MPa	7 MPa
Poisson's Ratio, ν	0.15	0.17
Pore Gas Pressure, Pg	-	5.0 MPa
Volume of Gas, "Q"	-	2.0 m^3/tonne

B) Energy Calculations

Potential energy of elastic deformation, W_y	4600 kg-m/tonne	4850 kg-m/tonne
Potential energy of compressed gas, W_r	-	48000 kg-m/tonne
Total potential energy (rock + gas), W (W_y+W_r)	4600 kg-m/tonne	52850 kg-m/tonne
Energy consumed in volume change, W_z	1700 kg-m/tonne	1900 kg-m/tonne
Energy consumed during the destruction process, A	8400 kg-m/tonne	8400 kg-m/tonne

Note: 1 kg-m = 7.23 Joules

CRITERION FOR PENNY SHAPED CRACK CONTAINING HIGH PRESSURE GAS

FIGURE 4.1

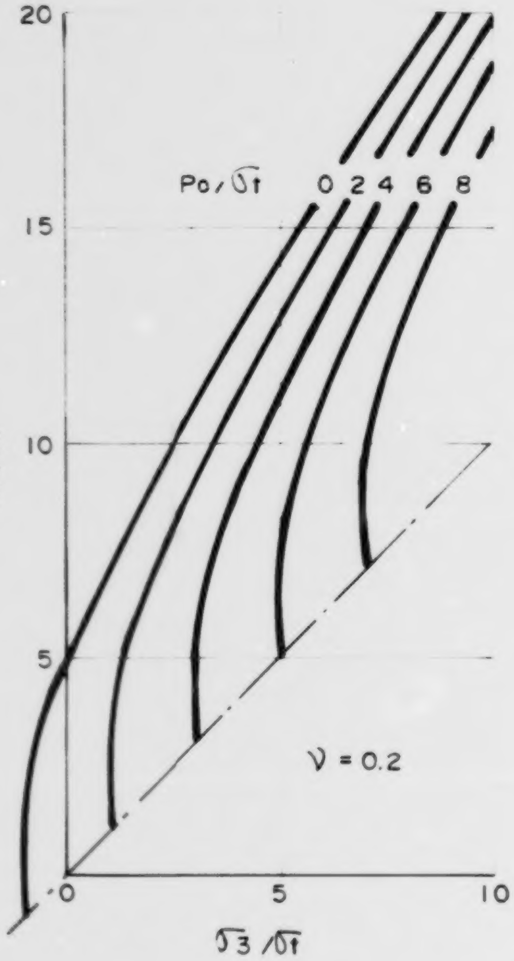

AFTER HIRAMATSU et al, (1983)

Date FEB. 3, 1986
Project 861-1290

Golder Associates

Drawn D M
Chkd

FAILING DISC IN RELATION TO ITS INITIAL SURROUNDING STRESS STATE

FIGURE 4. 2

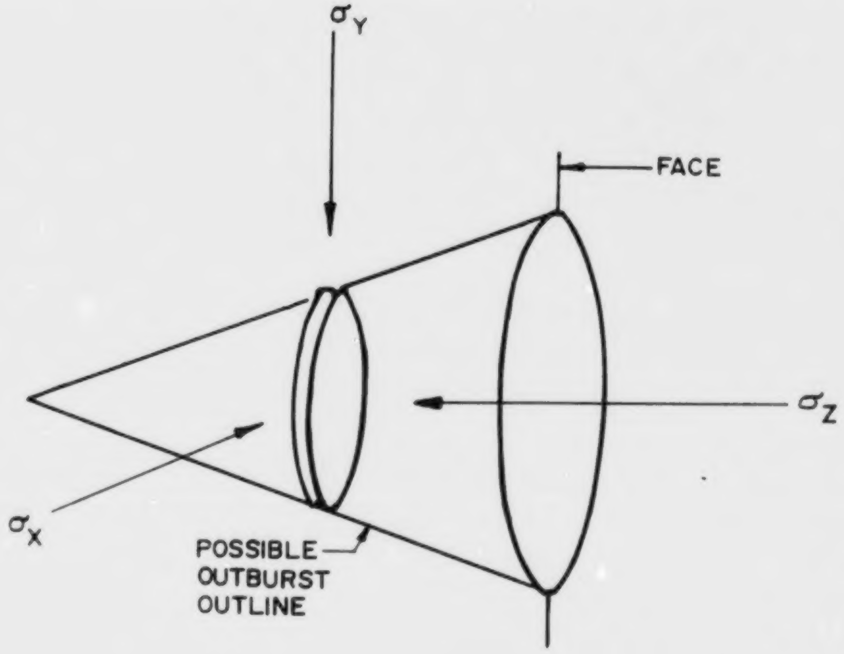
σ_Y
FACE
σ_Z
σ_X
POSSIBLE OUTBURST OUTLINE

AFTER GRAY, (1980)

Date FEB. 24, 1987
Project 861-1290

Golder Associates

Drawn TMG
Chkd

THE PROCESSES OF SECONDARY FAILURE OF FLAKED PIECES AND THE CREATION OF A CONICAL SHAPE CAVITY

FIGURE 4.3

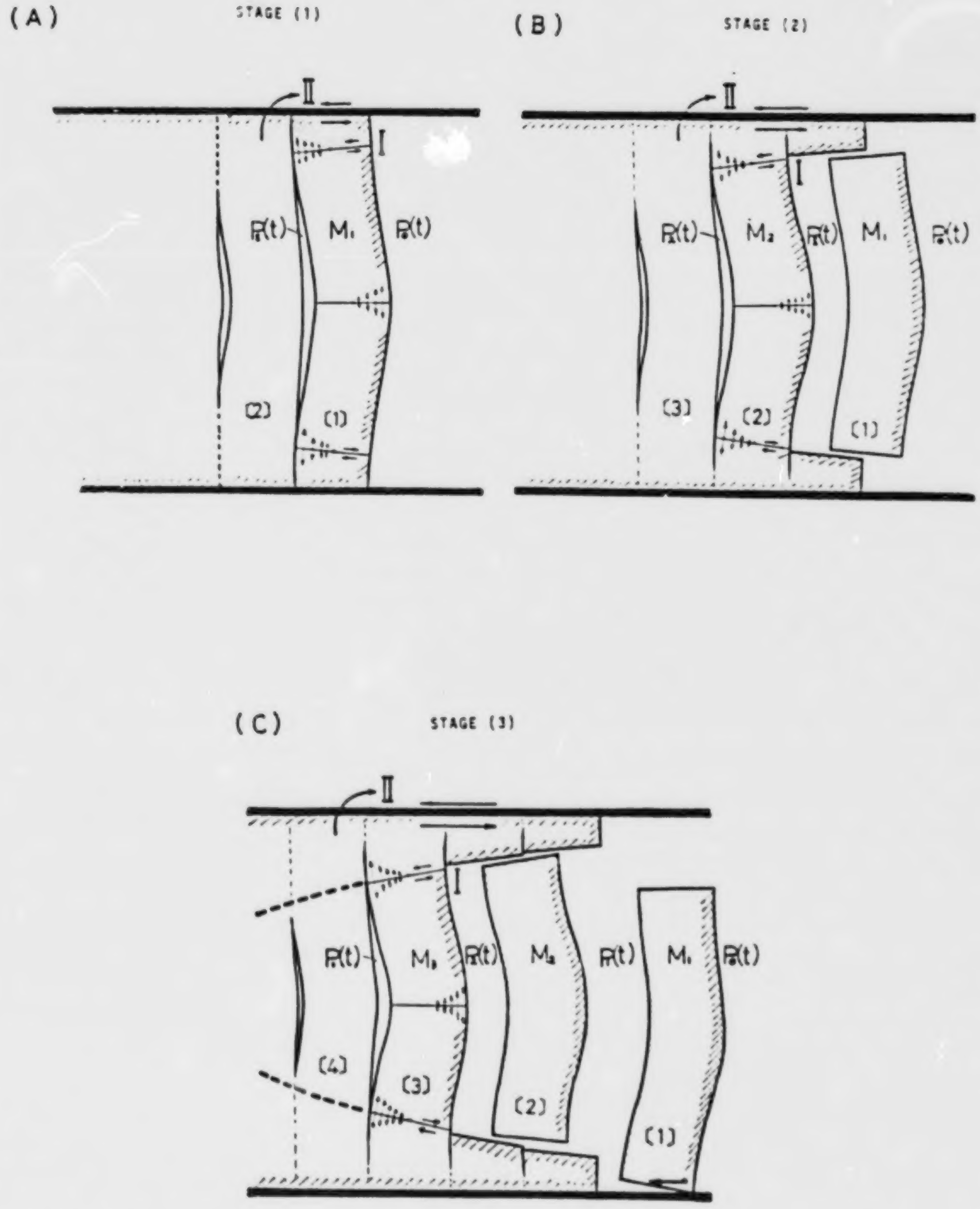
(A)
STAGE (1)
II
I
P1(t)
M1
P2(t)
(2)
(1)
(B)
STAGE (2)
II
I
P1(t)
M2
P2(t)
M1
P2(t)
(3)
(2)
(1)
(C)
STAGE (3)
II
I
P1(t)
M3
P2(t)
M2
P2(t)
M1
P2(t)
(4)
(3)
(2)
(1)

NOT DRAWN TO SCALE

AFTER UJIHIRA et al, (1965)

Date FEB 2, 1987
Project 861-1290

Golder Associates

Drawn D M
Chkd

MODEL OF ROCK AND GAS OUTBURST

(AFTER SEVELEV 1974)

FIGURE 4.4

A) FOUR DISTINCT AREAS DURING THE EVENT

I - BURST-PRONE UNDISTURBED ROCK MASS
II - FRACTURING, DEFORMATION (STRESS CONCENTRATION)
III - OUTBURST CAVITY
IV - VENTILATION NETWORK

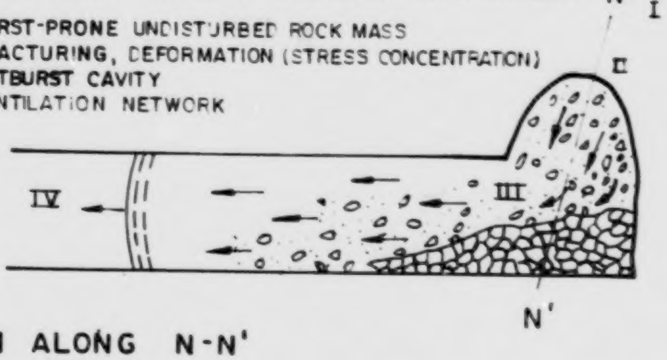

B) SECTION ALONG N-N'

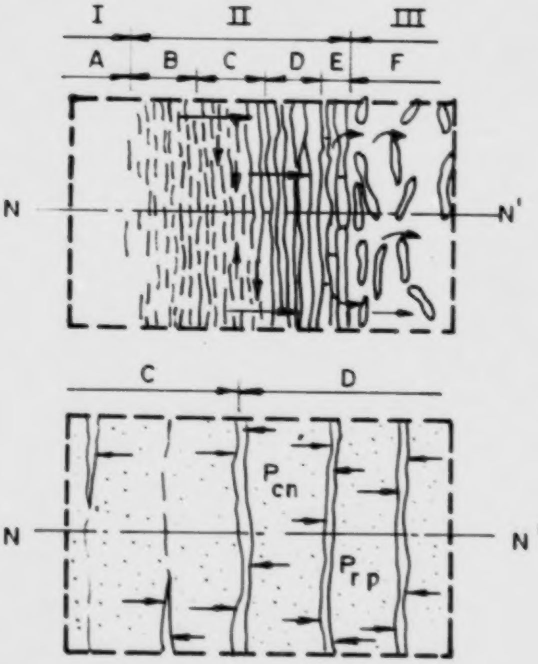

C) GAS PRESSURE VARIATION WITH TIME DURING OUTBURST

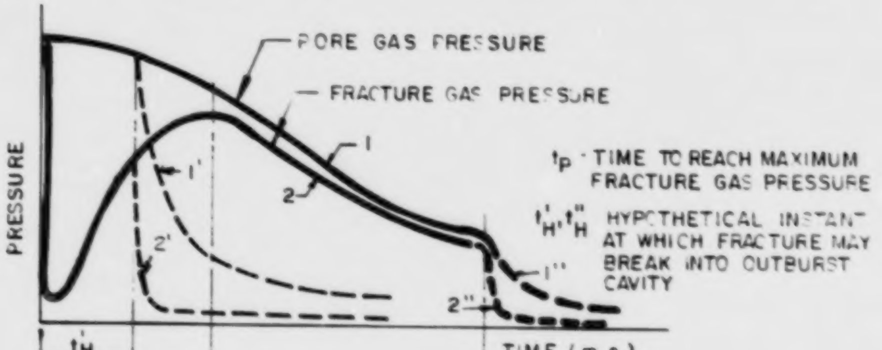

t_p - TIME TO REACH MAXIMUM FRACTURE GAS PRESSURE

t'_H, t''_H HYPOTHETICAL INSTANT AT WHICH FRACTURE MAY BREAK INTO OUTBURST CAVITY

Date FEB 2, 1987
Project 861-1290

Golder Associates

Drawn D M
Chkd

FORM PRODUCED JUNE 1986
Form G.A.-D-4m (metric)

STATES OF EQUILIBRIUM IN THE STRESS-STRAIN RELATIONSHIP

FIGURE 4.5

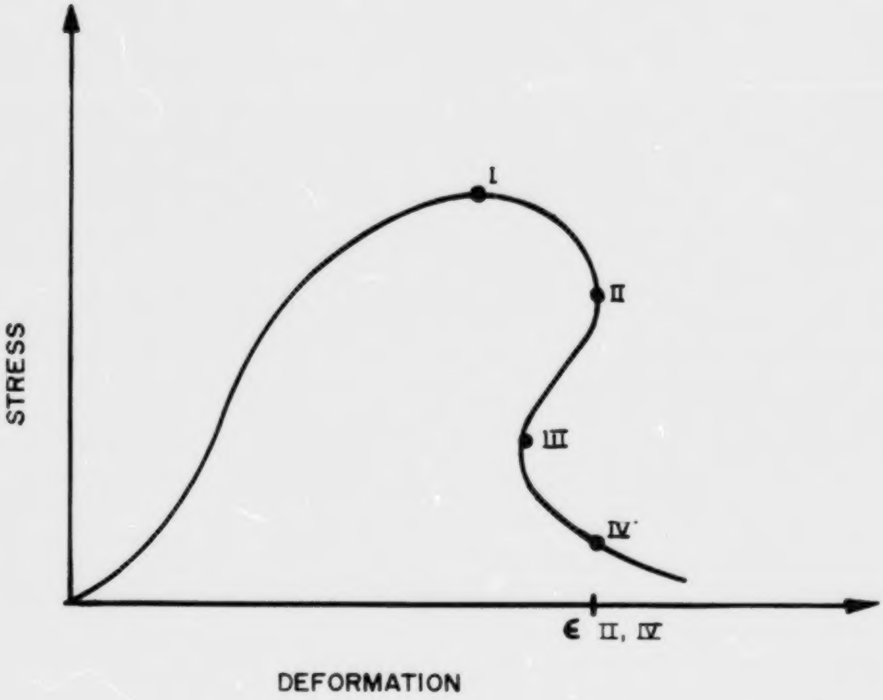

(AFTER HUECKEL, 1980)

Date FEB. 24, 1987.
Project 861-1290

Golder Associates

Drawn TMG
Chkd

5. FACTORS AFFECTING THE OCCURRENCE OF OUTBURSTS

5.1 Introduction

The outburst case history and model reviews, the analysis of the Sydney Coalfield data, the review of field data related to the effect of shotfiring on stresses and rock mass behaviour around underground excavation, and the results of laboratory testing carried out for this study have identified a wide spectrum of parameters believed to be involved in the physical mechanisms associated with coal, and rock and gas outbursts. This section presents a review of these parameters and a description of their interrelationships. Their relevance in a conceptual model of rock and gas outburst is also discussed.

During the review, consideration was given to retain the original nomenclatures used by various authors (where practicable) to illustrate the difference in the proposed concepts. However, due to the widely different terminologies used by different authors, it is considered, for reason of clarity, that the commonly used rock mechanics terminologies be employed to describe the proposed concepts and the factors involved. For example, the term "gas quantity" referred to by some authors likely relates to "gas pressure" while the term "critical depth of overburden" can be described by using the more commonly used term "initial in situ stresses".

Factors considered to be relevant to the outburst phenomenon were identified by various researchers and they are listed in Table 5.1. The matrix of factors presented in the table provides a useful perspective of the relative significance of the factors considered to be affecting the outbursts either in initiating the outburst or in providing an indication of burst-prone conditions.

The following section discusses the influence of these factors on the physical mechanisms of rock and gas outbursts. The role they are likely to play in the events reported in the Sydney Coalfield are then analysed.

5.2 Stresses in Rock Mass

5.2.1 In-situ Stresses

The influence of rock stresses on the initiation of dynamic event was recognized by many researchers. The fact that a majority of the cases presented in Table 3.2 took place in development headings or faces advancing in virgin districts is illustrative of the influence of in situ stress on the occurrence of outbursts.

The stresses existing in an undisturbed rock mass are related to the weight of the overlying strata and the geological history of the rock mass. For a relatively horizontal deposit, the vertical stress can be approximated by the overburden load, i.e.

$$\sigma_v = \gamma h \qquad (5.1)$$

where γ = Density of the strata above
h = Depth below ground surface

The horizontal stresses in totally undisturbed conditions are related to the vertical stress based on elasticity.

$$\sigma_h = \sigma_v(\nu/(1-\nu)) \qquad (5.2)$$

where ν = Poisson's ratio

However, field measurements around the world (Hoek and Brown, 1980) have demonstrated that the horizontal stresses were generally found to be higher than the vertical stress. They are considered to be the results of a combination of gravitational, tectonic and thermal loading.

Anomalies in the in-situ stress regime could be created by the presence of geological features such as faults, dykes and other intrusions, strata dip changes and thickness variations. Differences in elastic properties of the rock strata could also alter the stress distribution. Fault planes and, to some extent, the contact between stiff and soft rock mass will generally transmit normal stresses while the tangential stresses will be altered according to the frictional characteristics of the contact plane. Accordingly, the boundaries of irregular shaped inclusions such as sandstone channels could be under highly anisotropic stress conditions.

5.2.2 Stresses Around Mine Openings

Not-withstanding the origin of the horizontal and vertical in-situ stresses, the creation of a cavity in the rock mass causes stress redistribution and hence alters both the directions and magnitudes of these stresses around the cavity. The volume of rock disrupted by the stress changes is related to the size and geometry of the excavation. The radial stress component will be zero at the cavity boundary and gradually increase to the virgin stress state at some distance from the cavity boundary. The tangential stress component, however, will either increase or decrease at the cavity perimeter depending on the location of the point on the boundary, and the ratio of the in-situ horizontal to vertical stresses.

The stress concentration/reduction around the cavity will bring the rock into different states of stress. At the cavity perimeter, the rock is essentially subjected to a biaxial stress field. As the distance from the cavity perimeter increases, the increasing confining effect of the rock mass will bring along a triaxial state of stress.

For a rock mass subjected to anistropic in situ stresses, the direction of drivage in relation to the major principal stress will significantly affect the stress concentration around the underground opening. Variations in the stress concentration patterns along different alignments were numerically analysed by Revalor, et al, (1985). It is also recognized that when the strata consist of materials of different elastic and strength properties (such as coal measures strata), considerable stress variation could develop at their interface and the overall rock mass behaviour may be difficult to assess even with numerical modelling as it often involves simplifications.

A study on the occurrence of outbursts must encompass an assessment of the influence of a chosen mining method. An appreciation of the stress configurations resulting from mining operation would often provide guidance in the planning and sequencing of mining layouts. Of interest in this aspect of the study are the stresses in the vicinity of longwall panels.

High vertical stress in the abutments of the longwall panels are expected but the exact location of the stress concentration peak can vary due to the strength properties of the strata. For instance, the peak vertical stress can be displaced away from the perimeter of the opening due to failure or yielding of the unconfined material in this zone.

A stress monitoring programme carried out at Hickleton Colliery (U.K.) by Shepherd and Kellet, (1973) indicated high concentration (≈120 MPa) of vertical stress in the front abutment of an advancing longwall face under a rigid sandstone unit. The stress change was approximately equal to six times the vertical stress (calculated using the overburden load) when the face came within 10 ft. of the instrumented station (located ahead of the face).

Figure 5.1 shows the vertical stress concentration in the front and side abutment zones of a typical longwall operation in U.K. (Whittaker 1983). Although these conditions may not be directly applicable to the Sydney Coalfield, the overall stress distribution is illustrative of the magnitudes of stress concentration factors that may be anticipated.

However, the influence of the longwall panel over the distribution of horizontal stresses is more difficult to evaluate. The horizontal stress distribution is affected by the layering of the strata, the caving and subsidence zones (of reduced elastic modulus) above the longwall panel and hence is strongly dependent on the elasticity modulus of the surrounding strata. There are also indications of the existence of horizontal stress shadow effects in the immediate vicinity of the longwall panel.

Maximum advantage can be taken of the relaxed ground immediately adjacent to the longwall panel when the gate roads are developed some distance behind the face and this layout is in use in the Sydney Coalfield. Similarly, the development of other headings, such as airways, could be sequenced to maximize the drivage within stress-relieved ground or stress shadow zones.

5.3 Mechanical Properties of Rock

The material involved in most of the reported rock and gas outbursts is sandstone. In all cases, the material was reported to be strong and rigid although, in the same sequence, non-bursting sandstone beds of higher strength and/or rigidity were often noted. The following is a summary of the reported mechanical properties of burst-prone sandstones from various locations.

Location	Mechanical Properties of Burst Prone Sandstone
1. France and Germany	σ_c = 60-80 MPa E = 20.7 GPa
2. Japan	σ_c = 78-108 MPa
3. Russia	σ_c = 90-120 MPa E = [illegible].5 GPa ν = 0.15 with pore gas pressure of 5 MPa: E = 17.7 GPa ν = 0.17 σ_t = 11.8 MPa

The mechanical properties of the material influence its behaviour under stress and determine the material failure characteristics. These aspects are discussed in the following paragraphs.

5.3.1 Stress-Strain Relationships

Conventional testing to study the mechanical and elastic properties of a rock material generally consists of monitoring the loading on the specimen and measurement of deformations parallel and perpendicular to the direction of loading. The stress-strain relationship of the material is obtained by plotting the stresses applied against the strains measured.

From this relationship, the elastic constants of the material, Young's Modulus and Poisson's Ratio, can be determined. It should be noted that these constants are dependent upon the loading conditions as they are different in compression and tension.

The development of stiff testing frame has permitted the definition of the post failure stress-strain relationship of rock materials. This part of the relationship is characterized by a negative slope and the brittleness of the material will be proportional to the magnitude of the negative slope.

5.3.2 Extension Fracture in Brittle Rock

5.3.2.1 Effective Tensile Stresses

It has been shown experimentally (Obert and Stephenson (1965), Fumagalli (1966), Trollope and Brown (1966) and Brown and Trollope (1967)) that by loading a cylinder (of low tensile strength) of rock laterally in a biaxial stress field, it is possible to fail the sample by longitudinal extension. This has led to the following definition of effective tensile stresses σ_x', σ_y' and σ_z' which are induced by the applied triaxial stress system.

$$\begin{aligned} \sigma_x' &= \sigma_x - v'(\sigma_y + \sigma_z) \\ \sigma_y' &= \sigma_y - v'(\sigma_x + \sigma_z) \quad (5.3) \\ \sigma_z' &= \sigma_z - v'(\sigma_x + \sigma_y) \end{aligned}$$

with $\sigma_x, \sigma_y, \sigma_z$ = 3 mutually perpendicular applied stresses
v' = parameter dependant upon the structure of the material

If the longitudinal stress (σ_z) is absent (i.e. $\sigma_z=0$), the material is subjected to a biaxial stress field and the induced tensile stress in the z direction is:

$$\sigma_z' = -v'(\sigma_x + \sigma_y) \quad (5.4)$$

or $\sigma_z' = -2v'\sigma_r$

with $\sigma_r = \sigma_x = \sigma_y$
(e.g. the confining stresses in a triaxial cell).

Biaxial failure would occur when

$$-2\,v'\sigma_r > f(\sigma_t) \quad (5.5)$$

where $f(\sigma_t)$ = a function of the tensile strength of the material

This mode of failure was observed when Pier Cap sandstone samples were tested (at the University of Toronto) for this study, using a conventional Hoek (triaxial) cell, a radial stress of only 22.8 MPa was required to create failure. More detailed discussion of the laboratory testing programme undertaken for this study is given in Section 6.2.

5.3.2.2 Extension strain criterion for Fracture Initiation

A very simple empirical extension strain criterion for fracture initiation in brittle rock was proposed by Stacey, (1981) on the basis of the effective stress theory. He stated that fracture initiation of brittle rock will take place when the total extension strain of the rock exceeds a critical value which is characteristic of that rock type or simply, fracture initiates when:

$$\epsilon \geq \epsilon_c \quad (5.6)$$

with ϵ_c = critical extension strain

For linear brittle material, the critical strain occurs in the direction of the minor principal stress and is given by:

$$\epsilon_3 = \frac{1}{E}[\sigma_3 - \nu(\sigma_1 + \sigma_2)] \qquad (5.7)$$

The critical extension strains for various rock types are summarized in Table 5.2. Strain levels shown in this table correspond to stress levels approximately equal to 30% of the uniaxial compressive strength of the material. These critical strains represent the strain associated with fracture initiation. Continuous fracturing, and failure would take place at higher value of extension strain, and a factor of 2 was suggested.

Coates, (1981) reported the results of model experiments on the evolution of fracture at low confining pressure. They showed that extension of fractures parallel to the major principal stress are coincident with the yield point on the lateral strain vs. axial stress curve.

5.3.2.3 Mechanism of Rock Fracturing Close to a Free Face

The fracturing of rock parallel to the direction of maximum compression was also studied by Fairhurst and Cook, (1966). They explained such failure on the basis of the extension of Griffith flaws (cracks) in a compressive stress field. A brittle rock loaded just beyond the "Griffith compressive strength" value (σ_g) is assumed to consist of numerous flaws parallel to the direction of loading. The "Griffith compressive strength" corresponds to the stress level on a stress-strain curve marking the change from the region of elastic compression without crack growth to the region of non-elastic compression. The cleavage parallel to the direction of maximum compression is a true mode of fracture initiation in brittle rocks.

These authors also examined the formation and subsequent buckling stability of laminated slabs close to a free face. They stated that on each incipient slab surface, the cleavage forces generated by Griffith flaws exactly balance the cohesive forces at the crack tips, provided that $\sigma_{applied} > \sigma_g$. For any slab to become fully developed, a finite amount of energy equal to the residual surface energy necessary to complete the formation of the slab must be supplied. As a result of the force and energy equilibrium between the cleavage forces (generated by $\sigma_{applied}$) and the cohesion, this slab will buckle in accordance with the Euler's relations. It should be recognized that when $\sigma_{applied} > \sigma_g$ the modulus, E, will probably have been reduced by the internal cleavage (microfracture) of the rock. Hence, the extent to which the individual slabs will develop depends upon how the applied stress varies as the column shortens by buckling. If the applied stress changes slowly with displacement, buckling may well proceed until the slabs are broken. If it changes rapidly, unbroken but buckled slabs may remain against the free face. The variation of applied stress with displacement under field condition depends upon the geometry of the excavation. It will change slowly if the excavation is wide in relation to the length of the stressed face, and rapidly if it is narrow.

Close to a free face, a biaxial state of stress exists and buckling of the first slab frees the next one which then buckles and the process repeats itself. In practice, the compressive stress acting normal to the free face of an underground opening increases toward the interior of the rock mass. This would tend to limit the formation of the slabs.

On the basis of the mode of failure described above, roof support could have a major bearing on the development of fractures as it would alter the confining forces on the rock undergoing failure. For example, successful results were obtained by bolting tunnel sidewalls subjected to slabbing (Fairhurst and Cook (1966)).

5.3.3 Core discing

Exploratory diamond drilling in the channel sandstone of No. 26 Colliery have produced core discing. This is a phenomenon that has been experienced in many other sites (e.g. Garood (1984), Gimm and Pforr (1964), Josien et al (1982), Seito et al (1983), and Paul (1983)) and it is generally considered that core discing is related to the strength of the rock and the in situ stresses in the rock mass into which the borehole is drilled (Obert and Stephenson(1965), Jaeger and Cook(1971). Similar core discing research are also taking place in France (Chemaou (1984), Josien (1985)).

Laboratory testing carried out by Obert and Stephenson, (1965) has shown the conditions under which core discing occurred. It was found that core discing did not occur indiscriminately in all rock types. For example, under laboratory conditions, core discing was induced in Indiana limestone, Nova Scotia sandstone, Vermont marble, Maryland marble and Georgia granite, but the South Dakota chalk did not disc under any combination of applied stresses. Triaxially loaded samples were cored under various confining and axial stresses. It was proposed that discing occurs when:

$$S_r \geq k_1 + k_2 S_a \qquad (5.8)$$

where S_r and S_a are the radial and axial stresses (with reference to the borehole axis) under which core discing occurred, and k_1 and k_2 are constants derived from a least square plot of various combinations of S_r and S_a.

By carrying out the experiment without applying axial stresses, the value of k_1 can be obtained. This constant was compared with the mechanical property constants of the various rock types tested and it was found that it correlated with the shear strength, S_o, (cohesion) of the rock by:

$$k_1 = 3400 + 2.0\ (S_o) \qquad \text{(in psi)} \qquad (5.9)$$

The value of k_2 for the various rock tested averaged to 0.7 although one of the rock types tested was called Nova Scotia sandstone, for which $k_2 = 0.59$.

Without any laboratory testing data on the No. 26 Colliery sandstone under the prescribed loading condition described by Obert and Stephenson (1965), it is difficult to discern whether expressions (5.8) and (5.9) are valid for the No. 26 Colliery sandstone under field conditions. It is known from the in situ stress measurements in No. 26 Colliery that the in situ stresses in the siltstone layer range from 23 to 25 MPa (Section 2). Stresses in the sandstone channels could be higher as they form irregular inclusions in the coal measures strata. Further laboratory scale tests could be pursued to study the validity of the above expressions for Lingan sandstone.

Nevertheless, the fact that consistent discing occurs in the sandstone when penetrated by a borehole indicates that the material is susceptible to failure by shear under low normal stresses. This is entirely consistent with the concept of rock failure by under biaxial loading at the free face of a development driven into the sandstone (Section 5.3.2.).

5.3.4 Effect of Rock Mass Properties on the Blasting Process

Blasting (shotfiring) is often used in underground development of coal mines. The blasting process is affected by the rock mass properties. They include the structural geology and the failure behaviour of the rock mass.

- Structural Geology

The effects of the rock structure on the blasting process and the rock fragmentation can be grouped in two categories: micro-scale and macro-scale effects. The effects of micro-fissures on blasting have been studied by Dally et al, (1976) in laboratory tests. It was concluded that flaws (micro cracks and pores) affect fragmentation in two different ways. First, they are acting as crack initiation sites by the passage of the reflected tensile wave from the blasting process. Secondly, the flaws enhance branching by reducing the energy requirement to drive the cracks. Micro-fissures also influence the elastic behaviour of the rock mass. Preferentially oriented micro-structures could induce large variations in the rock properties that can be revealed by wave velocity anisotropy.

Nevertheless, macro-fissures such as existing bedding and joint planes are the most important blasting variable as far as the degree of fragmentation and wave propagation are concerned. They override any of the physical and mechanical properties of the rock (Hagan and Harris, (1977)) and define the fragmentation limits. Where a new fracture is developed, it terminates prematurely where it intersects a pre-existing crack or bedding plane.

- Failure Behaviour

The failure behaviour and energy absorption property of the rock mass largely influence the blasting process (Kutter and Fairhurst (1971)). The physical properties of the material that relate to the ability of the material to absorb, store and release energy are of utmost importance.

It was found by Lang, (1976) that the elastic brittle behaviour of the rock affects the shock wave type of rock failure during blasting. The more brittle the rock mass, the higher is the fracturing effectiveness of the strain wave created by the blast. In this type of failure mode, the rock stores a large amount of energy and releases it violently. Hence, brittle rocks are more susceptible to outbursts.

In less brittle rocks, however, plastic deformation occurs. A considerable amount of energy will be absorbed instead of being used for the fragmentation of the rock mass during the blasting process (Pearse, (1955)). Failure of these types of rock, during blasting, is associated with the shearing action of the expanded gases causing outward deformation. This results in coarse fragmentation with large blocks and slabs.

The attenuation of the strain wave energy, within the burden distance, largely reduces the explosive potential to create tensile stresses. The attenuation of the strain wave varies inversely with the distance to the power of 1.4 in strong, brittle rocks whereas values up to 2.5 are used in less brittle rocks (Coates, (1981)). Attenuation of the strain wave also occurs in jointed rock mass. The greater the intensity of fracturing of the rock mass, the less brittle the failure behaviour of the rock mass.

5.4 Hydraulic Properties of Rock

5.4.1 Porosity

Gases in coal measures strata are trapped in the pore spaces within the formation rock. Porosity is a parameter which is defined as the ratio of the volume of voids and the total volume. It may be classified as absolute or effective. The absolute porosity considers all the void space, being interconnected or not. Effective porosity only takes into account the connected pore volume. The effective porosity can be determined using various porosimeters, whereas, the measurement of absolute porosity requires that the sample be crushed to its individual grain size. The grain volume being given by the weight and density of the materials.

The porosity of the strata is established and altered by the geological environment. The voids existing between the grains cemented during the initial formation of the strata create the primary porosity. It is, therefore, inversely proportional to the degree of cementation. Porosity is further reduced with increasing amount of fine grains and/or a reduction in the spheriness of the grains. In sandstone, the primary porosity makes the most of the rock porosity although further alteration of the strata by compaction, fracturation, solution and remineralization will produce the secondary porosity.

In Germany, burst prone sandstones have a porosity of 10-14% whereas non-burst prone ones have a porosity ranging from 2.7 to 6.9%. It was found that the porosity increased with an increase in the quartz-feldspar content and/or a decrease in the phyllosilicates - carbonates content. In addition, it was indicated that when less cementing materials (phyllosilicates-carbonates) are present, there is a higher grain-to-grain quartz binding, resulting in reduced tensile strength. It was also noted that the quartz grain size was twice as large in the burst prone strata than in the non prone ones (Paul, (1983)).

5.4.2 Permeability

Permeability is the property of the rock to permit fluid flow through the interconnected pores. Permeability is affected by the same factors as porosity, ie. grain size, angularity, distribution and packing, degree of cementation and consolidation. In addition, permeability of a rock to gas is greater than to liquid (Klinkenberg, (1941)). Rock permeability to a gas is a function of the mean free path of the gas molecules (eg. the average distance travelled by a molecule between collision with other gas molecules or rock material) which is further influenced by pressure (both rock and gas pressure), temperature and the type of gas. If the mean free path is small, ie. at high pressures, the rock permeability to gas approaches that for liquid. The effect of rock stresses on permeability is discussed in section 5.6.

5.5 Lithology

The sedimentation process itself is a source of variation in the rock properties. Within similar rock units, such as sandstone or siltstone, changes in grain size, distribution, degree of cementation, etc. are often noted. These form mini beds within the rock unit where rock properties would be altered. Furthermore, the deposition mechanism creates high anisotropy as the properties perpendicular to the bedding are often different from the ones measured parallel to it (Deere, (1968) and Hoek, (1968)). This includes mechanical properties, porosity and permeability, and wave propagation and attenuation characteristics.

In Russia, over 150 burst prone strata have been identified. The rock most frequently found to have an outburst hazard are alluvial sandstones, sandstone from underwater river drifts and offshore sandstones (Karagodin, 1983).

5.6 Variation in Rock Properties in a Changing Stress Regime

5.6.1 Effect of Confining Pressure on Rock Failure

The effect of confining pressure and the associated pore pressure on rock failure was studied by Cornet and Fairhurst, (1981). The following is a summary of their findings:

> "In the case of low confining pressure, the large opening of cracks would be associated with a marked decrease of pore pressure. Therefore, the associated effective stresses would be increased also. This corresponds to the well known 'dilatancy-hardening' phenomenon described by Brace and

> Martin, (1968). In the case of intermediate confining stresses, the phenomenon of dilatancy-hardening will still take place near the peak, but when shear occurs, it will be associated with an increase of pore pressure. The effective stresses in the solid will, therefore, be decreased, and failure will tend to be more unstable. This has sometimes been referred to as an 'increase of brittleness' due to the presence of fluids.
>
> In the case of higher confining pressure, the pore volume is decreased even at the peak. The associated pore pressure is thus increased and the effective stresses decreased. We can expect this phenomenon to be associated with a 'softening' or 'weakening' effect rather than a 'hardening' or 'strengthening' as is assumed to be the case."

5.6.2 Effects of Loading Rate

From their experiences, (Brace, and Martin, 1968) concluded that the law of effective stress holds for crystalline rocks of low porosity as long as loading rates are kept below a certain critical value. The critical rate is a function of such factors as the rock type and the type of fluid in the pores. The law of effective stress states that the strength of a porous material is a function of the effective stress which is given by:

$$\sigma^* = \sigma - P_p \qquad (5.10)$$

with σ^* = effective stress

σ = applied stress

P_p = Pore pressure

If a low porosity (generally low permeability) rock is subjected to a high strain rate, the fluid may not permeate the pore space completely. This effectively develops a transient condition of drainage and results in a non-uniform pore pressure distribution. (Cornet and Fairhurst, (1981)) however, expect this phenomenon to disappear at high confining pressure in drained conditions. In undrained conditions, the phenomenon would be reversed since it would be associated with increase in pore pressure.

5.6.3 Effect of Stress Changes on Rock Properties

Rock permeability also varies with changes in the stress regime. Petroleum engineers studying the flow behaviour in tight gas reservoir found that the flow rate was sometimes lower than that predicted using Darcy's Law. Vairogs et al, (1971) conducted a study to demonstrate that permeability reduction due to rock stress was more important in low permeability rock than high permeability ones. Samples were tested under a range of hydrostatic stress, the permeability at 3.5 MPa (500 psi) being taken as the reference permeability K_b. Figure 5.2 shows the permeability ratio vs. the effective confining pressure.

Similar tests were undertaken by Mordecai et al (1971). Sandstone samples were tested in triaxial state of stress to failure and permeability changes were monitored. Figure 5.3 shows typical results of permeability change vs. deviatoric stress at four confining pressures. They concluded that with increasing confining pressures, the reduction in permeability is larger as the axial stress is also increased. In all cases, the permeability reduction is followed by a sharp increase as the sample approaches the failure load. The point of minimum permeability is termed the fracture initiation point at which a small increase of axial stress would generate fracture initiation and thus increase the permeability. This increase in permeability is nevertheless smaller with increasing confinement (confining stresses). The results also showed that rock started to fracture long before ultimate failure. A similar conclusion was reached by Stacey (1981).

Rock elastic constants also change with changing stress regime. This was demonstrated by Kwaniewski (1983) on a series of triaxial tests on sandstone samples. In particular, the following parameters were investigated: Young's Modulus, ductility, and angle of internal friction. Figure 5.4 summarizes the reported results.

Recent work by Santarelli et al, (1986) illustrated the effects of using a confining pressure dependent elastic modulus on the computation of stress concentration around a circular opening in an hydrostatic stress field. Elastic analysis using a constant modulus predicts a maximum stress concentration factor of the order of 2 at the immediate wall perimeter. Analysis using a σ_3 dependent elastic modulus shows that the peak stress concentration was of lower magnitude.

5.6.4 Rock Behaviour Under High Rate of Stress Change

It is recognized that the rate of loading influences the uniaxial and triaxial failure strength of the material (Logan and Handin (1970); Brace and Martin (1968)). Similar results were reported by Golder Associates in the testing programme associated with this research project (Golder Associates report No. 841-1287-1,-2 (1984,1985). Similar rate effect was also noted when the material is tested in tension (Table 5.3).

Under field conditions, the stress changes, during the creation of an opening, do not generally occur at constant confining pressure. At the crown of a newly excavated heading, tangential stress increases while radial stress decreases. If blasting is used, this static stress change will occur rapidly. The dynamic stress effects of blasting will cause further changes in the stress regime.

Laboratory tests to simulate the effects of rapid stress changes have been undertaken by a number of researchers. Results of their experimental findings are summarized below.

Gimm and Pforr (1964) investigated the discing failure encountered in outburst prone materials in their study of salt and gas outbursts. They proposed that this type of failure, and the presence of exfoliation noted in outburst cavity, were the result of the change in the stress state from triaxial to biaxial.

Gas-free samples of salt rock were inserted in an open ended steel pressure cylinder provided with a circular opening of smaller diameter at the bottom end. The samples were loaded from the top end at a high rate of loading and were therefore subjected to triaxial stresses as a result of lateral constraints. The rock was permitted to deform only on the lower end where the circular opening was located. Around this open surface, the stresses were essentially biaxial. When the applied axial stress was brought close to the uniaxial compressive strength of the sample, pieces of rock fell out of the bottom end. The cavity produced in the samples were curved towards the direction of applied stress and showed the same bed separation caused by stress relaxation as had been found when coring outburst prone zones. They concluded that the intensity of bed separation and energy release is a function of the rock properties and the magnitude of sudden change in the nature of the stresses.

Khristianovich and Salganik, (1983) reported a series of experiments on coal cubes subjected to triaxial compression by loading plates. The front plate had a hatch which could be instantaneously opened.

In the first group of experiments, non-gas saturated specimens were tested. After being subjected to isotropic compression, the hatch was opened. No change was noticed up to 100 MPa. With further increase in loading, the coal was squeezed out of the hatch.

Specimens previously saturated with gas were then tested with isotropic compression up to 30 MPa. The hatch was opened and the outburst occurred. Further testing was also carried out in which the pressure on the front loading plate was considerably lowered in advance but each hatch opening was accompanied by an outburst. In the last series of tests, the loading on the side plates was lowered prior to opening of the front hatch and no outburst was observed.

Kobayashi et al, (1978) studied the rupture behaviour of two types of sandstone subjected to rapid reduction of confining pressure at constant differential stress. They found that the Mohr's stress circles representing the rupture of these sandstones (failed by rapid reduction of confining pressure), existed above the Mohr's failure envelope obtained by conventional triaxial compression test. They concluded that the sandstones failed violently under excessive elastic energy condition which is developed by rapid reduction of confining pressure.

The time required for reducing the confining pressure to atmosphere was approximately 0.2 seconds.

In a similar series of experiments carried out by the University of Toronto for Golder Associates (report no. 841-1287-1,-2 (1984-1985), samples of homogeneous sandstone (Pier Cap Sandstone) were first loaded to hydrostatic conditions of 30 MPa. The axial stress was then increased to values ranging between 50 and 200 MPa. Then, the confining pressure was instantaneously released keeping the applied axial load unchanged. The confining pressure at failure was recorded and the failure points (σ_1, σ_3) were found to correlate well with the failure envelope derived from the fast rate triaxial test (43.1 MPa/s uniaxial loading). This failure envelope is higher than that obtained from testing the same rock type using standard ISRM loading rate.

In a different series of tests, simultaneous rapid changes in axial and confining stresses were carried out using a servo-controlled system on both σ_1 and σ_3 loading mechanism. Three sandstone samples were tested and all failed at strength much lower than the ones predicted by the failure envelopes of various rate tests (testing at different loading rates including ISRM standard rate). It was concluded that the progressive decrease in confinement of the specimen during axial loading allowed accelerated dilation of the specimen when it started to yield, bringing forward the failure of the sample.

Cylindrical specimens of fine grained homogeneous sandstone was subjected to impact loading by Hawkes, (1959) in his study of stress rate effects on material behaviour. It was concluded that the rock behaves elastically when subjected to a rapidly applied load. On this basis, the laws which govern the behaviour of stress waves in elastic media could be applied to the material behaviour during blasting in which the dynamic stress changes in the rock is very rapid.

5.7 Gas Effects

The in situ sandstone pore gas pressure is one of the most important factors in the outburst process but it remains virtually unknown due to intrinsic difficulties in determining pore gas pressure in low permeability materials. These difficulties are not limited to the Sydney Coalfield but were also reported by others (Suchodolski (1971) and Belin (1981)).

The type of gas involved in rock and gas outbursts around the world is mostly methane (CH_4) although carbon dioxide (CO_2) and nitrogen (N_2) were also reported (see Section 3). There seems to be a correlation between the magnitude of the events and the type of gas involved. Outbursts with CO_2 in the pore space are more damaging than CH_4 outbursts, which are more violent than N_2 outbursts.

Ettinger, (1969) discussed the decrease in strength in fossil coals by the action of different gases, the greatest effect was shown by carbon dioxide followed by methane and hydrogen. The molecule diameter of the gas affects its mean free path and hence, the permeability of the medium to this particular gas. This, in turn, will influence the distribution of the gas pressure gradient. The following effective molecular diameters were calculated by Breault, (1987) of the Institut de

Recherche en Electricite du Quebec (IREQ) using the gas viscosity coefficients:

H_2 = 2.74 Å
N_2 = 3.74 Å
CH_4 = 4.14 Å
CO_2 = 4.59 Å

It is reasonable to assume that steeper gradients are developed by molecules of larger effective diameter.

Quoted gas pressure values for outburst prone sandstone is highly variable. In German Democractic Republic Mansfeld district, N_2 gas pressure ranged from 8.4 to 12.6 MPa (Suchodolski (1971)). In France, at Merlebach Colliery, CH_4 gas pressure was evaluated to range between 3 to 10 MPa (Revalor, (1985)). Belin, (1981) presented Russian gas pressure data which ranged between 1.5 to 7.0 MPa while Sevelev, (1974) used a value of 5 MPa in his study. In the Ibbenburen Colliery of West Germany, CH_4 gas pressure was determined to be 6.0 MPa (Paul, (1983)). In Poland, at the Nova Ruda mine, CO_2 gas pressure ranged between 0.3 to 4.0 MPa. In Sydney Coalfield, the sandstone pore gas pressure was estimated to range between 2.8 and 8.0 MPa (Aston, Cain, (1985)) which compares well with the other published values.

The importance of the gas pressure is two-fold. Firstly, according to the law of effective stress for crystalline rocks, the principal stresses would be reduced in magnitude by an amount equal to the pore gas pressure. The change in σ_1 in the vicinity of the opening would generally be small but the change in σ_3 could be very significant and could lead to effective negative confining pressure if the pore gas pressure is sufficiently high.

Secondly, the assumption of a uniform gas pressure distribution within the rock is a simplification of the actual situation especially in the vicinity of an underground opening. A gas pressure gradient will develop close to the cavity boundary. The pressure gradient is a function of the rock permeability which, in turn, is a function of the type of gas, temperature and initial pressure (Josien, (1985)). In a closed pore system, deformation under stress may reduce the pore volume and increase the pressure until the pore gets intercepted by a growing network of micro-fracture. However, there is a generally lack of experimental evidence in this aspect of research, not only in Canada, but in other countries as well.

5.8 Blasting Effects on Surrounding Rock Mass

The Sydney Coalfield data review and the case histories review have indicated a strong correlation between the initiation of dynamic events and shotfiring. Furthermore, the literature review has shown that there is a definite lack of comprehensive analysis of the shotfiring effects in regard to its influence on the occurrence of rock and gas outbursts.

In the following paragraphs, the fundamental aspects of rock blasting with regard to the dynamic stresses generated and the blast induced damages to the surrounding rock mass are presented.

5.8.1 Theoretical Considerations of the Dynamic Stresses caused by Shotfiring

Explosive Pressure Generation

The detonation reaction during blasting can be described as a chemical phenomena such that a shock wave advances down a column of explosive material reinforced and fed by the chemical reaction preceding it.

This reaction can be considered to be supersonic in nature since the following relationship must be obeyed for the detonation process to be established:

For supersonic conditions, (Chapman-Jouguet postulate):

$$D_V = W + C \qquad (5.11)$$

where: D_V = detonation velocity (m/sec)
W = particle velocity (m/sec)
C = velocity of sound - media (m/sec)

From flash X-ray photography where small lead pellets were added to formulations of detonating high explosives and then photographed using pulsed X-rays, particle velocity (W) was found to approximately equal one quarter the detonation velocity (0.25 D_V).

Figures 5.5 (A) and (B) show the regions in a longitudinal profile of a detonation reaction, for both unconfined and confined cases. Immediately in front of the leading edge of the reaction zone is a high pressure shock front. Alternatively, behind the reaction zone is a region of expanding gas products. The pressures associated with this region are substantially lower than those generated in the shock front.

The peak pressures generated by the detonation shock front are extremely high and can be considered to have a duration equivalent to the detonation time of a given mass of explosive material (i.e. the length of time required to completely detonate a specific quantity of explosive material). The peak pressure developed in this particular region of the reaction can be calculated from the following relationship developed from experimental

From thermohydrodynamics:

$$P = \gamma D_V W \tag{5.12}$$

where: P = detonation pressure
γ = explosive density
D_V = explosive detonation velocity
W = explosive particla velocity

The above expression can be simplified somewhat noting that W is equal to 0.25 Dv, and can therefore be reduced to the following:

Substituting for W:

$$Pd = \frac{(\gamma Dv^2)}{4} \times 0.00987 \tag{5.13}$$

where: Pd = detonation pressure (atmospheres)
γ = explosive density (gm/cc)
D = detonation velocity (m/sec)
0.00987 = conversion factor

The thermochemical pressure (Pt), (the maximum pressure available to do useful work - expansion for fully coupled charge against borehole wall) is generally taken to be equal to about one-half the above detonation pressure (Pd), as shown below:

For expansion;

$$Pt = Pd/2 \tag{5.14}$$

where: Pt = thermochemical pressure (atmospheres)
Pd = detonation pressure (atmospheres)

The above equation assumes that the explosive material is in intimate contact with the borehole wall, and in this case the thermochemical pressure (Pt) would equal the borehole pressure (Pb). Any decoupling (by the use of smaller diameter explosives or larger blast holes) of the explosive charge from the borehole wall would result in lower borehole pressures as follows:

Expansion due to decoupling:

$$P_b = P_t\ (C_d/H_d)^m \tag{5.15}$$

where: Pb = borehole pressure (atmospheres)
Pt = thermochemical pressure (atmospheres)
Cd = charge diameter (mm)
Hd = borehole diameter (mm)
m = decoupling constant
(m = 2.6 for air)
(m = 2.16 for water)
(m = 1.50 for aggregate)

These equations show that the peak pressure generated by the shock front is independent of the explosive charge weight, but dependent on the detonation velocity, and charge density. Such information is useful when designing explosive formulations to suit particular blasting characteristics and applications (e.g. wall control, low density explosive products, blasting vibration reduction, perimeter control in underground mines, etc).

Shock Wave Travel in Rock

The detonation of an explosive charge fully coupled in a borehole, results in high borehole pressures (Pb) obtained with steep risetimes. The high stresses (hoop stress - radial and tangential) induced around a borehole cause the rock medium to compress and acquire an outward particle motion. This motion transmits the stresses further into the rock mass and away from the shot point. Longitudinal compression wave velocity (P-wave) travels at the velocity of sound in the in situ rock mass which, in competent rock can approach 6200 m/sec. Shear wave velocities are much lower than the P-wave first arrival by approximately one-half the P-wave value. Cracks are formed due to hoop stresses and as a result, high borehole pressures are dissipated quickly, typically less than 10 milliseconds.

Following the removal of the blast induced compressive ground stress, rock which has not failed rebounds elastically to its original state in a damped mode. The short duration of the blast induced compressive ground stress limits the zone of rock under compression at any time to a very narrow cylindrical region around the borehole wall. The resulting particle displacement from a single detonation in an elastic medium is a non-oscillatory pulse having only a compression cycle. Particle velocity and acceleration, being the first and second derivatives of the particle displacement, are damped oscillations. Particle velocity pulses close to a detonating explosive charge can have frequencies of oscillation greater than 5 Khz.

The mechanisms associated with rock breakage are controversial, however high speed photography in transparent material reveals that cracks are formed by hoop stress even when detonating boreholes are placed near a free face. The effect of any free face is to reflect compressional wave fronts into a tensile mode. The returning tensile wave can produce both tensile and shear failures at joints and seams in stratified rock providing the magnitude of the tensile wave is sufficient to separate the jointing planes. The returning tensile wave also has the ability to extend cracks caused by hoop stress simply due to the action of imposing increased stress on crack tips, propagating them further.

The effect of the tensile wave is to induce tensile stresses in the strata close to the boundary of the excavation. This is superimposed onto the static tensile stresses brought about by the change of loading conditions at the free face from a triaxial to a biaxial state.

Scaling Laws and Geometrical Dispersion

In the context of blasting, scaling is the designation of relationships correlating measurable event levels (stress, particle velocity, etc) at various distances from detonating charge of explosives confined in boreholes drilled in rock. A scaling factor based on a dimensionless parameter for distance is used. The scaled distance is derived from the effects of geometrical dispersion on the outbound events occurring in a detonation.

The total energy of the ground motion wave occurring in the rock mass around a detonating borehole varies directly with the weight/energy of a given charge. As the ground motion wave propagates outwards from a detonating charge, the volume of rock subject to the compression wave increases. Since the energy in the ground shock is distributed over successively greater volumes of rock, to preserve mass flow, the peak ground motion levels must decrease.

The stress wave front resulting from a top primed blasthole propagates in the form of an expanding V - shape or cone. When a blasthole is bottom primed, the expanding stress wave front will take the form of an inverted V.

The stress wave front from a column charge having a length to diameter ratio of at least 120:1 take the form of a steeply inclined cone such that the volume of this stress cone varies as the square of its radius. Thus measurable events such as stress, particle velocity, etc. have magnitudes on any point of the stress cone that are inversely proportional to the square of the distance from the shot point. Therefore, scaled distance can be represented by the following:

$$S_d = \frac{r}{w^{0.5}} \qquad (5.16)$$

where: S_d = scaled distance
r = distance to shot point (m)
w = charge weight (kg)

Stress Wave Distribution and Attenuation in Rock Media

Stress wave dissipation or attenuation is attributed to three mechanisms;

(1) viscous damping of ground particle vibrations due to cohesion of particles composing the rock mass, leading to lower ground vibration frequencies with increasing distances from the shot point.

(2) absorption of energy in the ground stress wave due to reflections at discontinuities and strata inhomgeneities in the rock (foliation, dykes), in which interactions between reflected pulses are

> often accompanied by a trend to selectively attenuate high frequency vibrations to lower frequency vibrations. Frictional attenuation of the stress wave is due to the natural resistance of the material to rapid variations of the stress level. It is a form of stress hysteresis in which energy is removed from the wave and expanded as heat (Hawkes, 1986).

From the particle motion standpoint, ground motion waves travel through strata of different acoustical impedance. Scattering of the ground motion waves, initiated at boundary discontinuities by reflections, lowers the peak vibration levels. Interactions between reflected pulses alter the frequency composition of the wave train. Low frequencies are selectively attenuated while some higher frequencies are added to the ground vibrations.

The presence of joints, fractures, faults, or shear zones in the path of a ground motion wave also act to scatter the peak vibrations. Some of the lateral components of ground motion are lost as the wave crosses a discontinuity. The degree of redirection and dissipation of a ground motion wave is related to the nature and frequency of structural discontinuities in rock.

The influence of rock mass characteristics on ground motion waves are very complex. An empirical approach can be taken by determining site attenuation factors in a blast monitoring program. Particle velocity can be determined at several points from a given shot point and when combined with the scaled distance values at each monitoring point, an attenuation curve can be obtained so that particle velocity can be predicted for any point along the path of ground motion travel. Line labelled PLL in Figure 5.6 represents the attenuation curve relating peak particle velocity (in/sec) to scaled distance (ft./$lb^{0.5}$) parallel to the bedding surfaces of a sandstone/shale at a western coal mine. The equation representing the attenuation line is given by:

$$P_v = 61.2\ (S_d)^{-1.56} \qquad (5.17)$$

where: P_v = peak particle velocity (in/sec)
S_d = scaled distance (ft/$lb^{0.5}$)

The effects of layering in stratified material are also shown by line PDR in Figure 5.6 which represents the attenuation curve across layers of a sandstone/shale/coal (blasting on surface, measurements taken in underground exploration adit). This attenuation curve is represented by the equation:

$$P_v = 15.2(S_d)^{-1.06} \qquad (5.17)$$

where: P_v = peak particle velocity (in/sec)
S_d = scaled distance (ft/$lb^{0.5}$)

It is noted that the ground motion waves attenuate (or disperse) faster when propagating across the bedding surfaces.

Stress in Rock Mass due to Ground Vibration

The stresses due to ground vibration in rock masses close to a detonating cylindrical charge of explosive can be calculated using elastic theory. A spherical coordinate system (r,θ) with the origin at the charge centre can be used to give the stress levels in the ground motion wave at a distance from a shot point as follows:

In a homogeneous, elastic and infinite medium:

$$\sigma_r = \gamma C_l v(r,T) \qquad (5.18)$$

and;

$$\sigma_\theta = \gamma C_l v(r,T) \qquad (5.19)$$

where: σ_r = radial stress
σ_θ = tangential stress
γ = rock bulk density
C_l = P-wave velocity
$v(r,T)$ = Radial particle velocity (change with time)

These equations give the theoretical stresses. However, a rock mass is not an ideally elastic, homogeneous material. As a result, any calculations based on the assumptions give only approximate solutions. Field measurements of dynamic stresses would provide more realistic data. Evaluation of dynamic stresses from blast monitoring is presented in section 6.1 of this report.

5.8.2 Theoretical Considerations of Blast Induced Damages to Rock Masses

When shock waves propagate through an undisturbed medium, the shock wave patterns can be expressed specifically in terms of a given chosen parameter providing the equation of state is known. Thus temperature, pressure, and particle velocity may be expressed specifically in terms of the velocity of the shock wave.

When a shock wave intercepts a medium of lower density (e.g. fracture rock or free face) after travelling through a medium of high density, the stress front is reflected as a tensile wave back into the incident medium.

The peak particle velocity level which would cause blast induced tensile slabbing or spalling (the most common from of damage in underground openings) is as follows:

$$V = (1728\ \sigma t)\ (\rho C_1)\ \text{(in/sec)} \qquad (5.20)$$

where: 1728 = conversion factor

σt = dynamic tensile strength (psi)

ρ = mass density of the rock ($\text{lb-sec}^2/\text{ft}^4$)

C_1 = P-wave velocity of rock (ft/sec)

With stratified rock, the tensile strength perpendicular to the strata depends largely on the cohesion between bedding surfaces and could be significantly lower than that of intact rock. It may be noted from equation 5.20 that in order to minimize damage to the rock mass, the vibration level should be kept below a threshold level determined by the wave propagation and strength characteristics of the rock.

In order to investigate the effects of the current blasting practices on the surrounding rock mass in the Sydney Coalfield, a field blast monitoring program was undertaken at the Lingan Mine. Section 6 presents the details of the field program.

TABLE 5.1 FACTORS RELEVANT TO OUTBURST PHENOMENA

FACTORS REFERENCES	Tectonic Stresses	High Anisotropy of Virgin Stresses	Orientation of Heading vs σ_1	Stress Concentration Insitu Stresses	Critical Depth of Overburden	Area of Disturbance From Previous or Present Mining	Core Discing	Structural Abnormalities of Stress (Faults Dyke, Dip Change, etc)	Material Strength/ Elastic Properties	Material Hydraulic Properties (Porosity, Permeability)	Lithology	Properties of Adjacent Rock Masses	Low Moisture Content of Coal	Gas Pressure	Gas Pressure Gradient	Type of Gas	Quantity of Gas	Rate of Advance	Coincidental with Blasting	Dynamic Loading/ Unloading Due to Blasting
REVALOR, R., et al (1985) RE: Sandstone & Gas Outbursts		●	●				●	●	●					●					●	
SUCHODOLSKI, Z. (1971) RE: Rock & Gas Outbursts	●				●			●	●	●	●					●	●		●	
KUSZNIR, N.J.: FARMER, I.W. (1983) RE: Coal & Gas Outbursts				●				●	●			●		●			●			
KARAGODIN, L., et al (1983) RE: Rock & Gas Outbursts				●			●	●	●		●			●				●	●	●
HARGRAVES, A.J. (1967) RE: Coal/Rock & Gas Outbursts				●		●		●	●	●		●		●	●	●		●	●	●
IGNATIEFF, A. (1954) RE: Coal & Gas Outbursts	●			●	●	●		●	●	●				●						
FISEKEI, M.Y.: BARRON, K. (1975) RE: Coal & Gas Outbursts				●				●	●	●		●		●		●				
SHEPHERD, J., et al (1984) RE: Coal & Gas Outbursts	●				●	●		●	●	●		●		●		●	●	●	●	
SINGH, J.G. (1984) RE: Coal & Gas Outbursts	●				●	●		●		●		●	●			●	●	●		
MAHTAB, A. (1982) RE: Salt & Gas Outbursts		●			●	●	●	●	●					●	●				●	
GIMM, W.A.R.; PFORR, H. (1964) RE: Salt & Gas Outbursts				●			●		●	●				●						
KHRISTIANOVICH, S.A.; SALGANIK, R.L. RE: Rock & Gas Outbursts (1983)				●				●		●	●			●	●			●	●	
LITWINISZYN, J. (1985) RE: Coal & Gas Outbursts										●				●	●	●				
PATERSON, L. (1986) RE: Coal & Gas Outbursts				●	●			●	●	●					●			●		
BARRON, K. (1972) RE: Coal & Gas Outbursts				●						●				●	●					
DIKUNOV, E.A. (1971) RE: Rockbursts in Tunnel Headings				●					●											●
PETUKHOV, I.M.: LINKOV, A.M. RE: Rockbursts (1983)				●				●	●											
ZORIN, F.N., et al (1981) RE: Sandstone & Gas Outbursts				●					●									●	●	●
HIRAMATSU, Y., et al (1983) RE: Coal & Gas Outbursts				●				●	●	●				●	●		●		●	
GRAY, I. (1980) RE: Coal & Gas Outbursts				●				●	●					●		●				
HARGRAVES, A.J. in JACKSON, L.J. RE: Coal & Gas Outbursts (1984)	●				●			●		●			●				●			
BELIN, J. (1981) RE: Coal/Rock and Gas Outbursts		●		●			●	●	●	●	●	●		●	●	●			●	●
JOSIEN, J.P. (1985) RE: Rock & Gas Outbursts				●			●		●	●				●	●					
PATCHING, T.H. (1963) RE: Coal & Gas Outbursts	●			●	●	●		●	●	●		●					●			
FARMER, I.W.; POOLEY, F.D. (1967) RE: Coal & Gas Outbursts				●				●	●	●				●			●			
SEVELEV, G.A. (1974) RE: Sandstone & Gas Outbursts				●					●	●				●	●		●			
GIMM, W.A.R., et al (1976) RE: Salt & Gas Outbursts	●							●									●	●	●	
WATANABE, Y., et al (1981) RE: Sandstone & Gas Outbursts				●					●	●							●		●	●
UJIRIRA, M., et al (1985) RE: Coal & Gas Outbursts				●				●	●					●	●				●	●

TABLE 5.2

A) CRITICAL VALUES OF EXTENSION STRAIN - (Based on testing of core sample)
(after Stacey, (1981))

ROCK TYPE	CORE SIZE	SPECIMEN LENGTH/ DIAMETER RATIO	CRITICAL EXTENSION STRAIN
Quartzite A	BX	2	0.000120
Quartzite B	BX	2	0.000109
Quartzite C	AX	2	0.000081
Quartzite D	BX	2	0.000107
Quartzite E	BX	2	0.000130
Lava A	BX	2	0.000152
Lava B	BX	2	0.000138
Diabase	BX	2	0.000175
Norite	NX	2.5	0.000173
Conglomerate Reef A	BX	2	0.000086
Conglomerate Reef B	BX	2	0.000073
Conglomerate Reef C	BX	2	0.000083
Sandstone	BX	2	0.000090
Shale A	BX	2	0.000116
Shale B	BX	2	0.000150
Shale C	AX	2	0.000095

DISTRIBUTION OF VERTICAL STRESS PRODUCED BY LONGWALL EXTRACTION SHOWING FRONT AND FLANK ABUTMENT ZONES

FIGURE 5.1

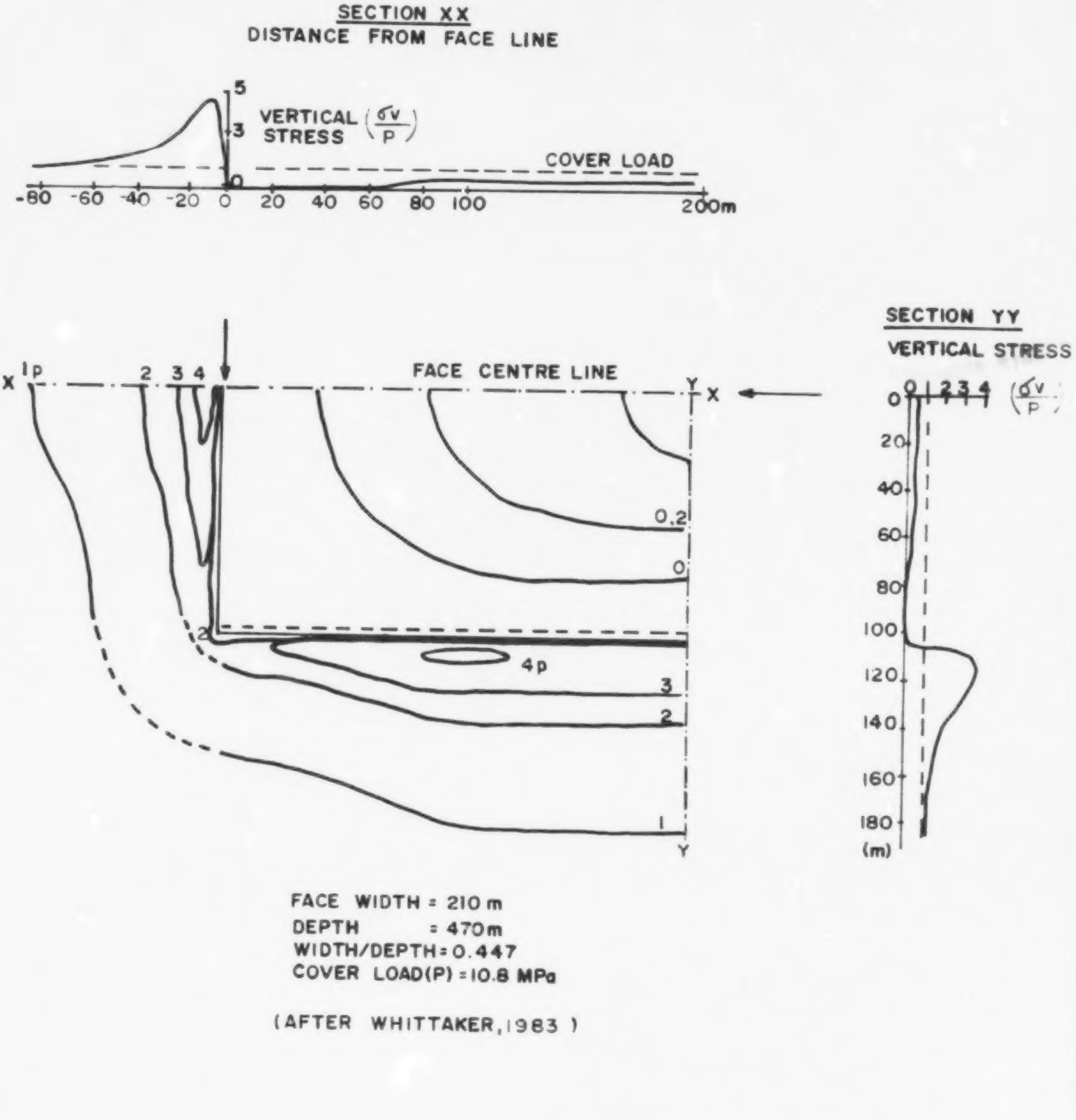

FACE WIDTH = 210 m
DEPTH = 470 m
WIDTH/DEPTH = 0.447
COVER LOAD (P) = 10.8 MPa

(AFTER WHITTAKER, 1983)

Date FEB. 23, 1987
Project 861-1290

Golder Associates

Drawn TMG
Chkd

PERMEABILITY REDUCTION DUE TO ROCK STRESS

FIGURE 5.2

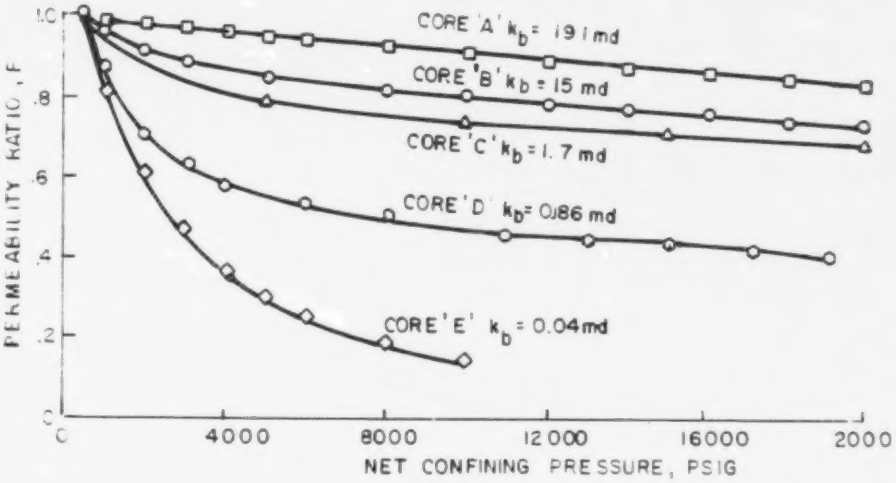

LEGEND

A - CHANUTE SANDSTONE
B - SAN ANDRES CARBONATE
C, D - SPRINGER SANDSTONE
E - FRIO SANDSTONE

ALL UNIFORM IN TEXTURE

(AFTER VAIROGS et al, 1971)

Date FEB. 9, 1987
Project 861-1290

Golder Associates

Drawn D M
Chkd

PERMEABILITY CURVES FOR INCREASING CONFINING PRESSURE

FIGURE 5.3

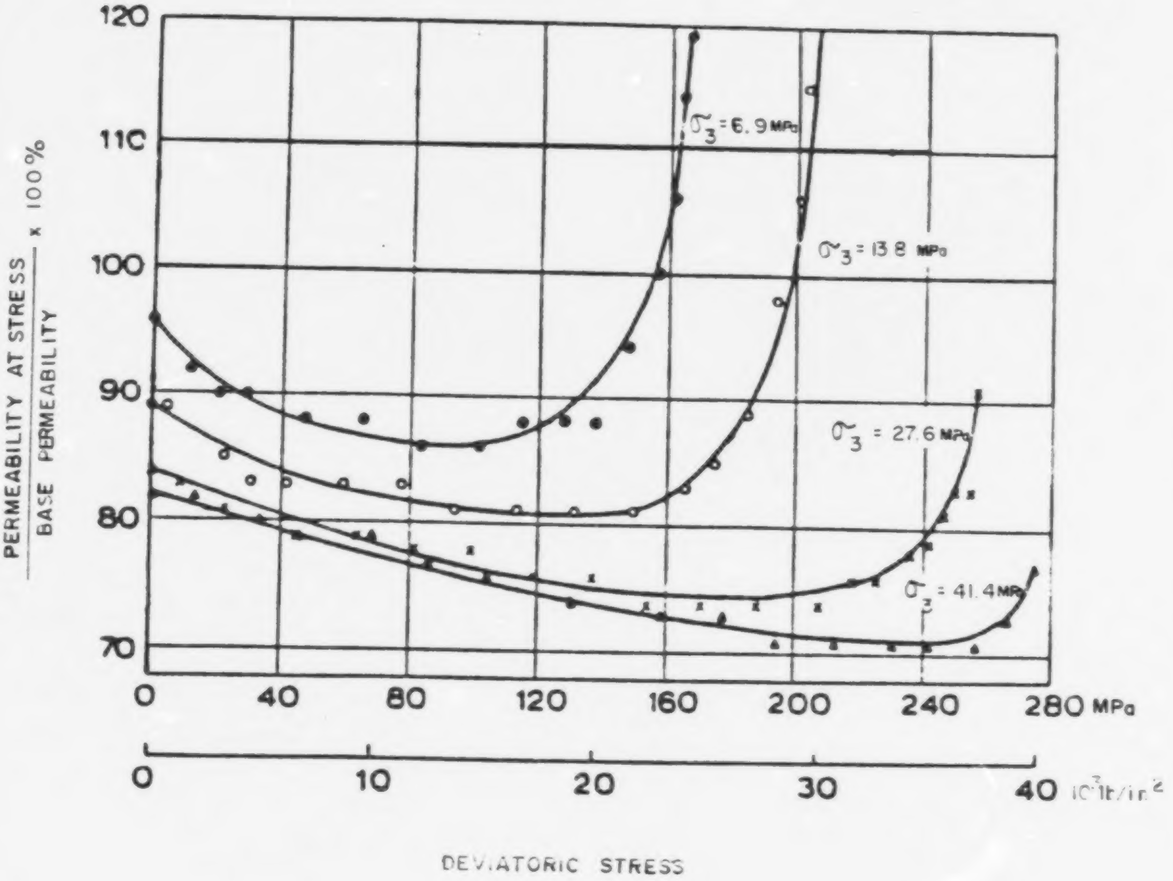

(AFTER MORDECAI AND MORRIS, 1971)

Date FEB. 6, 1987
Project 861-1290

Golder Associates

Drawn D.M.
Chkd

VARIATION IN ROCK PROPERTIES FOR 3 SANDSTONES WITH INCREASING CONFINING PRESSURE (after kwaniewski, 1983)

FIGURE 5.4

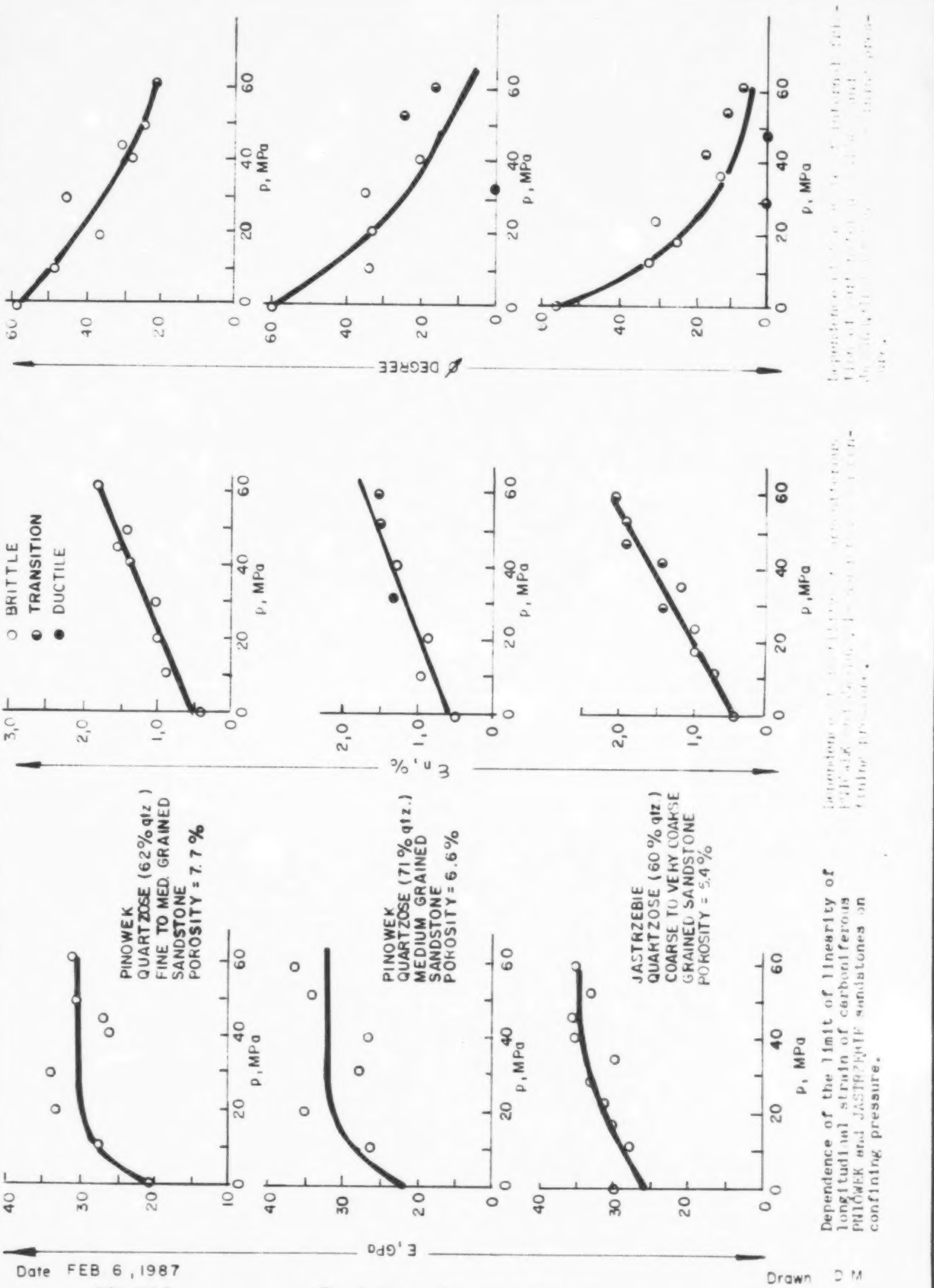

Date FEB 6, 1987

Project 861-1290

Golder Associates

Drawn D.M.

Chkd

PROFILE OF DETONATION IN AN INCOMPRESSIBLE AND A READILY COMPRESSIBLE MEDIUM

FIGURE 5.5

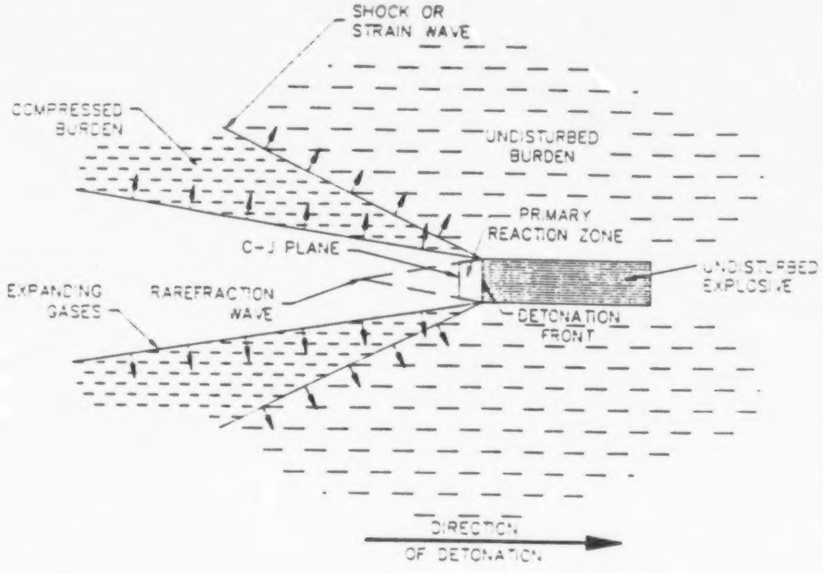
SHOCK OR STRAIN WAVE
COMPRESSED BURDEN
UNDISTURBED BURDEN
PRIMARY REACTION ZONE
C-J PLANE
UNDISTURBED EXPLOSIVE
EXPANDING GASES
RAREFRACTION WAVE
DETONATION FRONT
DIRECTION OF DETONATION

A) PROFILE OF DETONATION IN AN INCOMPRESSIBLE MEDIUM SUCH AS HARD, MASSIVE ROCK

REFERENCE: DUPONT - BLASTERS HANDBOOK

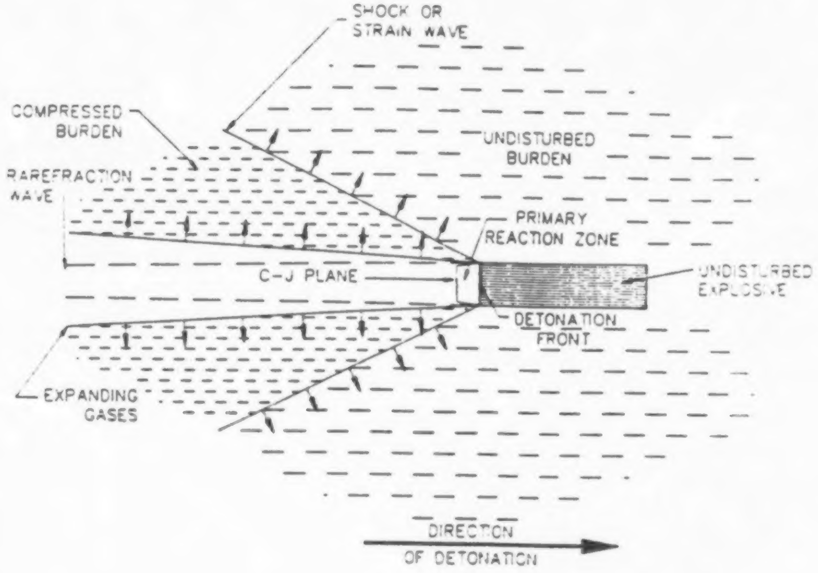
SHOCK OR STRAIN WAVE
COMPRESSED BURDEN
UNDISTURBED BURDEN
RAREFRACTION WAVE
PRIMARY REACTION ZONE
C-J PLANE
UNDISTURBED EXPLOSIVE
DETONATION FRONT
EXPANDING GASES
DIRECTION OF DETONATION

B) PROFILE OF DETONATION IN A READILY COMPRESSIBLE MEDIUM SUCH AS AIR, WATER OR SOFT ROCK

Date MARCH 1987
Project 861-1290

Golder Associates

Drawn D.M.
Chkd

FORM PRODUCED JUNE

TYPICAL COMPOSITE ATTENUATION PLOTS ACROSS LAYERS OF SANDSTONE/SHALE/COAL

FIGURE 5.6

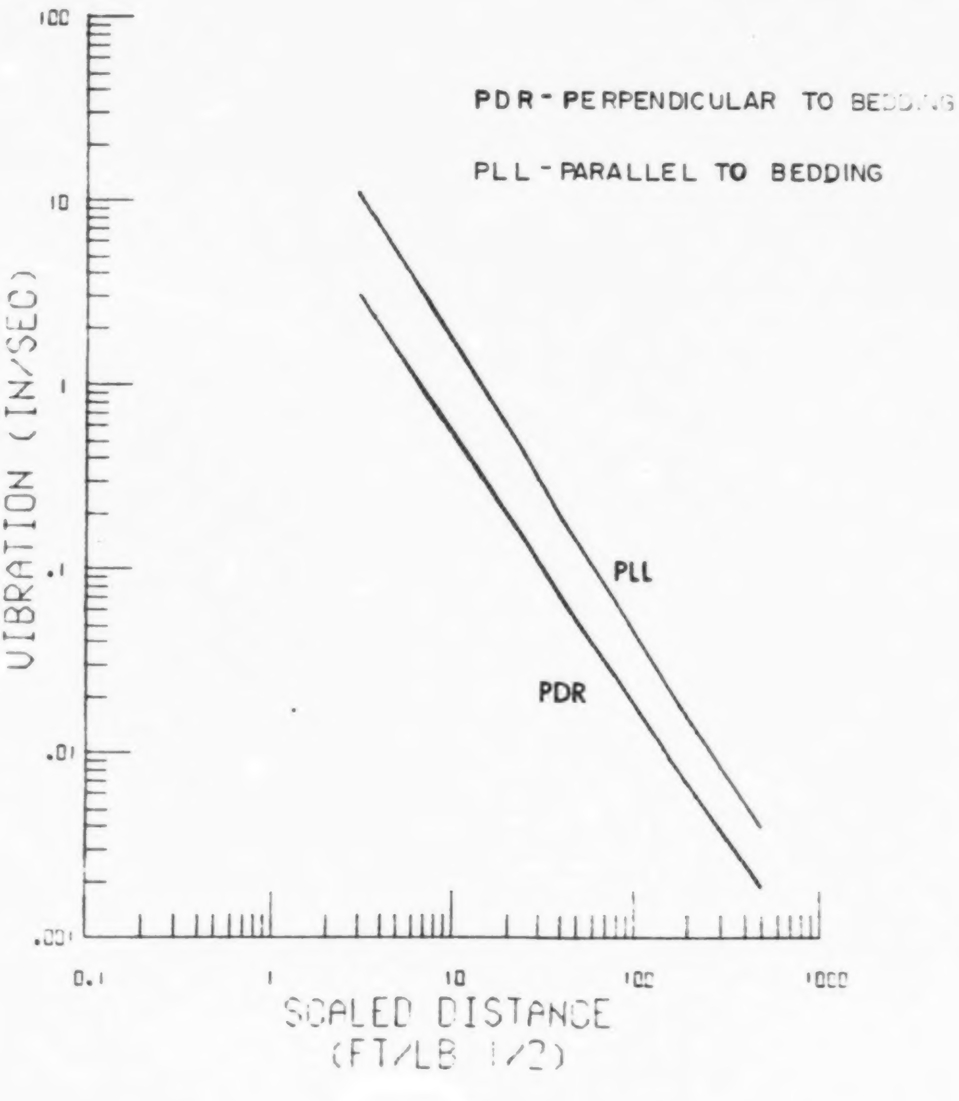

REFERENCE: DATA FROM DUPONT

NOTE: ORIGINAL DATA IN IMPERIAL UNITS

Date MARCH ,1987
Project 861-1290

Golder Associates

Drawn D M
Chkd [illegible]

6. EXPERIMENTAL PROGRAM

6.1 Blast Monitoring Program

6.1.1 Introduction

The occurrences of outburst events during roadway development in the Sydney Coalfield are known to be associated with shotfiring of the sandstones after the coal has been blasted (see Section 2). This phenomenon is indicative of the significance of the dynamic effects of blasting on the burst-prone sandstone.

Within the scope of this research study, a field program was undertaken by Du Pont Canada Inc. (Du Pont) to study the following aspects in the Lingan Mine.

(a) To review the current blasting practices employed in the Mine for roadway development.

(b) To monitor static and dynamic stress changes during the typical shotfiring rounds in roadway development.

(c) To develop a dynamic stress attenuation curve for the assessment of the dynamic stress regimes in the immediate vicinity of the roadway during shotfiring.

(d) To perform computer simulation to study the effect of blasting on the development of induced fractures on the basis of the current shotfiring practices at the Lingan Mine.

(e) To improve on the current blasting practices in the light of the blast simulation results.

6.1.2 Field Program and Procedures

The objectives of the field blast monitoring program were to determine the dynamic and background stresses generated during shotfiring using standard blast patterns employed at the Lingan Mine. The stress changes were monitored before and after each blasting round both in coal and sandstone. The data obtained was used in conjunction with other data obtained from similar sandstone (having similar rock properties) to predict the dynamic stress decay around the roadway. The field program was commenced on March 16 and completed on March 19, 1987.

The stress changes were monitored in 165 mm diameter boreholes using hydraulically coupled pressure sensors (ROCSCAN SYSTEM) developed by Du Pont (Figure 6.1). Prior to the actual tests in the mine, the "ROCSCAN" system was approved by CANMET for use in coal mines. The original field program called for two monitoring boreholes so that the dynamic properties of the rock could be measured from the cross hole data. However, because of drill breakdown and time constraint, the second borehole was not drilled.

The testing site at Lingan Mine was located in the No. 3 deep. The sensor was placed in a 165 mm (6.5 in.) diameter 3 m (10 ft.) long horizontal borehole drilled at 1.5 m (5 ft.) above the coal and sandstone contact (see Figure 6.1). The drillhole was about 4.5 m (15 ft.) behind the advancing face at the start of the field program.

The data collector was situated in a connecting adit about 75 m (250 ft.) from the face. The orientation of the monitoring borehole with respect to the blasthole centreline was 90 degrees. Shock waves arriving from the detonating boreholes would therefore intercept the monitoring borehole obliquely and geometric correlation is required to analyse the plane wave motion.

At the start of the experiment, the instrument was installed in the drillhole with a sensor pressure (prestress) of about 0.35 MPa (500 psi). This corresponds to a force of about 1750 kN (393 lbf) applied to the rock through the platens (12.7 mm or 0.625 in. diameter) which are in contact with the rock wall of the borehole. The contact area of the platen in a 165 mm (6.5 in.) diameter borehole is approximately 12 sq.mm. (0.05 sq.in.).

The measured dynamic pressure levels were always referenced to zero, whereas the static background pressure changes were referenced to the pre-trigger pressures measured prior to each blast.

The pressure signals, monitored in two directions, (horizontal and vertical) were transmitted to a data collector having a band-wdith of DC - 1000 HZ and a memory capacity of 0.5 Mbyte (internal). The information contained in the data collector was downloaded to a computer where pressure vs. time was displayed. Trigger levels were set as low as 117 KPa (17 psi) in order to capture blast events from both coal and sandstone.

A total of 6 rounds (approximately 3.5 m per round) was monitored, for a total advance of 21 m. In each round, the pressure changes arising from both the coal and rock (sandstone) were recorded.

6.1.3 Review of Current Blasting Practices at Lingan Mine

During developemnt of the roadway, in Lingan Mine as well as in other mines in the Sydney Coalfield, the coal seams, which are located in the lower part of the roadway, were often excavated first. The overlying sandstone layers are then blasted. Blastholes in coal were augered whereas the sandstone was drilled using a pneumatic percussion drill. A FEMCO 20 blasting machine was used to fire each production blast.

The drilled pattern, for both sandstone and coal are shown in Figure 6.2. It consisted of approximately 15-17 boreholes, 38 mm (1.5 in.) in diameter and 1.1 m (3.6 ft.) deep. The permissible explosive used was MONOBEL S-1 (CIL) 25 x 203 mm (1 x 8 in.) in dimension with each blasthole having a maximum loading of 0.45 kg (1 lb.). Each blasthole was bottom primed using MS delay CXB (SD) non-incendive blasting caps with copper leads. Period #1 to Period #7 were used with 3 delay periods/shot. For example, if Periods #1, #2 and #3 were used, then 5-7 blastholes were detonated per delay with 2.3 to 3.2 kg (5 - 7 lbs.) of MONOBEL S1. All blastholes were stemmed using a wetted clay type material. Explosives were lightly tamped.

The drilling patterns for both coal and sandstone were about 0.6 m (2 ft.) horizontal and 0.45 m (1.5 ft.) vertical. Blasts were opened in the centre. There was no attempt to provide a means of controlling the perimeter, in particular in the vicinity of the roof (arch). There did not appear to be excessive overbreak into the walls of the drift, however a great deal of overbreak appeared in the corners of the arch and were well into the roof. Part of this overbreak could be attributed to the drilling practice of angling the blastholes up into the roof in order to ensure clearance for the steel arches. This has led to poor perimeter control and enhanced crack propagation through seamy material.

Further examination of the effects of the current blasting practices on the surrounding rock mass and the suggested ways to improve the blast quality are presented in the following section.

6.1.4 Results of Stress Monitoring

The results of stress monitoring are summarized in Tables 6.1 and 6.2 for the dynamic and static stresses respectively.

In each Table, the blast number, the distance of the face from the monitoring station, the maximum weight of explosive used per delay and the vertical and horizontal pressures measured by the sensors for each blast are summarized.

For each set of results, the scaled distance based on the square root relationship (equation 5.16) and the stresses in the medium due to the compression wave were evaluated. The procedure for the evaluation of the dynamic stresses from the test data is presented below.

If the direction of the plane compression wave is known, the magnitude of plane dynamic stress (varying with time) at the instant of the pressure reading is evaluated according to the following expression:

$$\sigma d = \frac{(1-\nu)[2(1+\nu)+k]\ P\omega}{(1+\nu)[1+(1-2\nu)\cos^2(i)]} \quad (6.1)$$

where: σd = Dynamic stress
ν = Poisson's ratio
k = Ratio of Young's modulus of the medium monitored and bulk modulus of the hydraulic oil within the ROCSCAN system
i = Angle of incidence of the compression wave
$P\omega$ = measured pressure rise

The angle of incidence of the compression wave (i) can be evaluated by the following relationship:

$$i = \mathrm{Tan}^{-1} \frac{A}{D}$$

where: A = Acoustic medium velocity (for Lingan sandstone ≈ 13000 ft/sec) or 3980 m/sec)
D = Explosive Detonation velocity (7521 ft/sec or 2500 m/sec)

The data contained in the Tables are in imperial units in order to facilitate correlation with data from other sources which were given in imperial units. The required conversion factors to metric units are shown in the tables.

It may be noted from Table 6.1 that the dynamic effect of the shotfiring event is significant. The dynamic stress change at 4.5 m from the face (or about 6.2 m from the centre of the blast) could reach 24 MPa (3500 psi). The effect would tend to attentuate with distance as indicated by the gradual decrease of induced dynamic stresses with distance between the sensor and the source of the dynamic event.

The above results were plotted with the calculated dynamic stresses (σd in psi) against the scaled distance (S_d) and the following stress attentuation relationships were obtained by curve fitting.

CASE 1 - Vertical stresses in coal (CVI) $\sigma_{vc} = 2372/(S_d)^{2.12}$ (6.2)

CASE 2 - Vertical stresses in sandstone (SVI) $\sigma_{vs} = 23988/(S_d)^{3.08}$ (6.3)

CASE 3 - Horizontal stress in coal (CHI) $\sigma_{hc} = 4339/(S_d)^{2.47}$ (6.4)

CASE 4 - Horizontal stress in sandstone (SHI) $\sigma_{hs} = 3040/(S_d)^{2.31}$ (6.5)

Due to the set-up of the sensor in relation to the wave front of the plane dynamic wave, the interpretation of the vertical stresses from the recorded pressure rises were only approximate.

The equations for coal apply only in the case of shock wave transmission across the seam; whereas, for sandstone, the equations are applicable within the seam. In addition to the Lingan data, data from surface blasting of a coal mine in Western Canada (Du Pont, 1987) is also considered. The equation that represents the attenuation of dynamics across the coal measures strata is

$$\sigma d = 95/(S_d)^{1.02} \qquad (6.6)$$

To utilize the attenuation curves, it is necessary to consider the transmittion path for the determination of the peak dynamic stress either within a boundary layer or across a boundary layer.

The attenuation equation 6.5, developed for those readings taken in the horizontal direction (curve SHI) is considered to be applicable for the prediction of dynamic stresses within the sandstone layer. For prediction of stresses across the coal measures strata (wave transmission crosses boundaries of different rock units) equation 6.6 is considered to be applicable. These two equations are expressed as graphical plots in Figure 6.3.

As far as the static stresses are concerned, the stress changes due to shotfiring are relatively insignificant. The results appear to be consistent with the theoretical expectation that the static stress changes at the monitoring station (4.5 m from the face) due to face advance would be small.

6.1.5 Evaluation of Effects of Current Blasting _ Practices on Rock Fracturing in the Lingan Mine

To provide a quantitative evaluation of the blasting practices in Lingan Mine, computer modelling based on the currently used blast patterns was carried out to examine the degree of cracking around blast holes and the extent of overbreak for various blasting parameters and geological conditions.

The sensitivity of overbreak, decoupled cracking radius, coupled cracking radius and interpattern cracking radii were examined by varying the geological index burden distance, tensile strength and in situ stress ratio. The definition of these terms, the method of analysis and the results are contained in Appendix B of the report.

The results indicated that under the conditions at the Lingan Mine, the current blasting pattern would cause excessive overbreak and damage to the surrounding rock mass. The "cracking radii" calculations (see Appendix B), however, indicate that the interpattern cracking radius appears to break out within the existing pattern dimensions. The stress attenuation curves obtained from the blast monitoring program at Lingan Mine indicated that high tensile stresses due to reflection of the shock waves could develop near the boundary of the roadway.

To improve the quality of blasting at the Mine, the following modifications to the blast pattern in the sandstone are suggested for consideration by the mine operator:

- modify the delay system by keeping the perimeter blastholes on a minimum explosive weight/delay. The effects of a reduction in the explosive weight per delay was also examined and modelled. By reducing the weight of explosive per delay, the extent of potential overbreak would reduce.

- take out the centre of the sandstone using the same explosive loading but using delay periods no. 1, 2 and 3.

- use longer delay periods no. 6 and 7 to allow stress in the horizontal direction to equalize so that tensile failure occurs along the line of perimeter holes and results in a smooth post-shear failure zone.

- drill the perimeter holes perpendicular to the working face as close to the roof as possible. A drilling pattern that permits accurate drilling should be used.

A proposed blast pattern which may help to improve the blasting quality of the roadway at Lingan Mine is presented in Figure 6.4. A further modification to reduce blast damage at the perimeter is to use decoupled charges if deemed necessary. It is believed that above basic changes to the current blast pattern would result in better perimeter control and less overbreak and ultimately reduce of effects of dynamic stresses on the initiation of seismic events.

6.1.6 Summary

The following is a summary of the main findings of the blast monitoring and simulation study.

1. The drilling methods used during the testing period for the production blasting in the sandstone at the Lingan Mine were inadequate regarding the control of overbreak. Perimeter boreholes in the arch were drilled upwards to such a degree as to cause overbreak which may contribute to instability in the roof. It is also observed that there is very little support for the loose material produced.

2. Results of computer based blast simulation indicate that the current blast pattern would cause excessive overbreak and damage to the surrounding rock. Reduction of explosive weight per delay would results in reduced overbreak. Under the conditions at the Lingan Mine, the analyses indicate that the interpattern cracking radius appears to break out within the existing pattern dimensions.

3. The dynamic effect of the shotfiring event is significant. Such effect tends to attenuate with distance. The blast induced dynamic stresses follow the attenuation equations given below:

Within sandstone

$$\sigma_d = 3040/(S_d)^{2.31}$$

Across rock strata

$$\sigma_d = 95/(S_d)^{1.02}$$

4. Changes in the static stresses due to shotfiring are considered to be insignificant.

5. To improve the overbreak condition in roadway development at Lingan Mine, changes are required in overall blast design including drilling accuracy and layout of blast hole delays. A suggested blast pattern is given in Figure 6.4.

6.2 Laboratory Testing Program

6.2.1 Introduction

In conjunction with the study of the outburst problems in the sandstone at No. 26 Colliery, laboratory triaxial testing programs were undertaken on a reference sandstone (Pier Cap Sandstone) as well as on the sandstones from Lingan Mine and No. 26 Colliery. The results were contained in Golder Associates Report No. 851-1278.

For the purpose of this study, some of the fundamental behaviours of rock which relate to the initiation of failure during an outburst event were studied. A reference sandstone (Pier Cap Sandstone) used in previous laboratory testing programs for outburst studies was tested. The testing program included the following:

a. To study the stress-strain behaviour of the sandstone during unloading along the axial direction under constant lateral stress and a closed pore gas system (undrained condition).

b. To examine the drag effect (strain) on the sandstone sample as a result of gas flowing through the sample.

c. To study the strength of the sandstone under a system of biaxial loading.

The experimental procedures and results of the test programs are described in the following sections.

6.2.2 Axial Unloading under Constant Confining Stresses in a Closed Pore Gas System

This test was carried out in a Hoek type triaxial cell with strain measurements provided by 4 sets of strain gauges, two installed at the top end and two at the centre portion of the sample. Each strain gauge set comprised one vertical and one horizontal strain gauge. Two pressure transducers were used to measure the gas pressures at the top and bottom ends of the sample.

The test specimen was initially loaded uniformly in the axial (σa) and lateral ($\sigma 1$) directions ($\sigma a = \sigma 1$). A gas pressure (Pg) of 5 MPa was then introduced. The axial stress is then gradually reduced with no drainage provision for the gas (undrained case). The stresses, strains and pore gas pressures were monitored. The first series of test comprised the following:

Test 1 - Initial stresses: $\sigma_a = \sigma_1 = 10$ MPa
$P_g = 0$ MPa

Test 2 - Initial stresses: $\sigma_a = \sigma_1 = 15$ MPa
$P_g = 5$ MPa

Test 3 - Initial stresses: $\sigma_a = \sigma_1 = 25$ MPa
$P_g = 5$ MPa

The second series of tests comprised cylic loading of the sample with internal pore gas pressure. The loading and unloading sequence is as follows:

A - Initial loading to $\sigma a = \sigma 1 = 10$ MPa $Pg = 0$
Record $\sigma - \epsilon$ at intervals

B - Keep $\sigma a = \sigma 1 = 10$ MPa, introduce $Pg = 5$ MPa
Record $\sigma - \epsilon$ at $\sigma a' = \sigma 1' = 5$ MPa and $Pg = 5$ MPa
- Increase $\sigma a' = \sigma 1'$ to 10 MPa simultaneously
Record $\sigma - \epsilon$ and Pg
- Decrease $\sigma a' = \sigma 1'$ to 5 MPa and record $\sigma - \epsilon$ and Pg

C - Start at $\sigma a' = \sigma 1' = 5$ MPa and $Pg = 5$ MPa
- Keep $\sigma 1' =$ constant increase $\sigma a'$ to 10 MPa
- Keep $\sigma a' = 10$ MPa increase $\sigma 1'$ to 10 MPa

D - Keep $\sigma a' = 10$ MPa decrease $\sigma 1'$ to 5 MPa
- Keep $\sigma 1' = 5$ MPa decrease $\sigma a'$ to 5 MPa

E - Start at $\sigma a = \sigma 1 = 5$ MPa
- Keep $\sigma a' = 5$ MPa increase $\sigma 1'$ to 10 MPa
- Keep $\sigma 1' = 10$ MPa increase $\sigma a'$ to 10 MPa

F - Start at $\sigma a' = \sigma 1' = 10$ MPa
- Keep $\sigma 1' = 10$ MPa decrease $\sigma a'$ to 5 MPa
- Keep $\sigma a' = 5$ MPa decrease $\sigma 1'$ to 5 MPa

G - Start at $\sigma a' = \sigma 1' = 5$ MPa
- Keep $\sigma c' \sim 5$ MPa and decrease $\sigma a'$ to 0 MPa

The results obtained from these two series of tests are summarized below:

a. Under a closed system, the pore gas pressure decreases as the sample dilates (increases in volume). For a volumetric strain of 615 microstrains, the gas pressure reduced by 0.5 MPa. The internal gas pressure did not appear to have a significant effect on the stress-strain behaviour of the sample.

b. Under cyclic loading, the internal gas pressure under a closed system changed according to the effective stress changes. The pressure and volume change relationship appeared to be consistent with the gas law under isothermal condition.

6.2.3 Drag Effect of Gas Flowing Through a Sample

In this test, the test sample was coated with epoxy to restrict gas leakage from the sides of the sample. Gas was passed from one end of the sample to the other and the strain in the sample was monitored during passage of the gas. The internal gas pressure within the sample was allowed to stabilize prior to release at the downstream end of the sample. The sample was placed between the platens of a loading frame and a load cell was used to ensure that no positive axial load was applied to the sample.

The results indicated that there is no noticeable drag effect on the sample due to the passage of the gas. This might be attributed to the relatively high porosity (19%) of the Pier Cap Sandstone.

6.2.4 Strength under Biaxial Loading

In this experiment, confining pressures were applied to the samples with no axial load in a Hoek type triaxial cell. The confining stresses were increased gradually until failure occurred. The tests were carried out with and without lubricating the inside of the membrane of the triaxial cell to study the effect of friction on the failure load. The average uniaxial compressive strength of the sample is 45 MPa.

The samples tested failed by fracturing along a plane perpendicular to the sample axis. The confining pressures at which failures occurred are as follows:

Test	Maximum Confining Stress at Failure	
1	43.5 MPa	- membrane not lubricated
2	22.8 MPa	- membrane lubricated to reduce friction

It may be noted that the friction effect at the contact of the sample and the membrane is very significant under this loading condition. In essence, the friction developed at the sample/membrane interface resists the extension of the sample and thus acts as an axial stress component.

The observed mode of failure is consistent with the concept of effective tensile stress (e.g. Brown and Trollope, 1967) described in Section 5.3.2.

6.2.5 Discussion

The results of the experiments indicated that the general behaviour of gas within a relatively porous medium (porosity = 19%) appears to obey the gas law under isothermal condition. Of particular interest to this study is the mode of failure of the sandstone under a biaxial stress system. The change of the stresses around an underground opening from a triaxial to a biaxial state could create a condition conducive to failure as observed experimentally.

The gas pressure effects and the progressive development of the outburst events once rock fracturing was initiated has been described in Section 4.

The experimental results obtained in this and other previous studies were taken into consideration in the development of an outburst model for the Sydney Coalfiled presented in the next section.

TABLE 6.1: SUMMARY OF DYNAMIC STRESS MEASUREMENTS AND EVALUATIONS
LINGAN MINE NO. 3 DEEP

Blast Ref. No. (material)	Distance of Monitoring Station from face (ft.)	Explosive Charge per Delay (lb)	Scaled Distance $(lb)^{0.5}$	Measured Pressure Readings (psi)		Calculated Dynamic Stress Based on Plane Wave Theory (psi)	
				Vert.	Horl.	Vert.	Horl.
1a (coal)	15	6.0	6.1	112	112	1029	1029
1b (sandstone)	15	7.0	5.6	384	64	3526	588
2a (coal)	18.2	5.0	8.1	64	48	588	441
2b (sandstone)	18.3	6.0	7.4	80	112	735	1029
3a (coal)	24.6	6.0	10.1	38	42	349	386
3b (sandstone)	24.6	5.0	11.0	67	47	615	432
4a (coal)	28.1	6.0	11.5	28	18	257	165
4b (sandstone)	28.1	7.0	10.6	45	27	413	247
5a (coal)	33.8	6.0	13.8	(not recorded)		-	-
5b (sandstone)	33.8	7.0	12.8	23	18	211	165
6a (coal)	36.0	6.0	14.7	18	13	165	119
6b (sandstone)	36.0	7.0	13.6	16	11	147	101

NOTE: 1. Values are in imperial units to facilitate correlation with data from other sources.
Conversion factor: multiply (ft.) by 0.305 to convert to (m)
multiply (psi) by 6.895 to convert to (kPa)

2. Interpretation of vertical stresses is only approximate (see Section 6.1.4)

TABLE 6.2: SUMMARY OF MEASURED CHANGES IN STATIC STRESSES

LINGAN MINE NO. 3 DEEP

Blast Ref. No. (material)	Distance of Monitoring Station from face (ft)	Explosive Charge per Delay (lb)	Scaled Distance $(lb)^{0.5}$	Pre-Trigger Readings (psi)		Post Trigger Readings (psi)		Stress Changes (psi)	
				Vert.	Hort.	Vert.	Hort.	Vert.	Hort.
1a (coal)	15	6.0	6.1	594	370	653	462	41	92
1b (sandstone)	15	7.0	5.6	560	338	605	432	45	94
2a (coal)	18.2	5.0	8.1	516	358	583	450	67	92
2b (sandstone)	18.3	6.0	7.4	608	377	649	464	41	87
3a (coal)	24.6	6.0	10.1	525	358	595	453	90	95
3b (sandstone)	24.6	5.0	11.0	485	341	558	438	73	97
4a (coal)	28.1	6.0	11.5	515	358	584	450	69	92
4b (sandstone)	28.1	7.0	10.6	616	372	649	462	33	90
5a (coal)	33.8	6.0	13.8	512	352	581	447	69	95
5b (sandstone)	33.8	7.0	12.8	568	363	551	436	-17	73
6a (coal)	36.0	6.0	14.7	545	356	598	490	53	134
6b (sandstone)	36.0	7.0	13.6	492	344	549	434	57	90

NOTE: values are in imperial units to facilitate correlation with data from other sources.
Conversion factor: multiply (ft.) by 0.305 to convert to (m)
multiply (psi) by 6.895 to convert to (kPa)

LOCATION OF BLAST MONITORING TESTS IN LINGAN MINE

FIGURE 6.1

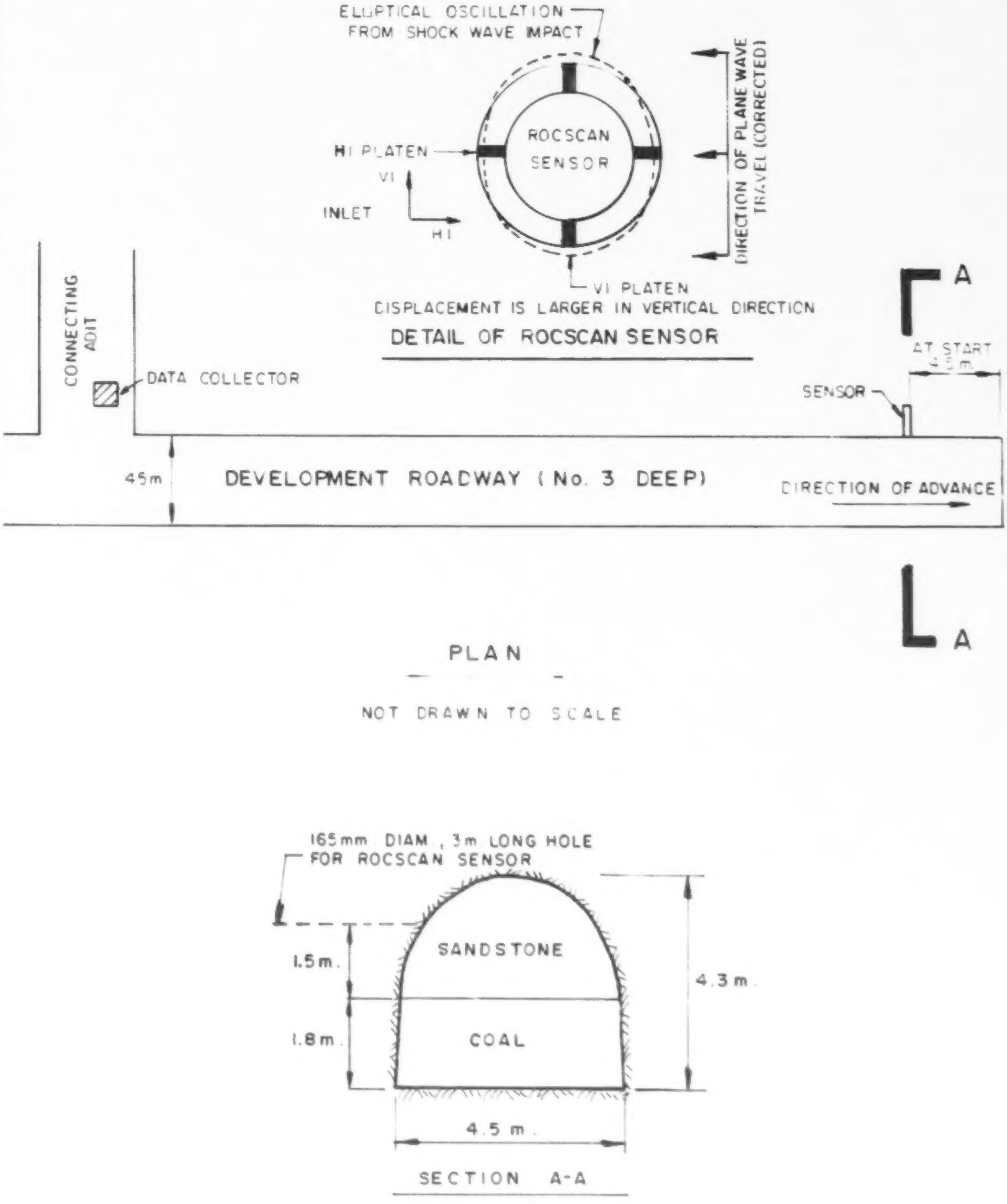
ELLIPTICAL OSCILLATION FROM SHOCK WAVE IMPACT
ROCSCAN SENSOR
H1 PLATEN
V1
INLET
H1
DIRECTION OF PLANE WAVE TRAVEL (CORRECTED)
V1 PLATEN
DISPLACEMENT IS LARGER IN VERTICAL DIRECTION
DETAIL OF ROCSCAN SENSOR
A
AT START
4.5m
SENSOR
CONNECTING ADIT
DATA COLLECTOR
45m
DEVELOPMENT ROADWAY (No. 3 DEEP)
DIRECTION OF ADVANCE
A
PLAN
NOT DRAWN TO SCALE
165mm DIAM., 3m LONG HOLE FOR ROCSCAN SENSOR
SANDSTONE
COAL
1.5m.
1.8m.
4.3m.
4.5 m.
SECTION A-A

NOTES

1) THE LINE OF THE SHOCK WAVE FRONT IS AT 60° TO THE LONGITUDINAL AXIS OF THE TUNNEL.

REFERENCE

DRAWING PREPARED BY DUPONT

Date MARCH, 1987

Project 871-1290

Golder Associates

Drawn D M

Chkd

Form GA-D-4m (metric)

TYPICAL BLASTING PATTERNS IN COAL AND SANDSTONE USED IN LINGAN MINE

FIGURE **6.2**

TOP PERIMETER HOLES ARE DRILLED UPWARDS INTO ROOF CAUSING EXTENSIVE OVERBREAK

PATTERN (SANDSTONE) 3X2 (FT.)

CHARGE WT VARIED 5-7 LBS/DELAY

PATTERN (COAL) 3X2 (FT.)

DIMENSIONS IN FT

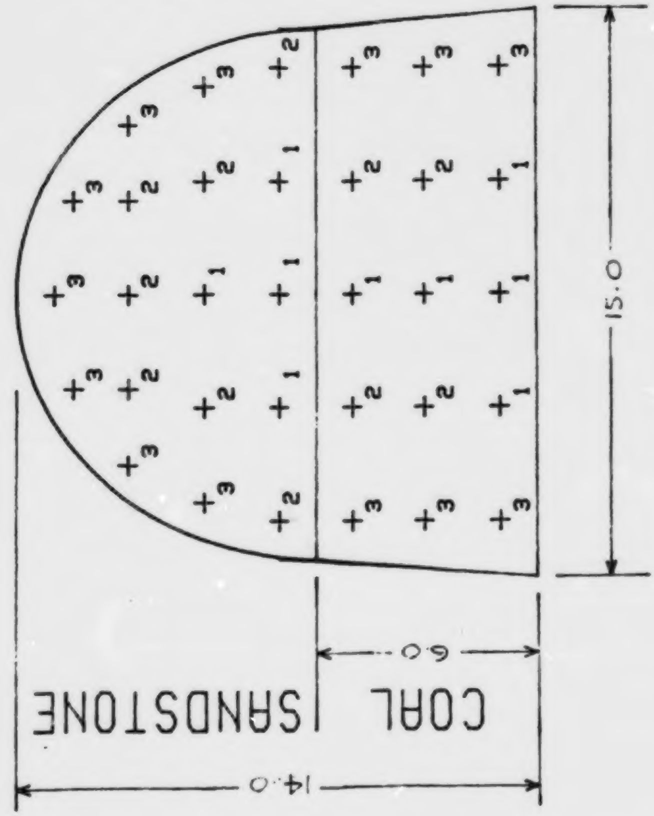

REFERENCE: DRAWING PREPARED BY DUPONT

Date JUNE 29, 1987
Project 871-1290

Golder Associates

Drawn D.M.
Chkd

PLOT OF DYNAMIC STRESS WITH SCALED DISTANCE

FIGURE 6.3

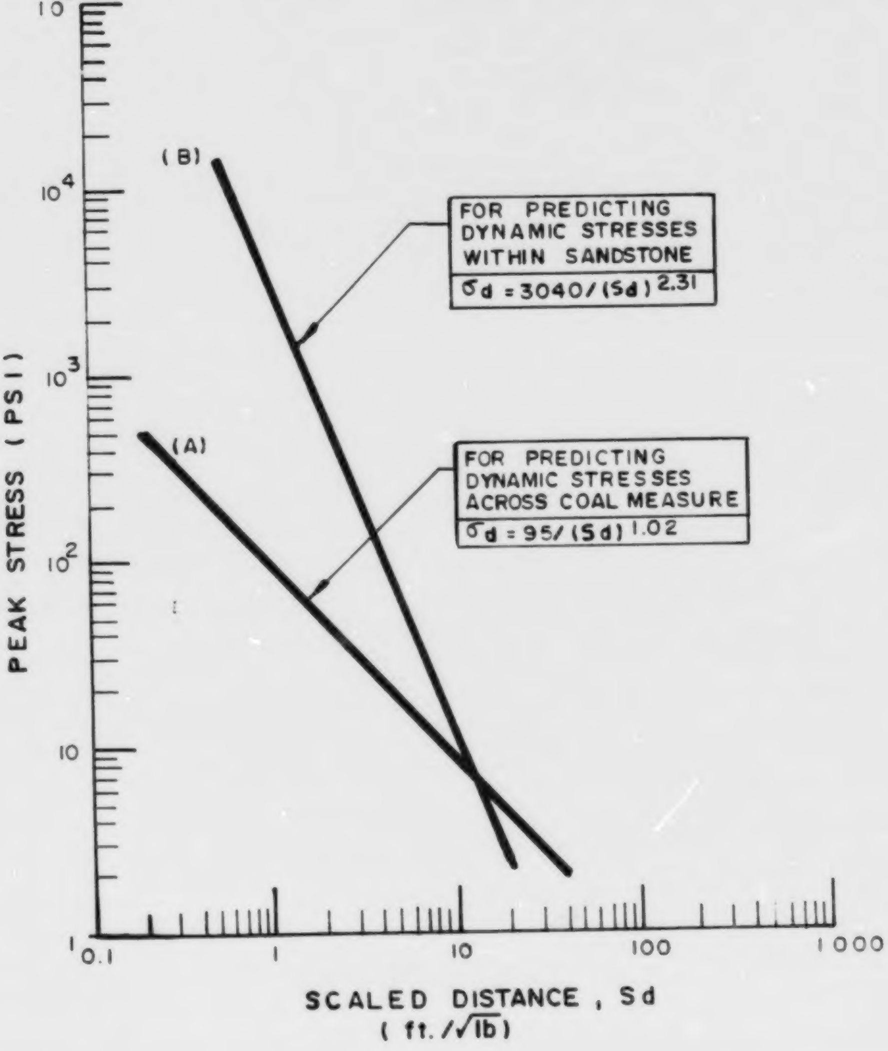

LEGEND

(A) DATA FROM COAL MINE IN WESTERN CANADA (DUPONT 1987)

(B) DATA FROM BLAST MONITORING IN LINGAN MINE CARRIED OUT FOR THIS STUDY

Date MARCH , 1987
Project 861-1290

Golder Associates

Drawn D M
Chkd

SUGGESTED MODIFICATIONS TO BLAST DESIGN FOR LINGAN MINE

FIGURE 6.4

BOREHOLES MUST BE DRILLED PERPENDICULAR TO FACE TO AVOID DAMAGE TO ARCH AND ROCK

PATTERN (SANDSTONE) 3X2 (FT.)

CHARGE WT RESTRICTED TO 3 LBS/DELAY AT ARCH PERIMETER

PATTERN (COAL) 3X2 (FT.)

DIMENSIONS IN FT

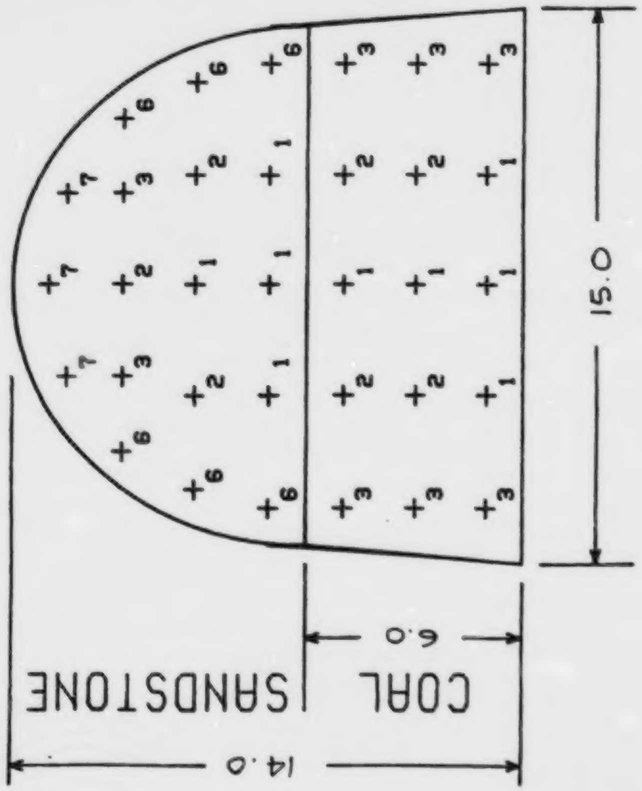

+7 +7 +7
+6 +3 +2 +3 +6
+6 +2 +1 +2 +6
+6 +1 +1 +1 +6
+3 +2 +1 +2 +3
+3 +2 +1 +2 +3
+3 +1 +1 +1 +3
SANDSTONE
COAL
6.0
14.0
15.0

REFERENCE · PREPARED BY DUPONT

Date MARCH, 1987
Project 861-1290

Golder Associates

Drawn C.M
Chkd

7. DEVELOPMENT OF AN OUTBURST MODEL

7.1 Introduction

Based on a review of the existing outburst models published by various researchers, various hypotheses were proposed to address:

(a) the initiating mechanism of the outbursts,

(b) the mechanism of rock and gas interaction during an outburst event, and

(c) the energy balance of the outburst events.

A number of researchers defined specific aspects which should be included in outburst model formulation. Farmer and Pooley (1986) pointed out that an outburst model must account for the initiation mechanism of the outburst and the ejection/transport phases of the phenomenon. Shepherd et al (1986) suggested that a model must also account for the transient effects, namely, audible and microseismic noises, instability of the face and temperature decrease prior to the outburst. Finally, Paterson (1986) specified that a model must include a gas flow description, a stress distribution formulation and a failure criterion.

In addition to the consideration of static stress distribution, the dynamic stresses would play a significant role in initiating the outbursts as indicated by the dynamic stress attenuation curves described in Section 6.

In this research project, the primary objective is to develop a model for rock and gas outbursts relating to the conditions in the Sydney Coalfield. The model will be calibrated using the data from the known events recorded in No. 26 Colliery to assess its overall validity and limitations in its applications. Subsequently, the model may be used to review conditions in other mines of the Sydney Coalfield to determine if rock and gas outbursts are likely to occur under a given set of conditions.

In keeping with the objective of the study and its intended applications, it is considered that the outburst model for the Sydney Coalfield should address the initiation mechanism of the outbursts rather than the associated disturbances following the events. The conditions governing the occurrence of the events are considered to be of greater practical significance in regard to the prediction and prevention of outbursts.

The following sections present

(a) the proposed outburst model for the Sydney Coalfield including a description of the hypothesis and the governing parameters and

(b) the calibration of the model based on No. 26 Colliery events.

7.2 Proposed Rock and Gas Outburst Model

On the basis of the available information presented in the preceding sections and the outburst data from No. 26 Colliery, the governing factors for the rock and gas outbursts in the Sydney Coalfield are:

(a) stresses in the strata including the static stress concentration around the underground opening and the dynamic stresses resulting from blasting (shotfiring)

(b) gas pressure

The proposed mechanistic model for the initiation of rock and gas outbursts in No. 26 Colliery is described as follows.

(1) The coal measures strata in No. 26 Colliery are subjected to a system of in situ stresses. The in situ stress measurements were undertaken mainly in the siltstone layers at a location approximately 760 m below sea level. The in situ stresses measured were fairly isotropic with the stress magnitudes ranging between 23 to 25 MPa. The channel sandstone has been identified as the burst prone strata and is known to exist as an irregular inclusion within the coal measures strata. As a result local concentration of stresses could occur within these sandstone units. It was also noted that the contact between this sandstone and other rock type often represents potential plane of weakness (see Section 2).

(2) All outbursts in the No. 26 Colliery occurred in roadways driven into virgin ground. The general mechanism of rock failure under static stresses is postulated as follows:

The creation of the roadway opening alters the stresses in the strata surrounding the roadway. Close to the excavation boundary the state of stresses varies from a biaxial loading (at the boundary) to a triaxial loading (farther away from the boundary) condition with low confining stresses.

Under a fairly isotropic state of stress the maximum stress (tangential stress) concentration factor at the boundary of the opening would be about 2. With increased anisotropy in the stress system and stress dependent elastic deformation parameters (Santarelli et al, 1986), the stress concentration factor would be higher.

The potential failure modes close to the excavation boundary (roof) of the roadway are as follows:

- under biaxial loading at the boundary potential extension fractures would develop parallel to the major principal stress direction

- under triaxial loading at low confining stresses, at locations relatively farther away from the boundary, potential shear type fractures would develop at a low angle to the direction of the major principal stress.

(3) In No. 26 Colliery, the coal measures strata comprise predominantly siltstone and sandstone and coal. Under the effects of static stress changes around the roadway, two cases are examined with regard to the stability of these rock units.

(a) Siltstone at the roof of the roadway. Under the anticipated biaxial stresses at the excavation boundary extension fracture would likely be induced in this rock unit and failure would take place in the form of slabbing due to induced bed separations as the extension fractures propagate along bedding surfaces.

Farther into the rock mass, the confinement would be increased and the corresponding triaxial strength of the rock would be higher. This would tend to limit the zone of overstress and bring about a state of equilibrium. The loosened rock fragments at the roof could generally be restrained or supported by rock support system for the roadway.

The failure would not be violent and the gas released from the failed siltstone would be small as this rock unit is not known to contain a significant amount of gas.

(b) Sandstone at the roof of the roadway. Outburst events recorded at No. 26 Colliery indicated that not all sandstones in the Sydney Coalfield are prone to burst. Core discing in rock core generally correlated with outburst events and could serve as an indicator for potential outburst hazard.

The potential failure modes in the sandstones would be similar to those described for the siltstone. However, the outburst-prone sandstones would exhibit a violent failure due to a combination of possibly higher stress concentration, brittle failure behaviour and gas pressure.

Records of the No. 26 Colliery outburst events presented in Section 2 indicate that outbursts took place in the channel sandstone whenever the sandstone is located within 2.7 m of the coal. Based on a typical roadway of 4.57 m wide by 3.67 m high, the top of the coal seam is generally located at about 2.2 m below the crown of the roadway. Hence, outbursts took place when the sandstone channel layer is located within 0.5 m (above) of the crown. The stress concentration effects in the immediate vicinity of the crown play a significant role in the observed trend of the outburst events.

(4) The postulated processes involved in an outburst event in the outburst-prone sandstone are summarized below.

When a roadway is driven into the channel sandstone, high stress concentration would occur at and close to the boundary (roof) of the excavation. The stress concentration factor would depend on the magnitude of in situ stresses existing in the sandstone unit. The stress changes could induce failure in the sandstone up to a certain distance above the roof because the strength of rock increases as the confining stresses increase.

At the onset of the creation of the opening, dynamic stresses from blasting (shotfiring) would superimpose additional stresses on the rock mass. Compressive stresses would be imposed by the compressional waves and tensile stress would be induced due to tensile waves resulting from wave reflections at the free boundary of the volume of rock to be excavated. Dynamic elastic recovery after a sudden release of the confinement could also exert traction on the rock material which may be sufficient to induce cracking in the rock mass. These dynamic effects would enhance the development of fractures parallel to the direction of the major principal stress. The fracture propagation path would generally follow the direction of least resistance very close to the boundary. In general, the fractures would closely follow the trajectory of the major principal stress. Beyond the boundary where some confinement is present, the plane of triaxial shear failure would be at a low angle with the direction of major principal stress.

Prior to initiation of fractures in the sandstone the gas originally trapped in the rock would respond to the changes in the stress regime under a closed system generally according to the principles of effective stresses. Increase in stresses in the medium would bring about a change in the gas permeability (generally a stress dependent parameter, see Section 5) and higher pore gas pressure. However, as fractures are developed in the rock strata, the pore gas pressure would partially escape through the fractures and would act in the stress (static and dynamic stresses) induced fractures as described by Sevelev (1979) (see Section 4.3.3.5).

If the fracture (crack) gas pressure is sufficient to overcome the confining stresses and if the fractures (primary extension fracture and/or secondary shear fractures) are allowed to propagate and eventually break into the cavity free face, materials in the form of thin flakes would be ejected from the cavity as the kinetic energy of the gas is dissipated. The fish scale type of failure surface observed in the outburst cavity of No. 26 Colliery is believed to be the result of the intense fracturing of the thin plates created by the fractures induced by biaxial loading and triaxial shear failure (under low normal stress) along the outburst cavity.

As the materials are ejected from the free face the new shape of the opening would cause further redistribution of the surrounding stresses and the process as described above would continue. Progressive fracturing within the outburst cavity and the development of a conical cavity shape as described by Ujihira et al (1985) (see section 4.3.3.4) would take place.

The outbursts would terminate under either one of the following conditions:

- the cavity extends to a geological contact where a non-outburst-prone material exists
- an equilibrium stress condition is reached
- the outburst event chokes itself due to
  - (a) friction along the cavity, delaying the creation of new cavity boundaries and/or
  - (b) the accummulation of outburst debris.

Even though a substantial amount of information has been collected at No. 26 Colliery, several fundamental parameters such as the in situ gas pressures, the stress related characteristics of the sandstone and the in situ stresses in the channel sandstone in which the events had taken place are still not well defined. Nevertheless, the model presented offers a reasonable description of the conditions leading to the outbursts in terms of the effects related to static and dynamic stresses and gas.

In the following sections, No. 26 Colliery data is used to calibrate the proposed model by considering the stress and gas pressure effects on roadway developments in the outburst areas.

7.3 Stress Analysis of a Development Roadway in No. 26 Colliery

To calibrate the proposed outburst model for the No. 26 Colliery events, a series of two dimensional plane strain finite element analyses were carried out to study the following aspects:

a. The effects of the following factors on the stresses at the roof (stresses behind the face are not as critical based on the work of Niwa et al, 1980) of a typical roadway in no. 26 Colliery:

   - location and thickness of the burst-prone sandstone layer
   - in situ stresses
   - relative rock mass stiffnesses of sandstone and siltstone

b. The stress condition at the roof of the 13N Airway which was driven through a sandstone channel without initiating a rock and gas outburst. The results are compared with those of the 14N Airway which generated outburst events no. 28 and 31 during drivage.

c. The effect of blast damage on the stress conditions at the roof of a typical roadway.

Table 7.1 summarizes the cases modelled under item (a) above, including the range of variations in some of the input parameters.

The rock types included in the models comprised coal, siltstone and sandstone. The rock mass parameters for these rock types are as follows:

Rock Type	σc (MPa)	E (GPa)	ν	m	s	γ (MN/m^3)
Coal	13.5*	3.45	0.1	0.005	0.0001	0.01
Siltstone	48.6	36.5	0.2	5.0	0.1	0.027
Sandstone	50.0	16.0	0.2	5.0	0.1	0.027

*perpendicular to bedding

where σc = uniaxial compressive strength
E = Deformation modulus
ν = Poisson's ratio
m,s = Rock mass strength parameters based on Hoek and Brown (1981) failure criterion
γ = unit weight

The Hoek and Brown failure criterion was used to assess the extent of the overstressed zone around the roadway based on static stresses and rock mass strength.

Dynamic stresses (based on the stress attentuation curve presented in Section 6) and pore gas pressures were superimposed on the static stresses to assess the overall stress regime at the onset of shotfiring.

7.3.1 Effects of the Location and Thickness of Sandstone in Relation to the Development Roadway

In this series of analysis, a typical roadway section (4.57 m wide by 3.67 m high) was modelled. The general stratigraphy represented by the model is based on the data available from CBDC (see Figure 7.1). The top of the coal seam is located at approximately the springline of the roadway and the seam is sandwiched between two siltstone layers. The upper siltstone layer is overlain by a channel sandstone layer.

It was observed in no. 26 Colliery that outburst took place when the channel sandstone was within 2.7 m of the top of the coal seam. The effects of the sandstone locations were examined in this analysis by considering the static stress conditions at the roof of the roadway and at the sandstone/siltstone contact for various positions of the sandstone layer. The sandstone layer thickness was kept constant at 5.7 m but the elevation of the sandstone/siltstone interface was varied from 1.3 m below to 1.7 m above the crown elevation of the roadway (about 3.5 to 3.9 m above the coal seam).

An additional set of analysis (Case 2 - Table 7.1) was also carried out by keeping the sandstone/siltstone contact at the roof (2.17 m above the coal seam) and varying the thickness of the sandstone layer; the other parameters remain unchanged.

The static principal stresses ($\sigma 1$ and $\sigma 3$) obtained from these two sets of analyses were plotted along a line (a-a) close to the vertical centre of the roadway as shown in Figure 7.1 for a range of positions (elevations) of the sandstone/siltstone contact; and in Figure 7.2, for a range of sandstone thicknesses.

The following points were noted from the results:

a. In general, the gradients of both tangential and normal stresses are high at and close to the free face of the excavation. A substantial increase in confining stress ($\sigma 3$) and reduction in tangential stress ($\sigma 1$) would occur at a short distance (approximately 0.5 m) from the free face. At about 2 times the height of the opening, the principal stresses are close to the in situ state of stresses (25 MPa, see Table 7.1).

b. The stress condition at the roof of the roadway is relatively independent of the position of the sandstone/siltstone contact when it is below the roof level (see Figure 7.1A to C).

c. The tangential stress ($\sigma 1$) at the roof is generally higher when the sandstone/siltstone contact is close to and above the roof. The closer the contact is to the roof, the higher is the tangential stress concentration (see Figure 7.1 D, E and F). This is primarily attributed to the concentration of stresses in the stiffer siltstone layer.

d. When the sandstone/siltstone contact occurs at the roof of the tunnel, the effect of the sandstone thickness on the stress conditions at the roof is relatively insignificant (see Figure 7.2).

e. Based on the Hoek and Brown failure criterion and the rock mass parameters described earlier, overstress would occur at the roof of the roadway. Theoretically, the extent of the overstressed zone would extend to about 0.5 m beyond the roof.

Hence, when the sandstone layer is at or very close to the roof of the tunnel, the static stress conditions would be such that overstress would occur in the sandstone and lead to initiation of fractures. When the sandstone/siltstone contact is located higher above the roof (such as the cases in Figure 7.1 f and g) the stress conditions in the sandstone would be more favourable (high confining stress and lower tangential stress). Figure 7.3 shows the variations in the magnitudes of the principal stresses with distance of the sandstone/siltstone contact (d) from the crown. The fact that outburst events took place in the burst prone sandstone where it occurred within 2.7 m of the coal (0.5 m of the crown of the roadway) is consistent with high stress concentration at the roof region.

It has been noted in Lingan Mine that the blastholes at the crown of the roadway were generally angled upwards. Furthermore, on the basis of the general blasting practices in the Sydney coalfield, the theoretical overbreak evaluated from blast simulation analysis is about 1 to 1.2 m, (which is consistent with field observations).

Such over-excavation would essentially shift the stress concentration front above the designed roof level of the roadway. As a result, even if the sandstone layer is located at some 1.2 m above the roof, it could still suffer from an adverse stress condition due to poor blasting practices.

7.3.2 Effect of In Situ Stresses

The cases presented and discussed in Section 7.2.1 pertains to the reference conditions at No. 26 Colliery where the in situ stresses are isotropic with $\sigma_h=\sigma_v = 25$ MPa. It is recognized that the in situ stresses may vary within the rock strata and between different mines. This would lead to different stress conditions around the roadway. The effect of in situ stresses was examined by analysing the same model used for case 1 in Table 7.1 for the following range of in situ stresses:

Insitu Stresses (MPa)

	σ_h^*	σ_v	$K = \sigma_h/\sigma_v$	
a.	20	20	1	(reference condition for No. 26 Colliery)
b.	25	25	1	
c.	30	30	1	
d.	25	10	2.5	(reference condition for Lingan Mine)
e.	37	15	2.5	
f.	50	20	2.5	

*σ_h is assumed to be perpendicular to the roadway axis.

The principal stresses at the contact of sandstone and siltstone above the roof of the roadway were evaluated for the above in situ stress conditions. The stresses are plotted against the distance of the contact (d) from the crown of the roadway (see Figure 7.4). It may be noted that with the exception of case 7.4(A) in which the magnitudes of the isotopic in situ stresses are at 20 MPa, all other cases would exhibit more adverse stress conditions in comparison with the reference case ($\sigma h=\sigma v$ = 25 MPa). Hence, all these conditions are also conducive to overstressing the rock mass and fracture initiation.

7.3.3 Effect of Relative Rock Mass Stiffness

The effect of relative rock mass stiffness on the stress conditions was examined by analysing the same model used for case 1 in Table 7.1 for the following range of deformation modulus for the sandstone layer.

Deformation Modulus, E (GPa)

Sandstone	Siltstone	Stiffness Ratio (S_r) E (sandstone)/E (siltstone)	Reference Figure
8.0	36.5	0.22	7.5 A
16.0	36.5	0.44*	7.5 B
36.5	36.5	1.00	7.5 C
54.8	36.5	1.50	7.5 D

* (reference condition for No. 26 Colliery)

The principal stresses at the contact of sandstone and siltstone above the roof of the roadway were evaluated for the above stiffness ratios. The stresses were plotted against the distance of the contact (d) from the crown of the roadway (see Figure 7.5).

It may be noted that the higher the stiffness ratio (E sandstone/E siltstone), the more unfavourable would be the stress condition in the sandstone. A comparison of Figures 7.5 (A) (S_r = 0.22) and 7.5 (D) (S_r = 1.5) indicates that σ_1 is higher and σ_3 is lower in the sandstone contact for the case of higher stiffness ratio.

Based on the data from no. 26 Colliery, the stiffness ratio is relatively low. The stiffness (deformation modulus) of the siltstone is about 2 times that of the sandstone. As a result, whenever the contact of sandstone/siltstone is close to the roof (Figure 7.1 E), the tangential stresses would be more concentrated in the siltstone layer. Overstressing of the siltstone layer and blast damage could break through the relatively thin siltstone cover at the roof and expose the sandstone to an adverse stress condition.

7.3.4 Analysis of the 13N Airway

Based on the outburst records of no. 26 colliery, no outburst took place during the drivage of 13N Airway although it intersected the same sandstone channel that caused events no. 10 to 12. It was noted that the 13N Airway was located about 60 m away from the initial position of the 13N longwall face. At the time when the airway heading crossed the sandstone channel, the longwall face has advanced about 550 m from its starting position.

During the development of the longwall mining, the rock strata are supported immediately behind the longwall face with hydraulic power supports. As the longwall face advances, the strata above the extracted coal seam will collapse into the mine-out area behind the face. The zone of collapse could be quite substantial and represents a region of low rock mass stiffness directly above the longwall panel. This would influence the distribution of ground stresses in the vicinity of the longwall panel.

For the purpose of this analysis, it is assumed that a zone of up to 28.5 m (approximately 10 times the height of the longwall panel) would be affected by the collapse of the longwall waste. The deformation moduli of the rock at various locations above the roof of the longwall panel are assumed as follows:

Distance Above Roof of Longwall Panel (m)	Rock Type	Deformation Modulus (GPa)
0 - 4.5	Sandstone	0.016
4.5 - 5.7	Sandstone	0.16
5.7 - 8.5	Siltstone	0.36
8.5 - 18.5	Siltstone	3.62
18.5 - 28.5	Siltstone	18.25

Note: Reference Deformation of undisturbed material $E_{(sandstone)}$ = 16 GPa; $E_{(siltstone)}$ = 36.5 GPa

The stress conditions at the roof of the 13N Airway were evaluated, taking into consideration the presence of the longwall panel located at 60 m from the Airway. The stratigraphy at the airway is shown in Figure 7.6(b). The channel sandstone, 5.7 m in thickness, directly overlies the coal seam. The in situ stresses used for the analysis were = $\sigma h = \sigma v$ = 25 MPa.

The principal stresses above the roof of the airway were presented in Figure 7.6b. This figure can be compared with Figure 7.6a which shows the stress conditions if the airway were developed without the influence of the 13N longwall panel. The minor principal stresses ($\sigma 3$) are generally similar in both cases. There is, however, substantial reduction in the major principal stress with the presence of the 13N longwall panel.

Further discussion of the overall stress regime at this location is given in Section 7.3.7.

7.3.5 Effects of Blast Damage

The potential for blast damage zone to develop around the roadway excavation was discussed in section 6 and earlier in this section. The effect of blast damage zone on the stresses at the roof of the roadway is illustrated in Figure 7.7. In this model, the main sandstone/siltstone contact is located at the crown of the roadway. Two thin layers of siltstones are present within the sandstone units. The in situ stresses used were $\sigma_h = \sigma_v$ = 25 MPa. The material within the blast damaged zone was considered to be fractured and has a deformation modulus which varies from 10% of the undisturbed value (16 GPa) at the excavation boundary to 90% of the undisturbed value at the outer limit of the blast damaged zone.

The results in Figure 7.7 clearly illustrate that immediately above the blast damage zone the confining stress (σ_3) is low and the tangential stress (σ_1) is high. The magnitudes of the stresses are similar to those at the roof of the roadway (e.g. Figure 7.1a) where blast damage was not considered in the analysis. Within the blast damage zone, however, the stresses are low as anticipated. The development of the blast damage zone has, in effect, created further stress re-distribution around the roadway and shift the stress concentration front upwards, as previously discussed. The effect of the stiffer siltstone layers on the major principal stress (σ_1) is also apparent from Figure 7.7.

7.3.6 Effects of Blast Induced Stresses

Based on the results of blast monitoring at the Lingan Mine, stress attenuation curves were developed for the dynamic stresses within the rock strata. The curve which is considered to be applicable for assessing the dynamic stresses in the sandstone is based on the following relationship:

$$\sigma_d = 3040/(S_d)^{2.31} \qquad (7.1)$$

where σ_d = Dynamic stress

S_d = scaled distance

Using this stress attenuation relationship, the dynamic stress levels generated during blasting of the roadway in No. 26 Colliery are assessed as described below.

Figure 2.12 in Section 2 shows the typical blast patterns used in No. 26 Colliery. Three reference blast patterns were available from CBDC. The maximum explosive weight per delay and the distance of the centroid of the blastholes for that particular delay to the crown of the roadway are summarized below together with the scaled distances (based on the square root relationship) and the dynamic stress levels at the crown. A correlation of the outburst events and these three reference blast patterns is presented in Table 2.5 of Section 2.

Blast Pattern	Max. Weight of Explosives per Delay (lb)	Approx. Distance between Centroid of Blast-holes to Crown of Roadway (ft)	Scaled Distance ft/(lb)$^{0.5}$	Dynamic Compressive Stress Level at Crown psi (MPa)	Dynamic Tensile Stress Level at Crown psi (MPa)
1. 14N Coal road	2 (burden holes)	4.3	3 (7.0)*	250 (1.7)	28 (0.2)
2. 13N Brushing face	7.5 (burden holes)	3.5	1.3 (4.0)	1100 (7.6)	150 (1.03)
3. 13S Airway	6 (perimeter holes)	2.5	1.0 (5)	2000 (13.8)	75 (0.52)

*Scaled distance for reflection of tensile wave

The dynamic stress levels at various distances above the crown of the roadway were evaluated according to the stress attenuation curve shown in Figure 6.3 and the results are summarized in Table 7.2. These results represent the potential dynamic stresses that could be developed in the rock mass as a result of the compressional wave and tensile wave due to reflection at the boundary of the excavation. It must be recognized however that these stresses are transient stresses generated at the onset of shotfiring. Superposition of the dynamic and static stresses are discussed below.

7.3.7 Combined Effects of Pore Gas Pressure and Stresses

The static and dynamic stresses resulting from the creation of the roadway have been addressed in Section 7.3.1 to 7.3.6. The dynamic phenomena of the outburst events are due to the combined effects of the pore gas pressure and the stresses in the rock mass. This section examines the probable critical stress levels at which outbursts took place in No. 26 Colliery by considering the mode of failure of the sandstone.

The mode of failure and the postulated processes involved in an outburst event in the outburst prone sandstone have been described in Section 7.2. In order to quantitatively address the failure of the sandstone at the on set of an outburst event, the Griffith criterion of brittle fracture (Griffith, 1924) was used to examine the stress conditions for the initiation of fracture in the sandstone in a biaxial stress field (the effect of the intermediate principal stress was not considered to be significant (Farmer 1968)).

The stress components that are relevant to the dynamic failure of the sandstone include:

a the static stresses near the surface of the outburst cavity prior to the event,
b the dynamic (tensile) stresses induced by blasting, and
c the pore gas pressure acting in the sandstone.

The combined effects of these stress components would produce a transient state of stress which could become critical for the intiation of fractures according to the Griffith's failure criterion:

$$\frac{-(\sigma 1-\sigma 3)^2}{8(\sigma 1+\sigma 3)} \geq \sigma t \qquad (7.2)$$

where σt = tensile strength of the material
$\sigma 1$ = major principal stress
$\sigma 3$ = minor principal stress

That is, fracture initiation would take place if the condition in expression (7.2) is satisfied. If the effective stresses are used, the effective major principal stress component is given by

$$\sigma 1' = \sigma 1(\text{static}) - Pg \qquad (7.3)$$

and the effective minor principal stress is given by

$$\sigma 3' = \sigma 3'' - (Pg+\sigma d) \qquad (7.4)$$

where $\sigma 1$(static) = static major principal stress
Pg = pore gas pressure
σd = dynamic stress due to reflection of tensile wave (tensile)
$\sigma 3''$ = induced static effective tensile stress

Equation 7.2 can be rewritten in terms of effective stresses as follows:

$$\frac{-(\sigma 1'-\sigma 3')^2}{8\ (\sigma 1'+\sigma 3')} \geq \sigma t \qquad (7.5)$$

$\sigma 3''$ is the induced effective tensile stress discussed in section 5.3.2. The equations governing the effective tensile stresses in the directions of σ_1, σ_2 and σ_3 are as follows:

$$\begin{aligned}\sigma_1'' &= \sigma_1 - v' (\sigma_2 + \sigma_3) \\ \sigma_2'' &= \sigma_2 - v' (\sigma_1 + \sigma_3) \\ \sigma_3'' &= \sigma_3 - v' (\sigma_1 + \sigma_2)\end{aligned} \qquad (7.6)$$

At or close to the boundary (roof) of the excavation, the stress system would be biaxial ($\sigma_3 = 0$) or triaxial with low normal stress.

Hence for $\sigma_3 = 0$

$\sigma_3'' = -v' (\sigma_1 + \sigma_2)$ is tensile

and for the case that σ_3 is low

$\sigma_3'' = \sigma_3 - v' (\sigma_1 + \sigma_2)$ could still be tensile.

At the roof of the roadway, these tensile stresses would act approximately perpendicularly to the bedding of the strata and contribute to reduce the effective confining stresses.

Based on the strength data for the sandstone from No. 26 Colliery, the uniaxial and tensile strengths reported are as follows:

	σ_c (MPa)	σ_t (MPa)
a.	59.3	7.8
b.	49.0	5.0
Av.	54.1	6.4

For an uniaxial compression test, ($\sigma_2 = \sigma_3 = 0$) the induced tensile stresses at failure, based on Eqt (7.6), is:

$$\sigma_3'' = -v' \sigma_c$$

Failure would develop if σ_3'' exceeds the tensile strength of the rock. Based on the above set of data, the average value for σt is 6.4 MPa and the average value for $v' = 0.12$.

According to Griffith's criterion (7.5) the uniaxial compressive strength is equal to $8\sigma t$ or $\sigma t/\sigma_c = v' = 0.125$.

Hence, the strength data is consistent with the Griffiths theory of fracture.

Pore Gas Pressure

Gas pressure measurements in the Sydney Coalfiled has been reviewed in Section 2.5. It is noted that the actual reservoir gas pressure in the sandstone has yet to be established. The best estimate of the gas pressure is between 2.8 and 8.0 MPa. The internal gas pressure would reduce the principal stresses generally according to the principles of effective stresses (Eqts 7.3 and 7.4).

Stress Conditions for the outburst events in No. 26 Colliery

On the basis of the stress concept formulated above, the stress conditions for the outburst events in No. 26 Colliery were examined. For comparison purposes, the stress conditions at the interface of sandstone and siltstone at 2 m from the crown of the roadway was also analyzed. This is the condition where no outburst has occurred in the sandstone. The case records considered included:

(a) 13N Airway (blast pattern no. 1)

(b) outburst events no. 1 to 9, and 13 to 37 (blast pattern no. 1)

(c) outburst events no. 10 to 12 (blast pattern no. 2)

(d) sandstone and siltstone interface at 2 m above crown (siltstone above crown) (blast pattern no. 1)

The stress conditions for each of these cases were evaluated according to Eqts (7.3) and (7.4) and compared with Griffith's criterion of fracture initiation (Eqt. 7.5). For cases (a) to (c), the average stress condition within a 0.2 m layer of rock immediately above the roof of the roadway was considered. For case (d), the average stress at 2 m from the crown in the sandstone was examined. The static stresses were evaluated on the basis of the finite element analyses presented in Section 7.3 and an isotropic in situ stress system of $\sigma h = \sigma v = 25$ MPa. For comparison purposes, the stress condition at the interface of sandstone and siltstone at 2 m from the crown of the roadway was also analysed. This is the conidition where no outburst has occurred in the sandstone.

The induced effective tensile stresses ($\sigma 3''$) were calculated based on Eqt. (7.6) and $v' = 0.12$. The dynamic stresses (σy) were based on the dynamic stress attentuation curve (Eqt. 7.1) and the reference blast patterns given in Figure 2.12 and table 2.5. The pore gas pressure ranges from 2.8 to 8.0 MPa as previously described. Table 7.3 summarizes the stress calculations and the Griffith's criterion for fracture initiation.

Discussion of Results

It may be noted that in cases (a) to (c) where the sandstone is located above the roof, the combined effects of the static and dynamic stresses and the gas pressure would develop tensile minor principal stresses within the surficial layer of the sandstone. In case (d), where the sandstone is located at 2 m above the roof, the combined stress could be compressive or tensile depending on the pore gas pressure. However, the induced tensile stress would be substantially less than those in cases (a) to (c). Eqt (7.5) can be used to evaluate whether the stress condition is critical on the basis of Griffith's criterion of fracture initiation.

The results indicated that for all the outburst events, the Griffith's failure criterion was met. Hence, fracture would have been initiated in each case. It is also of interest to note that even without gas pressure the combined effects of the static and dynamic stresses alone would have exceeded the fracture initiation criterion. As the fractures were formed, the pore gas pressure would start to act in the fractures and enhance the fracture propagation as previously described in Section 7.2.

For the case of the 13N airway, the fracture initiation criterion was not exceeded without gas pressure. With gas pressure ranging from 2.8 to 8 MPa, the fracture initiation criterion would be exceeded at a gas pressure of about 6 MPa. Hence the risk of an outburst occurring at the 13N airway would have been less compared with the other sites where outburst events were observed.

For the case of the sandstone located at 2 m from the crown, the tensile stresses based on Griffith's theory are less than the tensile strength of the sandstone. This is consistent with the record that no failure was observed under such condition.

It must be recognized that in view of the complexity of the outburst problems, and the lack of data regarding some governing parameters (e.g. the pore gas pressure), assumptions and generalization of the condition have been made to allow quantitative assessment of the proposed model. On the basis of the analyses undertaken and the calibration of the results with the documented case histories from No. 26 Colliery, it appears that the proposed stress concept for outburst initiation is consistent with the occurrence of the outburst events.

More detailed analyses might be carried out to determine the gas pressure distribution around the roadway (e.g. pore gas pressure gradient), but more specific data would be required on the porosity and gas permeability of the rock mass, the initial reservoir gas pressure and the stress dependency of these parameters. In this regard, the proposed model is limited in defining the relationship of the transient pore gas pressure under stress at the moment of fracture initiation. The significance of gas pressure in outburst occurrence is illustrated in Table 7.3 which shows that a reduction in the gas pressure could have reduced the risk of the outburst hazards especially for marginal cases.

Another significant implication of the static and dynamic stress effects is also noted from the analysis. The dynamic stresses are very much a function of the scaled distance which relates to the distance from the dynamic energy source (blast) and of the explosive weight used for the blast delay. The blast induced tensile stress in most of the roadway development (based on blast pattern no. 1) were relatively low except for events no. 10 to 12. This was attributed to the use of uncharged holes on the roadway periphery and the separate firing sequence of the wing burden holes. However, outbursts consistently occurred in the sandstone despite these measures. This indicates that the static stress concentration and pore gas pressure would also have contributed significantly to the occurrence of the dynamic events. In all the analyses the reference in situ stress system is isotropic. Increase in anisotropy of the in situ stresses will result in higher stress concentration and consequently higher induced tensile stresses.

TABLE 7.1

CASES FOR FINITE ELEMENT ANALYSIS OF TYPICAL ROADWAY DEVELOPMENT

CASE	DESCRIPTION	REFERENCE FIGURE
1	o Roof of roadway at elevation -787.9 m o Sandstone thickness = 5.7 m o Contact between sandstone and underlying siltstone layer varies from elevation -786.2 to -789.2 m (1.7 m above to 1.3 m below crown of roadway) o Insitu stresses $\sigma_h = \sigma_v = 25$ MPa	7.1
2	o Roof of roadway at elevation -787.9 m o Sandstone and siltstone contact at crown of roadway (elevation -787.9 m) o Thickness of sandstone varies from 0.5 m to 5.7 m o Insitu stresses $\sigma_h = \sigma_v = 25$ MPa	7.2
3	o Roof of roadway at elevation -787.9 m o Sandstone and underlying siltstone contact varies from 0 m to 2.2 m above crown of roadway o Insitu stresses $\sigma_h = \sigma_v = 25$ MPa	7.3
4	o Roof of roadway at elevation -787.9 m o Sandstone and underlying siltstone contact varies from 0 to 20 m o Insitu stresses varying between the following values: $\sigma_h=\sigma_v = 20$ MPa $\sigma_h=\sigma_v = 25$ MPa $\sigma_h=\sigma_v = 30$ MPa $\sigma_h=25$ MPa $\sigma_v=10$ MPa $\sigma_h=37$ MPa $\sigma_v=15$ MPa	7.4
5	o Roof of roadway at elevation -787.9 m o Sandstone and underlying siltstone contact varies from 0 to 20 m o Insitu stresses $\sigma_h=\sigma_v = 25$ MPa o Deformation modulus of sandstone varies between 8 GPa and 54.8 GPa	7.5

TABLE 7.2 DYNAMIC STRESS GENERATED FROM REFERENCE BLAST PATTERNS USED IN NO. 26 COLLIERY

Blast Pattern	Dynamic Stresses (MPa) with distance above crown (m)								
	0	0.5	1	1.5	2	3	4	6	10
1. 14N coal road	1.7 (0.2)*	1.1 (0.17)	0.8 (0.10)	0.68 (0.07)	0.55 (0.06)	0.45 (0.05)	0.36 (0.05)	0.13 (<0.05)	<0.1 (<0.05)
2. 13N brushing face	7.6 (1.03)	4.8 (0.62)	2.1 (0.48)	1.5 (0.28)	0.8 (0.26)	0.62 (0.16)	0.34 (0.11)	0.15 (0.07)	<0.1 (0.06)
3. 13S airway	13.8 (0.52)	6.9 (0.38)	2.7 (0.28)	1.4 (0.22)	0.8 (0.15)	0.62 (0.10)	0.34 (0.05)	0.15 (<0.05)	<0.1 (<0.05)

* Figures in brackets are dynamic tensile stresses due to wave reflection.

TABLE 7.3

INDUCED TENSILE STRESSES ON A 0.2 M THICK LAYER ABOVE ROOF OF ROADWAY STRESS CONDITION AT THE ROOF OF THE ROADWAY IN NO. 26 COLLIERY

	Average Stress Conditions within a 0.2 m thick layer at the roof			Induced Effective Tensile Stress Due to Static Stresses	Induced Tensile Stress Due to Shotfiring	Pore Gas Pressure	Combined Effective Stresses (MPa)		Griffith's Fracture Criterion	Average Tensile Strength
	σ_1 (MPa)	σ_2 (MPa)	σ_3 (MPa)	σ_3'' (MPa)	(MPa)	P_g (MPa)	σ_1'	σ_3'	$-\frac{(\sigma_1'-\sigma_3')^2}{8(\sigma_1'+\sigma_3')}$	σt (MPa)
(a) 13W Airway[(1)]*	32	25	4	-2.8	-0.2	2.8 to 8	29.2 to 24	-5.8 to -11	- 6.5 to -11.8	7.0
(b) Event No. 1 to 9 and 13 to 37[(1)]	50	25	4.5	-4.5	-0.2	2.8 to 8	47.2 to 42	-7.5 to -12.7	- 9.4 to -12.8	7.0
(c) Event No. 10 to 12[(2)]	50	25	4.5	-4.5	-1.0	2.8 to 8	47.2 to 42	- 8.3 to -13.5	-10.0 to -13.5	7.0
(d) Sandstone[(1)] at 2 m from crown	40	25	14	+6.2 (compressive)	-0.6	2.8 to 8	37.2 to 32	+ 3.3 to - 1.9	- 4.2 to - 4.7	7.0
	(Average stress conditions at 2 m from crown)									

NOTES:
1. σ_1, σ_2 and σ_3 are principal stresses
2. In situ stress $\sigma_h = \sigma_v = 25$ MPa
3. * blast pattern
4. See Section 7.3.7 for calculation of combined effective stresses.

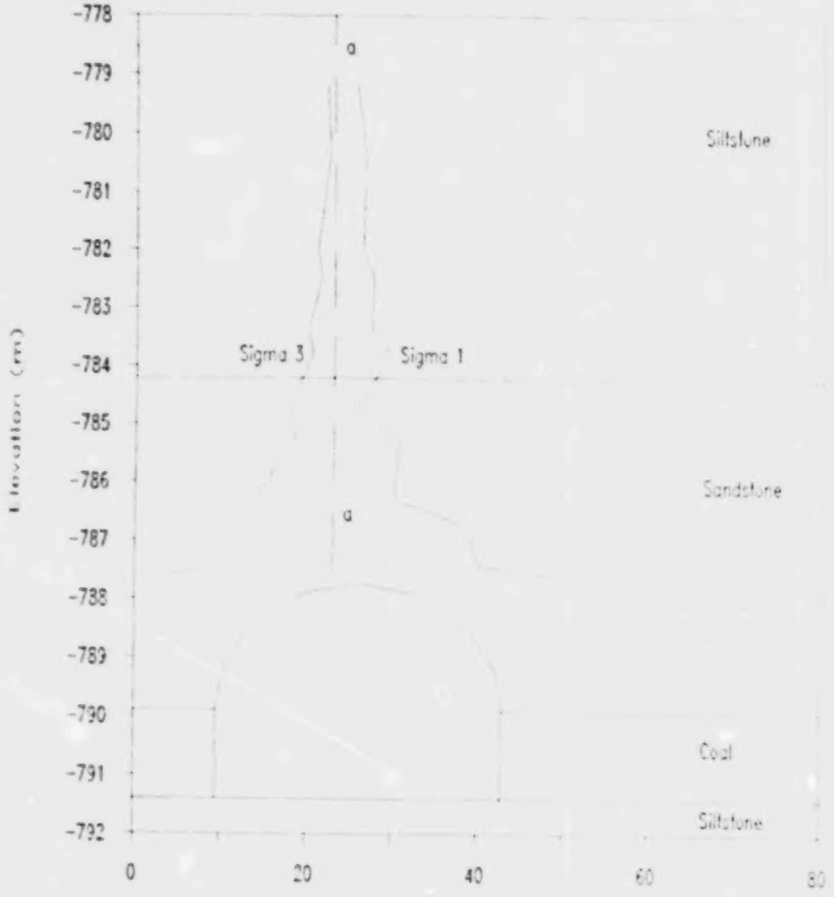
-778
-779
-780
-781
-782
-783
-784
-785
-786
-787
-788
-789
-790
-791
-792
Elevation (m)
a
a
Sigma 3
Sigma 1
Siltstone
Sandstone
Coal
Siltstone
0
20
40
60
80
Stress along line a-a (MPa)

(A)

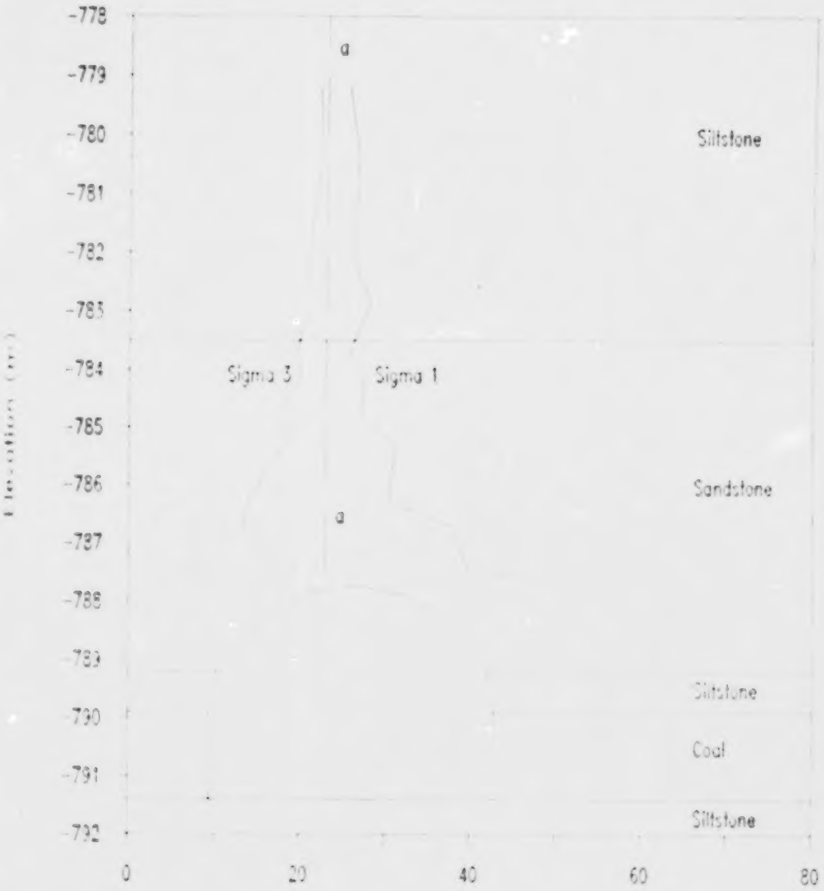
-778
-779
-780
-781
-782
-783
-784
-785
-786
-787
-788
-789
-790
-791
-792
Elevation (m)
a
a
Sigma 3
Sigma 1
Siltstone
Sandstone
Siltstone
Coal
Siltstone
0
20
40
60
80
Stress along line a-a (MPa)

(B)

-778
-779
-780
-781
a
Siltstone

-778
-779
-780
-781
a
Siltstone

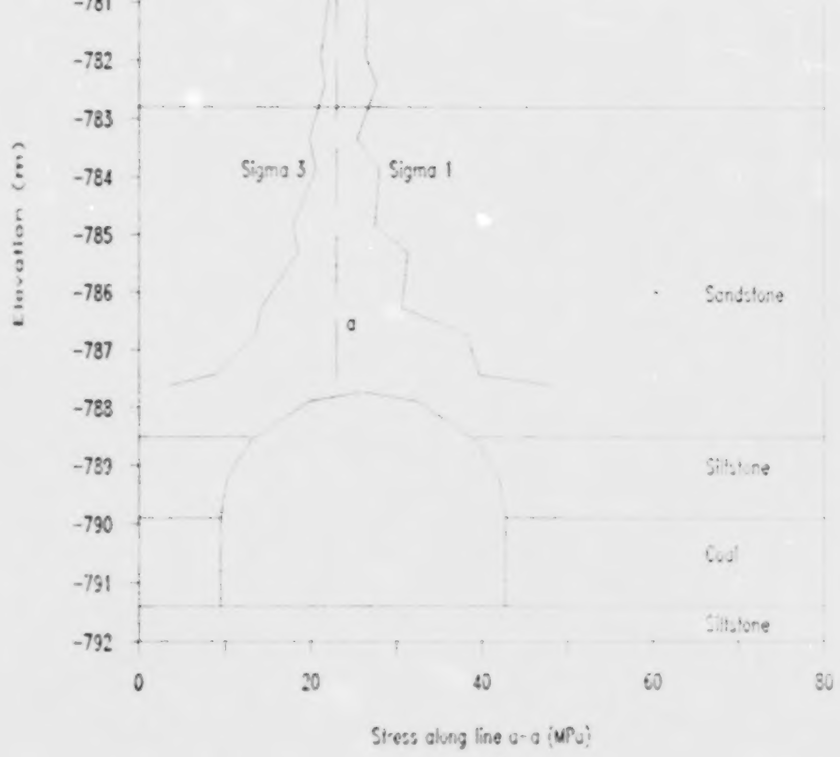
-781
-782
-783
-784
-785
-786
-787
-788
-789
-790
-791
-792
Elevation (m)
Sigma 3
Sigma 1
a
Sandstone
Siltstone
Coal
Siltstone
0
20
40
60
80
Stress along line a-a (MPa)

(C)

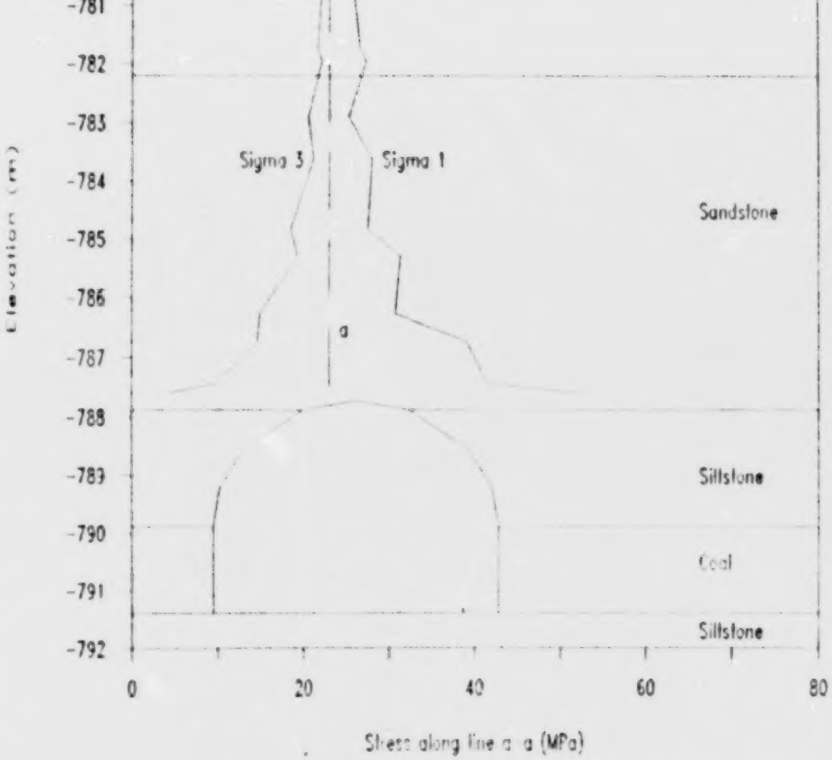
-781
-782
-783
-784
-785
-786
-787
-788
-789
-790
-791
-792
Elevation (m)
Sigma 3
Sigma 1
a
Sandstone
Siltstone
Coal
Siltstone
0
20
40
60
80
Stress along line a-a (MPa)

(D)

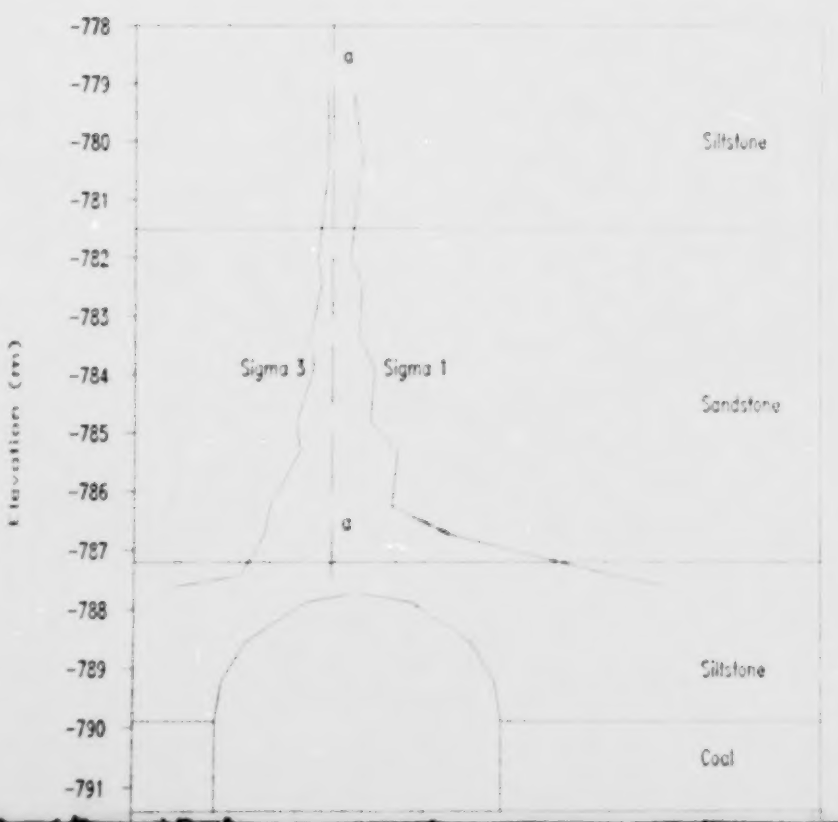
-778
-779
-780
-781
-782
-783
-784
-785
-786
-787
-788
-789
-790
-791
Elevation (m)
a
Sigma 3
Sigma 1
a
Siltstone
Sandstone
Siltstone
Coal

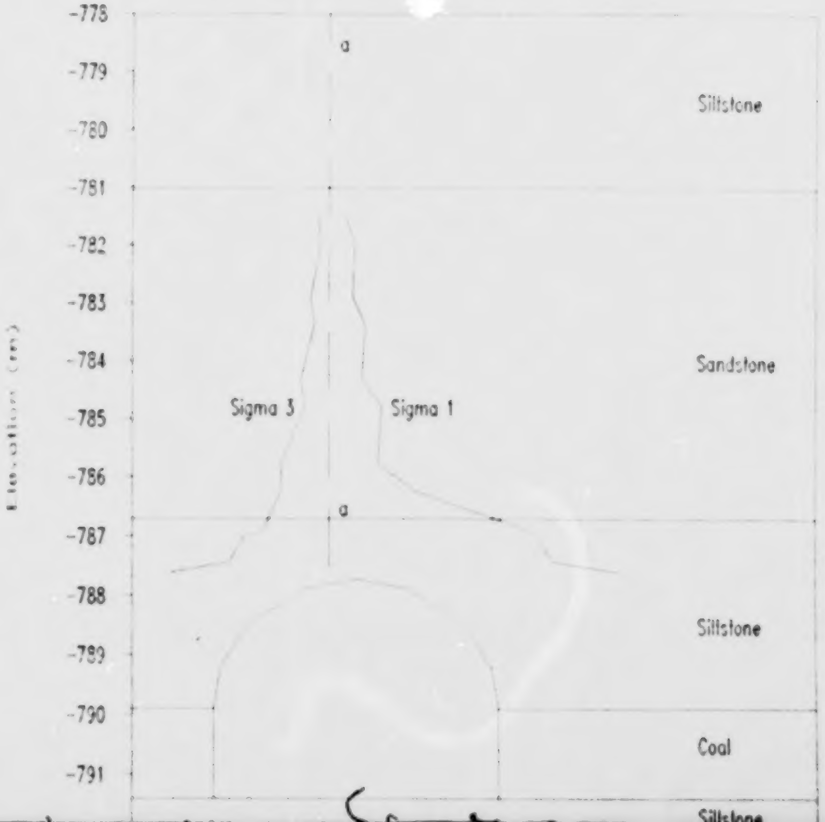
-778
-779
-780
-781
-782
-783
-784
-785
-786
-787
-788
-789
-790
-791
Elevation (m)
a
Sigma 3
Sigma 1
a
Siltstone
Sandstone
Siltstone
Coal
Siltstone

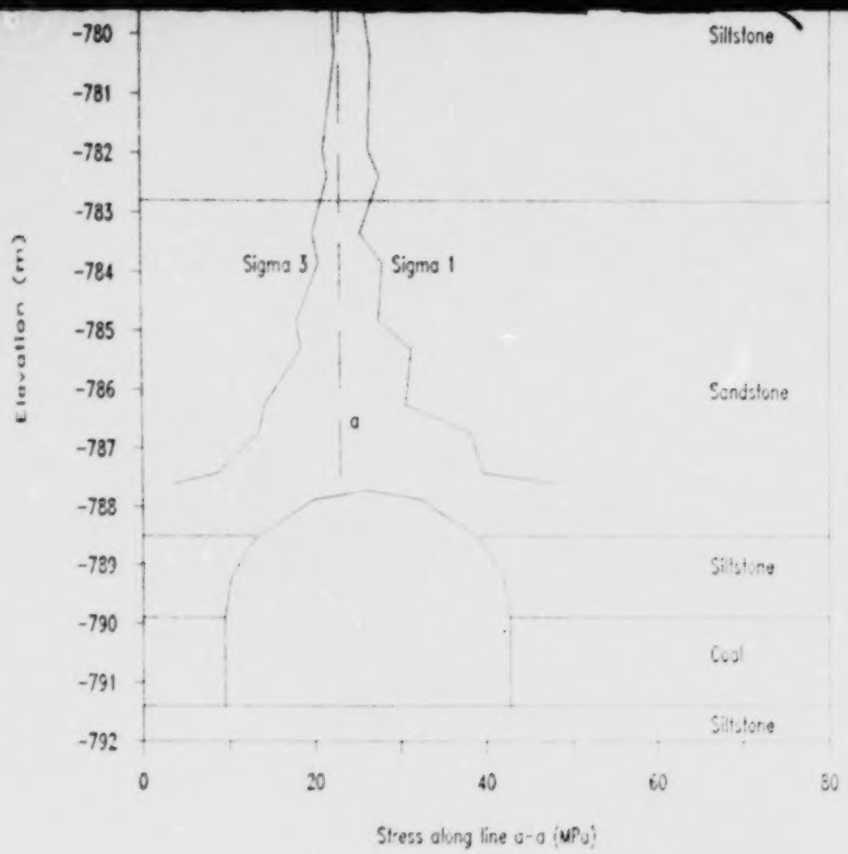
Elevation (m)
-780
-781
-782
-783
-784
-785
-786
-787
-788
-789
-790
-791
-792
Siltstone
Sandstone
Siltstone
Coal
Siltstone
Sigma 3
Sigma 1
a
0
20
40
60
80
Stress along line a–a (MPa)

(C)

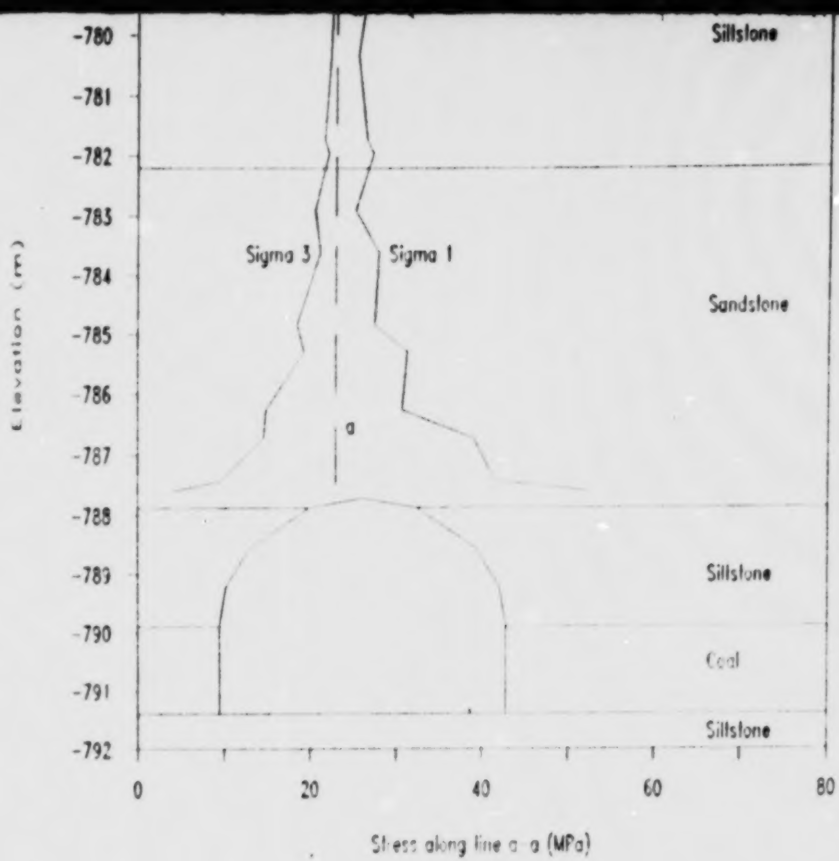
Elevation (m)
-780
-781
-782
-783
-784
-785
-786
-787
-788
-789
-790
-791
-792
Siltstone
Sandstone
Siltstone
Coal
Siltstone
Sigma 3
Sigma 1
a
0
20
40
60
80
Stress along line a–a (MPa)

(D)

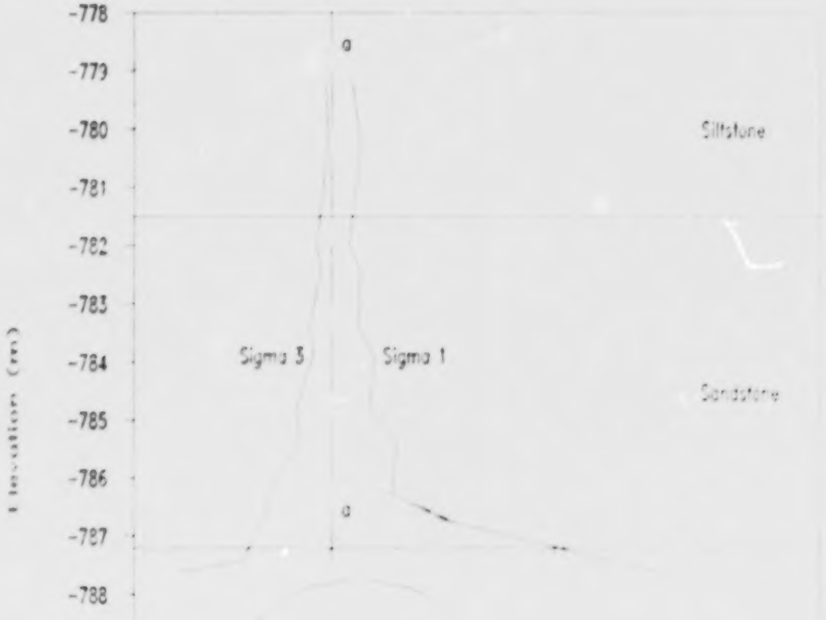
Elevation (m)
-778
-779
-780
-781
-782
-783
-784
-785
-786
-787
-788
Siltstone
Sandstone
Sigma 3
Sigma 1
a
a

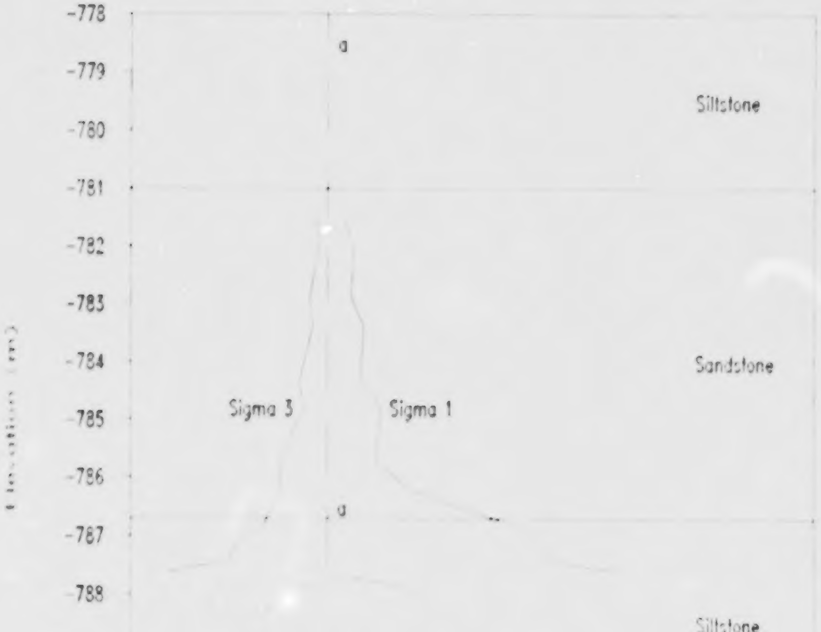
Elevation (m)
-778
-779
-780
-781
-782
-783
-784
-785
-786
-787
-788
Siltstone
Sandstone
Siltstone
Sigma 3
Sigma 1
a
a

PRINCIPAL STRESSES AT THE ROOF OF A TYPICAL ROADWAY IN No. 26 COLLIERY FOR VARIOUS POSITIONS OF SANDSTONE LAYER

FIGURE 7.1

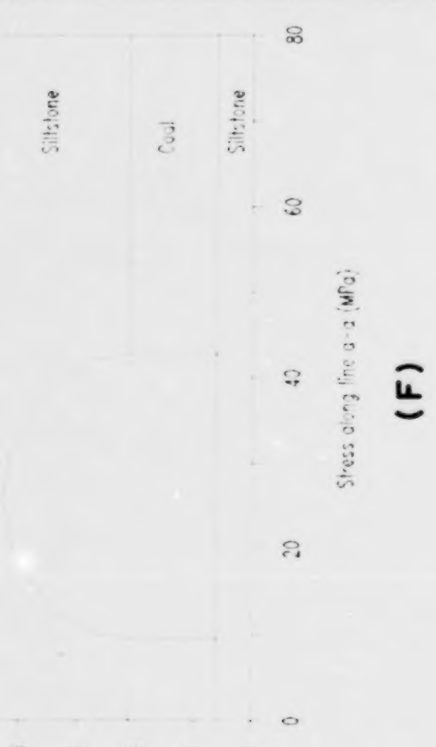

(F)

NOTES:

1. DIMENSIONS OF TYPICAL ROADWAY ARE [illegible] m WIDE BY [illegible] m HIGH.
2. SIGMA 1 [illegible] AND SIGMA 3 [illegible] ARE MAJOR AND MINOR PRINCIPAL STRESSES RESPECTIVELY.
3. LINE A-A IS SLIGHTLY OFF VERTICAL CENTRE LINE OF ROADWAY.
4. GENERAL STRATIGRAPHIC DATA AVAILABLE FROM [illegible]

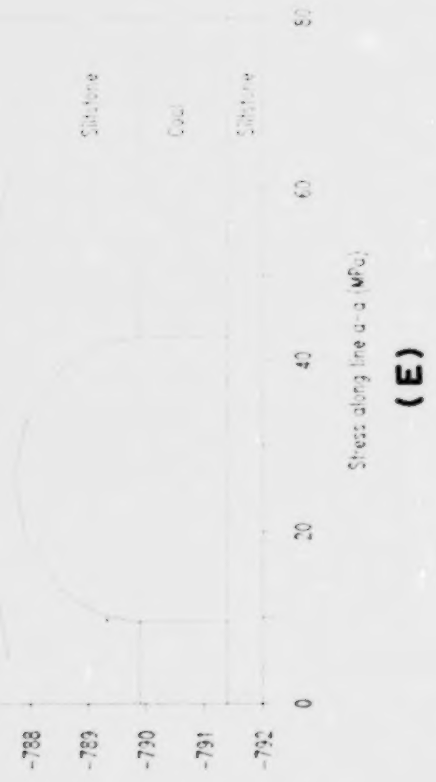

(E)

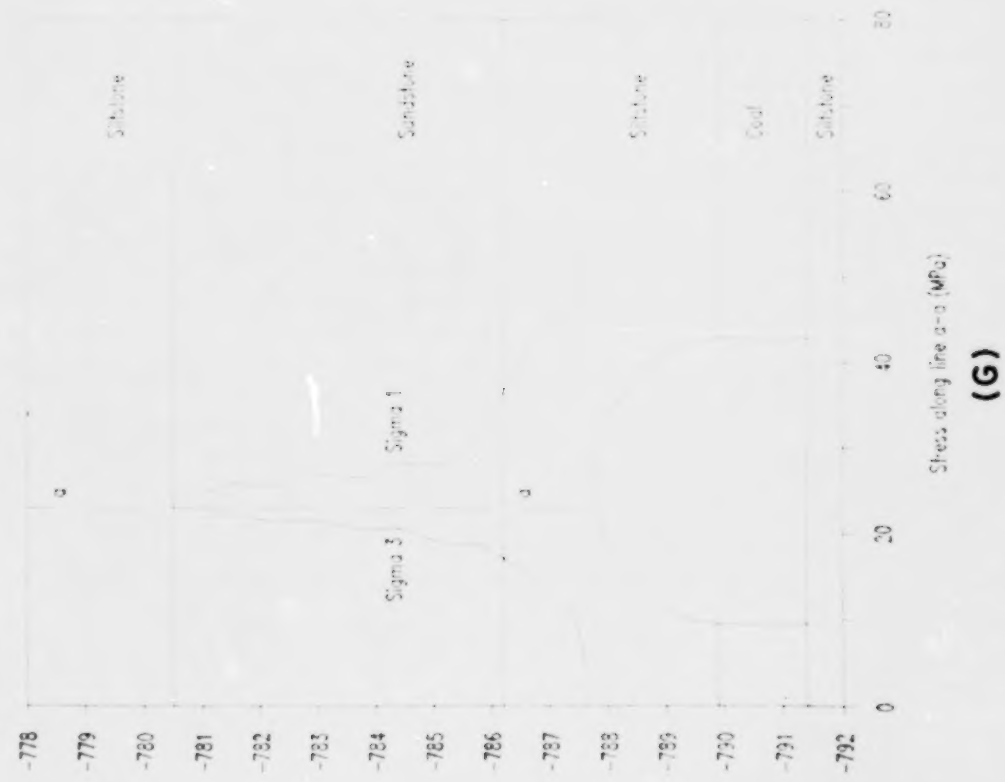

(G)

Date FEB 17, 1987
Project 861-1290

Golder Associates

Drawn RWR
Chkd

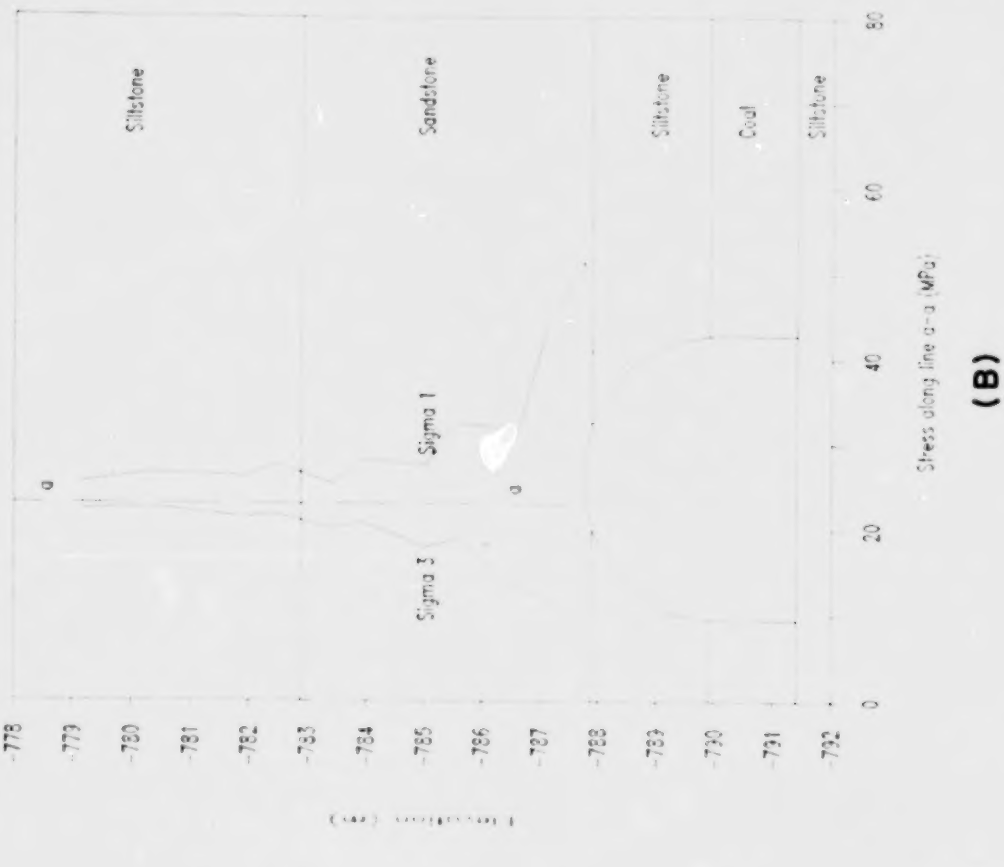
Siltstone
Sandstone
Siltstone
Coal
Siltstone
Sigma 1
Sigma 3
a
a
-778
-779
-780
-781
-782
-783
-784
-785
-786
-787
-788
-789
-790
-791
-792
Elevation (m)
0
20
40
60
80
Stress along line a–a (MPa)

(B)

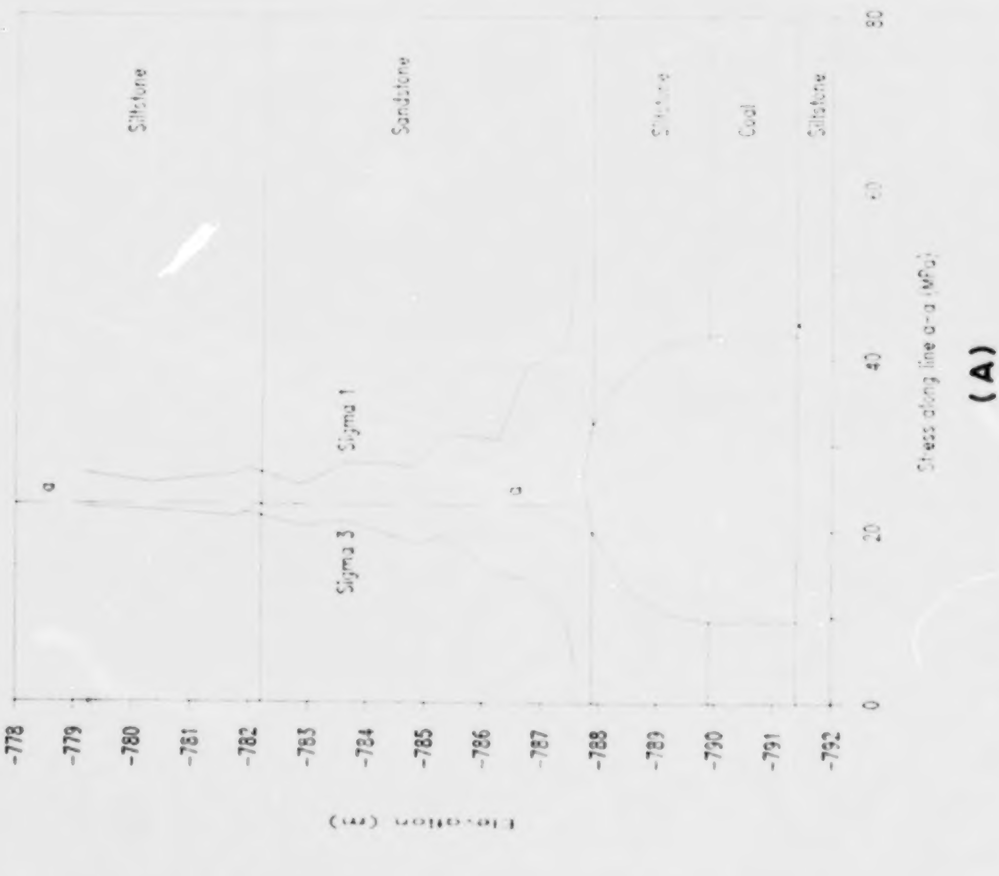
Siltstone
Sandstone
Siltstone
Coal
Siltstone
Sigma 1
Sigma 3
a
a
-778
-779
-780
-781
-782
-783
-784
-785
-786
-787
-788
-789
-790
-791
-792
Elevation (m)
0
20
40
60
80
Stress along line a–a (MPa)

(A)

Siltstone
a
-778
-779
-780
-781
-782

Siltstone
a
-778
-779
-780
-781
-782

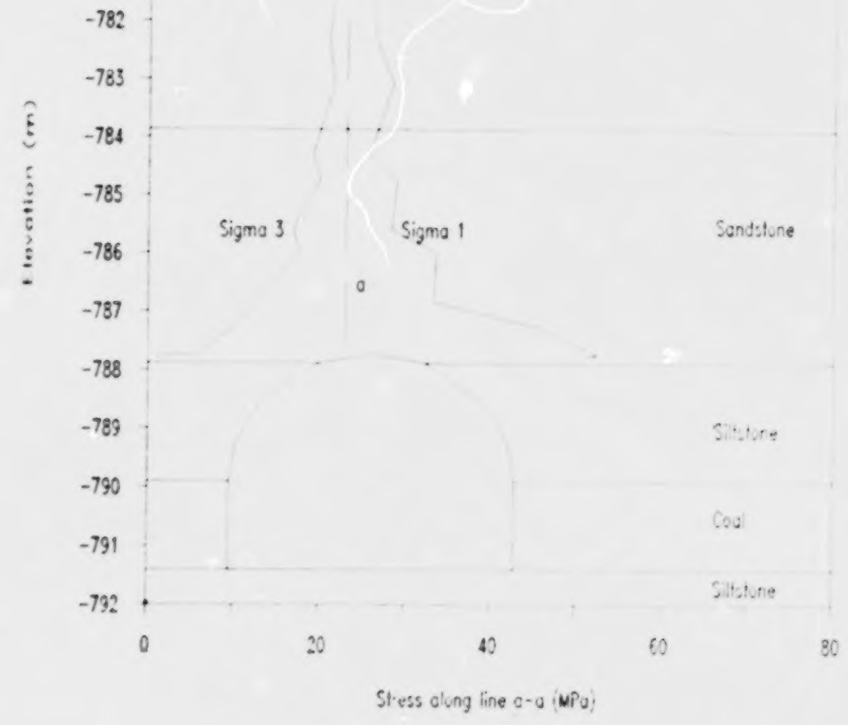
Elevation (m)
-782
-783
-784
-785
-786
-787
-788
-789
-790
-791
-792
Sigma 3
Sigma 1
a
Sandstone
Siltstone
Coal
Siltstone
0
20
40
60
80
Stress along line a-a (MPa)

(C)

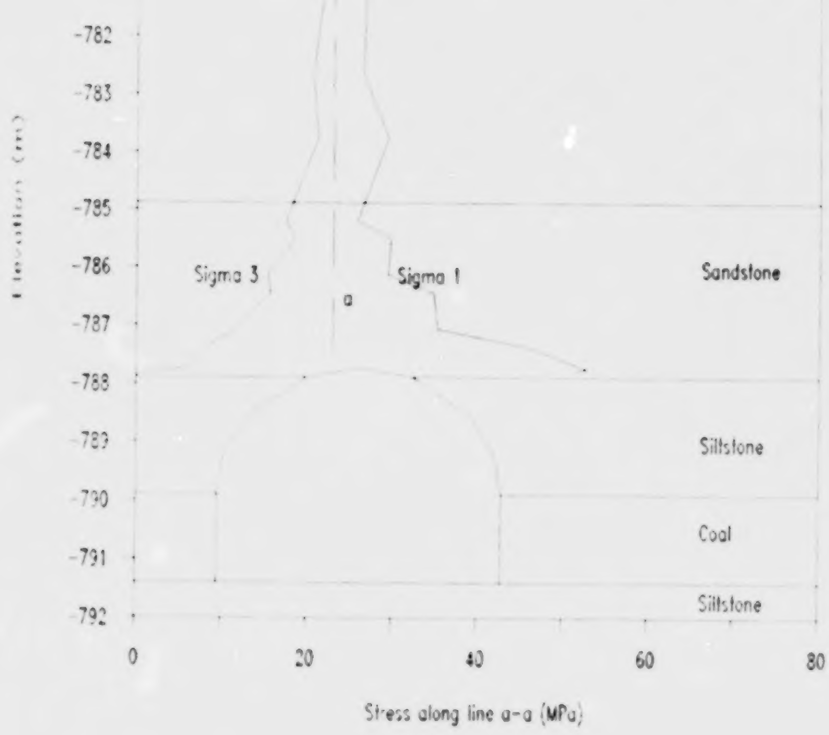
Elevation (m)
-782
-783
-784
-785
-786
-787
-788
-789
-790
-791
-792
Sigma 3
Sigma 1
a
Sandstone
Siltstone
Coal
Siltstone
0
20
40
60
80
Stress along line a-a (MPa)

(D)

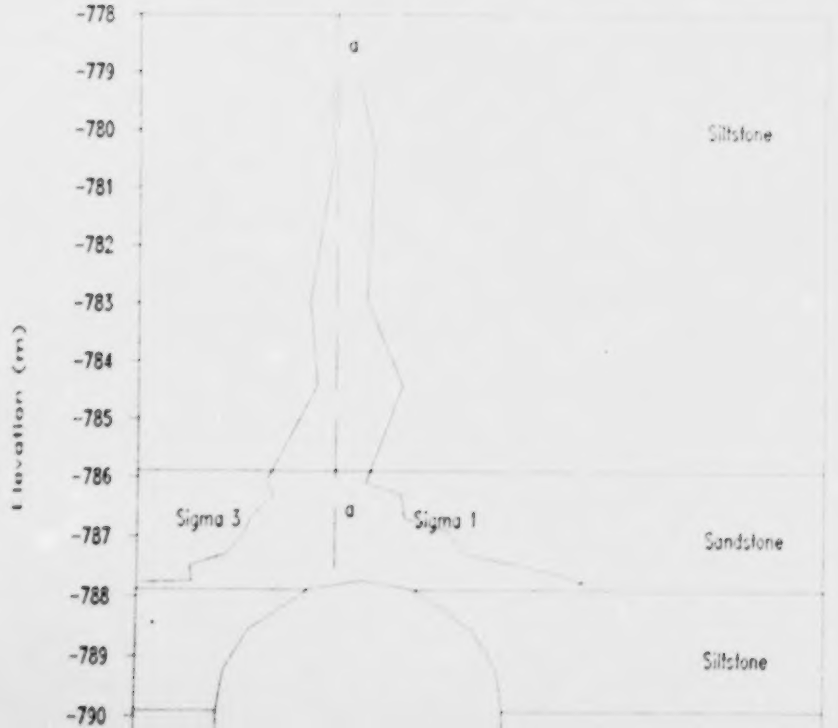
Elevation (m)
-778
-779
-780
-781
-782
-783
-784
-785
-786
-787
-788
-789
-790
a
Siltstone
Sigma 3
Sigma 1
Sandstone
Siltstone

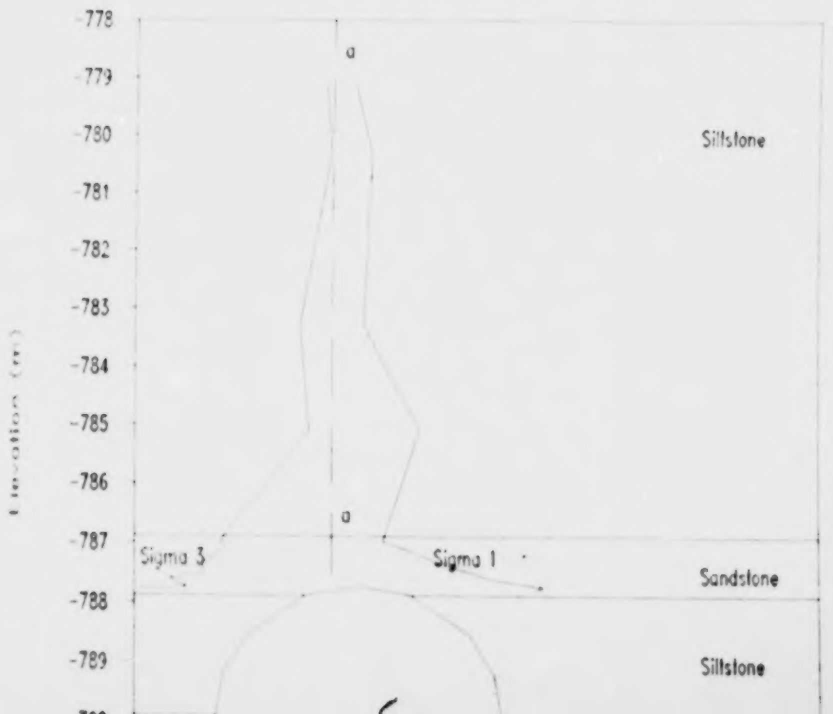
Elevation (m)
-778
-779
-780
-781
-782
-783
-784
-785
-786
-787
-788
-789
a
Siltstone
Sigma 3
Sigma 1
Sandstone
Siltstone

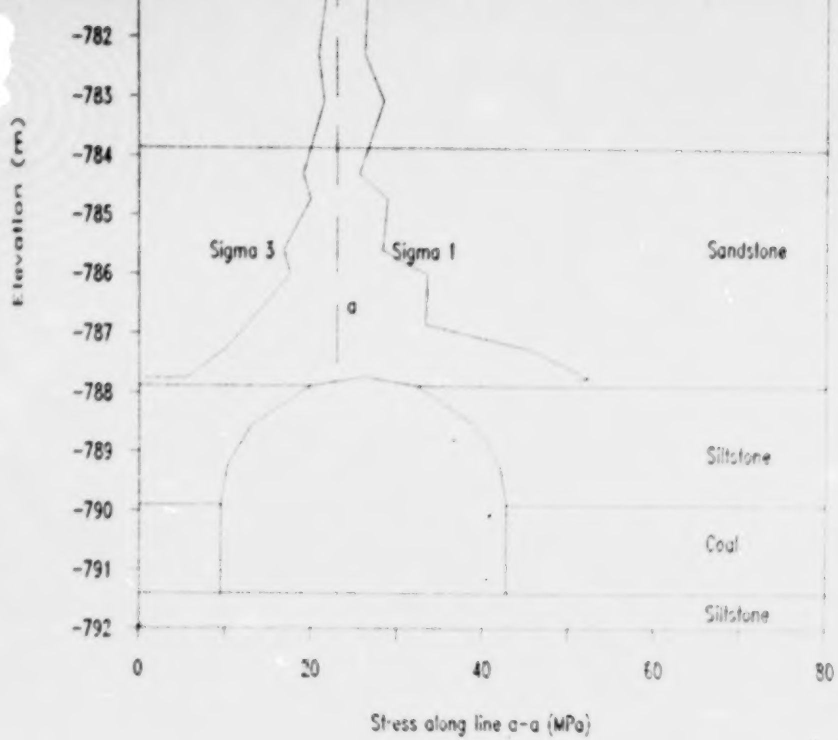
Elevation (m)
-782
-783
-784
-785
-786
-787
-788
-789
-790
-791
-792
Sigma 3
Sigma 1
a
Sandstone
Siltstone
Coal
Siltstone
0
20
40
60
80
Stress along line a-a (MPa)

(C)

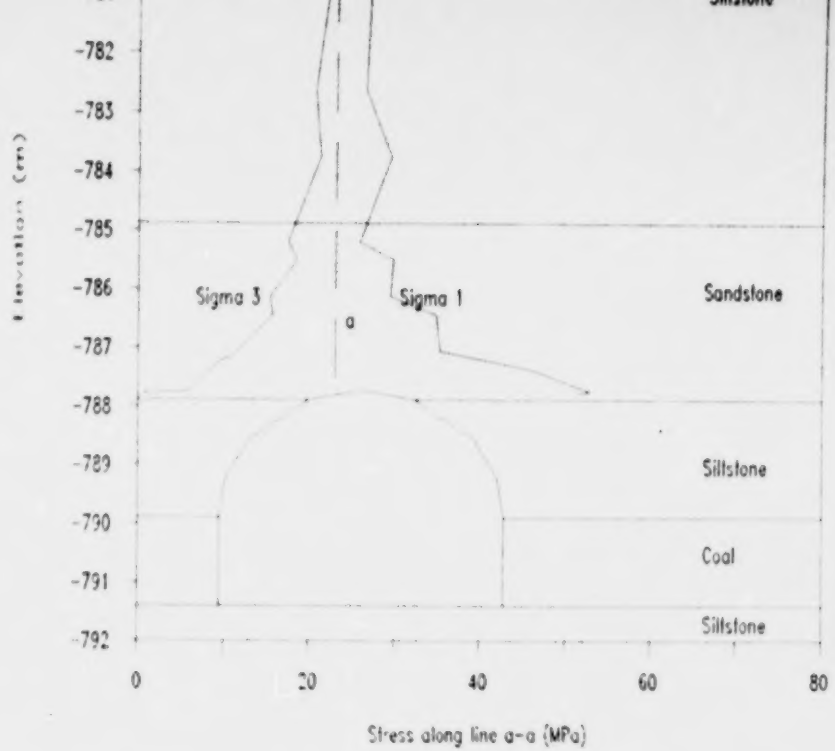
Elevation (m)
-782
-783
-784
-785
-786
-787
-788
-789
-790
-791
-792
Sigma 3
Sigma 1
a
Sandstone
Siltstone
Coal
Siltstone
0
20
40
60
80
Stress along line a-a (MPa)

(D)

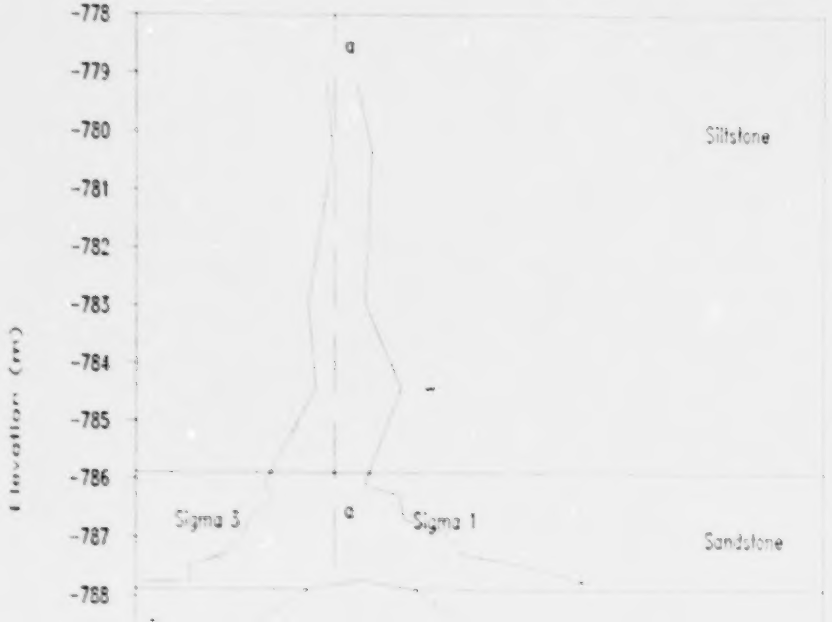
Elevation (m)
-778
-779
-780
-781
-782
-783
-784
-785
-786
-787
-788
a
Siltstone
a
Sigma 3
Sigma 1
Sandstone

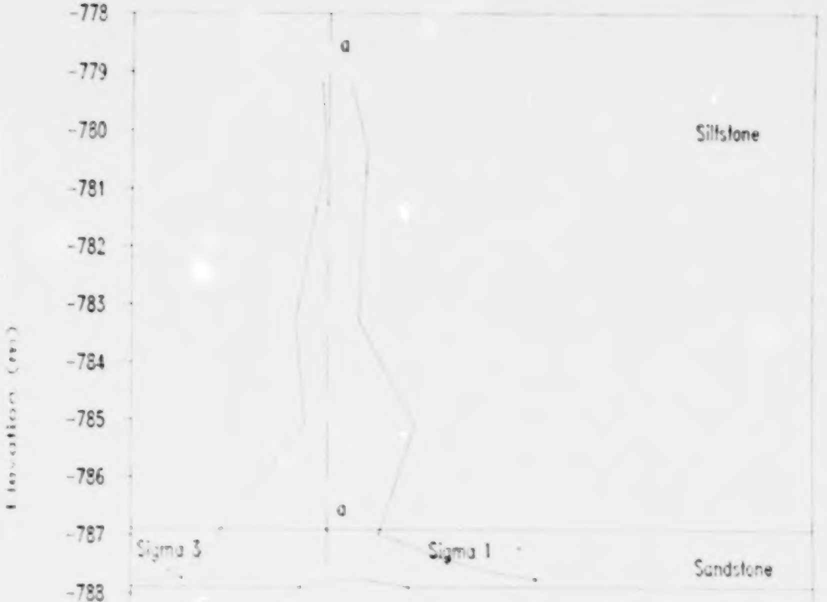
Elevation (m)
-778
-779
-780
-781
-782
-783
-784
-785
-786
-787
-788
a
Siltstone
a
Sigma 3
Sigma 1
Sandstone

PRINCIPAL STRESSES AT THE ROOF OF A TYPICAL ROADWAY IN No. 26 COLLIERY FOR VARIOUS THICKNESS OF SANDSTONE LAYER

FIGURE 7.2

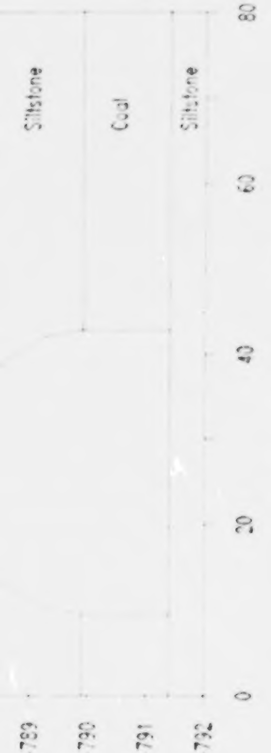

(F)

NOTES:

1. DIMENSIONS OF TYPICAL ROADWAY ARE [illegible] m WIDE BY [illegible] m HIGH.
2. SIGMA 1 ([illegible]) AND SIGMA 3 ([illegible]) ARE MAJOR AND MINOR PRINCIPAL STRESSES RESPECTIVELY.
3. LINE a-a IS SLIGHTLY OFF VERTICAL CENTER LINE OF ROADWAY.
4. [illegible]

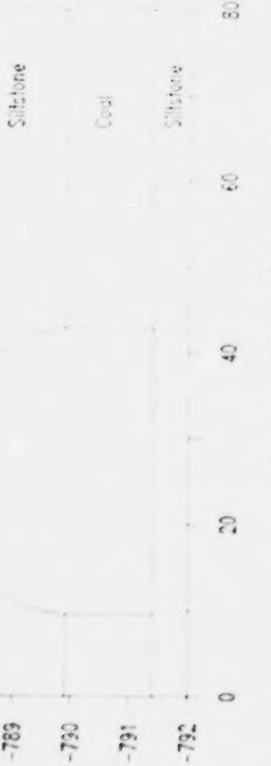

(E)

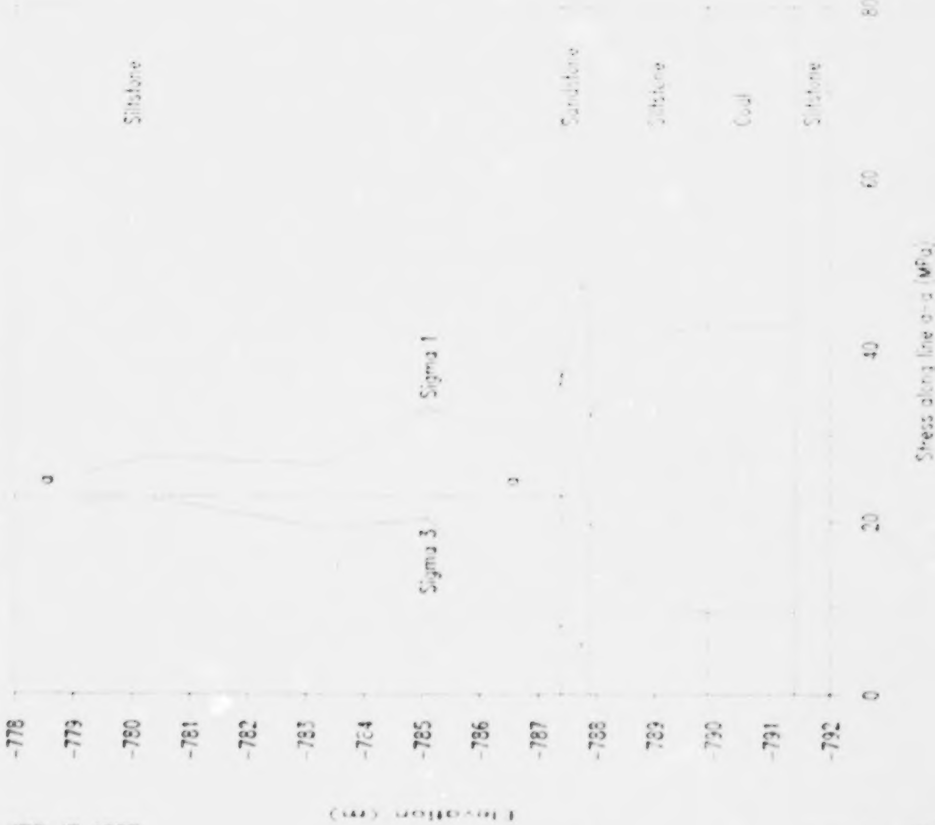

(G)

Date FEB 17, 1987

Project 861-1290

Golder Associates

Drawn RWR

Chkd

VARIATIONS OF PRINCIPAL STRESSES WITH DISTANCE OF SANDSTONE/SILTSTONE CONTACT FROM CROWN OF ROADWAY - REFERENCE CASE

FIGURE 7.3

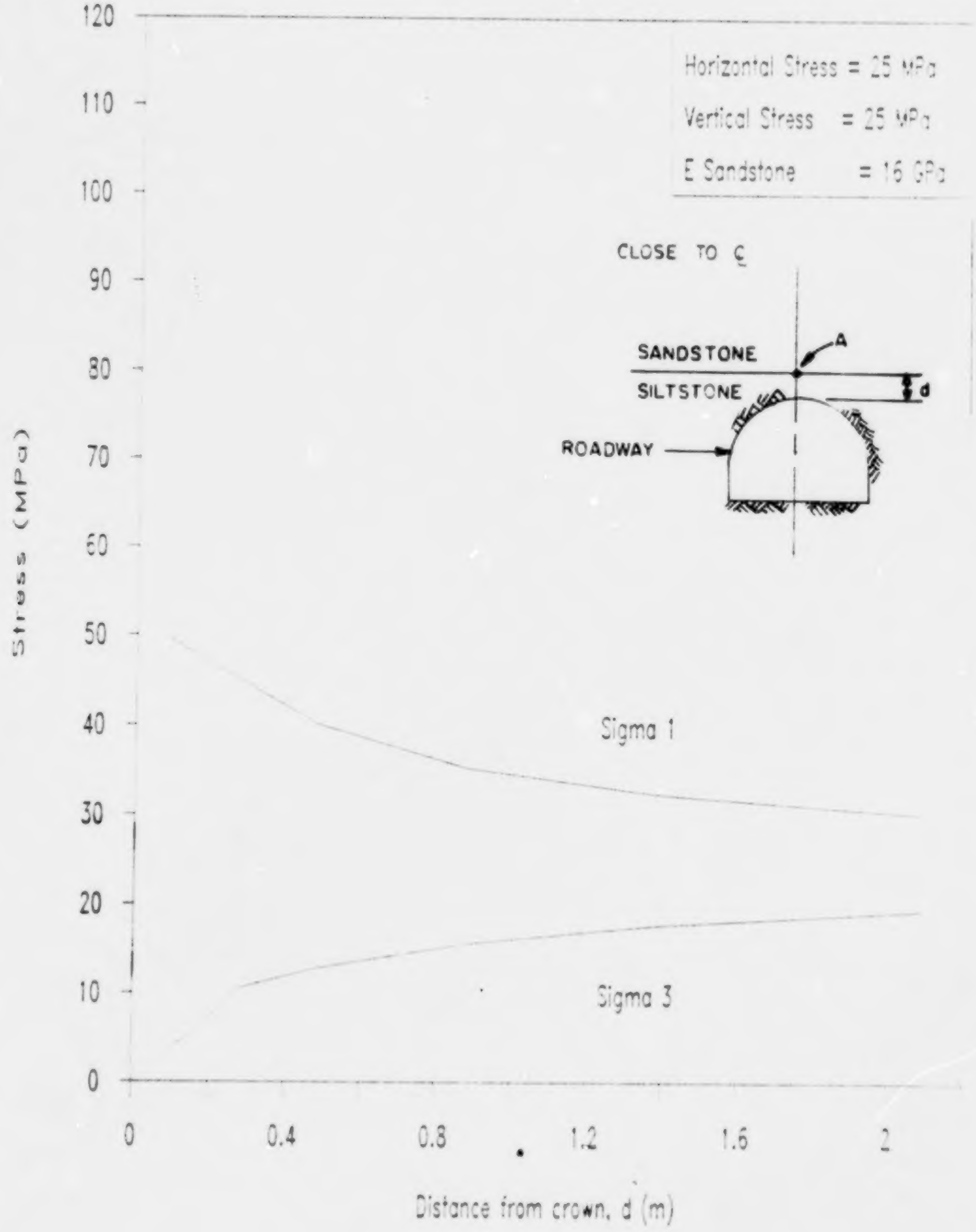

NOTE: STRESSES SHOWN ARE PRINCIPAL STRESSES AT POINT A.

Date MARCH, 1987
Project 861 - 1290

Golder Associates

Drawn D. M.
Chkd

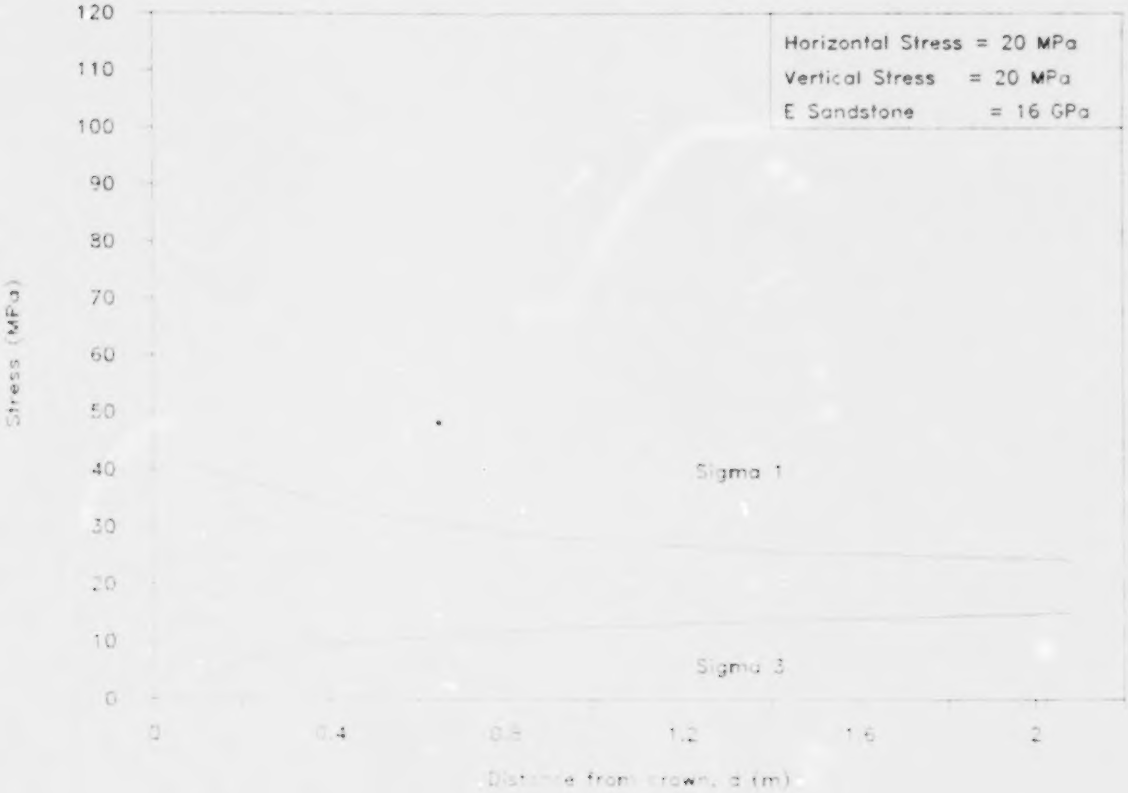
Horizontal Stress = 20 MPa
Vertical Stress = 20 MPa
E Sandstone = 16 GPa
Stress (MPa)
120
110
100
90
80
70
60
50
40
30
20
10
0
Sigma 1
Sigma 3
0
0.4
0.8
1.2
1.6
2
Distance from crown, d (m)

(A)

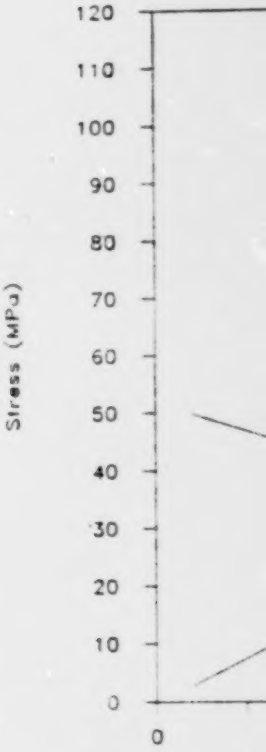
Stress (MPa)
120
110
100
90
80
70
60
50
40
30
20
10
0
0

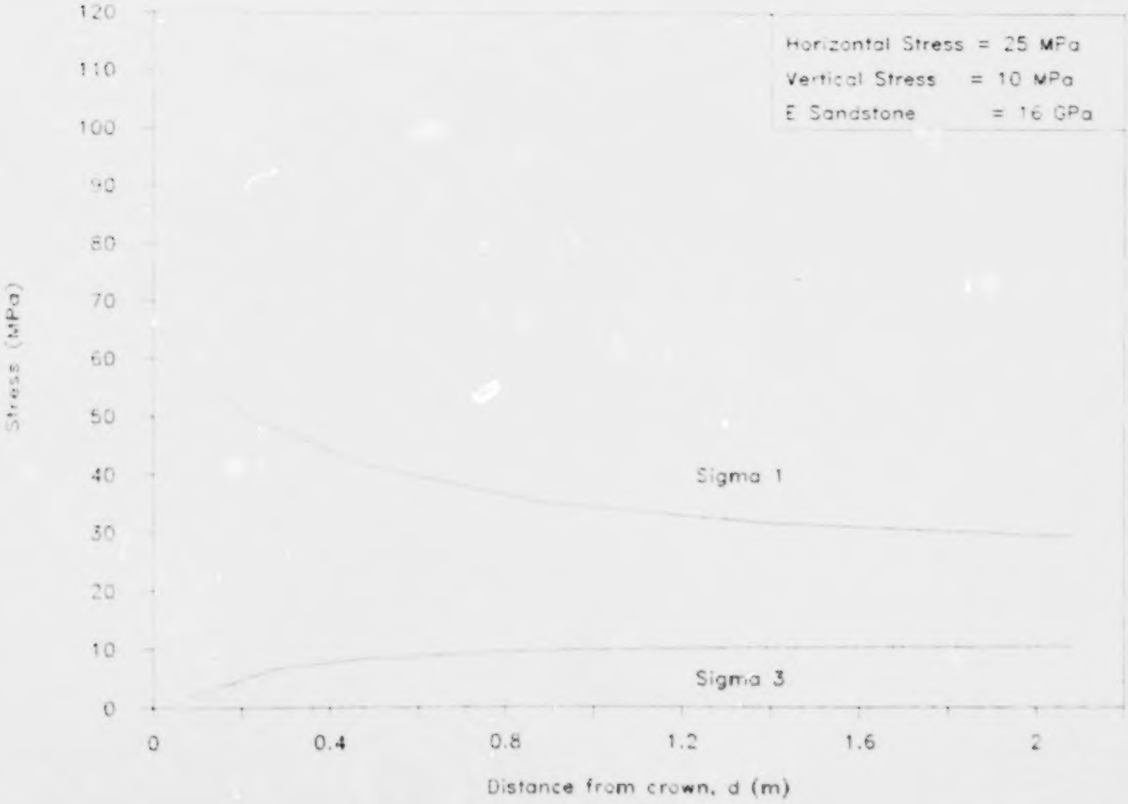
Horizontal Stress = 25 MPa
Vertical Stress = 10 MPa
E Sandstone = 16 GPa
Stress (MPa)
120
110
100
90
80
70
60
50
40
30
20
10
0
Sigma 1
Sigma 3
0
0.4
0.8
1.2
1.6
2
Distance from crown, d (m)

(D)

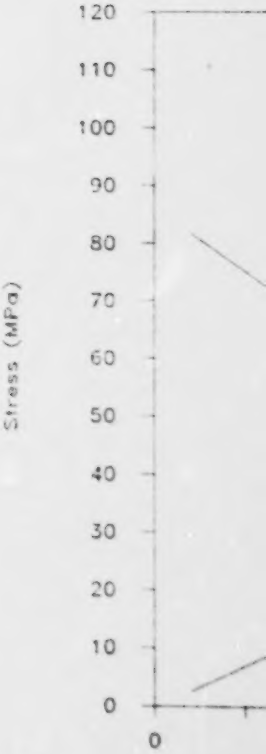
Stress (MPa)
120
110
100
90
80
70
60
50
40
30
20
10
0
0

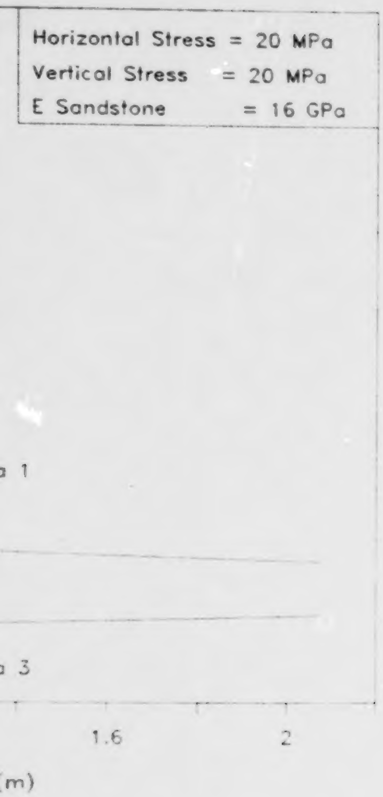
Horizontal Stress = 20 MPa
Vertical Stress = 20 MPa
E Sandstone = 16 GPa
a 1
a 3
1.6
2
(m)

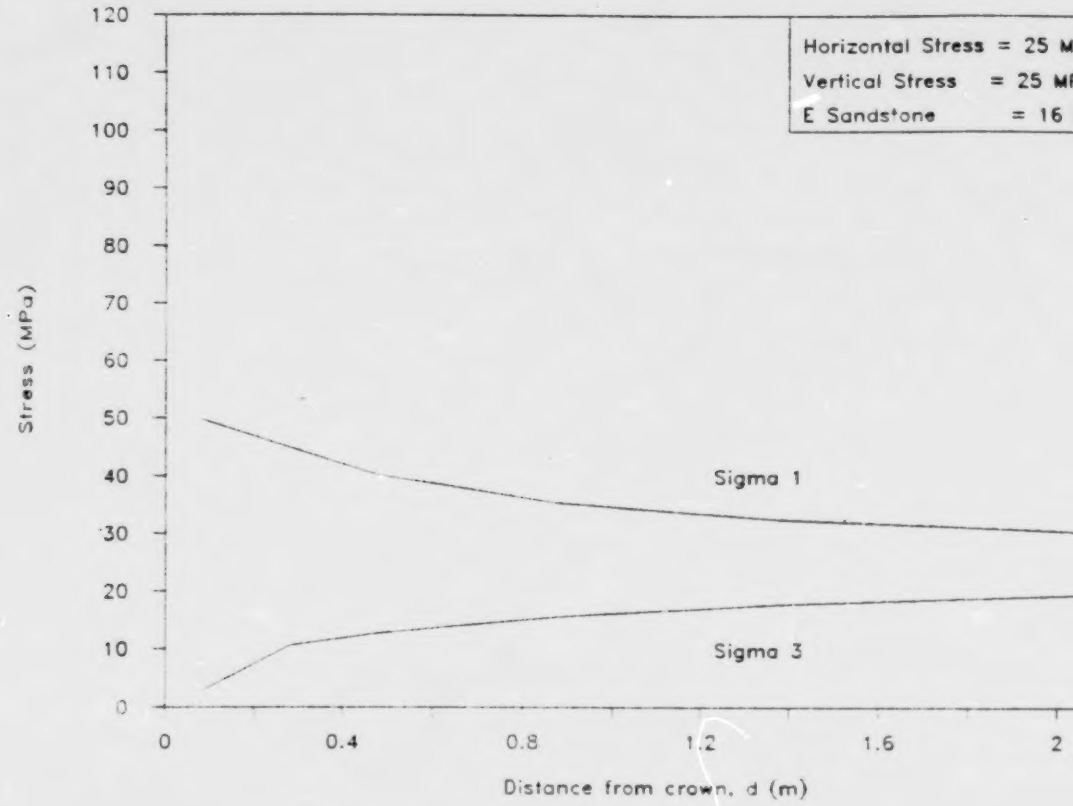
120
110
100
90
80
70
60
50
40
30
20
10
0
Stress (MPa)
Horizontal Stress = 25 M
Vertical Stress = 25 M
E Sandstone = 16
Sigma 1
Sigma 3
0
0.4
0.8
1.2
1.6
2
Distance from crown, d (m)

(B)

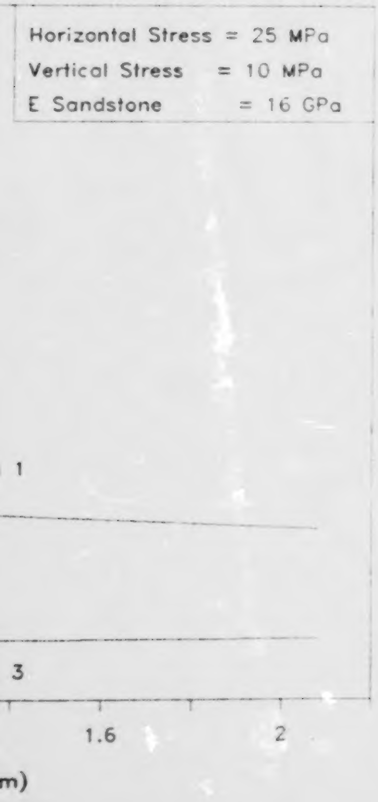
Horizontal Stress = 25 MPa
Vertical Stress = 10 MPa
E Sandstone = 16 GPa
1
3
1.6
2
m)

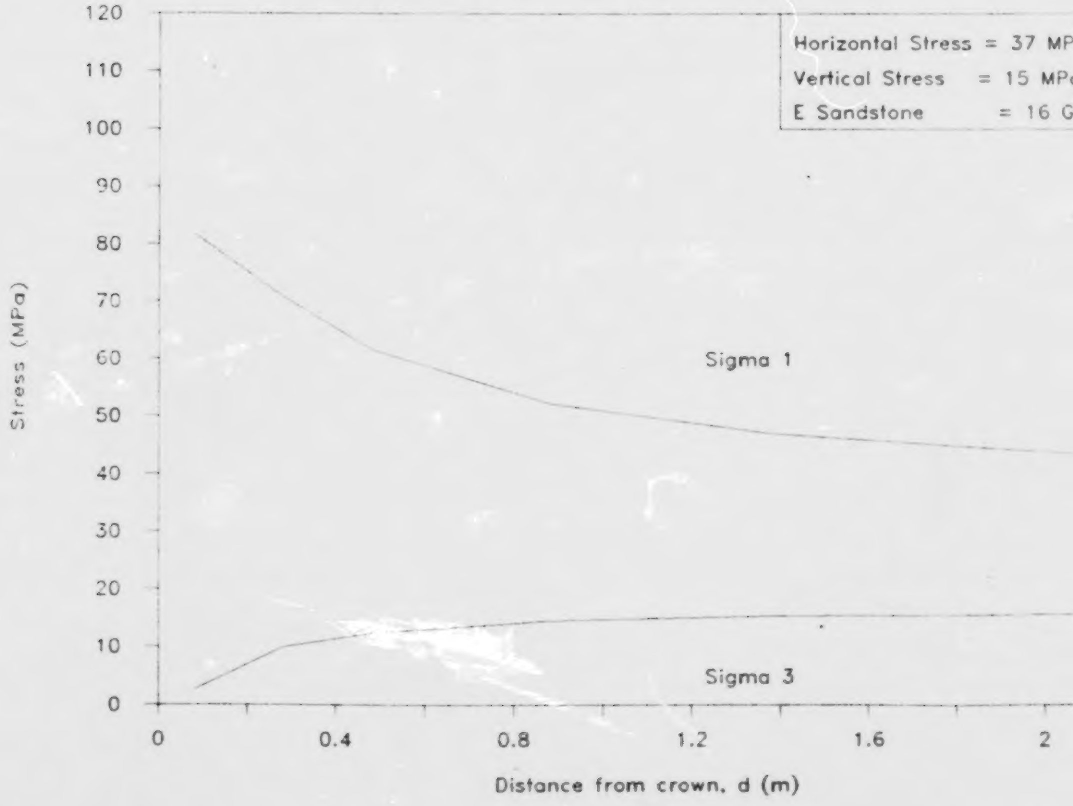
120
110
100
90
80
70
60
50
40
30
20
10
0
Stress (MPa)
Horizontal Stress = 37 MP
Vertical Stress = 15 MP
E Sandstone = 16 G
Sigma 1
Sigma 3
0
0.4
0.8
1.2
1.6
2
Distance from crown, d (m)

(E)

VARIATIONS OF PRINCIPAL STRESSES
DISTANCE OF SANDSTONE / SILTSTO
CONTACT FROM CROWN OF ROADW
VARIOUS IN SITU STRESS COND

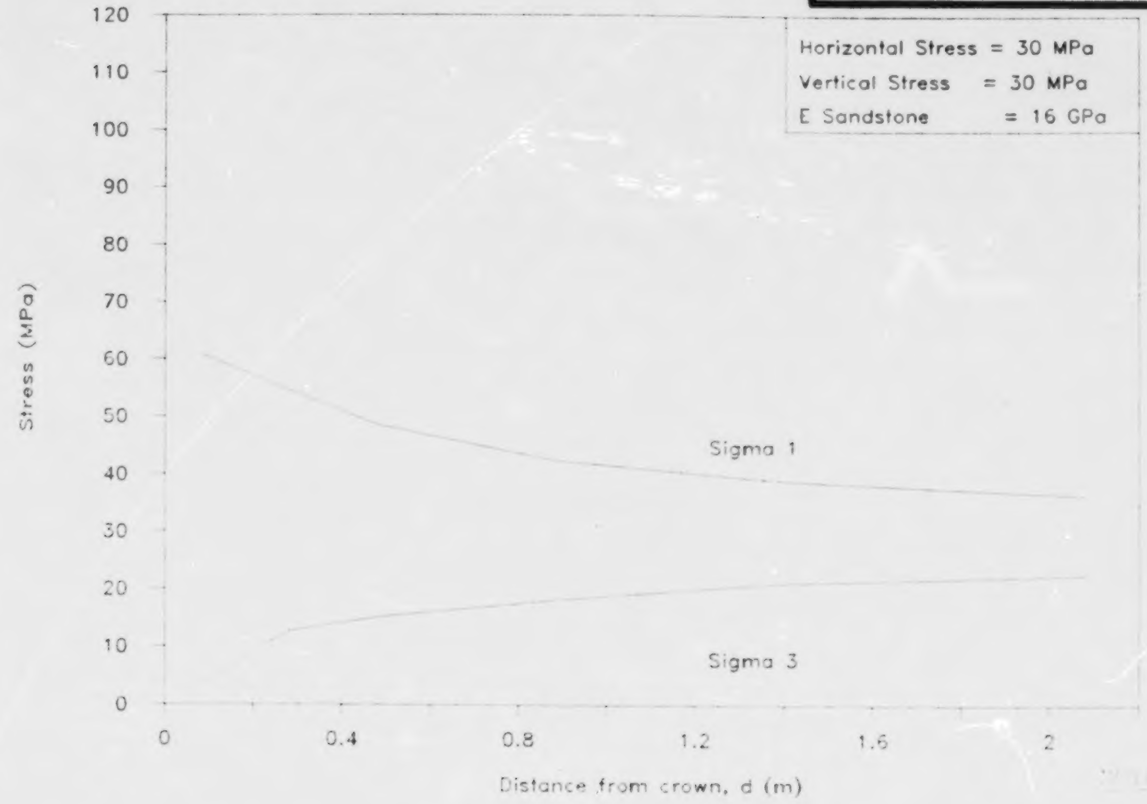

(C)

CR
SANDST
SILTSTO
ROADWAY

NOTES:

1. STRESSES SHOWN ARE
2. CASE (B) IS THE REF
GEOMETRY.

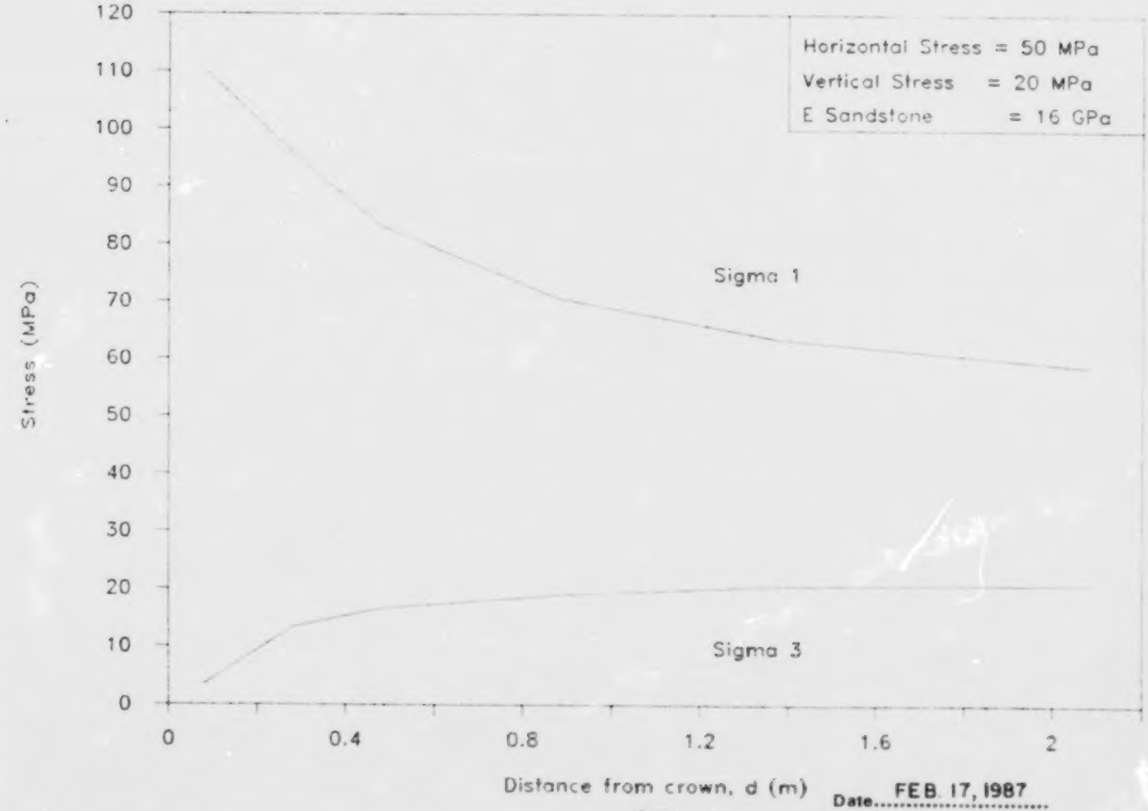

(F)

Date FEB. 17, 1987
Project 861-1290

Golder Assoc

VARIATIONS OF PRINCIPAL STRESSES WITH DISTANCE OF SANDSTONE / SILTSTONE CONTACT FROM CROWN OF ROADWAY FOR VARIOUS IN SITU STRESS CONDITIONS

FIGURE 7.4

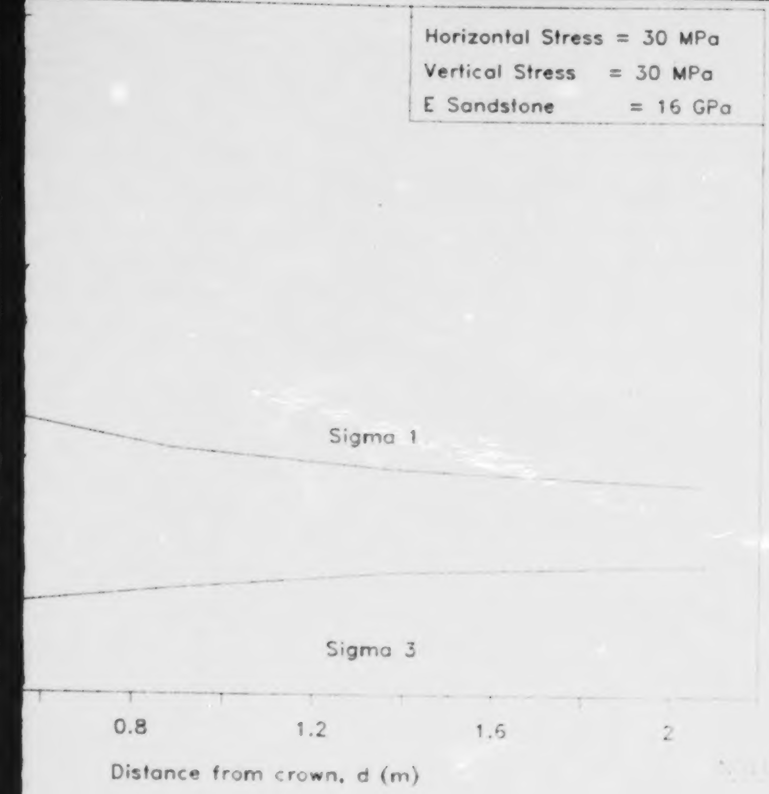

(C)

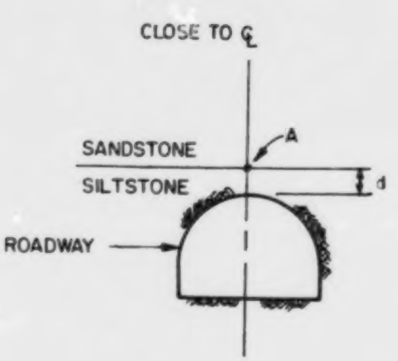
CLOSE TO ℄
A
SANDSTONE
SILTSTONE
d
ROADWAY

NOTES:

1. [illegible]
2. [illegible]

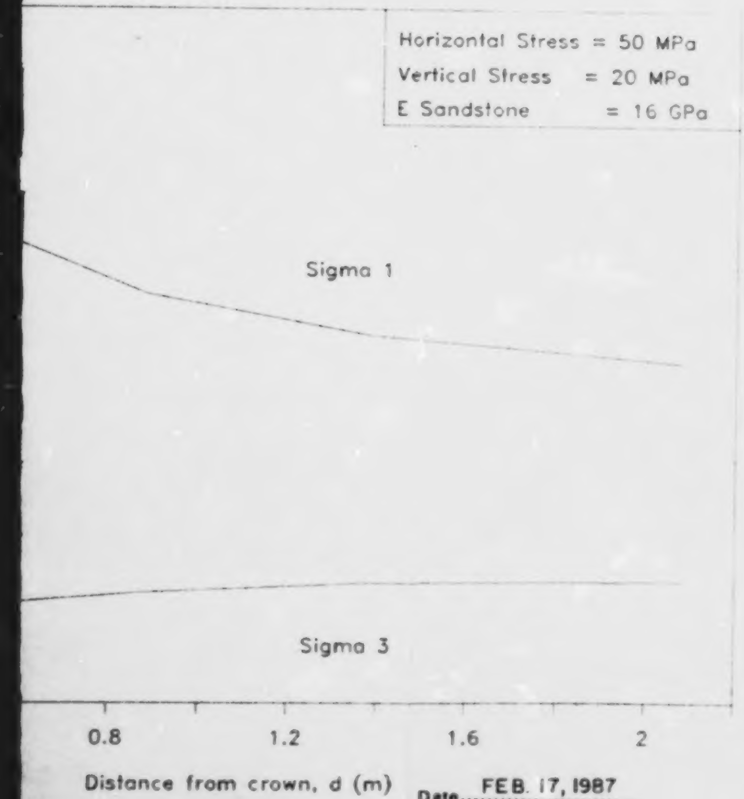

(F)

Date FEB. 17, 1987
Project 861-1290

Golder Associates

Drawn RWR
Chkd

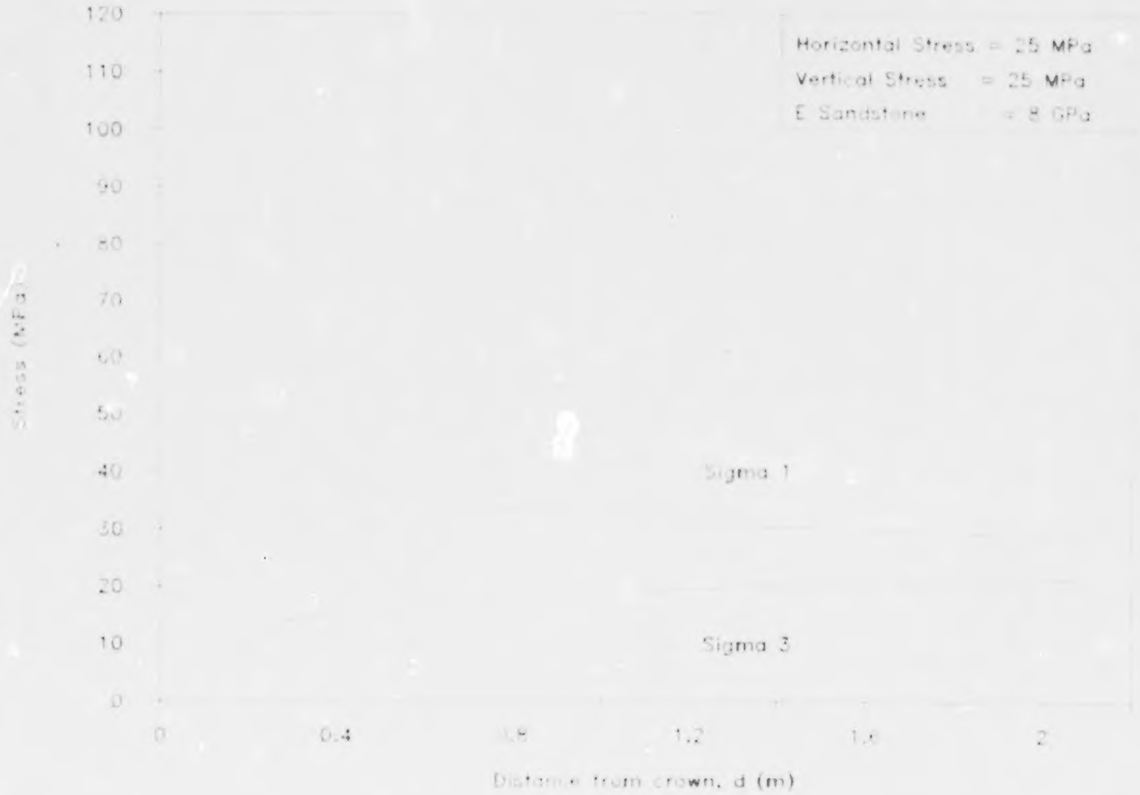

Horizontal Stress = 25 MPa
Vertical Stress = 25 MPa
E Sandstone = 8 GPa
Sigma 1
Sigma 3
Stress (MPa)
120
110
100
90
80
70
60
50
40
30
20
10
0
0
0.4
0.8
1.2
1.6
2
Distance from crown, d (m)

(A)

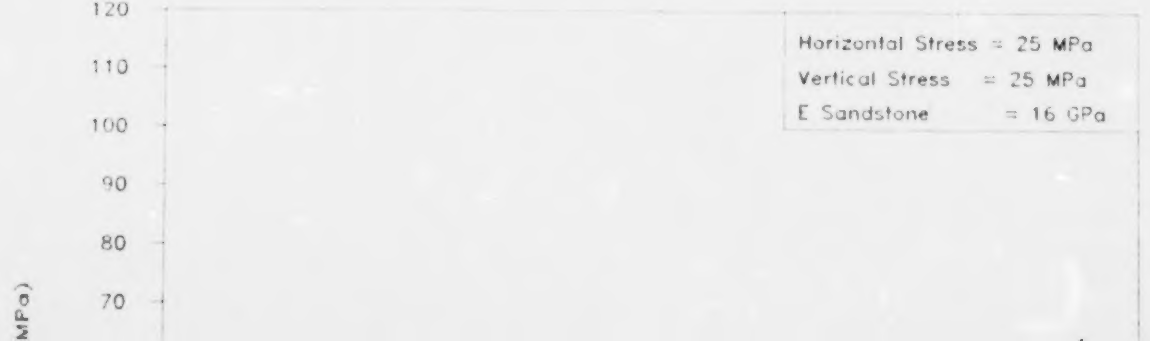

Horizontal Stress = 25 MPa
Vertical Stress = 25 MPa
E Sandstone = 16 GPa
120
110
100
90
80
70
MPa)

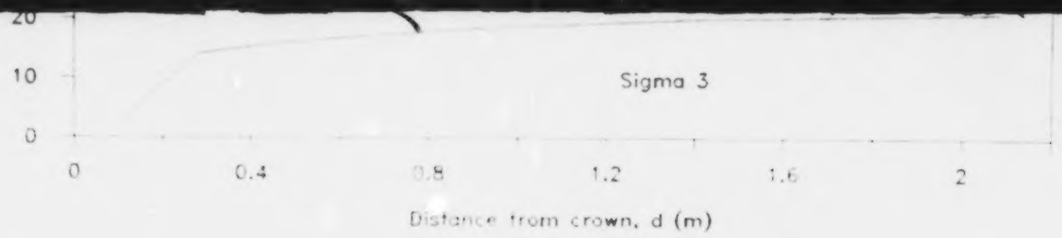
20
10
0
Sigma 3
0
0.4
0.8
1.2
1.6
2
Distance from crown, d (m)

(A)

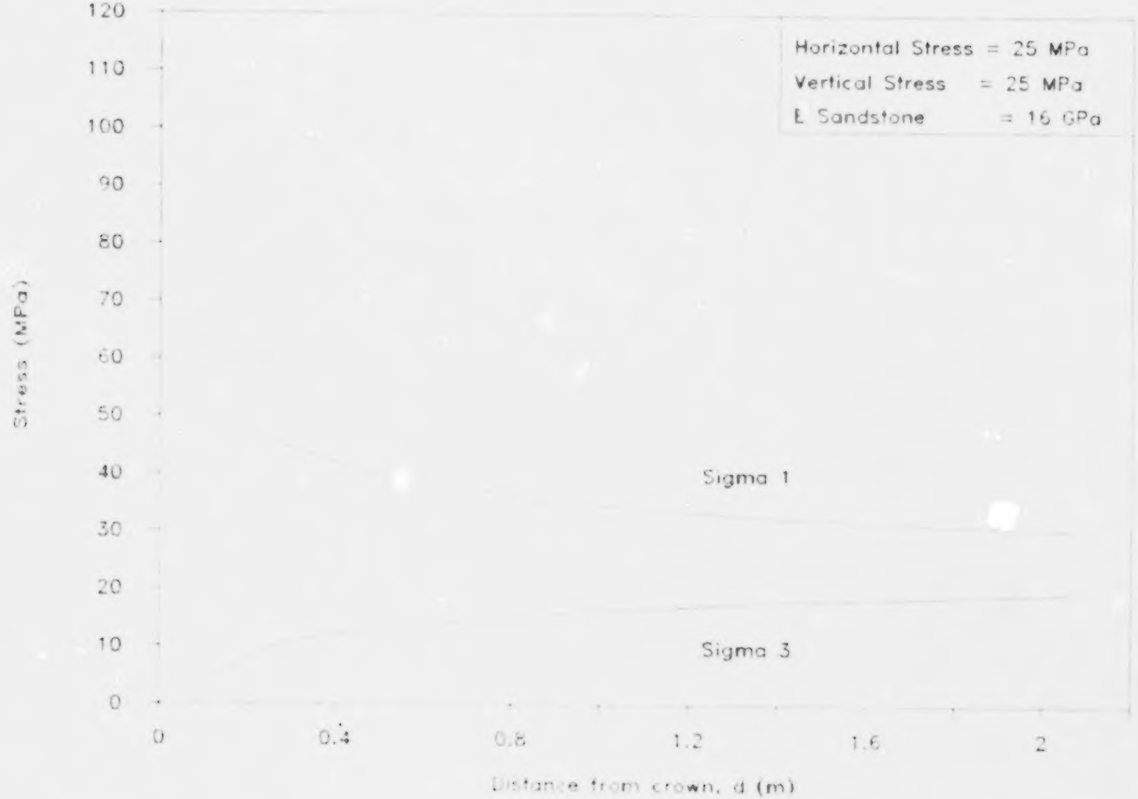
120
110
100
90
80
70
60
50
40
30
20
10
0
Stress (MPa)
Horizontal Stress = 25 MPa
Vertical Stress = 25 MPa
E Sandstone = 16 GPa
Sigma 1
Sigma 3
0
0.4
0.8
1.2
1.6
2
Distance from crown, d (m)

(B)

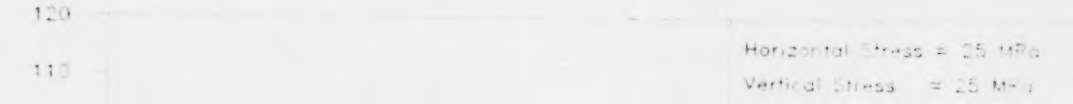
120
110
Horizontal Stress = 25 MPa
Vertical Stress = 25 MPa

VARIATIONS OF PRINCIPAL ST
DISTANCE OF SANDSTONE / SIL
CONTACT FROM CROWN OF R
VARIOUS STIFFNESSES OF SA

(C)

[illegible]

Date FEB. 17, 1987
Project 861-1290

Golder As

VARIATIONS OF PRINCIPAL STRESSES WITH DISTANCE OF SANDSTONE / SILTSTONE CONTACT FROM CROWN OF ROADWAY FOR VARIOUS STIFFNESSES OF SANDSTONE

FIGURE 7.5

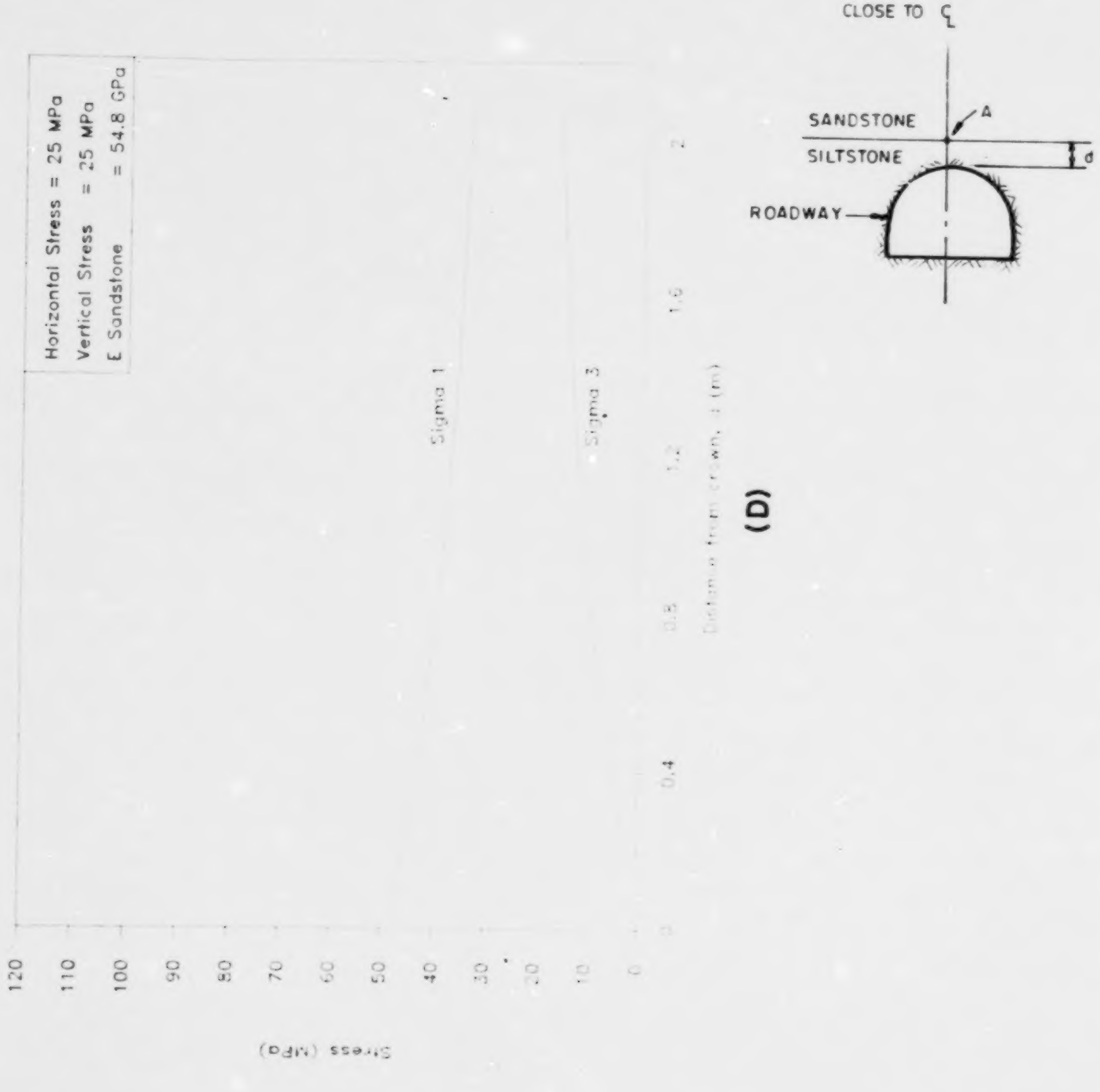

(D)

Date FEB. 17, 1987
Project 861-1290

Golder Associates

Drawn RWR
Chkd

PRINCIPAL STRESSES AT THE ROOF OF A TYPICAL ROADWAY AND 13 N. AIRWAY IN No. 26 COLLIERY

FIGURE 7.6

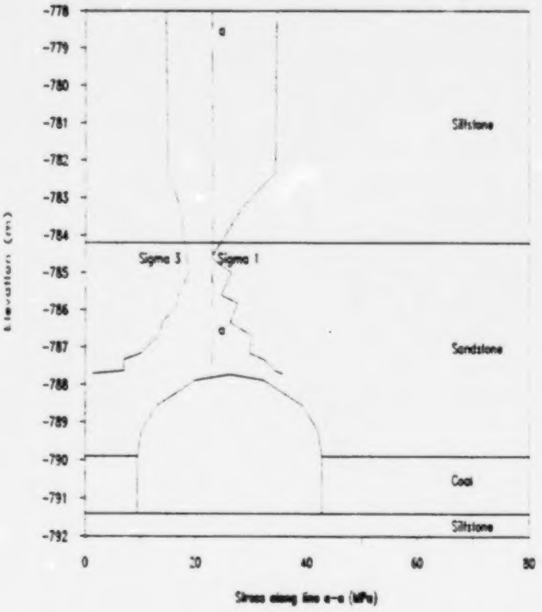

A) 13N AIRWAY WITH 13N LONGWALL PANEL AT 60 m. AWAY

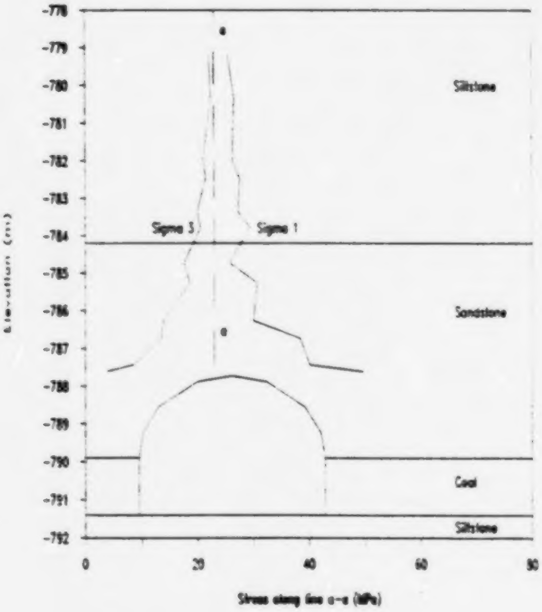

B) TYPICAL ROADWAY DRIVEN IN UNDISTURBED GROUND

Date MARCH, 1987
Project 861-1290

Golder Associates

Drawn D.M.
Chkd.

PRINCIPAL STRESSES AT THE ROOF OF A TYPICAL ROADWAY. IN NO. 26 COLLIERY. WITH THE PRESENCE OF A BLAST DAMAGED ZONE.

FIGURE 7.7

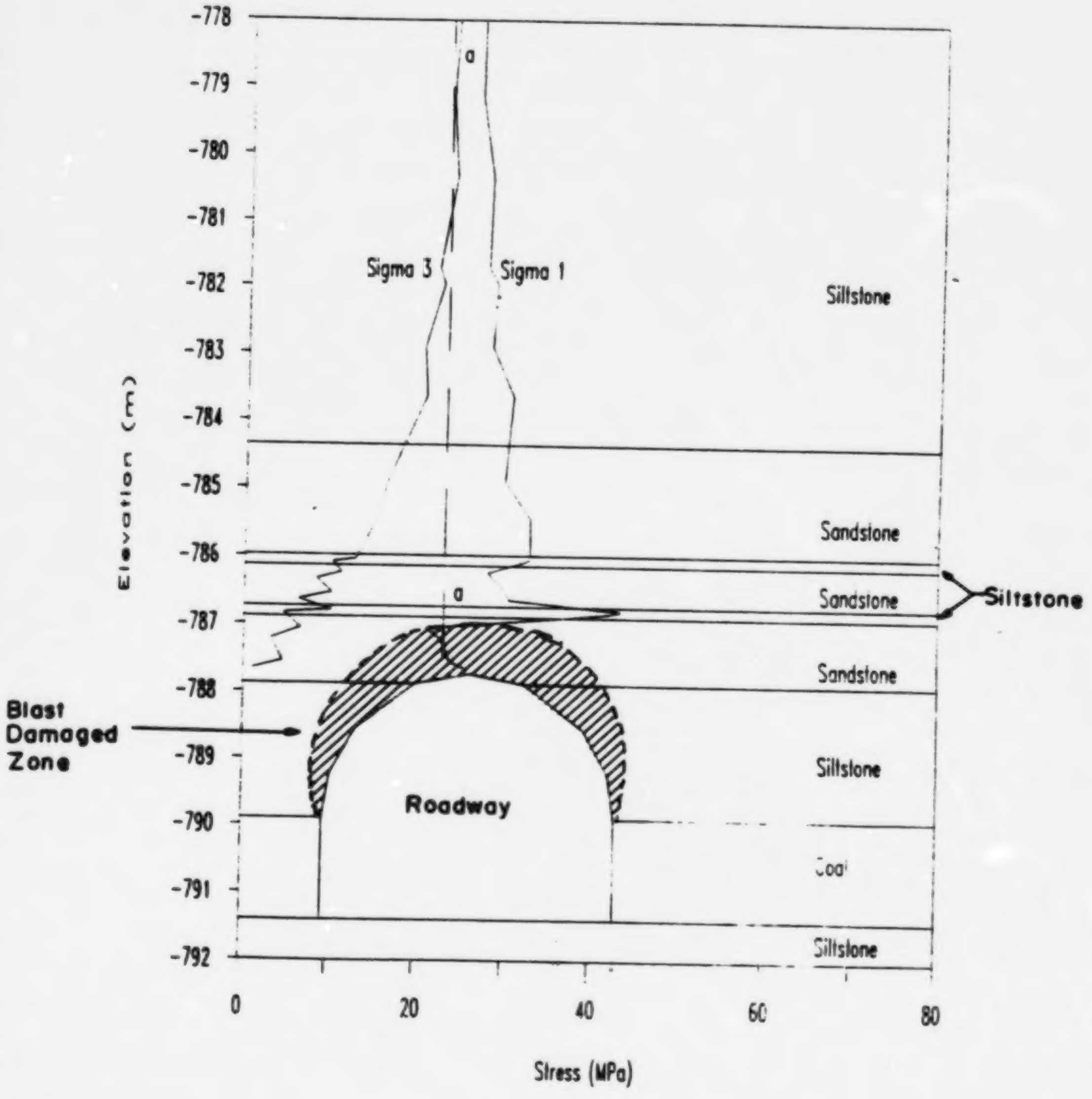

Date MARCH, 1987

Project 861-1290

Golder Associates

Drawn S. de K.

Chkd.

8. COAL MINING UNDER OUTBURST PRONE CONDITIONS

The proposed mechanistic model for the outburst events identifies the conditions under which the outburst prone sandstone is vulnerable to dynamic rock failure. Coal mining under such conditions have experienced various degrees of distress as described in Section 3. The general characteristics of the outburst activities in No. 26 Colliery of the Sydney Coalfield is consistent with the experiences documented in different countries. In the following sections the outburst risk assessment methodology and the predictive and prevention measures implemented by other countries under similar mining (outburst-prone) conditions are examined. The applicabilities of these methods to the Sydney Coalfield are discussed.

8.1 Outburst Risk Assessment

The most universally recognized method of risk assessment for rock and gas outbursts is based on the phenomenon of core discing, also termed "the Freiberg core prognosis". In Germany, core discing clearly correlated with the risk of outburst (Paul, 1983). Similarly, core discing in sandstone correlated with outburst events in No. 26 Colliery of the Sydney Coalfield. It is generally regarded as a reliable indicator for outburst hazards. Belin (1981), however, pointed out that discing of core is a necessary but not a sufficient condition as the drilling procedure (hole diameter, penetration and rotation rate) can influence the discing effect. Airuni et al. (1976) described a rating system to determine the potential outburst hazard in sandstone based on the number of discs present in 1 m of core of 59-76 mm diameter:

30 to 40 discs/m:	high outburst hazard
20 to 30 discs/m interspaced by fissured short (50-100 mm) rock columns:	medium outburst hazard
Fissured short columns (150-200 mm in length) separated by some single discs:	low outburst hazard

In Russia, an elaborate method of detection is based on the various properties of the material and the depth. Table 8.1 shows the risk assessment table used in USSR based on the outburst-prone sandstone in that country. The index is obtained by arithmetic mean and a value between 0.8 and 1.0 indicates a very high risk outburst hazard.

In Japan, Acoustic-Emission (AE) monitoring was proposed by Watanabe et al. (1981) to forecast imminent outbursts. Acoustic emission is the term applied to transient high-frequency elastic waves, generated by stress changes in a solid. Their study showed that sufficient information to predict impending rock and gas outbursts could be obtained by monitoring the rock mass only a few minutes after blasting, since during the process of stress redistribution high levels of fracturing activity occur.

In the German potash mines, in addition to the core discing method, gas pressure prognostics are established by monitoring the gas pressure in boreholes 2 to 3 m longer than the blasthole round. The potential of outburst occurrence is considered to be proportional to the gas pressure. In addition, an assessment of outburst potential is carried out by dissolving a quantity of salt rock in water and by measuring the intensity of the crepitation caused by the gas liberated in the water.

The noises are monitored by microphones and transformed in volt readings. Outburst potential are evaluated using a range of critical values.

In the Sydney Coalfield a formalized method of assessing the outburst risk has yet to be established. On the basis of the depth of mining, core discing and laboratory strength data, No. 26 Colliery could be considered as having a medium risk of outburst hazard according to the classification described above. As mining in other mines in the Sydney Coalfield is approaching greater depths, a systematic risk assessment procedure relating to the characteristics of the outburst-prone channel sandstone and the pertinent geological conditions of the coalfield should be developed.

8.2 Prediction of Outburst Hazards

Risk assessment of outburst hazards generally provides an overall evaluation of the risk of outburst potential in the mining area. Prediction of the hazard requires more in-depth investigation of the zones identified. Mapping and test drilling are the usual field procedures for collecting the required data.

In the Sydney Coalfield mapping of the channel sandstone in No. 26 Colliery had been ongoing prior to the fire which caused closure of the mine. In other mines (e.g. the Lingan Mine) which will be approaching the depths at which there is potential for outburst to occur, a systematic prediction would be beneficial for the planning and sequencing of the mining operation. The procedure may consist of the following:

- Project locations of burst-prone channel sandstone deposits based on existing geological data.

- Drill cored holes from current mining levels to intersect potential burst-prone strata.

- Examine the cores carefully with particular emphasis on core discing as this is a relatively reliable indicator of outburst hazard. A systematic procedure of recording drilling parameters (such as drilling pressures, penetration rates) would be useful to correlate the results from different drillholes.

- Should core discing be noted from the drill holes, further investigation program for delineating the extent of the zone of potential outburst hazard should be considered.

  Depending on the dip of the strata, this may consist of detailed probe drilling to project the location of the burst-prone layer ahead of the development heading. These probe holes should cover about 6 m of the strata above the roof of the roadway. As experiences are acquired from the drilling program, the depths and distances between the probe holes could be optimized.

- Considerations should also be given to in situ stress measurement programs in the areas where high stresses may be anticipated (i.e. areas of core discing). Existing stress data is useful but may not be sufficient to define the stress condition in the burst-prone strata.

- Measure the reservoir gas pressure within the outburst-prone sandstone. Previous measurements in No. 26 Colliery did not provide conclusive results.

Using the model described in Section 7, it is possible to assess the potential for outburst to occur in the development heading based on the location of the sandstone, the in situ stresses, the rock properties, the blasting patterns and parameters and the pore gas pressures.

As outburst events are very disruptive to the mining operation and is a safety hazard, predictive measures and outburst risk assessment are necessary to provide as much advance warning as possible to allow: (a) review of the potential impact on future mining operations and (b) preventive procedures to be implemented.

8.3 Prevention of Outbursts

Several methods have been used for the prevention of outbursts in different countries. They included:

- gas drainage of the outburst-prone strata
- destressing the rock mass by: blasting, creation of a stress relief zone or drilling
- modify the blasting parameters to reduce the effects of blast induced dynamic stresses
- use of mechanical excavation equipment
- isolation of the volume of rock to be excavated from the surrounding rock mass
- secondary safety measures comprising protection of the personnel and equipment and reinforcing the rock mass

These methods have achieved varying degrees of success in different parts of the world.

The procedures for these measures and their possible applications in the Sydney Coalfield are discussed in the following sections.

8.3.1 Gas Drainage

Gas drainage has been used successfully in degassing coal seams by the use of long drill holes ahead of a longwall (Matuszewski et al., 1979). However, this procedure may not be efficient in the outburst-prone sandstone in the Sydney Coalfield due to the intrinsically low permeability of the material and a potential reduction in permeability around a gas drainage borehole due to stress concentration around the hole.

8.3.2 Destressing of the Rock Mass

Destressing comprises the relief of the initial stresses in the area through which the roadway will be driven through. It can be achieved by either one of the following methods.

Destressing by Shotfiring

In this method, the sandstone ahead of the face is deliberately fractured by shotfiring. This process would create a zone of low stiffness within the rock mass so that the initial stresses in the sandstone are reduced. Such rock destressing has been used successfully in hard rock mines but there is limited data on the degree of success in burst-prone sandstones. The disadvantage of this method is the damage of the rock surrounding the roadway. Unless the zone of destress is sufficiently extensive, the stress concentration at the boundary of the destressed zone in combination with the dynamic stresses and gas pressure could still be sufficient to trigger an outburst which would perhaps be smaller or not occur at all. The event following No. 37 in No. 26 Colliery was an event triggered by the removal of material from an outburst cavity.

Destressing by Drilling

Destressing drilling has been used in relieving the stresses in coal seams (Kozlowski, 1983). It consisted of drilling a series of small diameter (42 mm) borehole in the coal seam being developed. The use of such methods in outburst-prone sandstone (Paul, 1983) at Ibbenburen Coal Mine had not been successful. It was found that little if any gas emerged from the holes. The methane was not released until the rock was broken up at the time of the burst. It was considered that the influence of the destressing borehole was too small. Core drilling tests had shown that the destressed zone, even around outburst cavities, extended only a few metres into the rock.

Creation of a Stress Relief Zone

An alternative method of reducing the initial (in situ) stresses in the sandstone is to create a stress relief zone by adjacent excavations. This may be achieved by working a reliever (protective) seam or by sequencing the mining operation.

The mining of a protective seam is generally considered effective in the context of prevention (e.g. Matuszewski et al, 1979). This is done by undermining the gas bearing strata in an underlying seam. It requires that the protective seam be mined out completely to effect the stress relief in the upper seam. The effectiveness of such methods, however, decreases as the distance between the seams increases.

In the context of the Sydney Coalfield, the only protective seam that could be considered for the Harbour seam would be the Phalen seam which is about 2.7 m thick and is located about 150 m deeper. Hence, it is not practical to use the Phalen seam as the protective seam.

On the basis of the outburst records from from No. 26 Colliery, it was noted that the 13N airway was driven through the outburst prone sandstone but did not result in an outburst event. Stress analysis of this roadway indicated that the 13N longwall panel located 60 m from the roadway has caused stress relief in the rock mass in the vicinity of the 13N airway and has this caused a reduction in the stress concentration at the roof of the roadway (see Section 7.2). Similar mining sequences could be implemented in the Lingan mine to protect the airways from potential outburst hazards.

The absence of any outburst events in the gate roads adjacent to the longwall panel is also indicative of the stress relief effects on the reduction of outburst risks.

8.3.3 Modification of the Blasting Parameters

The effect of shotfiring and the associated dynamic stresses on the rock mass presented in Section 6 indicated that there could be reduction in the dynamic stress level by modifying the blasting parameters.

Mindelli (1965) has compared the effects of the following types of blast round:

- normal shotfiring in a single round
- blowing of the coal in the lower part of the cross section and then firing the rest of the face, to increase the time for stress relaxation to occur

- pre-splitting along the upper half of the roadway with perimeter holes spaced at 0.3 m; break out the lower part of the roadway and then fire the upper part

- line drilling of uncharged holes at 0.15 m around the entire profile of the roadway, the ground then being broken in two stages

It was found that none of the above procedures has prevented the outburst in the roadway. During development of the 14N coal road, in No. 26 Colliery (Sydney Coalfield), the use of uncharged perimeter holes appeared to have produced relatively low dynamic stress levels but have not prevented the outbursts (see discussion in section 7). However, as all the outbursts experienced in the Sydney Coalfield were triggered by shotfiring, the impact of the dynamic effects of shotfiring should be further examined.

The blast monitoring program undertaken in this study indicated that there is room for improvement in the blast practices implemented at Lingan Mine. A systematic experimental program aimed at improving the quality of the blasts (including drilling and blast design) and reducing the dynamic effects on the surrounding rock would prove to be beneficial in the long term planning for the control and prevention of outbursts.

8.3.4 Use of Mechanical Excavation Equipment

The use of a mechanical excavation equipment such as a road header had been considered as a means of reducing the dynamic impact of the excavation process. Belin (1981) indicated that by excavating a circular section and a hemispherical face and by limiting the rate of advance to 0.5 m/hr for high risk (outburst risk) sandstone, and 1 m/hr for medium risk sandstone, the risk of outburst could be reduced. The disadvantage of this method, however, is that the equipment and the operator would be exposed to the risk of outburst occurring during the excavation process. Shotfiring avoids the direct exposure of equipment and personnel to the potential outburst hazard and therefore remains a safer operation.

8.3.5 Isolation of the Volume of Rock to be Excavated

This method comprises the drilling of a relief slot around the periphery of the roadway to isolate the volume of rock to be excavated from the surrounding rock mass. In general, data on the use of such procedures in burst-prone sandstone is very limited. This has been applied in the USSR for relieving stresses in the coal seams prior to shotfiring (Airuni, 1976). However, the work reported by Mindelli (1965) indicated that such procedure was not successful in preventing outbursts. Zorin (1974) suggested that the stress relieving slot should be more than 50 mm wide to ensure isolation of the block which was then removed by blasting.

8.3.6 Pre-support Ahead of the Face

Results of laboratory testing indicated that the strength of rock increases with increase in confinement. In particular, regions of low confinement could be substantially strengthened by increasing the confining stresses. This principle may be applied to rock burst prevention by pre-supporting the roof strata up to about 2 m above the roadway and ahead of the face. This could be achieved by upwardly inclined (30°) fully resin grouted (untensioned) rock bolts. As the protruding end of the bolts are to be cut off after the round is fired, a non-metallic material such as a high strength fibre-glass could be used.

The use of this method for control of outburst has not been tried but should be considered as an adjunct to other methods.

8.3.7 Safety Measures

Despite the use of various methods for outburst prediction and prevention, the risk of outburst occurrence in outburst-prone strata always exists. In order to provide the best possible protection to men and equipment, the following safety measures are generally implemented:

- Blasting should be executed from a large distance from the heading (at least 150 m).

- The mining crew should be withdrawn into the through-going fresh air ventilation current. In the Sydney Coalfield, shotfiring is usually undertaken at the end of a shift thus allowing sufficient waiting period for re-entry of the heading.

- A barrier be set up at some distance (say 10 to 15 m) from the face to slow down the violent ejection of the material. This procedure has been implemented in German Potash Mines.

- The ventilation system should be designed to divert the methane from the potential outburst zones away from the active longwall panels or other development works.

8.3.8 Summary

Preventive measures for outbursts have been developed in different countries on the basis of the specific features of the outburst prone materials, the mining methods and the perceived concepts of outburst initiation. Some of these methods have been implemented and some of them are still at the experimental stage. The degree of success achieved was also varied. Hence, these experiences may not be directly transferable to the Sydney Coalfield. Nevertheless, on the basis of the site conditions in the Sydney coalfield and the findings obtained in this study, the following methods are considered to be applicable to the prevention of potential outbursts.

a. The creation of a stress relief zone by sequencing the development of the longwall panels and the development roadway/airway. The relative distance between the roadway/airway and longwall development may be planned to suit the stress relief requirements.

b. Establish an experimental blasting program aiming at improving the blast quality and reducing the effects of dynamic stresses. The effectiveness of line drilling or slotting around the excavation in controlling outbursts has not been proven but may be considered as part of the experimental program.

c. Pre-support of the roof strata ahead of the face using fully resin grouted rock bolts would increase the confinement and reduce the induced tensile stresses in the roof strata. It may be considered as an adjunct to other methods.

TABLE 8.1

METHOD OF RISK ASSESSMENT FOR OUTBURST-PRONE SANDSTONE USED IN USSR

Index Considered			Risk Level (	increasing)		
	0	0.2	0.4	0.6	0.8	1
% detrital quartz	<30	30-40	40-50	50-60	60-70	>70
% regenerated quartz	<2.5	2.5-5.0	5.0-7.7	7.5-10.0	10.0-12.5	>12.5
% argillaceous and micaceous minerals	>45	45-35	35-25	25-15	15-5	<5
Weighted average of grain dimensions (mm)	<0.12	0.12-0.13	0.13-0.16	0.16-0.2	0.2-0.28	>0.28
Extent of intergranular contact (mm)	<0.1	0.1-0.2	0.2-0.3	0.3-0.4	0.4-0.5	>0.5
% open pore space	<2.5	2.5-4.5	4.5-6.5	6.5-8.5	8.5-10.5	>12
Tensile strength (MPa)	9.8	9.8-8.4	8.4-7.0	7.0-5.7	5.7-4.3	<3.9
Percentage of pore space filled by gas (in terms of mass)	<40	40-50	50-60	60-70	70-80	>80
Depth (m)	<500	500-700	700-900	900-1100	1100-1300	>1300

Reference: Safety Rules for Operations in Outburst-prone Seams. USSR Ministry of the Coal Industry (Moscow, NEDRA, 1977).

9. CONCLUSIONS

A study has been undertaken to develop a mechanistic model for the initiation of rock and gas outbursts experienced in No. 26 Colliery of the Sydney coalfield. The findings of the study and the conclusions derived are summarized below.

(a) A comprehensive record of the outburst events has been compiled by CBDC and CANMET and is shown in Table 2.6. The burst-prone material is the channel sandstone deposit. The general characteristics of the outbursts in No. 26 Colliery are consistent with those experienced in other countries.

(b) Published rock and gas outburst models were reviewed. Different hypotheses had been put forth by various researchers to explain the outburst initiation mechanisms and the processes during an outburst event. The salient points noted from the review are summarized below:

- The change in the state of stresses from a triaxial to a biaxial loading condition near the free face of the underground opening was considered to be the likely cause for induced tensile stresses which could lead to the initiation of rock fractures.
- The effect of blasting (shotfiring) is the rapid reduction of confinement of the burst-prone material. This in turn, mobilizes the gas pressure gradient as the change in stress during blasting is considered to be faster than the change in gas pressure.

Furthermore, blasting also superimposes dynamic tensile stresses over and above the static stresses.

- Gas plays a major role in the initiation of rock failure as well as in the subsequent manifestation of the event (violent expulsion of the failed material). A description of the interaction of the gas and rock mass during an outburst as postulated by Sevelev (1979) is presented in Section 4.3.3.5.

- The conical shape of the outburst cavity is considered to be related to the configuration of the shear failure surfaces within the outburst cavity. The intense fish scale fracturing along the cavity perimeter is the breakage of the material which has failed along the stress trajectory around the outburst cavity.

- An outburst would terminate itself under any one of the following conditions
    - the cavity extends to a geological contact where a non-outburst-prone material exists
    - an equilibrium stress condition is reached
    - the outburst event chokes itself due to friction along the cavity, delaying the creation of new cavity boundaries.

(c) Based on the literature review of case histories and models for rock and gas and coal and gas outbursts, factors considered to be relevant to the outburst events by various researchers are summarized in Table 5.1 in a matrix form. The current trend of thinking in outburst research study is apparent from the summary. The governing factors include the in situ stresses, geological structures, material strength and properties (including hydraulic properties) gas pressure effects and dynamic effects due to blasting.

(d) An experimental blast monitoring program was undertaken in a development heading in the Lingan Mine to monitor the dynamic and static stress changes during typical shotfiring rounds in roadway development. A review of the current blasting practices at the Lingan Mine was carried out together with computer simulation of the development of induced fractures. The following is a summary of the findings from the blasting study.

- the drilling methods used during the testing period for the production blasting in the sandstone at the Lingan Mine were inadequate regarding the control of overbreak. Perimeter boreholes at the crown of the roadway were drilled upwards to such a degree as to cause overbreak which may contribute to instability in the roof. It is also observed that there is very little support for the loose material produced.

- results of computer based blast simulation indicate that the current blast pattern would cause excessive overbreak and damage to the surrounding rock. Under the conditions at the Lingan Mine, the analysis indicates that the inter-pattern cracking radius appears to break out within the existing pattern dimensions.

- the dynamic effect of the shotfiring event is significant. Such effect tends to attenuate with distance. The blast induced dynamic stresses follow the attenuation equations given below:

  Within sandstone

  $$\sigma d = 3040/(S_d)^{2.31}$$

  Across rock strata

  $$\sigma d = 95/(S_d)^{1.02}$$

  where σd = dynamic stress

  S_d = scaled distance

- changes in the static stresses due to shotfiring are considered to be insignificant.

- to improve the overbreak condition in roadway development, changes are required in overall blast design including drilling accuracy and layout of blast hole delays. A suggested blast pattern is given in Figure 6.4.

(e) A laboratory program has been undertaken to study some of the fundamental behaviours of rock which relate to the initiation of failure during an outburst event. A reference sandstone used in previous laboratory testing programs for outburst studies was tested. The results of the laboratory program indicated that the general behaviour of gas within a relatively porous sandstone (porosity = 19%) appears to obey the gas law under isothermal condition. It was also noted that under a biaxial stress system, the samples failed due to induced tensile stresses normal to the plane of the applied stresses, as observed by other researchers. The implication is that the changes of stresses around an underground openings from a triaxial to a baxial state would create a condition conducive to failure as observed experimentally

(f) In keeping with the objective of the study and its intended applications, it is considered that the outburst model for the Sydney coalfield should address the initiation mechanism of the outbursts rather than the associated disturbances following the events. The proposed model was developed on the basis of the effects of static and dynamic (due to shotfiring) stresses, and gas pressure and a tensile mode of failure based on Griffith's criterion of fracture initiation. The postulated processes involved in an outburst event in the burst-prone sandstone are described in Section 7.2. In summary, stresses and gas pressure all play a part in inducing the tensile stresses in the rock mass near the free face. The gas released from the rock at failure tends to eject the failed material away from the burst cavity.

(g) A series of stress analyses was carried out to study the effects of the parameters related to the otubursts in No. 26 colliery. They included the location and thickness of the outburst-prone sandstone layer, the in situ stresses, the relative rock mass stiffnesses of the sandstone and siltstone and the effect of blast damage on the stress conditions. The stress condition at the roof of the 13N airway which was driven through a sandstone without initiating a rock and gas burst was also examined and the results were compared with those of 14N airway which generated outburst events no. 28 and 31 during drivage. The results indicated that:

- at the roof of the roadway, tangential stresses are generally high and become higher when the sandstone/siltstone contact is close to and above the roof.

- the stress condition at the roof of the roadway is relatively independent of the position of the sandstone/siltstone contact when it is below the roof level.

- based on the Hoek and Brown failure criterion and the in situ stress data pertaining to No. 26 colliery, overstress would occur at the roof of the roadway.

- the presence of a blast damage zone would tend to shift the stress concentration front away from the designed excavation boundary.

- the stress condition at the 13N airway was found to be influenced by the 13N longwall panel located at about 60 m away. As a result, the tangential stresses were reduced compared with development heading driven into virgin ground.

(h) The combined effects of pore gas pressure and static and dynamic stresses were studied by considering the induced effective principal stresses for all the outburst events, the 13N airway and the sandstone and siltstone interface at 2 m above the crown. Griffith's criterion of fracture, initiation was used to examine the outburst potentials of the cases studied.

It was noted that based on the range of estimated gas pressures, the stress conditions in the sandstone for all the outburst events are such that fracture initiation would take place based on Griffith's failure criterion. The probability of outburst in 13N airway however is substantially lower. For the case where the sandstone and siltstone interface is at 2 m above the crown, the stress defined by Griffith's theory is less than the tensile strength of the rock. This is consistent with the record that no failure was observed under such condition.

It appears that the stress concept and the mode of failure proposed in the model is consistent with the observed events in No. 26 colliery.

(i) As outburst events are very disruptive to the mining operation and is a safety hazard, predictive measures and outburst risk assessment are necessary to provide as much warning as possible to allow: (i) review of the potential impact on future mining operations and (ii) preventive procedures to be implemented. The suggested predictive measures are as follows:

- Project locations of burst-prone channel sandstone deposits based on existing geological data.
- Drill cored holes from current mining levels to intersect potential burst-prone strata. Examine cores carefully with emphasis on core discing as this is a relatively reliable indication of outburst hazard.

- Should core discing be noted from the drill holes, more detailed investigation should be implemented to delineate the extent of the burst-prone strata.

- Consideration be given to in situ stress measurement programs where high stresses may be anticipated (i.e. areas of core discing). Existing stress data is useful but may not be sufficient to define the stress condition in the burst prone strata.

- Measure the reservoir gas pressure within the outburst-prone sandstone. Previous measurements in No. 26 colliery did not provide conclusive results.

The data collected could be synthesized and used in the proposed model to predict the potential of the outburst hazard.

(j) Preventive measures for outbursts have been developed in different countries on the basis of the specific features of the outburst prone materials, the mining methods and the perceived concepts of outburst initiation. The degree of success of these methods was varied. Nevertheless, the following preventive methods are considered to be applicable to the Sydney coalfield.

- The creation of a stress relief zone by sequencing the development of the longwall panels and the development roadway/airway.

- Establish an experimental blasting program aiming at improving the quality of blasting and reducing the effects of dynamic stresses. Line drilling or slotting around the excavation may be considered as secondary activities.

- Pre-support of the roof strata ahead of the face using fully resin grouted rockbolts would increase the confinement and reduce the induced tensile stresses in the roof strata. It may be considered as an adjunct to other methods.

10. RECOMMENDATIONS FOR FURTHER RESEARCH

The study presented in this report revealed several items of significance that were not fully addressed in the research study plan. The following is an outline of items which requires further research efforts.

Core Discing

Apart from the careful examination of this phenomenon from rock cores, core susceptible to bursting should be tested using the procedures reported by Obert and Stephenson (1965). Both the channel sandstone and non-outburst-prone sandstone should be tested under various uniaxial and biaxial stresses, and triaxial stress with low axial confinement. The mode of failure should be observed in each case. The introduction of gas pressure in the sample could be incorporated if possible (previous experiments indicated that it was difficult to pass gas into the burst prone sample of the Sydney Coalfield).

Gas Pressure and Gas Permability of Rock

Gas pressure, quantity of gas and gas permeability of the rock in the outburst prone sandstone are important parameters which governs the gas-rock interaction during an outburst. Field program should be undertaken to measure the reservoir gas pressure and the in situ gas permeability of the rock surrounding the roadway. The quantity of gas in the sandstone can be readily determined based on the pressure and the porosity of the rock.

At present, little is known about the gas pressure gradient around a roadway at the on set of shotfiring. A study of the reservoir gas pressure, the gas permeability distribution and the anticipated fracturing of the rock (increase or decrease in gas permeability) due to the excavation/shotfiring process would provide a better estimate of the gas pressure at the time of fracture initiation.

Blasting

The blasting program outlined in Section 8.0 should be implemented as part of the long term research study in the coal mine. While outburst is not an imminent problem in the coalfield at present, optimization of blasting pattern and good blasting practices may take some time to establish.

11. Acknowledgements

Golder Associates would like to thank the Cape Breton Development Corporation and CANMET for their assistance in the provision of the background data relating to the outbursts in No. 26 colliery, and in arranging the field program. Special thanks are also due to Dr. Peter Cain for his helpful discussions during the study. The invaluable contribution of Mr. Guy Le Bel (formerly of Golder Associates) of Cambior is also gratefully acknowledged.

GOLDER ASSOCIATES

Clement

Clement M.K. Yuen, P. Eng.

REGISTERED PROFESSIONAL ENGINEER
C.M.K. Yuen
PROVINCE OF ONTARIO

CMKY/dh

REFERENCES

1. Airuni, A.T., et al; Methods of Driving Development Workings in Outburst Prone Seams; Prezeglad Gorniczy (Mining Journal) No. 11, 1976.

2. Abel, J.F.; Lee, F.T.; Stress Changes Ahead of an Advancing Tunnel; Intl. J. Rock Mech. Min. Sci. & Geomech. Abstr. V.10, 1973.

3. Aston, T.R.C., et al; Coal Strength Parameters Derived From Point Load Index Tests, Sydney Coalfield, Nova Scotia; Dept. Energy, Mines and Resources, Canada, CANMET Report #ERP/CRL 84-21(TR), 1984.

4. Aston, T.R.C.; Theoretical Insitu Strata Reservoir and Pore Pressure Calculations for Material From No. 26 Colliery, N.S.; Dept. Energy, Mines and Resources Canada, CANMET Report, #ERP/CRL 85-15(TR), March 1985.

5. Aston, T.R.C., Cain, P.; Gas and Rock Outburst at No. 26 Colliery, Sydney Coalfield, Nova Scotia - A Case History; Proceedings of the 21st Intl. Conf. on Safety in Mine Research Institutes, Sydney, Australia, October 1985.

6. Barron, K.; An Analytical Approach to the Study of Outbursts; Dept. Energy, Mines and Resources, Canada, Internal Report, Mine Branch, #72/29-ID, March 1972.

7. Belin, J.; Prevention of Instantaneous Outbursts of Methane and Coal or Rock; Working Party on Ventilation, Firedamp and other Mine Gases, Safety and Health Commission for the Mining and Other Extractive Industries, Commission of the European Communities, Doc. 6093/81 EN., Nov. 1981.

8. Brace, W.F., Martin, R.J. III; A Test of the Law of Effective Stress for Crystalline Rocks of Low Porosity; Intl. J. Rock Mech. Min. Sci., V5, 1968.

9. Breault, R.; Personal Communication, March 1987.

10. Brown, E.T., Trollope, D.H.; The Failure of Linear Brittle Materials under Effective Tensile Stress; Rock Mech. Engng. Geol. V, pp 229-241, 1967.

11. Chemaou Elfihri, O.; Etude des Phenomenes Dynamiques dans les Creusements au Rocher et Recherche de Methodes de Prevision; These de l'Institut National Polytechnique de Lorraine, France, Octobre 1984.

12. Coal in Nova Scotia; Senior Author was Calder, J.H.; Nova Scotia Dept. of Mines and Energy, 1985.

13. Coates, D.F.; Rock Mechanics Principles; Dept. Energy, Mines and Resources, Canada, CANMET, Monograph 874, 1981.

14. Cornet, F., Fairhurst, C.; Variation of Pore Volume in Disintegrating Rock, Proceedings of the ISRM Symp. on Percolation Through Fissured Rock, Stuttgart, 1972.

15. Dally, J.W., Fourney, W.C., Holloway, D.C.; The Role of Flaws in the Fragmentation Process, Rock Fragmentation Session, 17th U.S. Symposium on Rock Mechanics, Brown, Green, Hakala et al Editors, August 27th, 1976.

16. Deere, D.V.; Geological Considerations, Rock Mech. in Engng. Practice, Stagg and Zienkiewics Editors, John Wiley & Sons, London, 1968.

17. Dikunov, E.A.; Nature and Mechanism of Sudden Rock Bursts and a Method for Preventing Them; Ugol'Ukrainy (Ukrainian Coal), V15, No. 5, 1971.

18. Development and Use of Triaxial Rock Testing Procedures for Samples of the Sydney Coalfield, Nova Scotia, Phase 1; Golder Associates Report No. 841-1287-1, 1984.

19. Development and Use of Triaxial Rock Testing Procedures for Samples of the Sydney Coalfield, Nova Scotia, Phase 2; Golder Associates Report No. 841-1287-2, 1985.

20. Ettinger, I.L.; Sudden Outbursts of Coal and Gas and the Structure of Coal; Nedra, Moscow, 1969.

21. Fairhurst, C., Cook, N.G.W.; The Phenomenon of Rock Splitting Parallel to the Direction of Maximum Compression in the Neighbourhood of a Surface; Proceedings of the 1st. Intl. Congress of Rock Mech., Lisbon, Portugal, 1966.

22. Fairhurst, C., Cornet, F.; Rock Fracture and Fragmentation; Proceedings of the 22nd Rock Mech. Symp., 1981.

23. Farmer, I.W., Pooley, F.D.; A Hypothesis to Explain the Occurrence of Outbursts in Coal, Based on a Study of West Wales Outburst Coal; Intl. J. Rock Mech. Min. Sci., V4, 1967.

24. Farmer, I.W.; Engineering Properties of Rocks; E. & F.N. Spon Ltd., London, 1968.

25. Fisekci, M.Y., Barron, K.; Methane Pressure and Flow Measurements in Coal and Surrounding Strata; Dept. Energy, Mines and Resources, Canada, CANMET Report, #ERP/MRL 75-32 (OP), 1975.

26. Forgeron, S., et al; The Effects of Geological Features on Coal Mining, Sydney Coalfield, Nova Scotia; Can. Inst. Min. Metal. Bulletin, V79, No. 891, July 1986.

27. Fumagalli, E.; Stability of Arch Dam Rock Abutments; Proceedings of the 1st Intl. Congress on Rock Mech., Lisbon, Portugal, 1966.

28. Gallant, W.D., Aston, T.R.C.; Measurement of Insitu Strata Gas Pressure at No. 26 Colliery, Sydney Coalfied, N.S.; Dept. Energy, Mines and Resources, Canada, CANMET Report, #ERP/CRL 85-10(TR), January 1985.

29. Garrood, P.S.; Ground Control Aspects of the Development at Creighton No. 11 Shaft; Proceedings of the 14th Canadian Rock Mech. Symp. Vancouver, 1982, Can. Inst. Min. Metal. special volume No. 30, 1984.

30. Gimm, W.A.R., Pforr, H.; Breaking Behaviour of Salt Rock Under Rockbursts and Gas Outbursts; Proceedings of the 4th Intl. Conf. on Strata Control and Rock Mechanics, Columbia Univ., New York, USA, May 1964.

31. Gimm, W.A.R., et al; *The Present Status of Controlling Co$_2$ Gas Hazards in the Werra Potash Mines of the German Democratic Republic*; New Mng. Engng., V6, 1976.

32. Gorski, B.; *Laboratory Test Results of Rock Cores From No. 26 Colliery, Sydney Coalfield*; Dept. Energy, Mines and Resources, Canada, CANMET Report, #ERP/MRL 84-25(TR), March 1984.

33. Gray, I.; *The Mechanism of, and Energy Release Associated with Outbursts*; Proceedings of Aus. I.M.M. Southern Queensland Branch Symp. on The Occurrence, Prediction and Control of Outbursts in Coal Mines, 1980.

34. Hagan, T.N., Harries, G.; *The Effects of Rock Properties on Blasting Results*, Chapter 4 of the Australian Mineral Foundation Workshop Course Manual, Drilling and Blasting Technology, Adelaide, 1977.

35. Hargraves, A.M.; *Failure of Porous Rocks with Contained Gas*; Proceedings of the Symp. on Stress and Failure Around Underground Openings, University of Sydney, Australia, March 1967.

36. Hawkes, I.; *A Study of Stress Waves in Rocks and the Blasting Action of an Explosive Charge*; Colliery Engineering, May 1959, pp. 186-196.

37. Hiramatsu, Y., et al; *Studies on the Mechanism of Gas and Coal Bursts in Japanese Coal Mine*; Proceedings of the 5th Intl. Congress on Rock Mech., Melbourne, Australia, 1983.

38. Hoek E., *Brittle Failure of Rock*; Rock Mech. in Engng. Practice, Stagg and Zienkiewics Editors, John Wiley & Sons, London, 1968.

39. Hoek, E., Brown, E.T.; *Underground Excavations in Rock*; IMM, London, 1980.

40. Hueckel, T.; *Analysis of Dynamic Effects Influencing Rockbursts in Board and Pillar Systems*; Gornictwo (Mining), V5, No. 4, 1981.

41. Hueckel, T.; *Analysis of Dynamic Effects Influencing Roof Rockbursts in Longwall Excavations*; Gornictwo (Mining), V6, No. 2, 1982.

42. Ignatieff, A.; Outbursts in Coal Seams; Can. Inst. Min. Metal Transactions, V.57, 1954.

43. Insitu Stress Determination in No. 26 Colliery, Cape Breton, Nova Scotia; Golder Associates Report No. 831-1296, 1984.

44. Insitu Stress Determinations, Prince and Lingan Mines, Cape Breton, Nova Scotia; Golder Associates Report No. 851-6025, 1986.

45. Jackson, C.J.; Outbursts in Coal Mines; Draft Report, Tech. Infor. Serv., Coal Research, International Energy Agency, February 1984.

46. Jaeger, J.C.; Cook, N.G.W.; Fundamentals of Rock Mechanics; Reprint by Champman & Hall, London, 1971.

47. Josien, J.P., et al; The Dynamic Effects of Strata-Pressure-Rock Bursts; Proceedings of the 7th Intl. Strata Control Conference, Sept. 1982.

48. Josien, J.P.; Personal Communication, March 1985.

49. Joughin, N.C.; Jager, A.J.; Fracture of Rock at Stope Faces in South African Gold Mines; Proceeding of the Symposium Rockbursts: Prediction and Control, IMM, 1983.

50. Jovanovic, G., et al; Energy Spread of Free Gas in Oligomiocenic Coalfields and Its Outburst Capacity; Proceedings of the 18th Intl. Conf. on Safety in Mining Research Institutes, Cavtat, Yugoslavia, October 1979.

51. Karagodin, L.; et al; Method of Forecasting and Suppression of Rock and Gas Outbursts in Dombass; Proceedings of the 20th Intl. Conf. on Safety in Mine Research Institutes, Sheffield, U.K., October 1983.

52. Khristianovich, S.A., Salganik, R.L.; Several Basic Aspects of the Forming of Sudden Outbursts of Coal (Rock) and Gas; Proceedings of the 5th Intl. Congress on Rock Mech., Melbourne, Australia, 1983.

53. Kidybinski, A.; Bursting Liability Indices of Coal; Intl. J. Rock Mech. Min. Sci. & Geomech. Abstr., V18, 1981.

54. Klinkenberg, L.J.; The Permeability of Porous Media to Liquids and Gases; API Drill. and Prod. Prac. 1941.

55. Kobayashi, R., et al; Fundamental Studies on Rock Burst; J. of the Min. and Metal. Inst. of Japan, V94, No. 1084, June 1978.

56. Konda, B.W., Kochhar, J.K.; Undersea Longwalling at Cape Breton; Engineering and Mining Journal, V187, No. 5, May 1986.

57. Kozlowski, B., Kalisz, E.; Results of Research Into the Background of the Gas and Outburst Hazard in Crosscuts Driven Under Very Difficult Mining Conditions; Proceedings of the 19th Intl. Conf. on Safety in Mine Research Institutes, Poland, 1981.

58. Kusznir, N.J., Farmer, I.W.; Rockburst Phenomena in British Coal Mines; Proceedings of the Symp. on Rockbursts: Prediction and Control; IMM, 1983.

59. Kutter, H.K., Fairhurst, C.: On the Fracture Process in Blasting, Int. J. Rock Mech. Min. Sci., Vol. 8, pp. 181-202, 1971.

60. Kwasniewski, M.; Deformational and Strength Properties of the Three Structural Varieties of Carboniferous Sandstones; Proceedings of the 5th Intl. Congress on Rock Mech., Melbourne, Australia, 1983.

61. Lang, L.C.; New Permafrost Blasting Methods Developed at Asbestos Hill, Canadian Mining Journal, March 1976.

62. Lee, F.T., et al; Some Relations Between Stress, Geologic Structure and Underground Excavation in a Metamorphic Rock Mass West of Denver, Colorado; U.S. Geol. Survey Prof. Paper 650-C, Geological Survey Research, 1969.

63. Litwiniszyn, J.; A Model for the Initiation of Coal-Gas Outbursts; Intl. J. Rock Mech. Min. Sci. & Geomech. Abstr., V22, No. 1, 1985.

64. Logan, J.M., Handin, J.; Triaxial Compression Testing at Intermediate Strain Rates; Proceedings of the 12th Symp. on Rock Mech. (Nov. 1970), SME of AIME, 1971.

65. Longwall Techniques in Nova Scotia; Davis, H., Senior Editor,; Coal Age Second Operating Handbook of Underground Mining, McGraw-Hill, 1980.

66. Mahtab, A.; Geomechanical Aspects of Gas Outbursts in Louisiana Salt Mines; Bull. Ass. Engng Geol., Vol. XIX No. 4, 1982.

67. Matuszewski, J., Kozlowski, B., and others; Control of Gas and Rock Burst Hazard Demonstrated by Example of the Bitumiuous Coal Mine "Nowa Ruda"; Proceedings of the 18th International Conference of Mining Safety Research, Cavat, Yugoslavia, 1979.

68. Measurement and Analysis of Rock Deformation and Support System Response in the Drill and Blast and Bored Access Drivages at the Donkin-Morien Project; Golder Associates Report No. 831-6014, 1985.

69. Mindelli, E.O.; Some Shotfiring Problems in Ejection-Prone Stone Drifts; Sakhtonoe Stroitelstvo, 1965.

70. Moore, R.D., Hanes, J.; Bursts in Coal at Leichhardt Colliery, Central Queensland, and The Apparent Benefits of Mining by Shotfiring; Proceedings of Aus. I.M.M. Southern Queensland Branch Symp. on The Occurrence, Prediction and Control of Outbursts in Coal Mines, 1980.

71. Mordecai, M., Morris, L.H.; An Investigation Into the Changes of Permeability Occurring in a Sandstone When Failed Under Triaxial Stress Conditions; Proceedings of the 12th Symp. on Rock Mech. (Nov. 1970), SME of AIME, 1971.

72. Niwa, Y., et al; Stresses and Displacements Around an Advancing Face of a Tunnel; Proceedings of the 4th Intl. Congress on Rock Mech., V. 1 ISRM, Montreux, (Switzerland), 1979.

73. Obert, L., Stephenson, D.E.; Stress Conditions Under Which Core Discing Occurs; Transactions of SME of AIME, V.232, pp 227-234. September 1965.

74. Outbursts of Gas and Rock in the Werra Potash Mines; Editors, World Mining, V.20, No. 3, March 1967.

75. Patching, T.H.; Investigations Related to Sudden Outbursts of Coal and Gas; Proceedings of the 1st Rock Mech. Symp. (Sept. 1962), Dept. of Mines and Technical Surveys, Canada, 1963.

76. Paterson, L.; A Model for Outbursts in Coal; Intl. J. Rock Mech. Min. Sci. and Geomech. Abstr. Vol. 23, No. 4, 1986.

77. Paul, K.; Methane Bursts Involving the Ejection of Rock Material; Proceedings of the Symp. on Methane Bursts Involving the Ejection of Coal or Rock; Luxembourg, July 1983.

78. Pearse, G.E.; Rock Blasting: Some Aspect of the Theory and Practice, Mine and Quarry Engineering, January 1955.

79. Petrographic Study of Outburst Material, Sydney Coalfield, N.S.; Corelab-Canada Ltd. Report #70687-86-128, 1986.

80. Petukhov, I.M., Linkov, A.M.; Theoretical Principles and Fundamentals of Rock Burst Prediction and Control; Proceedings of the 5th Intl. Congress on Rock Mech., Melbourne, Australia, 1983.

81. Preston, C.J., Tienkamp, N.J.; New Techniques in Blast Monitoring and Optimization; Can. Inst. Min. Metal. Bulletin, V77 No. 867, July 1984.

82. Revalor, R., et al; In Situ Rock Stress Measurements in French Coal Mines. Relation Between Virgin Stresses and Rock Bursts; Proceedings of the 26th U.S. Symp. on Rock Mech., Rapid City, S.D., 26-28th June 1985.

83. Saito, T., et al; Study on Rockbursts at The Face of a Deep Tunnel, The Kan-ETSU Tunneel in Japan Being an Example; Proceedgins of the 5th Intl. Congress on Rock Mech., Melbourne, Australia, 1983.

84. Santarelli, F.J., Brown, E.T. Maury, V.; Analysis of Borehole Stresses Using Pressure-Dependent, Linear Elasticity; Intl. J. Rock Mech. Min. Sci. & Geomech. Abstr. Vol. 23, No. 6, 1986.

85. Sevelev, G.A.; Mechanism of Outbursts; Ugol'Ukrain (Ukrainian Coal), May 1974.

86. Shepherd, R.; Kellet, W.H.; Strata Behaviour, A Study on Faces and Roadways in Workings under a Sandstone Roof Liable to Rock Bumps; Colliery Guardian, V. 221 N. 3, March 1973.

87. Shepherd, J., et al; Instantaneous Outbursts of Coal and Gas with Reference to Geological Structures and Lateral Stresses in Collieries; Proceedings of the Symposium on Rockbursts and Seismicity in Mines; Gay and Wainwright Editors, The South African Institute of Mining and Metallurgy, Johannesburg, 1984.

88. Shepherd, J., et al; Outbursts and Geological Structures in Coal Mines: A Review; Intl. J. Rock Mech. Min. Sci. & Geomech. Abstr., V18, 1981.

89. Singh, J.G.; A Mechanism of Outbursts of Coal and Gas; Mining Science and Technology, 1, 1984.

90. Skempton, A.W.; Effective Stresses in Soils, Concrete and Rocks; Pore Pressure and Suction in Soils, Butterworths, London, 1961.

91. Stacey, T.R.; A Simple Extension Strain Criterion for Fracture of Brittle Rock; Intl. J. Rock Mech. Min. Sci. & Geomech. Abstr., V18, No. 6, 1981.

92. Stacey, T.R.; Page, C.H.; Practical Handbook for Underground Rock Mechanics; Trans Tech Publications, FRG., 1986.

93. Suchodolski, Z.; The Character of Gas Manifestations in the Lubin Bassin; Przeglad Gorniczy (Mining Journal), V.27, N. 5, 1971 (Poland).

94. Tanton, J.H., et al; The Introduction of Stabilizing Pillars to Reduce Rockbursts at Western Deep Levels Limited; Proceedings of the 1st Intl. Congress on Rockbursts and Seismicity in Mines, Johannesburg 1982, SAIMM, 1984.

95. Trollope, D.H., Brown, E.T.; Effective Stress Criteria of Failure of Rock Masses; Proceedings of the 1st Intl. Congress on Rock Mech., Lisbon, Portugal, 1966.

96. Trollope, D.H., The Mechanics of Discontinua or Clastic Mechanics in Rock Problems; Rock Mech. in Engng. Practice, Stagg and Zienkiewics Editors, John Wiley & Sons, London, 1968.

97. Ujihira, M., et al; On the Flaking - Destructive Phenomena of Porous Material Induced by Involved High Pressure Gas; Journal of the Mining and Metal. Inst. of Japan, V.100, No. 1153, March 1984.

98. Ujihira, M., et al; On the Process of Destruction of Porous Material in which High Pressure Gas is Involved; Journal of the Mining and Metal. Inst. of Japan, V.100, No. 1155, May 1984.

99. Ujihira, M., et al; The Relation Between Gas Pressure and Stress Distribution in the Vicinity of the Exposed Surface of Porous Materials; Journal of the Mining and Metal. Inst. of Japan, V.101, No. 1167, May 1985.

100. Ujihira, M., et al; On the Triaxial Compression Test of Coal and Other Specimens in which High Pressure Gas is Involved; Bulletin of the Faculty of Engineering, Hokkaido University No. 128, 1985.

101. Ujihira, M., et al; Scale Models Studies and Theoretical Considerations on the Mechanism of Coal and Gas Outbursts; Proceedings of the 21st. Intl. Conf. on Safety in Mining Research Institutes, Sydney, Australia, October 1985.

102. Vairogs, J., et al; Effect of Rock Stress on Gas Production From Low-Permeability Reservoirs; J. of Petroleum Technology, September 1971.

103. Watanabe, Y., et al; The Application of AE Techniques as a Forecasting Method to the Rock and Gas Outburst in Coal Mine; Proceedings of the 19th Intl. Conf. on Safety in Mining Research Institutes, Katowice, Poland, 1981.

104. Whittaker, B.N.; Longwall Planning With Reference to Rockbursts; Proceedings of the Symposium Rockbursts: Prediction and Control, IMM, 1983.

105. Zorin, F.N., et al; Driving Near Burst-Prone Rocks; Ugol'Ukrainy (Ukrainian Coal), 1981.

APPENDIX A

BOREHOLE LOG
B162, B163
B164

March 1987 861-1290

FORM 1076

CAPE BRETON DEVELOPMENT CORPORATION

LOG SHEET

BOREHOLE NUMBER B-162

LOCATION No. 26 12 North Coal near 2nd cund

COORDINATES N ~~S~~ 10,070 (3069.336 (m))

E ~~W~~ 22,225 (6774.18 (m))

ELEVATION TOP OF CASING -2121.3 (- 646.57m)

TOP OF GROUND -2121.3 (-646.57m)

TOTAL LENGTH 152.4 m (500 ft)

DATE STARTED Sept 4/80 FINISHED Oct 18/80

PURPOSE OF HOLE To intersect Phalen seam and determine thickness and quality

SEAM OF INTEREST Phalen

SEAM INTERSECTED Phalen - Boutillier - Backpit

Photographs of seam available

CONTRACTOR Longyear Canada Inc.

DRILL PERSONNEL FOREMAN John Newsome

RUNNERS J. Newsome; J.G. Belanger; R. Laroque; R. Lloyd

DRILLING METHOD EHS-38 - ten foot core barrel

CORE SIZE HQ-3 NQ-3

BEARING OF HOLE N.A.

INCLINATION Vertical

OVERBURDEN DEPTH N.A.

CASING USED 6' (1.83m) left in hole

CEMENTED YES ☒ NO ☐

TESTS TAKEN IN HOLE No tests

GEOPHYSICAL LOGGING Not available

REMARKS Many problems with rods sticking, etc: at 332 HQ rod stuck. Left 300' (91.44m) HQ rods and HQ core barrel and HQ-3 bit and reaming shell in hole. Reduced hole to NQ-3 after drilling out core barrel and bit. "Polydrill" mud used from 350 [illegible] to 500 [illegible]. No further sticking problems.

[illegible] logged [illegible]

LOGGED BY

[illegible]

DEPTH (ft) (m)	THICKNESS (ft) (m)	DESCRIPTION
		Start of hole to 19.3' is represented by only 6 feet of broken core. Good recovery from 17' on.
0 - 19.3' 0 - 5.88 m		SANDSTONE: light grey, medium grained, locally fine grained, bedding planes contain micaceous bands and trace amounts of carbonaceous material, no discing noted
19.3' - 29.2' 5.88 - 8.90 m	9.9' 3.02 m	SILTSTONE: dark grey, generally massive with a slight tendancy to break at approximately 10° - 6 feet core recovered - Joints @ 22.6' is 45° 6.04 - 6.13 m (19.8 - 20.1') sandstone lense, fine grained 8.51 - 8.66 (27.9' - 28.4') zone remenisant of a seatearth contains numerous stigmaria remains
29.2 - 30.5' 8.90 - 9.30 m	1.3' 0.4 m	MUDSTONE: grey black, massive, soft fossil content is high with leaves, ferns, branches common, minor amount of listric surfaces. 30 - 40 run: 8' core recovered.
30.5 - 32.5' Zone 9.30 - 9.91 m	0.2' Recovered	COAL: coal to impure splinty coal some shiny
32.5 - 32.7' 9.91 - 9.97 m	0.2' 0.6 m	MUDSTONE: as 29.2' - 30.5' 8.90 - 9.30 m
32.7 - 33.6' 9.91 - 9.97 m	0.9' 0.27 m	LIMESTONE: Interlayered limestone fauna units containing ostracods and trace lamellebracs, these occur in thin 1 cm black layers wavy interbands common in top half; limestone is lighter grey in colour.
33.6 - 41.4' 10.24 - 12.62 m	7.8' 2.38 m	MUDSTONE: grey, massive, abundant calcareous nodules, (rusty) many are 1 mm but range up to 5 cm 36.2' (9.94 m) Worm burrow infilled 38.5' - 39.1' (11.73 - 11.92 m) Sandstone inclusion, fine grained finely cross-bedded

DEPTH	THICKNESS	DESCRIPTION
41.4 - 45.8' 12.62 - 13.96 m	4.4' 1.34 m	2 SANDSTONE: light grey, fine to medium grained, very massive and competent; cross-bedding common localized silty phases. No discing noted.
45.8 - 48.8' 13.96 - 14.87 m	3.0' 0.91 m	INTERBEDDED MUDSTONE AND SILTSTONE: 2' recovered (possibly lost 1' at 47.8 - 48.8') minor fine grained sandstone, ironstone lenses common along bedding, unit weakens in water.
48.8 - 57.9' 14.87 - 17.65 m	9.1' 2.78 m	3 SANDSTONE: light grey, fine grained, ironstone blebs very common, massively bedded but with locallized bedding and cross bedding as at 54.6'. Dip 10° - 20°. No discing noted. 53.5' - 45° fracture 56.6' - 70° fracture
57.9 - 58.8' 16.65 - 17.92 m	0.9' 0.27 m	MUDSTONE: greenish grey, soft, deteriorates when wet, sharp lithological contacts (may be lost due to drilling as short run 50'-58.2')
58.8 - 65.8' 17.92 - 20.06 m	7.0' 2.14 m	4 SANDSTONE: light grey, fine to medium grained micaceous, cross-bedding common unit is hard and competent. Discing noted between: 61.5' -62.15' 62.29' - 62.52'. Calcareous cement in disced locations.
65.8 - 72' 20.06 - 21.95 m	6.2' 1.89 m	MUDSTONE: grey, generally semi-soft as deteriorates easily in water, ironstone concretions (stained brown) are common and effervesce easily, minor amounts of sandy and silty fractions present.
72 - 73.4' 21.95 - 22.73 m	1.4' 0.43 m	LIMESTONE: greenish grey, hard, dense, fine grained crystalline, difficult to find exact contact as a gradational contact is present expecially in foot wall
73.4 - 79.1' 22.37 - 24.11 m	5.7' 1.74 m	5 SANDSTONE: light grey, fine grained, locally calcareous; top portion contains calcareous iron stone nodules (approximately 1 mm) interbedded siltstone and some mudstone present.
79.1 - 82.1'	3.0'	LIMESTONE: dark green grey, ophitic texture, small ostracod like fauna present, however, they are somewhat curved. This unit much like that at 32.7 - 33.6'; lower section is more crystalline, rock hard and dense, sharp foot wall contact, fauna increase upward in section.

DEPTH	THICKNESS	DESCRIPTION
82.1 - 100.0' 25.02 - 33.53 m	27.9' 8.50 m	**MUDSTONE:** dark grey, generally soft with the following zones; 85 - 87' (25.93 - 26.54 m): listric zones, polished soapy surfaces 96.5 - 98': many listric zones parallel to horizontal axis. 99 - 101': fissile 102.7': 45° joint 104': 5° - 10° bedding 106.5 - 109': whispy silty interbands at 15°
100.0 - 147.7' 33.53 - 34.86 m	4.7' 1.43 m	**SILTSTONE:** light grey to grey, locally some fine grained sandstone with some heavy crossbedding, interbanding with mud stone also common.
114.7 - 118.7' 34.96 - 36.18 m	4.0' 1.22 m	6 **SANDSTONE:** white, looks bleached, medium grained, breaks easily as in box along bedding perpendicular to core axis and crumbles; not strong! Moderately calcareous
118.7 - 119.1' 36.18 - 36.30 m	0.4' 0.12 m	**MUDSTONE:** dark grey
119.1 - 128.9' 36.30 - 39.29 m	9.8' 2.99 m	7 **SANDSTONE:** light grey, silty to very fine grained cross bedding extremely pervalent due to a carbonaceous material along bedding planes. Less turbulent at base.
128.90 - 133.1' 39.29 - 40.57 m	4.2' 1.28 m	**MUDSTONE:** (slightly silty): dark grey mainly massive and uniform but local bedding at 10° - 15°
133.1 - 147.0' 40.57 - 44.81 m	13.9' 4.24 m CHANNEL SANDST.	8 **SANDSTONE:** light grey, fine to medium grained, carbonaceous material along bedding planes, cross bedding becoming common. 145.2 - 145.9' Calcareous zone 146.7 - 147.0' LAG: reminants of erosional features (mudstone) Discing noted between: 143.5' - 147.17' 144.375' - 145.33'; 145.625' - 146.33'; 146.58' - 146.92'.
147.0 - 150.0' 44.81 - 45.72 m	3.0' 0.91 m	**SILTSTONE:** dark grey, massive, oxidized, ironstone blebs and nodules present throughout core.

DEPTH	THICKNESS	DESCRIPTION
150.0 - 156.0' 45.72 - 47.55 m	6.0' 1.83 m	9 **SANDSTONE:** light grey, fine grained, locally cross-bedded, typically micaceous on ends. Gradational contact from above over 4 inches. Unit ends as a LAG consisting of a mixture of mudstone clasts on the bottom contact. Oxidized ironstone nodules and zonations common on bottom .3 feet. Discing noted between 152'-156.04'.
156.0 - 159.0' 47.55 - 48.46 m	3.0' 0.91 m	10 **SANDSTONE:** fine to medium grained, zones of finer and darker siltstone within unit. Ironstone clasts present, dip approximately 20°.
159.0 - 166.5' 48.46 - 50.75 m	7.5' 2.29 m	11 **SANDSTONE:** grey, medium to coarse grained, generally massive bedding, Progressively coarser towards base, numerous claystone fragments and many oxidized fragments; coaly fossil remains present with locally large 1 mm muscovite micas present. Claystone seems to form the matrix as it encompasses the grains; pebbles up to 1 cm common on unti base. Rock is competent; but would not likely be very strong under compression; tendency to crumble.
166.5 - 167.7' 50.75 - 51.11 m	1.2' 0.36 m	**SEATEARTH:** a light green-grey silty mudstone makes up 40% of unit. Remainer is a highly contorted unit of swirls and flexures, coaly material with fossil branches, as well as fossil rootlets (?) are abundant. Pyrite blebs at base. Some of core ground
167.7 - 171.4' 51.15 - 52,28 m	3.7' 1.13 m	12 **SANDSTONE:** light grey, fine grained, 168 - 169': tendency for sandstone to break into 5 mm dimes along bedding, not strong at this point Discing noted between 168.16' - 169.66'; 169 - 171.4': sandstone is heavily crossbeddid and whispy in nature; a 40% constituent of silt becomes common in the cross-bedding.
171.4 - 174.5' 52.28 - 53.22 m	3.1' 0.94 m	**MUDSTONE:** (shaly) grey to brownish grey, massive will break easily.

DEPTH	THICKNESS	DESCRIPTION
174.5 - 175' 53.22 - 53.38 m	0.5' 0.16 m	LIMESTONE: black speckled, hard dense unit containing only a few noticeably fossils i.e. ostracods. A small presence of coaly material present. Contacts are extremely sharp. Does not exhibit sugary texture feted odor.
175 - 188' 53.38 - 57.34 m	13' 3.96 m	INTERBEDDED MUDSTONE AND SILTSTONE: 30% siltstone 70% mudstone, fine cross-bedding, lenses and clasts of pyrite common in 186-188 Shaly tendency.
188 - 189.0' 57.34 - 57.65 m	1.0' 0.31 m	SHALE: blackish, fissile
189.0 - 189.7' 57.65 - 57.86 m	0.7' 0.31 m	LIMESTONE: feted, hard, dense, competent approximately pyrite as specs
189.7 - 191.0' 57.86 - 58.26 m	1.3' 0.40 m	LIMEY MUDSTONE: dark, extremely incompetent after 9 months prior to logging, strong H_2S odor, with HCl disintergrates in H_2O.
191.0 - 192.7' 58.26 - 58.77 m	1.7' 0.51 m	MUDSTONE: grey, extremely broken with numerous polished sides; abudant carbonates as stringers.
192.7 - 192.85' 58.77 - 58.82 m	0.15' 0.05 m	LIMESTONE: greyish brown, hard, dense, slight sugary texture, pyrite blebs and specs throughout sample approximatel 1%, sample weathers to a whitish bleached colour.
192.85 - 203' 58.82 - 61.92 m	10.15' 3.10 m	MUDSTONE: grey, extremely soft and water absorbant, localized irregular carboate blebs 198' sediment is slightly coarser, non-calcareous, hard and competent. Pyrite is common (less than 1%) in much of the core as small localized blebs, probably after carbonaceous material. Gradation into siltstone.
203.1 - 203.9; 61.92 - 62.19 m	0.9' 0.27 m	SILTSTONE: light to dark grey, finely laminated interbeds of silts and clays; crossbedding common.
203.9 - 204.9' 62.19 - 62.49 m	1.0' 0.30 m	LIMESTONE-MUDSTONE: mottled light and dark grey, intertwined. Possibly an erosional feature weather and infilled (?) . Polished surfaces on mudstone.

DEPTH	THICKNESS	DESCRIPTION
204.9 - 205.3' 62.49 - 62.62 m	0.4' 0.13 m	MUDSTONE: greenish grey, soft.
205.3 - 205.7' 62.62 - 62.74 m	0.4' 0.12 m	LIMESTONE: brownish grey
205.7 - 205.85' 62.74 - 62.78 m	0.15' 0.04 m	MUDSTONE: greenish grey, soft, broken
205.85 - 208.8' 62.78 - 63.68 m	2.95' 0.90 m	LIMESTONE: brownish grey, small zones of mudstone, polished slickensided fractions; feted odor.
208.8 - 209.8' 63.68 - 63.99 m	1.00' 0.31 m	LOST CORE: reconstruction This zone felt to be lost coal 1'. This evedenced by 1" bands of poor quality coal: and the underlying rock as described below.
209.8 - 211.6' 63.99 - 64.54 m	1.8' 0.55 m	MUDSTONE: dark grey to blackish, unit soft, highly polished with numerous listric surfaces slight indication of stigmaria.
211.6 - 213.65' 64.54 - 65.16 m	2.05' 0.62 m	SILTSTONE: lightish grey, numerous stigmaria; the lower portion of rootlets have been replaced by pyrite.
213.65 - 218' 65.16 - 66.49 m	4.35' 1.33 m	SILTSTONE: light grey, same as above but void of stigmaria, localized carbonate blebs throughout 216.6 - 217' localized contorted sandstone, steep dip
218 - 220.8' 66.49 - 67.34 m	2.8' 0.85 m	MUDSTONE: dark grey to black, competent looking but easy to break into pieces.
220.8 - 222.6' 67,34 - 67.89 m	1.8' 0.55 m	MUDSTONE: medium grey, approaching a "TECTONITE"; extremely polished, internal listric surfaces; small pyrite blebs replacing carbonaceous matter.
222.6 - 225.9' 67.89 - 68.90 m	5.6' 1.01 m	SILTSTONE: medium grey,grading into a (0.5') fine grained sandstone which is slightly calcareous and contains carbonaceous material.
225.9 - 231.9' 68.90 - 70.73 m	5.6 1.83 m	MUDSTONE: greenish grey, massive, semi-competent unit abundant with numerous ironstone blebs and blobs. 229; - small silty zone
231.9 - 233.6' 70.73 - 71.20 m	2.1' 0.47 m	SILTSTONE: grey, gradation change to silty mudstone to siltstone

DEPTH	THICKNESS	DESCRIPTION
233.6 - 235' 71.20 - 71.68 m	1.4' 0.48 m	(3 SANDSTONE: light grey, fine grained easily breaks into 1" pieces.
235 - 240.5' 71.68 - 73.35 m	5.5' 1.67 m	MUDSTONE: dark grey, larg ironstone nodules with numerous listric surfaces. rock is weak and breaks easily.
240.5 - 245.3' 73.35 - 74.82 m	4.8' 1.47 m	SILTSTONE: brownish grey, with interbeds of fine grained sandstone; carbonate blobs that effeversce, sandstone; is often crossbedded.
245.3 - 250.5' 74.82 - 76.40 m	5.2' 1.58 m	MUDSTONE: grey, eventually grades into a siltstone; ironstone nodules are present throughout 245.3 - 246.3' extremely soft approaching a tectonite.
250.5 - 255.6' [illegible]	5.1'	(4 SANDSTONE: light grey, interbedded sandstone, cross bedded easily breaks along bedding planes, Discing noted between 250.5' - 253' and 254.75' - 255.17'. gradation into siltstone.
		NOTE: 253-263: 3 feet missing core, suspect missing 258.9'-261.9' may be Bouthillier.
255.6 - 257.6' 77.96 - 78.57 m	2.0' 0.61 m	MUDSTONE: dark grey,soft, easily broken, poor rock.
257.6 - 294.2' 78.57 - 89.73 m	36.6' 11.16 m	MUDSTONE: dark grey to green grey, soft broken, stigmaria common, well polished, slickensided. Approaches tectonite, incompetent locally. Numerous ironstone nodules. 277.2 - 277.3' Calcareous zones 278.2 - 278.3'
294.2 - 300.4' 89.73 - 91.62 m	6.2' 1.89 m	(5 SANDSTONE: light grey, fine grained, not competent. Discing noted; Intense between 295.0' - 296.0'
300.4 - 302' 91.62 - 92.11 m	1.6' 0.49 m	LIMESTONE: brownish grey, eroded by sandstone, somewhat mottled, one ostracod observed. 301.0 - 302.0' interbedded limestone and mudstone hard, dense, speckled, (looks like concrete.)

DEPTH	THICKNESS	DESCRIPTION
302.0 - 325' 92.11 - 99.13 m	23' 7.02 m	INTERBEDDED SILTSTONE AND MUDSTONE: grey and dark grey, 70% mudstone: with ironstone nodules soft, listeric surfaces, 25% siltstone: most competent, 5% fine sandstone. Discing noted between 322.75'and 323.17' and 324.083' - 325.33'.
325.0 - 326.4' 99.13 - 99.55 m	1.4' 0.42 m	15 SANDSTONE: light grey, fine to medium grained most of core broken into dimes.
326.4 - 331.0' 99.55 - 100.96 m	4.6' 1.41 m	INTERBEDDED SILTSTONE AND MUDSTONE: as 302-325.
331.0 - 331.5' 100.96 - 101.11 m	0.5' 0.15 m	SHALE: black, lamellabracs' shells smeared on core faces; minor pyrite as traces
331.5 - 332.0' 101.11 - 101.26 m	0.5' 0.15 m	LIMESTONE: almost black, crenulated wavy unit with fauna as layers.
		NOTE: change to NQ-3 core. Core barrel and rods became stuck and it was impossible to free same. The inner tube was removed and the landing ring was drilled out with NQ impregnated bit. 300' of HQ rods and HQ core barrel left in hole.
332.0 - 101.26 -	Missing Core	COAL: Backpit seam 1.5' recovered Approximately 2.2' of lost core sample used for CH_4 gas test.
- 337.8' - 103.03 m		SILTY: mudstone seatearth, stigmaria common, generally competent.
337.8 - 339.8' 103.03 - 103.64 m	2.0' 0.61 m	SILTSTONE: light grey, competent massive unit
339.8 - 340.8' 103.64 - 103.94 m	1.0' 0.30 m	SILTY MUDSTONE: dark grey, finely interbedded.
340.8 - 341.3' 103.94 - 104.10 m	0.5' 0.16 m	MUDSTONE: dark grey, incompetent, soft
341.3 - 346' 104.10 - 105.53 m	1.43 m	INTERBEDDED SILTSTONE AND MUDSTONE: occasional ironstone nodules
346.0 - 353' 105.53 - 107.67 m	2.14 m	SANDSTONE: light grey, fine grained ground pieces, micaceous.
		Lost core 347 - 354 only 1.5' removed

DEPTH	THICKNESS	DESCRIPTION
353.0 - 365.0' 107.67 - 108.58 m	3' 0.91 m	MUDSTONE: greenish grey, very soft and easy to break on wet surfaces, ironstone nodules present.
356.0 - 362' 108.58 - 110.41 m	6' 1.83 m	INTERBEDDED SILTY MUDSTONE AND SILTSTONE: with fine grained sandstone, a few ironstone nodules and lenses present.
362.0 - 394.2' 110.41 - 120.23 m	32.2' 9.82 m	SANDSTONE: light grey, fine to medium grained generally broken into 4" pieces or less; generally massive bedding with cross-bedding 387' dark zone to carbonaceous material (0.2') tendency to become coarser towards base and generally more massive. Intire unit disced with the exception of bottom 1.25' (392.95-394.2') Calcareous zones at 378.3' (115.38 m) 380.0' (115.90 m) 383.0' (116.83 m) 385-386' (117.43-117.73 m) 393.9-394.2'(120.14-120.23m)
394.2 - 395.0' 120.23 - 120.48 m	0.80' 1.25 m	MUDSTONE: dark grey, soft with many listric surfaces, top is slicensided, 393.85-393.95' limestone band, light brown, possible ostracods present.
395.0 - 399.2' 120.48 - 121.76 m	4.2' 1.28 m	SILTSTONE: dark grey, quite competent, ironstone nodules present, 396.9-397.7' fine grained sandstone with cross-bedding.
399.2 - 422.2' 121.76 - 128.77 m	23.0' 7.01 m	SANDSTONE: light grey, fine to medium grained, carbonaceous material whispy along bedding; unit appears to have been deposited under varying energies in coarser ss. feldspar present. 403.0'steep dips, moderate elsewhere 408.0-409.0 (124.44-124.75 m) coarse grained section 410.8-412' (125.29-125.66) coarse grained section 412-413.4' (125.66-126.07 m) lag coarse constituents with calcareous fragments 416.6-417.4' (127.06-127.31 m) coarse grained section Entire unit disced. (Average thickness - 7mm) The base at 422' becomes finer grained grading into dark grey siltstone.
422.2 - 447' 128.77 - 136.34 m	17.8' 7.57 m	INTERBEDDED SILTSTONE AND MUDSTONE SECTION: grey to dark grey; mudstone 30% with many elongated and nodular ironstone nodules siltstone 65% fine sandstone 5% 438-439.5' mudstone, soft with abundant listric surfaces. 445-447' numerous ferns and plant debris.

DEPTH	THICKNESS	DESCRIPTION
447.0 - 449.2' 136.24 - 137.01 m	2.2' 0.67 m	MUDSTONE: dark grey to grey black, quite broken, many listric surfaces as well as abundant fossil plant material with some pyrite replacement slight amounts of coalification in bottom section.
49.2 - 456.4' 37.01 - 139.20 m	7.2' 2.19 m	COAL - PHALEN: 86-1/2 inches drilled and recovered: see coal description
56.4 - 479.1' 39.20 - 146.13 m	22.7' 6.93 m	MUDSTONE: dark grey to blackish grey, numerous ironstone nodules and blebs; some reactive to HCl others not, a few whispy silty zones throughout but especially at 466.9-468, 476-478' 470-471 dark grey black soft mudstone 478-479,1
79.1 - 482' 46.13 - 147.01 m	2.9' 0.88 m	LIMESTONE: hard, dense, extremely competent, brownish grey, speckled, extremely calcareous.
82.0 - 484.3' 47.01 - 147.71 m	2.3' 0.70 m	INTERBEDDED: calcareous mudstone zone with limestone grey and light brown, a mottled unit with blebs and blotches of carbonate.
84.3 - 488! 47.71 - 148.84 m	3.7' 1.13 m	MUDSTONE: dark grey, semi-competent, flora fossil fragments, abundant listric surfaces.
88 - 489' 8.84 - 149.15 m	1' 0.31 m	SHALE: coaly black, coalification present, pyrite abundant as blebs and seamlets; some plant remains visable.
9 - 494' 49.15 - 150.67 m	5' 1.52 m	INTERBEDDED SILTSTONE AND MUDSTONE: 60% siltstone. slightly calcareous, 40% mudstone. Minor ironstone nodules and lenses.
4 - 494.7' 50.67 - 150.88 m	.7' 0.21 m	SHALE: dark grey to black grey, soft with a few lamellibracs.
4.7 - 495.4' 50.88 - 151.10 m	0.7' 0.22 m	SHALE: black, with calcareous banding, lamellibracs extremely prevalent, in beds and layers Pyrite as swirls and irregular shapes.
5.4 - 495.7' 51.10 -151.19 m	0.3' 0.09 m	STONY COAL: Poor
5.7 - 498' 51.19 - 151.89 m	2.3' 0.70 m	SILTY SEATEARTH: stigmaria present with coalification present, no bedding
8 - 1.98		

END OF HOLE

FORM 1076

CAPE BRETON DEVELOPMENT CORPORATION

LOG SHEET

BOREHOLE NUMBER B-163

LOCATION No. 26 12 North Coal No. 2 Drive

COORDINATES N ~~S~~ 2923.032 (m) 9,590

E ~~W~~ 8420.10 (m) 27,625

ELEVATION TOP OF CASING -685.28 m -2248.3

TOP OF GROUND -685.28 m -2248.3

TOTAL LENGTH 161.85 m (531')

DATE STARTED Oct 20/80 FINISHED Nov 10/80

PURPOSE OF HOLE Test seams and stratigraphy between Harbour and Gardiner

SEAM OF INTEREST Phalen

SEAM INTERSECTED Phalen - Backpit

CONTRACTOR Longyear Canada Inc.

DRILL PERSONNEL FOREMAN John Newsome

RUNNERS J. Newsome; R. Lloyd; D. Fournier

DRILLING METHOD EHS-38 - ten foot core barrel

CORE SIZE HQ-3 2.406 in. 61.1 mm BEARING OF HOLE N.A.

INCLINATION Vertical OVERBURDEN DEPTH N.A.

CASING USED (20') 6.10 m CEMENTED YES ☒ NO ☐

TESTS TAKEN IN HOLE No tests taken

GEOPHYSICAL LOGGING Not available

REMARKS Polydrill used from start to finish. No hole problems. Hole to be drilled to 320 m (1050'). However, due to a change in ventilation, drill was curtailed at 161 m.

LOGGED BY F.M. Isenor, K. MacPherson

HOLE B-163

DEPTH (m)	THICKNESS (m)	DESCRIPTION
0 - 6.55	6.55	1 **SANDSTONE** - Light grey; very fine - fine grained, highly micaceous; contains an abundance of plant fossils; unit is covered by a calcareous coating, but is not calcareous; first 2.74 m is highly ground up, contains much more carbonaceous matter than the remainder; abundance of coal shards between 4.42 - 4.88 m; highly broken up in core box; direction of bedding is not apparent; lower contact is very sharp; generally competent.
6.55 - 7.13	.58	**MUDSTONE** - dark grey; very silty; contains abundant plant fossils; somewhat micaceous; non calcareous; gradational lower contact; competent.
7.13 - 15.11	7.98	**SILTSTONE** - light-medium grey; fine grained; massive; slightly calcareous; micaceous; 5 cm bed of coal located at 13.14; plant fossils generally absent; gradational lower contact; very competent.
15.11 - 15.39	.28	**MUDSTONE** - medium grey; very silty; listric surfaces throughout; plant fossils absent; calcareous; abrupt lower contact; competent.
15.39 - 15.91	.52	2 **SANDSTONE** - light grey; fine grained; highly micaceous; slightly calcareous; slightly cross bedded; contains a few mudstone fragments (.6 cm); abrupt lower contact; competent.
15.91 - 18.56	2.65	**MUDSTONE** - medium grey; very silty; contains numerous bands of siltstone (.3 cm thick); plant fossils absent; slightly micaceous; gradational lower contact; relatively competent.
18.56 - 20.76	2.20	3 **SANDSTONE** - light grey; fine-medium grained; contains numerous interbeds of coarse grained siltstone throughout unit; cross bedded; slightly micaceous; calcareous; mudstone fragments throughout; erosive lower contact; bedding not apparent; competent.
20.76 - 21.9	1.14	**MUDSTONE** - dark grey; very silty; plant debris noted; slightly calcareous; abrupt lower contact; slightly competent.

DEPTH (m)	THICKNESS (m)	DESCRIPTION
21.9 - 22.25	.35	LIMESTONE - black; sugary texture; fetid odor; abrupt lower contact; competent
22.25 - 23.32	1.07	SILTSTONE - medium grey; fine grained; slightly calcareous; non micaceous; no plant fossils noted; massive; structureless; bedding not well developed; gradational lower contact; competent.
23.32 - 23.59	0.27	LIMESTONE - medium grey; sugary texture; impure; ironstone nodules to 1 cm diameter noted throughout section; gradational lower contact; competent.
23.59 - 25.05	1.46	SILTSTONE - medium grey; medium grained; plant fossils absent; non micaceous; calcareous pods noted throughout; massive; erosive lower contact; competent.
25.05 - 27.16	2.11	SANDSTONE - SILTSTONE - medium-dark grey; sandstone - fine grained; siltstone - coarse grained; highly micaceous; slightly calcareous; ironstone nodules throughout; plant fossils absent; gradational lower contact; competent.
27.16 - 53.89	26.73	SANDSTONE - light-medium grey; fine to medium grained; highly micaceous; slighty calcareous; massive; plant fossils noted; lower contact - abrupt; competent. 27.16 m - 28.96 m unit contains interbeds of siltstone (medium grained) and is cross-bedded. At 30.39 m and 30.45 m fractures noted. Dipping at an angle of 25° to core axis. 31.9 m - 32.37 m - unit of medium grey; fine grained siltstone noted; 47.9 m - 48.3 m - unit is highly crossbedded and contains an abundance of fossil matter. 51.17 m - 51.36 m - band of highly polished mudstone. At 53.6 there is a 5 cm bed of coal. Sandstone becomes very fine grained in the last 1.2 m.

DEPTH (m)	THICKNESS (m)	DESCRIPTIONS
53.89 - 63.61	9.72	MUDSTONE - SILTSTONE (interbedded) - medium to dark grey; siltstone is medium to coarse grained; plant fossils abundant; entire unit is calcareous; highly micaceous; localized listric surfaces; interbands of siltstones are highly variable in thickness; lower contact is gradational; direction of bedding is not apparent; unit is generally competent. Limestone interbeds noted at the following locations: 55.1 (5 cm) 57.73 (5 cm) 61.08 (.55 cm) 60.75 (13 cm)
63.61 - 75.59	11.98	MUDSTONE - dark grey; contains silt sized material; few plant fossils noted; listric surfaces found throughout section; unit contains numerous calcareous pods (up to 5 cm) in diameter; a 10 cm coal seam is found at 68.70m; limestone interbeds were found at 78.87m (10 cm thick), and 74.13 m (3 cm thick); a medium grained siltstone interbed was located from 70.10 to 70.59; abrupt lower contact; unit is slightly competent.
75.59 - 77.27	1.68	SANDSTONE - light grey, fine grained; massive; slighlty calcareous; micaceous; slightly cross bedded; contains numerous interbeds of siltstone and mudstone from 76.35 - 76.93; abrupt lower contact; competent.
77.27 - 77.97	.70	MUDSTONE - dark grey to black; contains an abundance of fossiliferous matter; a 5 cm bed of limestone was located at 77.48 m; gradational lower contact; slightly competent.
77.97 - 80.86	2.89	SILTSTONE - medium grey; coarse grained; slightly calcareous; micaceous; massive and structureless; no plant fossils noted; ironstone staining throughout; gradational lower contact; competent.
80.86 - 81.14	.28	MUDSTONE - refer to 77.27 - 77.97 for description
81.14 - 81.47	.33	COAL - no signs of pyritic accumulations; badly broken up in core box.
81.47 - 86.93	5.46	MUDSTONE - medium to dark grey; massive and structureless; no plant fossils noted; non calcareous; ironstone staining throughout; localized listric surfaces; lower contact - gradational; incompetent.

DEPTH (m)	THICKNESS (m)	DESCRIPTION
86.93 - 88.36	1.43	SILTSTONE - medium grey; medium grained; slightly calcareous; micaceous; small plant fossils noted; fine grained sandstone interbed from 87.36 - 87.69; ironstone staining throughout; abrupt lower contact; competent.
88.36 - 88.94	.58	SANDSTONE - light grey; fine grained; micaceous; highly calcareous; ironstone staining throughout; no plant fossils noted; abrupt lower contact; competent.
88.94 - 91.13	2.19	MUDSTONE - dark grey; highly slickensided, plant fossils generally absent; non calcareous; somewhat silty; gradational lower contact; incompetent.
91.13 - 95.80	4.67	SILTSTONE - medium grey; fine to medium grained; ironstone staining throughout; micaceous; calcareous; bedding not apparent; no plant fossils noted; gradational lower contact; competent.
95.80 - 103.48	7.68	MUDSTONE - dark grey to black; very silty; localized slickensided surfaces; plant fossils are abundant, ironstone staining noted; calcareous pods throughout; abrupt lower contact; slightly competent. - small coal bed from 98.85 - 98.94. - limestone interbeds noted at the following locations: 98.05 (3 cm) 98.69 (15 cm) 100.92 (12 cm)
103.48 - 108.36	4.88	7 SANDSTONE - light grey; fine grained; massive and structureless; slightly calcareous; micaceous; plant fossils absent; abrupt lower contact; competent.
108.36 - 110.79	2.43	MUDSTONE - medium grey; very silty; localized listric surfaces; plant fossils absent; calcareous fragments throughout; gradational lower contact; competent.
110.79 - 116.13	5.34	SILTSTONE - light to medium grey; fine grained; non calcareous; non micaceous; unit is cross-bedded; no evidence of plant fossils; lower contact - gradational; competent.
116.13 - 128.17	12.04	8 SANDSTONE - light grey; fine grained; highly calcareous; massive; abundance of plant fossils; bedding not apparent; slightly crossbedded in sections; ironstone nodules throughout unit; conglomeritic sandstone from 125.12 - 125.27; gradational lower contact; competent.

DEPTH (m)	THICKNESS (m)	DESCRIPTION
128.17 - 132.28	4.11	SILTSTONE - light to medium grey; fine to medium grained; abundance of fossil fragments; calcareous; numerous narrow (.65 cm) interbeds of mudstone; (mudstone from 71.32 - 72.2).)
132.28 - 133.12	0.84	MUDSTONE - dark grey; slightly silty; plant fossils common along bedding.
133.12 - 135.33	2.21	MISSING CORE (records show the Phalen roof to be composed of a slightly silty, hard shaly mudstone.)
135.33 - 137.33	2.00	PHALEN SEAM
137.33 - 137.53	0.20	MISSING CORE (records indicate the Phalen floor to be composed of a grey siltstone seatearth, slightly argillaceous; disseminatated pyrite common; competent.)

DEPTH.(m)	THICKNESS (m)	DESCRIPTION
137.53 - 151.85	14.32	INTERBEDDED MUDSTONE-SILTSTONE - light to medium grey; siltstone is medium to coarse grained; entire unit is very silty; few plant fossils noted; calcareous fragments throughout; slightly micaceous; gradational lower contact; coal seam noted from 150.63 - 150.85; limestone noted at (151.06 - 151.18); unit is competent.
151.85 - 154.93	3.08	SILTSTONE - medium grey; fine grained; plant fossils absent; non calcareous; non micaceous; slightly crossbedded; gradational lower contact; competent.
154.93 - 160.51	5.58	MUDSTONE - medium grey; very silty; localized listric planes throughout; calcareous pods; few plant fossils noted; gradational lower contact; slightly competent. - Coal noted at 155.75 - 155.87, 158.13 - 158.19 - limestone noted at 159.01 - 159.19.
160.51 - 161.85	1.34	SILTSTONE - refer to 151.85 - 154.93 for description.

END OF HOLE

SECTION AND SAMPLING RECORD

SEAM: PHALEN

DEPTH 135.33m
(444')

BOREHOLE B-163

DATE: 1981-03-03

Logged by: S.V. Forgeron
F.M. Isenor

TOTAL HEIGHT	INTERVAL (METRE)	MEGASCOPIC DESCRIPTION OF SEAM INTERVALS	SAMPLE	
			NO.	THICKNESS (METRE)
		ROOF: Composed of slightly silty, hard shaly mudstone. Plant fossils common along bedding.		
		TOTAL SEAM THICKNESS 2.00 m RECOVERED 0.775 m (38.6%)		
1.40	1.40 m	LOST CORE ZONE: 17.8 cm coal recovered Broken: Bright Ankerite common along cleat. Ply probably represents composite of lost core zone No pyrite observed. One piece 2 cm thick composed of splint.	1	1.40 m
1.55	0.15	Bright banded coal Well developed cleat contains one 2 mm pyrite band Fusain common along bedding Contain one 1 cm durain band	2	0.15m

B-163

TOTAL HEIGHT	INTERVAL (METRE)	MEGASCOPIC DESCRIPTION OF SEAM INTERVALS	SAMPLE NO.	SAMPLE THICKNESS (METRE)
1.70	0.15	Intermediate to bright banded coal. Contains two 1 cm thick durain bands. First is 2 cm from top of ply Second is 10 cm from top of ply Some fusain along bedding containing pyrite	3	0.15 m
1.85	0.15	Bright banded coal. Some ankerite along cleat. Fusain quite common in sample and locally the fusain is soaked with pyrite.	4	0.15 m
2.00	0.15	Intermediate to Bright banded coal Contains a 2 cm splint band 10 cm above floor; contains 5mm shale band immediately under splint band Ankerite common along cleat; Contains some fusain locally soaked with pyrite. Pavement: Grey siltstone seatearth, slightly argillaceous. Dissemintated pyrite common. Hard	5	0.15 m

APPENDIX B

EVALUATION OF EFFECTS OF CURRENT BLASTING PRACTICES ON ROCK FRACTURING IN THE LINGAN MINE

March 1987

861-1290

B.1 INTRODUCTION

It is important to define the extent of all cracks produced in the blasting process in order to define their limit concerning overbreak in a given blasting configuration.

Previous experience in underground mines has indicated that it is possible to preshear/postshear in the direction of the major stress field (generally horizontal), but very difficult to extend a shear fracture perpendicular to this stress field. High horizontal stresses tend to squeeze cracks oriented in the vertical direction and begin to propagate them in the horizontal direction. Under blasting conditions, such cracks can migrate for substantial distances and ultimately form failure envelopes to any major contact thus defining a detachment zone. In stratified materials, the zones of detachment are usually well defined by individual layering even within a given stratification layer. The tendency of blasting operations is to extend existing failure planes and provide the vibrational displacements to precipitate detachment.

Using the SHEAR4.BST program (proprietary blast simulation program developed by Du Pont) it was possible to simulate the current conditions, including both the geological conditions and blasting pattern including blast hole locations, orientations (as drilled) and explosive loading found at Lingan Mine. The computer runs were completed using a set of both fixed and variable parameters. The uniqueness of the SHEAR4.BST program is such that it can interpret the effects of geology on computer output. A range of values for a given geological condition can be plotted and interpreted.

It should be mentioned here that only the sandstone was evaluated from both a computer simulation and field measurement standpoint.

The following geological conditions for Lingan Mine were used in the blast simulation analyses:

Sandstone Rock Properties:

Young's Modulus :	30 GPa (4.4 x 10^6 psi)
Bulk Modulus :	15.8 GPa (2.3 x 10^6 psi)
Poisson's Ratio :	0.18
Tensile Strength:	6.9 MPa (1000 psi)
Geological Index:	0.51
In situ Stress Ratio :	(variable)

Explosive Loading Data:

Depth of Boreholes:	1.1 m (3.6 ft.)
Borehole Diameter :	38 mm (1.5 in.)
Collar (Burden) :	0.7 m (2.3 ft.)
Charge Length :	0.4 m (1.3 ft.)
Explosive Loading :	0.46 kg. (1.0 lb.) (per hole)
Delay Usage :	Usually 3 periods (5-7 lb/ delay)

The effects of overbreak, decoupled cracking radius, coupled cracking radius and interpattern cracking radius were examined by varying the geological index (GI), burden distance (BD), tensile strength (T), and the stress ratio (SR). All of these terms, in conjunction with other computer outputs, are defined in section B.3 (definition of terms).

B.2 RESULTS OF ANALYSIS

Approximately 50 computer simulations were completed using the SHEAR4.BST program to examine the effects of the specific parameters on the distribution of cracks around a geometric configuration that represented the Lingan blasting conditions. For the most part, the rock properties given for sandstone were used.

The parameters tested were:

(1)	geological index	(GI)
(2)	burden distance	(BD)
(3)	tensile strength	(T)
(4)	in situ stress ratio	(SR)

The following output parameters were plotted:

(1)	overbreak	(OBK)
(2)	confined cracking radius	(CCK)
(3)	burden distance	(BD)
(4)	decoupled cracking radius	(DCK)
(5)	interpattern cracking radius	(INT)

The results of the analyses are presented in Figure B.1 to B.6. The fixed and variable parameters used are summarized below.

Figure	Fixed Parameters	Variable Parameters
B.1	GI, T, BD	SR
B.2	GI, BD, SR	TS
B.3	GI, T, SR	BD
B.4	BD, T, SR	GI
B.5	GI, T, SR	BD
B.6	GI, T, SR	BD

Each of the plots are presented and discussed in the following sections.

Effects of Insitu Stress Ratio (Figure B1):

For this plot, GI/BD/T were fixed and SR was variable. From the plot, it can be seen that the maximum extent of cracking considering a totally confined state (CCK) is about 0.59 m (1.93 ft.). However, the decoupled cracking radius (DCK) with an SR of 1 is about 0.4 m (1.32 ft.) illustrating the effect of a decoupled charge for the same geometric and confinement configuration. The SR strongly affects the extent of cracking especially in the direction of the major stress field. At an SR=2, it can be seen that the decoupled cracking radius extends out to the limit of a confined charge (in the direction of the major stress field). Overbreak with this charge geometry appears to be always significant considering the pattern size. Interpattern cracking appears to be consistent with the burden since at SR=2, cracking is roughly equal to the pattern size.

Effects of Tensile Strength of Rock (Figure B2):

For this plot, GI/BD/SR are fixed, with T made variable. From this plot the strong influence of tensile strength (T) is shown. It is noted that both the confined cracking radius (CCK) as well as the decoupled cracking radius (DCK) are affected. Overbreak is still extensive with this charge configuration which would indicate that such a configuration would not be appropriate for perimeter blastholes. At T = 6.8 MPa (1000 psi), interpattern cracking (INT) again approaches the pattern size.

Effects of Burden Distance - GI = 0.1 (Figure B3):

For this plot, GI/T/SR are fixed, with BD variable. It should be noted that both the confined cracking radius (CCK) and the decoupled cracking radius (DCK) are not sensitive because of their dependence on tensile strength (T) and geological index (GI). At a BD = 0.76 m (2.5 ft) there is substantial interpattern cracking (INT) to provide breakout with approximately 0.33 m (1.1 ft.) of overbreak (OBK) which may be detrimental near the perimeter. The geological index reflected homogeneous conditions (GI = 0.1) with still enough energy for breakout. This run was repeated in Figure C6 using a geological index equal to 0.51 (generally used for sedimentary rock) to represent the Lingan sandstone condition.

Effects of Geological Index of Rock (Figure B4):

For this plot, BD/T/SR are fixed, with GI variable. From this plot, all output are sensitive particularly considering the confined cracking radius (CCK) and the decoupled cracking radius (DCK). At GI = 0.51 overbreak would still be considered to be excessive especially near the perimeter of the blast configuration. Again the interpattern cracking radius (INT) appears to breakout within the pattern dimensions.

Effects of Burden Distance - GI = 0.5 (Figure B5):

For this plot, essentially a repeat of Figure B4, GI/T/SR are fixed, with BD variable. From this plot, a change of the geological index (GI) from GI = 0.1 to GI = 0.51 has increased the confined cracking radius (CCK) and the decoupled cracking radius (DCK) from 0.4 m (1.3 ft.) and 0.37 m (1.22 ft.) to 0.6 m (1.92 ft.) and 0.59 m (1.87

ft.) respectively. Both overbreak (OBK) and interpattern cracking radii (INT) are strongly affected. For this material type (sandstone), the blasting configuration is such that it may be overblasted with the result of producing unacceptable overbreak.

Effects of Burden Distance - Reduction in Explosive Charges (Figure B6):

This plot is a duplicate of Figure B5 with the charge rate reduced from 0.45 kg (1 lb) per hole to 0.23 kg (0.5 lb) per hole. From the graph it can be seen that the overbreak (OBK) has been substantially reduced from a maximum of 0.44 m (1.45 ft.) (see Figure C5) at a burden distance (BD) of 0.85 m (2.8 ft.) to a maximum of 0.27 m (0.9 ft.) (see Figure B5) for the same burden distance. The interpattern cracking radius (INT) is also correspondingly lower. It is noted that a reduced change weight will definitely reduce overbreak into the perimeter region.

From the above computer simulations, it appears that the current blasting configuration (pattern) used at Lingan may not match the rock type as the results indicate that excessive overbreak would occur. There does not seem to be procedures in place that will protect the perimeter. Unfortunately, if poor blasting practices are followed repetitively, an inherited condition will exist with all other environmental aspects simply becoming additive or superimposed on an already undesirable condition.

B.3 DEFINITION OF TERMS (COMPUTER ANALYSIS)

The following terms are defined with reference to the results of the SHEAR4.BST computer analyses presented in Figures B1 to B6:

Dynamic Tensile Rock Strength (T) - tensile breaking strength of a specific rock type - (in psi)

Ratio of Stress Field (SR) - the ratio of horizontal stress to vertical stress as found in underground and/or surface mining operations.

Average Dynamic Compressive Strength - compressive breaking strength of a specific rock type calculated from tensile strength value and includes effects of geological index (psi).

Geological Index (GI) - combines the static/dynamic bulk modulus and Young's modulus into a value that reflects the geology of a specific rock type. For sedimentary rock GI = 0.5.

Confined Crack Radius (CCR) - maximum cracking radius obtained from an explosive charge having a specific energy and geometric configuration, under infinite burden conditions (no free faces present) and no influence of all environmental effects (in situ stresses).

Cracking Radius - Interpattern (INT) - maximum cracking radius obtained from explosive charges having a specific energy and geometric configuration, with free faces present and all environmental effects included (insitu stress ratio). Also includes the effects of an adjacent loaded borehole (same configuration). Direction of cracking is toward free face and in direction of major stress field.

Decoupled Crack Radius (DCK) - similar to confined crack radius except it includes the effects of decoupled charges only under infinite burden conditions (no free faces present) and includes also the effects of environment (insitu stress ratio).

Overbreak (OBK) - extent of cracking behind borehole and away from free face. Usually the direction of cracking follows the major stress field. Includes effects of free faces, environment and adjacent similar loaded boreholes.

Burden Distance (BD) - maximum burden distance between rows or adjacent boreholes and/or free face.

Borehole Collar Height - collar height of borehole determined from percentage of column loaded value.

EVALUATION OF CRACKING RADII BASED ON CURRENT BLASTING PATTERN USED IN LINGAN MINE

FIGURE B1

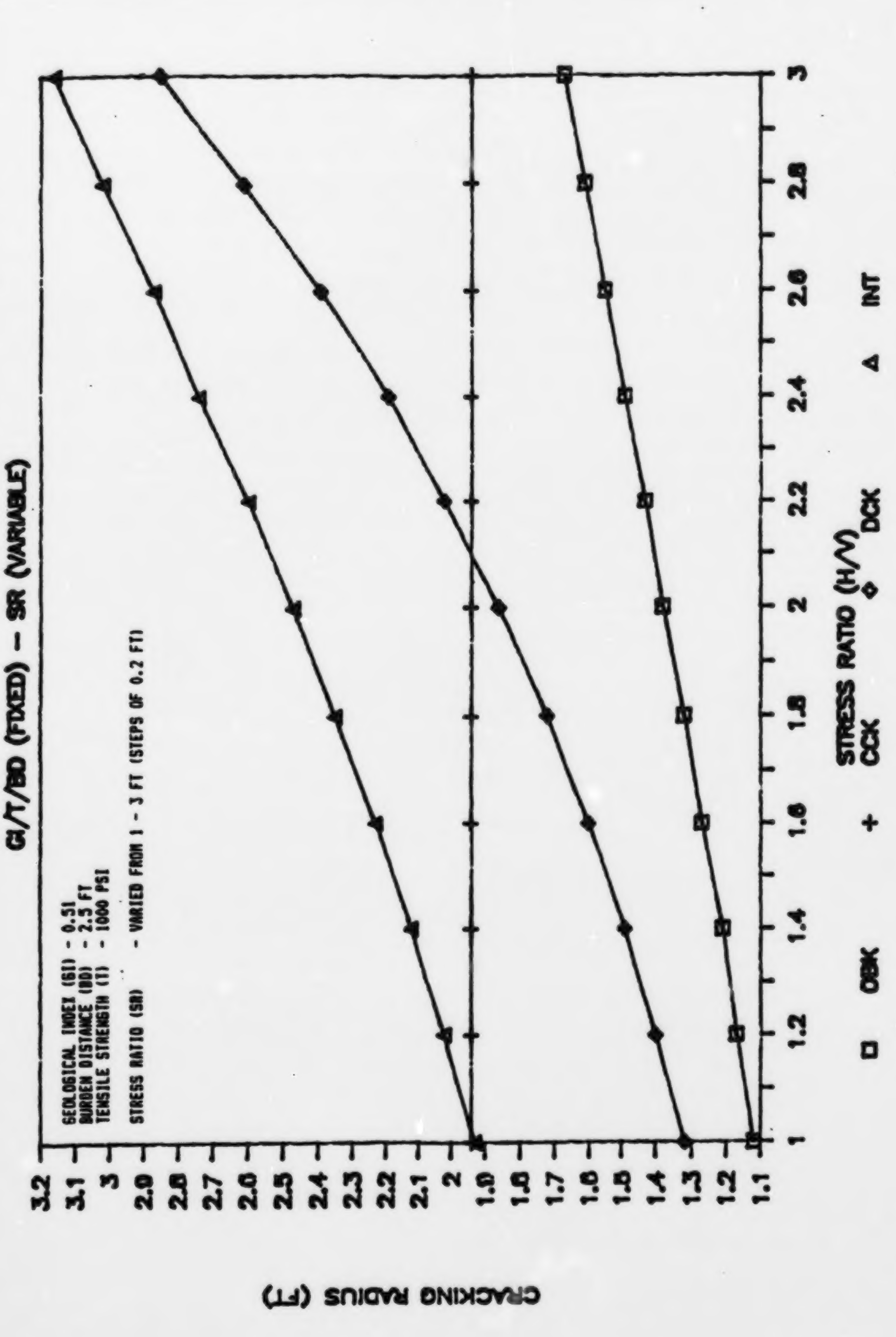

NOTE 1 - PLOT PREPARED BY DUPONT. RESULTS OBTAINED BY USING SHEAR 4 PROGRAM

Date AUG. 11, 1987
Project 861-1290

Golder Associates

Drawn LL
Chkd.

EVALUATION OF CRACKING RADII BASED ON CURRENT BLASTING PATTERN USED IN LINGAN MINE

FIGURE B2

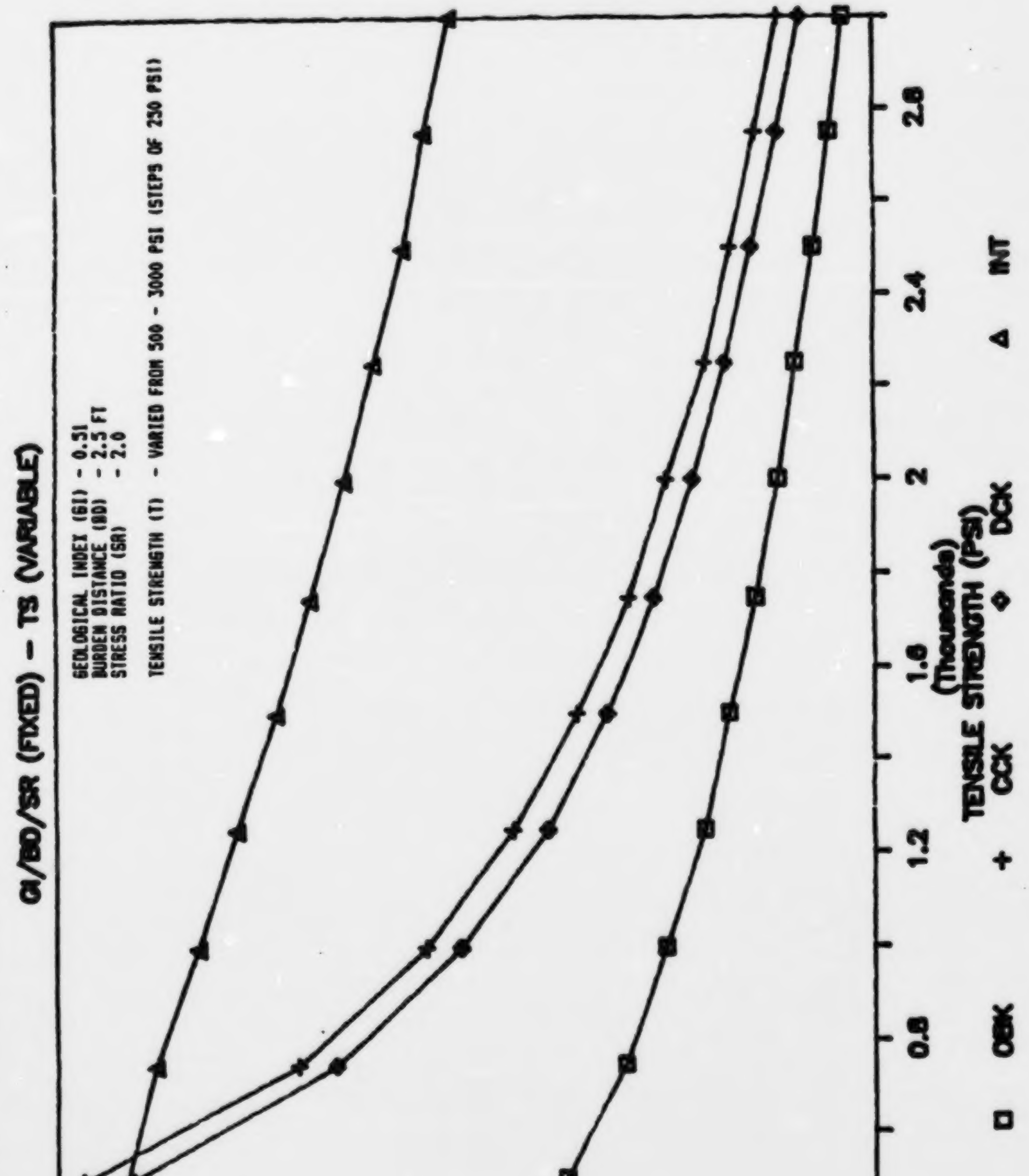

NOTE : - PLOT PREPARED BY DUPONT . RESULTS OBTAINED BY USING SHEAR 4 PROGRAM

Date AUG. 11, 1987

Project 861-1290

Golder Associates

Drawn LL

Chkd.

EVALUATION OF CRACKING RADII BASED ON CURRENT BLASTING PATTERN USED IN LINGAN MINE

FIGURE B3

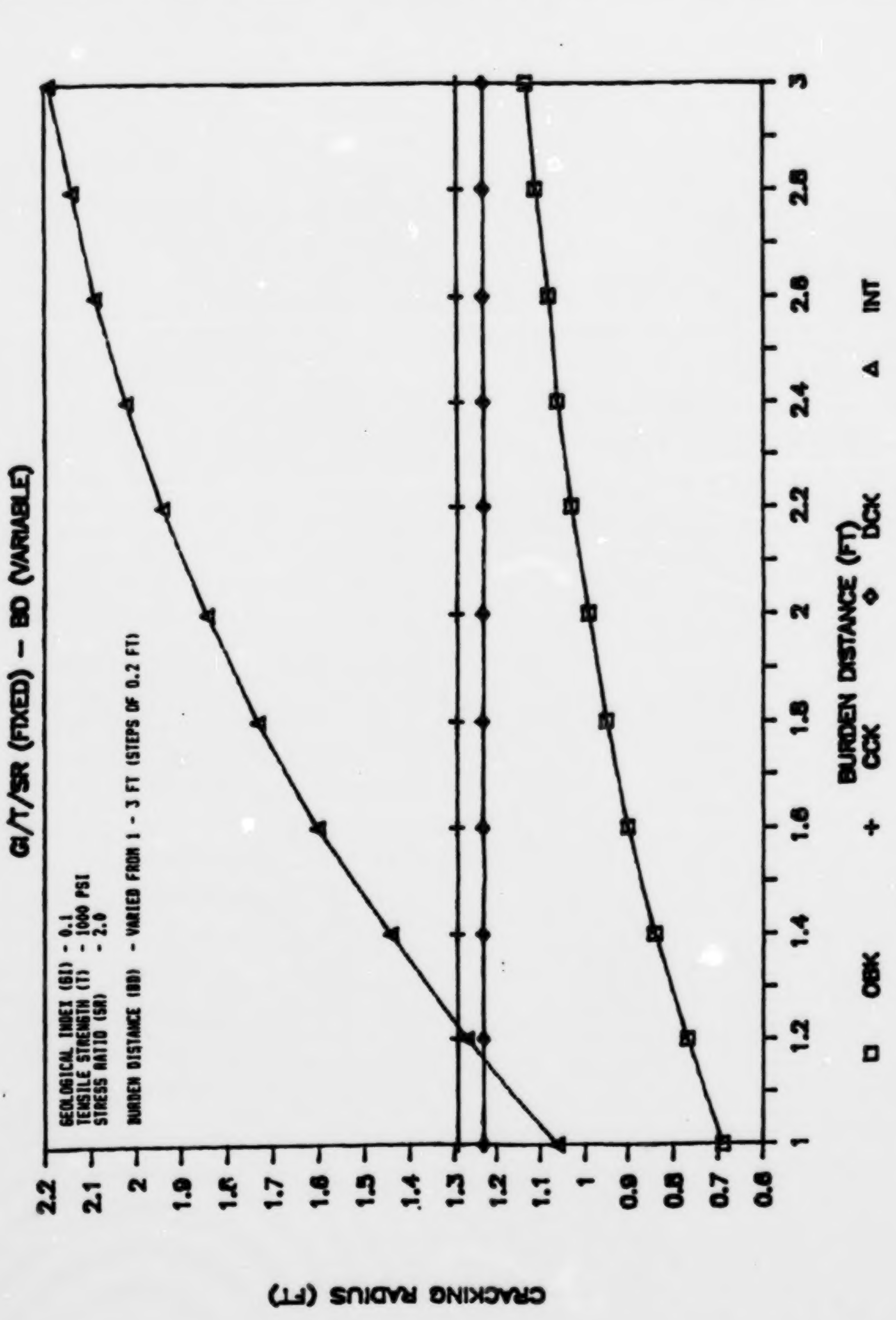

NOTE : - PLOT PREPARED BY DUPONT. RESULTS OBTAINED BY USING SHEAR 4 PROGRAM

Date AUG. 11, 1987
Project 861-1290

Golder Associates

Drawn L L
Chkd. CJ

EVALUATION OF CRACKING RADII BASED ON CURRENT BLASTING PATTERN USED IN LINGAN MINE

FIGURE B4

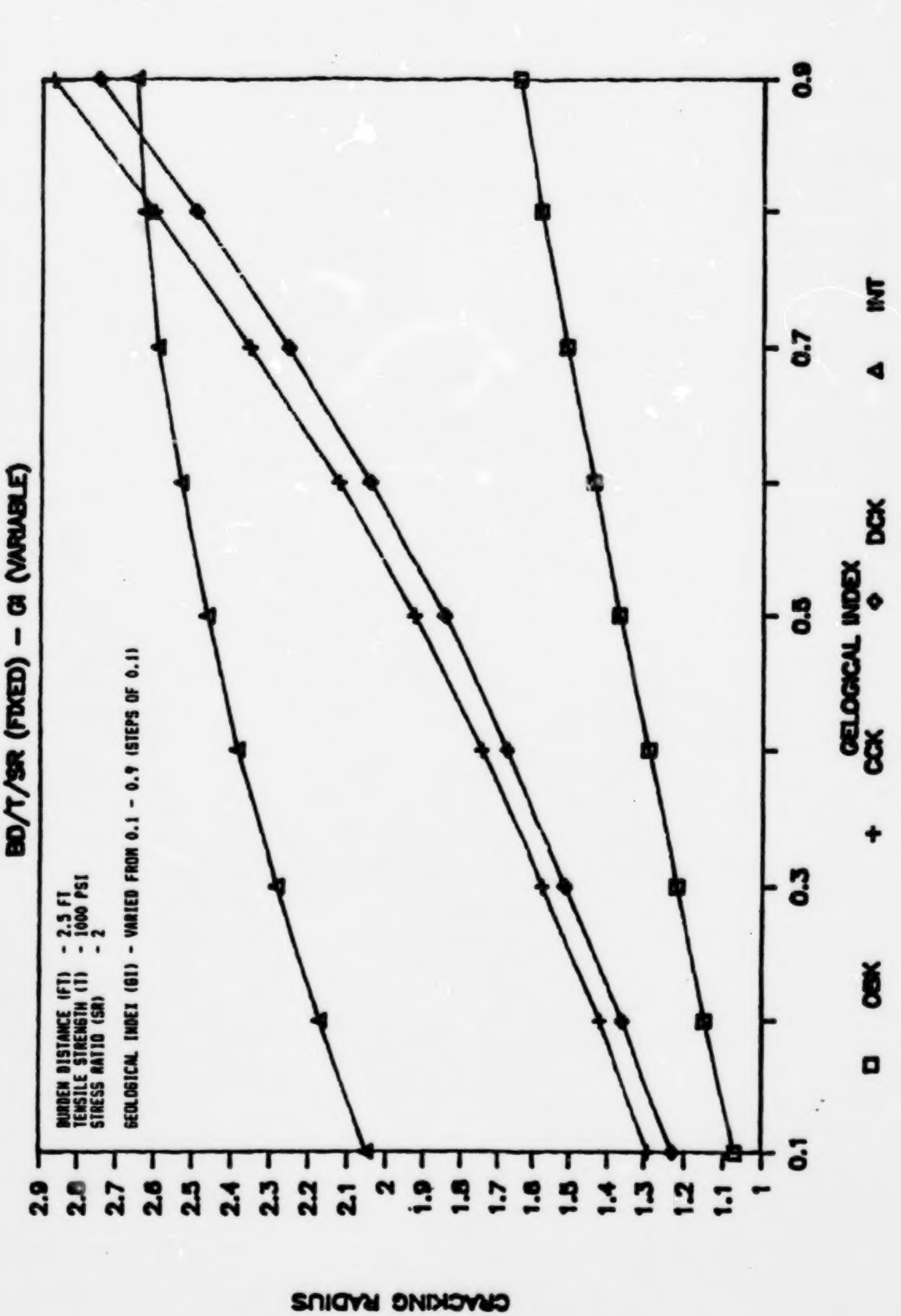

NOTE : - PLOT PREPARED BY DUPONT. RESULTS OBTAINED BY USING SHEAR 4 PROGRAM

Date AUG. 11, 1987
Project 861-1290

Golder Associates

Drawn LL
Chkd.

EVALUATION OF CRACKING RADII BASED ON CURRENT BLASTING PATTERN USED IN LINGAN MINE

FIGURE B5

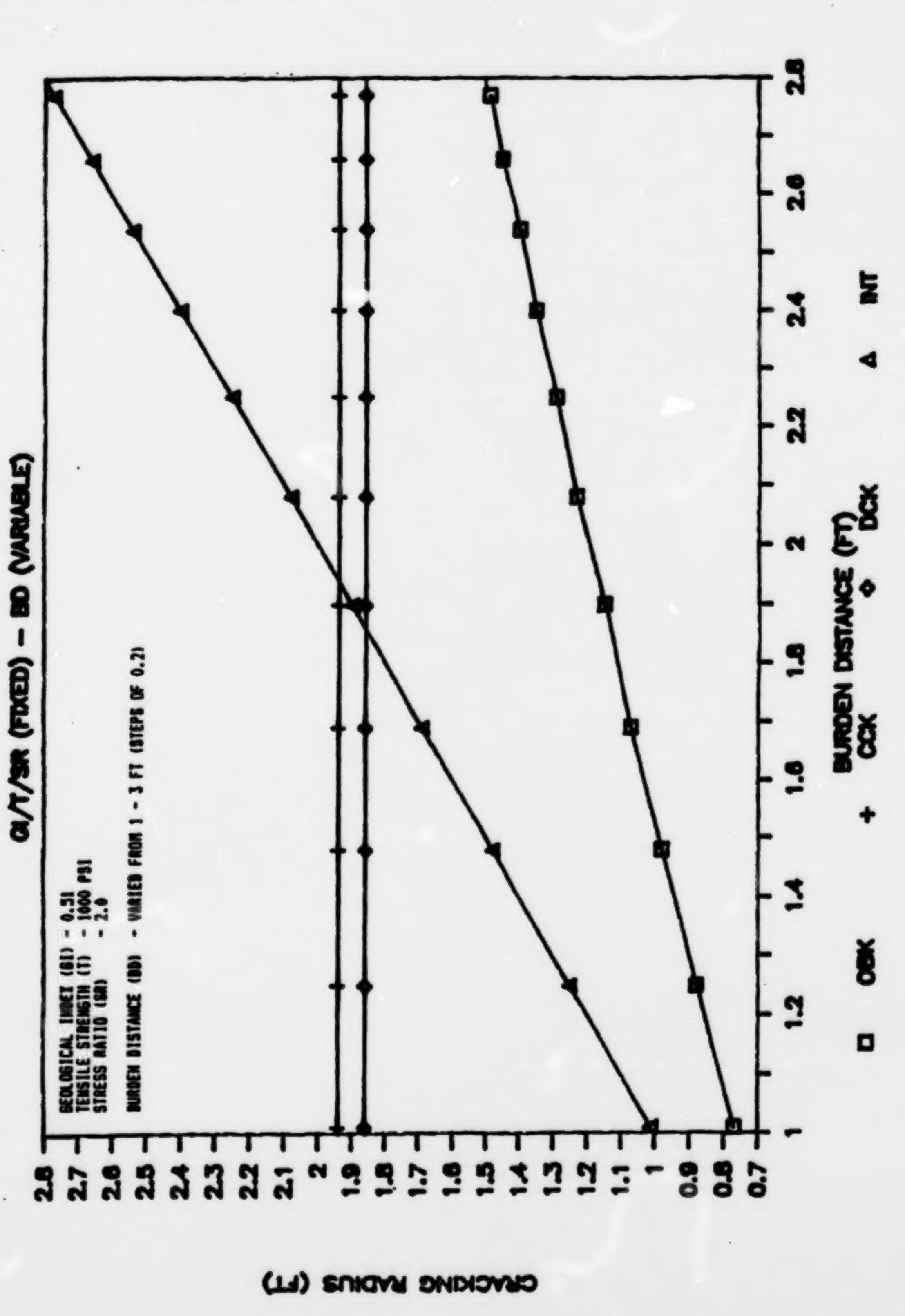

NOTE : - PLOT PREPARED BY DUPONT . RESULTS OBTAINED BY USING SHEAR 4 PROGRAM

Date AUG. 11, 1987
Project 861-1290

Golder Associates

Drawn L L
Chkd.

EVALUATION OF CRACKING RADII BASED ON CURRENT BLASTING PATTERN USED IN LINGAN MINE

FIGURE B6

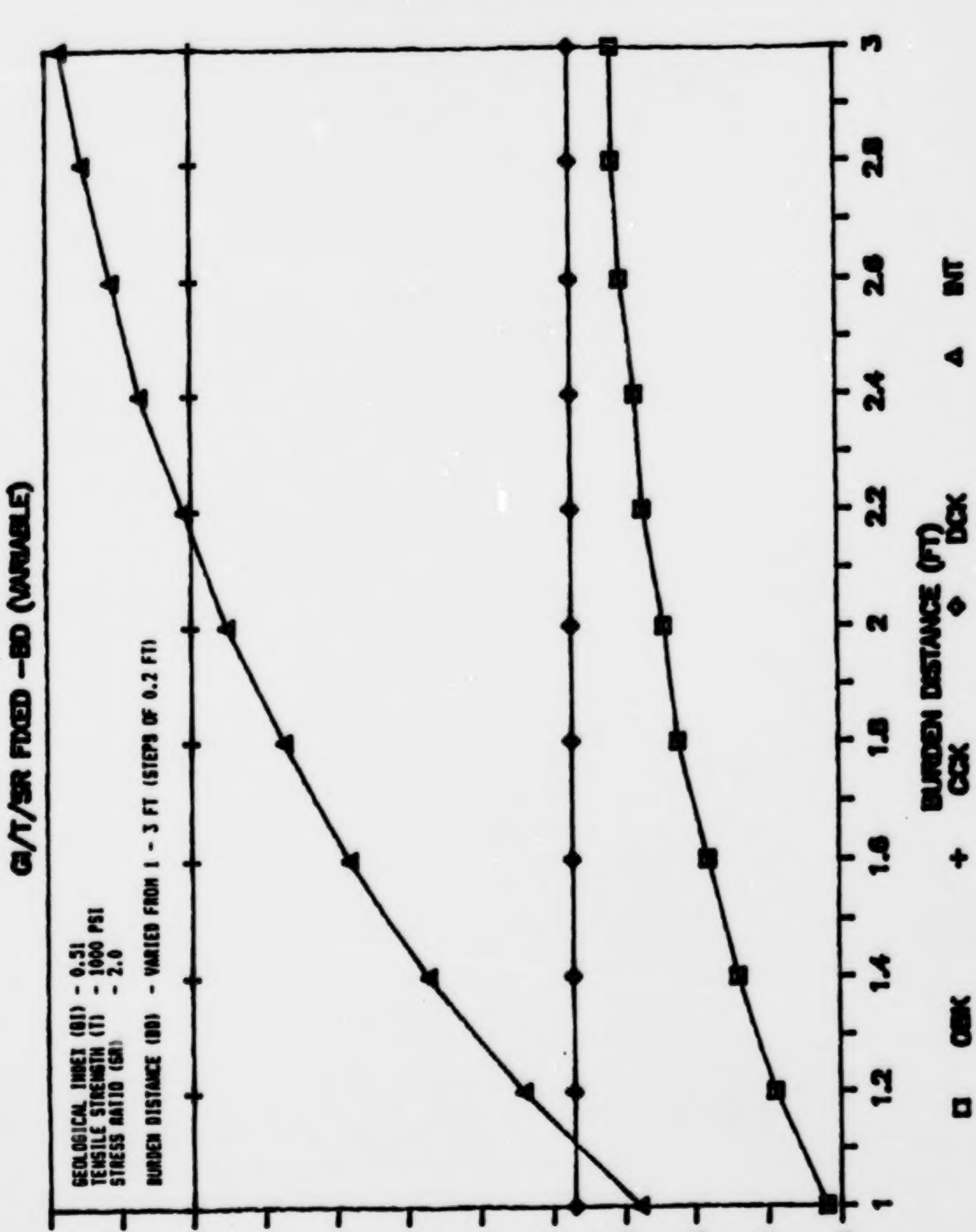

NOTE 1 - PLOT PREPARED BY DUPONT. RESULTS OBTAINED BY USING SHEAR 4 PROGRAM

Date AUG. 11, 1987
Project 861-1290

Golder Associates

Drawn L L
Chkd.

REPORTED AT NO. 26 COLLIERY, SYDNEY COALFIELD, N.S.

EVENT NO.	DATE	LOCATION	TYPE OF DRIVEAGE	DIRECTION OF DRIVEAGE	TRIGGER MECHANISM	ARCHES DOWN OR DAMAGED	ROCK TYPE EJECTED	BURST ACCOMPANIED BY GAS	VOLUME OF GAS (m^3)	POSITION OF BURST	APPROX. DIMENSIONS OF CAVITY (m) L x W x H	ESTIMATED VOLUME OF CAVITY m^3	HT OF SANDSTONE ABOVE COAL (m)	ADVANCE SINCE LAST FALL (m)	DISTANCE TO NEAREST ROADWAY/WALL	ELEVATION BELOW SEA LEVEL
1	Summer 77	13 North Material Level	Development	West	?	?	Sandstone	?	?	?	?	?	1.8	?	120(D)/W24	703
2	Jan 5-78	13 North Coal Road	Development	West	Shooting at face	2 damaged	Sandstone	Unknown	-	above face	0.9 x 4.3 x 1.2	5	.609	?	91.44(D)/W304.8 12N	737
3	Jan 23-78	13 North Coal Road	Development	West	Shot in coal and stone	0	Sandstone	No gas reported	-	above face	1.8 x 4.26 x 3.05	24	0 (on coal)	?	91.44(D)/W304.8 12N	735
4	Jan 25-78	13 North Coal Road	Development	West	Shot in coal and stone	0	Sandstone	No gas reported	-	above face	1.8 x 4.26 x 3.05	24	0 (on coal)	1.82	91.44(D)/W304.8 12N	735
5	Aug 30-78	13 South Material Level	Development	East	Shot in coal and stone	2 damaged	Sandstone	No gas reported	-	at face	4.26 x 4.57 x 1.22	23	2.13	?	85.39(D)/W182.88 12S	724
6	Sept 1-78	13 South Material Level	Development	East	Shot in stone	1 damaged	Sandstone	No gas reported	-	at face	2.74 x 4.57 x 1.22	15	1.52	4.57	92.9(D)/W182.88 12S	724
7	Sept 5-78	13 South Material Level	Development	East	Shot in coal and stone	1 damaged	Sandstone	No gas reported	-	at face	2.74 x 4.57 x 1.22	15	0.3048	2.13	95.4(D)/W182.88 12S	724
8	Sept 6-78	13 South Material Level	Development	East	Shot in coal and stone	0	Sandstone	3.5 - 5% after shooting	?	above face	.91 x 4.57 x 1.22	5	0 (on coal)	.914	96.3(D)/W182.88 12S	724
9	Sept 21-78	13 South Material Level	Development	East	Shot in coal and stone	0	Sandstone	No gas reported	-	above face	.91 x 4.57 x 1.22	5	0 (on coal)	14.93	109.73(D)/W182.88 12S	724
10	Jan 24-79	13 North Material Level	Top Brushing	West	Not recorded	0	Sandstone (1)	-	-	-	-	-	1.83	-	On Wall	703
11	Jan 30-79	13 North Material Level	Top Brushing	West	Not recorded	0	Sandstone	-	-	-	-	-	1.22	-	On Wall	703
12	Feb 8,9, 10-79	13 North Material Level	Top Brushing	West	Not recorded	0	Sandstone	No gas reported	-	-	6.09x4.26x1.83 8th 1.52 9th 3.65 10th	-	0.3048	-	On Wall	703
13	Oct 23-80	Main Deep	Development	North	Shot in coal and stone	4	Sandstone	Yes, 20 min to clear	?	above face and ribs	7.62 x 5.79 x 2.4	107.6	0 (on coal)	-	45.72(D)/W396.24 13N 13S	782
14	Oct 30-80	Main Deep	Development	North	Shot in stone	12	Sandstone	Yes, 5% after shooting, 0.5% end of shift	?	above face and ribs	10.66 x 6.09 x 2.74	178	0 (on coal)	6.09	45.72(D)/W396.24 13N 13S	782
15	Mar 5-81	14 North Coal Road	Development	West	Shot in coal	0	Sandstone and coal	Yes 3%, 5 min to clear	?	ahead of face and ribs	L x H = 2.39 m^3 W = 4.26 m	10	0 (on coal)	first	47.24(D)/W335.28 13N	777
16	Mar 9-81	14 North Coal Road	Development	West	Shot in coal and stone	0	Sandstone	Yes, 4% after shooting	?	at face	Included above	Included above	0 (on coal)	2.13	49.37(D)/W335.28 13N	777
17	Mar 23-81	14 North Coal Road	Development	West	Shot in coal and stone	4 down	Sandstone	Yes +5%, 25 min to clear	?	at face	L x H = 3.45 m^3 W = 2.66 m	9	0 (on coal)	2.13	51.51(D)/W335.28 13N	777
18	Mar 25-81	14 North Coal Road	Development	West	Not recorded initiation	0	Sandstone	Unknown, not recorded	?	above face	Included above	Included above	0 (on coal)	0	51.51(D)/W335.28 13N	777
19	Apr 3-81	14 North Coal Road	Development	West	Unknown	0	Sandstone	No gas reported	-	above face	L = 1.76 m W x H = 2.75 m^3	5	0 (on coal)	5.48	57.30(D)/W335.28 13N	777
20	Apr 7-81	14 North Coal Road	Development	West	Unknown	0	Sandstone	No gas reported (2)	-	above arch	L x H = 0.276 m^3 W = 4.26 m	1	0 (on coal)	3.05	60.35(D)/W335.28 13N	777

18	Mar 25-81	14 North Coal Road	Development	West	Not recorded initiation	0	Sandstone	Unknown, not recorded	?	above face	Included above	Included above	0 (on coal)	?	51.51([illegible])/W335.28 13N	777
19	Apr 3-81	14 North Coal Road	Development	West	Unknown	0	Sandstone	No gas reported	-	above face	L = 1.76 m W x H = 2.75 m^3	5	0 (on coal)	5.48	57.30(D)/W335.28 13N	777
20	Apr 7-81	14 North Coal Road	Development	West	Unknown	0	Sandstone	No gas reported (2)	-	above arch	L x H = 0.276 m^3 W = 4.26 m	1	0 (on coal)	3.05	60.35(D)/W335.28 13N	777
21	Apr 14-81	14 North Coal Road	Development	West	Shot in stone	0	Sandstone	Yes 5%, 15 min to clear	?	at face	L x H = 4.26 m^3 W = 8.53 m	37	0 (on coal)	6.70	66.44(D)/W335.28 13N	777
22	Apr 27-81	14 North Coal Road	Development	West	Shot in coal and stone	Unknown	Sandstone	Yes 5%, 10 min to clear	?	at face	L = 1.82 m W x H = 14.40 m^3	27	0 (on coal)	7.90	65.88(A)/W335.28 13N	777
23	May 4-81	14 North Coal Road	Development	West	Shot in coal	1 damaged	Sandstone	Yes 5%, 20 min to clear	?	at face	L X H = 7.04 m^3 W = 6.70 m	43	0 (on coal)	4.26	61.13(A)/W335.28 13N	777
24	May 7-81	14 North Coal Road	Development	West	NIL (3)	1 damaged	Sandstone	Yes 3%, 45 min to clear	?	at face	L x H = 11.13 m^3 W = 6.62 m	67	0 (on coal)	2.44	52.42(A)/W335.28 13N	777
25	May 12-81	13 North Airway	Development	South	Shooting	0	Sandstone	Yes, 2-2.4% after shooting	?	-	?	?	0.6	-	24.38(D)/W51.81 13N	741
26	May 14-81	14 North Coal Road	Development	West	Shot in coal	2 down 2 damaged	Sandstone	Yes 5%, 40 min to clear	?	at face	L X H = 15.27 m^3 W = 5.25 m	81	0 0.4	4.26	48.16(A)/W335.28 13N	777
27	June 6-81	14 North Coal Road	Development	West	Shot in coal	2 damaged	Sandstone	Yes 5%, 35 min to clear	?	at face	L = 4.57 m W x H = 4.39 m^3	20	1.04	6.09	42.67(A)/W335.28 13N	777
28	June 10-81	14 North Airway	Development	North	Shot in coal and stone	3	Sandstone	Yes 5%, 15 min to clear	?	above face	4.57 x 4.26 x 3.04	59	1.52	first	48.78(14NCR)/W274.32 13N	776
29	June 19-81	14 North Coal Road	Development	West	Shot in coal and stone	4 down	Sandstone	Yes 5%, 20 min to clear	?	at face	L x H = 1.93 m^3 W = 5.86 m	11	1.52	7.92	34.13(A)/W335.28 13N	776
30	June 26-81	14 North Coal Road	Development	West	Shot in stone	3 down	Sandstone	Yes 5%, 20 min to clear	?	at face	L = 2.74 m W x H = 9.89 m^3	27	1.52	3.05	31.08(A)/W335.28 13N	776
31	July 14-81	14 North Airway	Development	North	Shot in stone	2 down	Sandstone	Yes 5%, 15 min to clear	?	above face	3.05 x 4.26 x 2.44	32	.91	17.68	30.48(14NCR)/W289.56 13N	776
32	Nov 10-81	14 North Coal Road	Development	West	Shot in coal	0	Sandstone	Yes 5%, 25 min to clear	?	above face	L X H = 6.49 m^3 W = 3.65 m	24	2.28	18.29	12.8(A)/W335.28 13N	776
33	Dec 7-82	Belt Deep	Development	North	Shot stone and coal	1 damaged	Sandstone	Yes, 1.[illegible]% after shooting	?	above face	2.13 x 3.65 x 2.13	17	2.28	?	30.48(D)/W228.6 14N	789
34	Jan 11-83	Belt Deep	Development	North	Shot stone and coal	0	Sandstone	Yes 2.65%, 25 min to clear	?	above face	?	14	2.28	first	48.77(D)/W243.84 14N	789
35	Jan 19-83	Belt Deep	Development	North	Shot stone and coal	7 down	Sandstone	Yes 5%, 60 min to clear	?	above face	4.57 x 4.88 x 3.05	68	1.52	?	48.77(D)/W243.84 14N	789
36	Nov 23-83	Main Deep	Development	North	Shooting	16-18 down	Sandstone	Yes, +5% after shooting	753	above face and west side rib	Variable	316	0.6 - 2.74	first	24.38(D)/W213.36 14N	789
37	Jan 6-84	Main Deep	Development	North	Shooting 12 holes in coal and ribs	15 down	Sandstone	Yes, no record	3171	above face, west & east side ribs	Variable	145	0 (on coal)	3.65	24.38(D)/W213.36 14N	790

NOTES:

1) SANDSTONE EXHIBITING CLEAVAGE CHARACTER BUT NO SERIOUS ROOF CONTROL PROBLEM.
2) 3% GAS CONCENTRATION NOTED ON MATERIAL LEVEL BY INSIDE REGULATOR DOORS ON FOLLOWING SHIFT
3) HAD 9 HOLES STEMMED WHEN BUSHING FACE CAVE IN, NO TIME TO SHOOT.

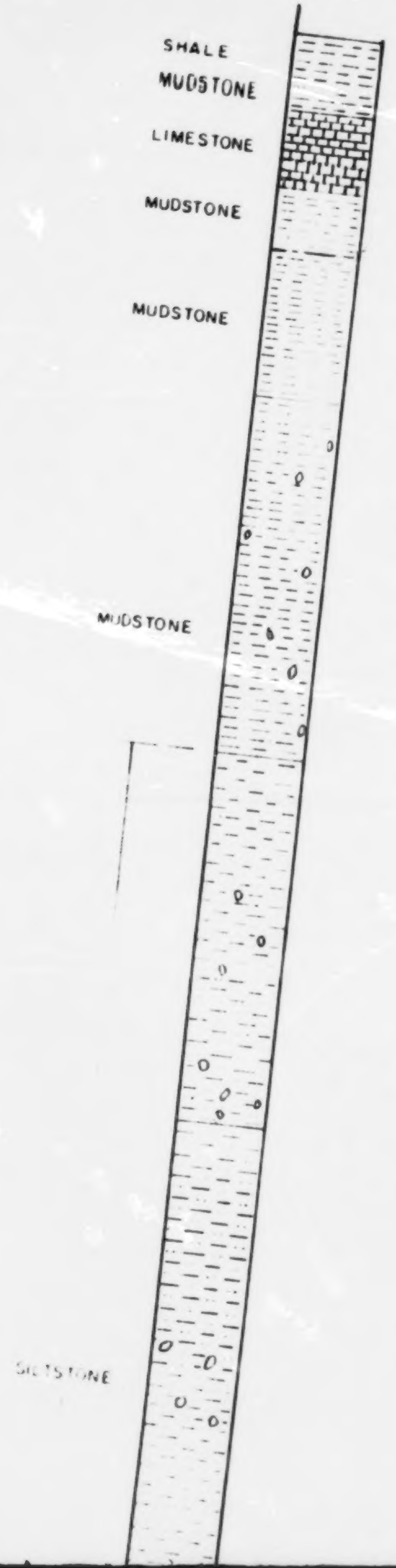
SHALE
MUDSTONE
LIMESTONE
MUDSTONE
MUDSTONE
MUDSTONE
SILTSTONE

PROJECTED TRUE SECTION
SECTION

ECTION

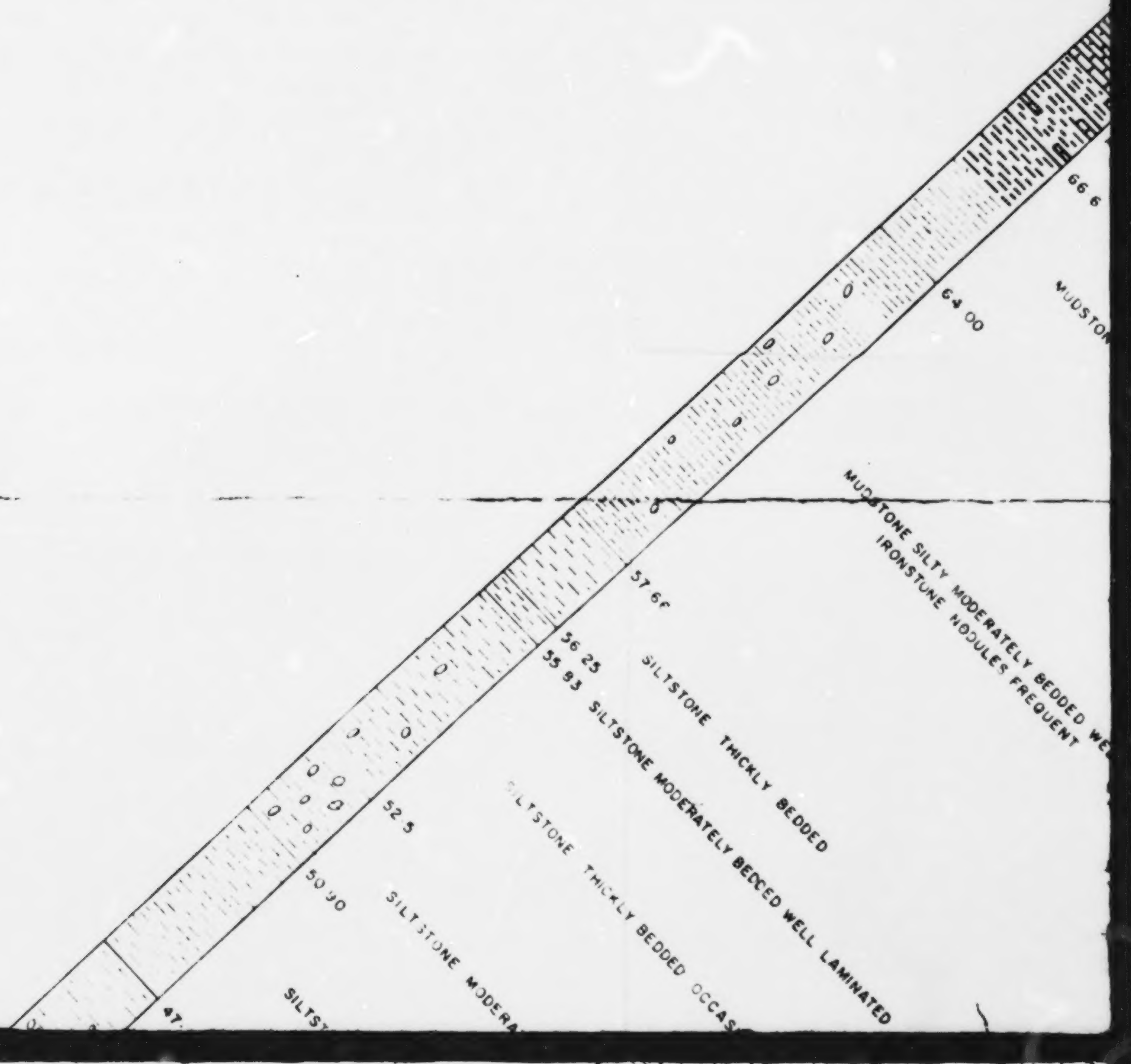

66 6
MUDSTON
64 00
MUDSTONE SILTY MODERATELY BEDDED WE
IRONSTONE NODULES FREQUENT
57 6F
56 25
SILTSTONE THICKLY BEDDED
55 93 SILTSTONE MODERATELY BEDDED WELL LAMINATED
SILTSTONE THICKLY BEDDED OCCAS
52 5
50 90
SILTSTONE MODERA
SILTST
47

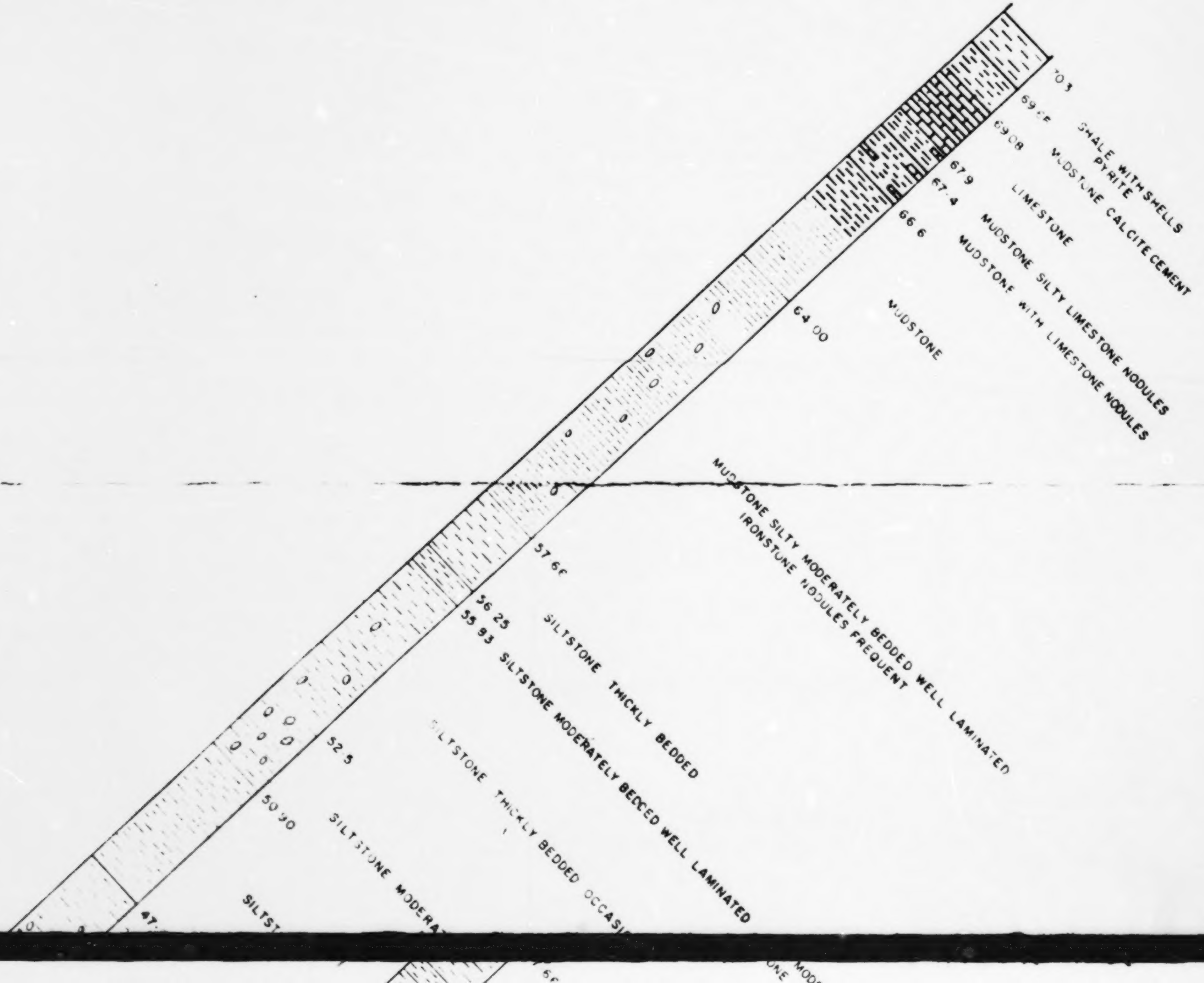
70 3
69 66
SHALE WITH SHELLS
PYRITE
69 08
MUDSTONE CALCITE CEMENT
67 9
LIMESTONE
67 4
MUDSTONE SILTY LIMESTONE NODULES
66 6
MUDSTONE WITH LIMESTONE NODULES
64 00
MUDSTONE
MUDSTONE SILTY MODERATELY BEDDED WELL LAMINATED
IRONSTONE NODULES FREQUENT
57 66
56 25
SILTSTONE THICKLY BEDDED
55 93
SILTSTONE MODERATELY BEDDED WELL LAMINATED
52 5
SILTSTONE THICKLY BEDDED OCCASI
50 90
SILTSTONE MODERAT
SILTST
47

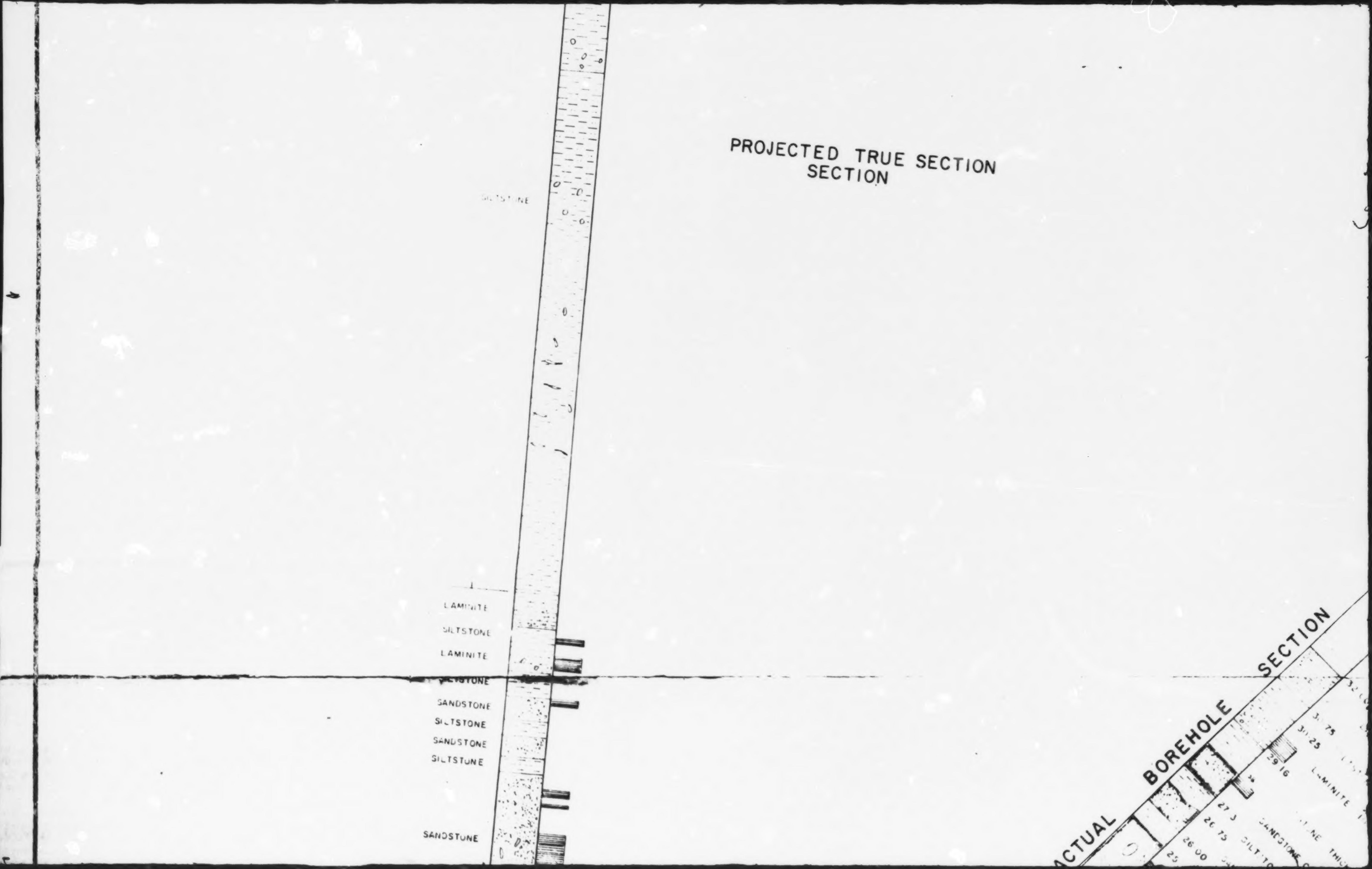
PROJECTED TRUE SECTION
SECTION
SILTSTONE
LAMINITE
SILTSTONE
LAMINITE
SILTSTONE
SANDSTONE
SILTSTONE
SANDSTONE
SILTSTONE
SANDSTONE
ACTUAL BOREHOLE SECTION
30.75
30.25
29.16
LAMINITE
27.5
26.75
26.00
25
SANDSTONE
SILTSTONE

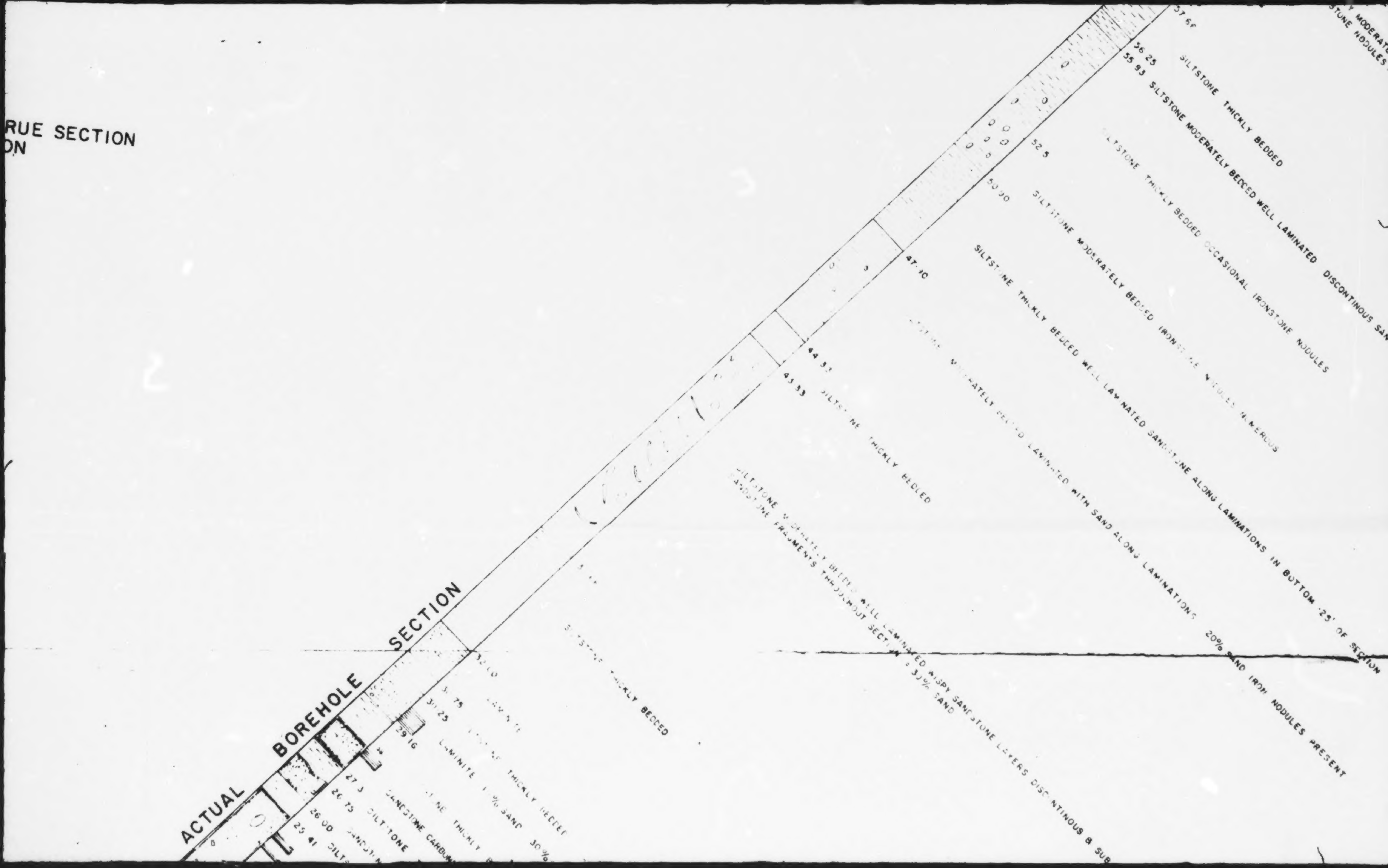
RUE SECTION
ON
ACTUAL BOREHOLE SECTION
0
25 41 SILTS
26 00 SANDSTON
26 75 SILTSTONE
27 3 SANDSTONE CARBON
STONE THICKLY B
29 16 LAMINITE 1 % SAND 30 %
30 25 STONE THICKLY BEDDED
31 75 LAMINITE
32 00
SILTSTONE THICKLY BEDDED
SILTSTONE MODERATELY BEDDED WELL LAMINATED WISPY SANDSTONE LAYERS DISCONTINOUS & SUB
SANDSTONE FRAGMENTS THROUGHOUT SECTION ≈ 30% SAND
43 33 SILTSTONE THICKLY BEDDED
44 33
SILTSTONE MODERATELY BEDDED LAMINATED WITH SAND ALONG LAMINATIONS 20% SAND IRON NODULES PRESENT
47 40
SILTSTONE THICKLY BEDDED WELL LAMINATED SANDSTONE ALONG LAMINATIONS IN BOTTOM ·25' OF SECTION
50 90
SILTSTONE MODERATELY BEDDED IRONSTONE NODULES NUMEROUS
52 5
SILTSTONE THICKLY BEDDED OCCASIONAL IRONSTONE NODULES
55 93 SILTSTONE MODERATELY BEDDED WELL LAMINATED DISCONTINOUS SAN
56 25 SILTSTONE THICKLY BEDDED
57 66
Y MODERATE
STONE NODULES

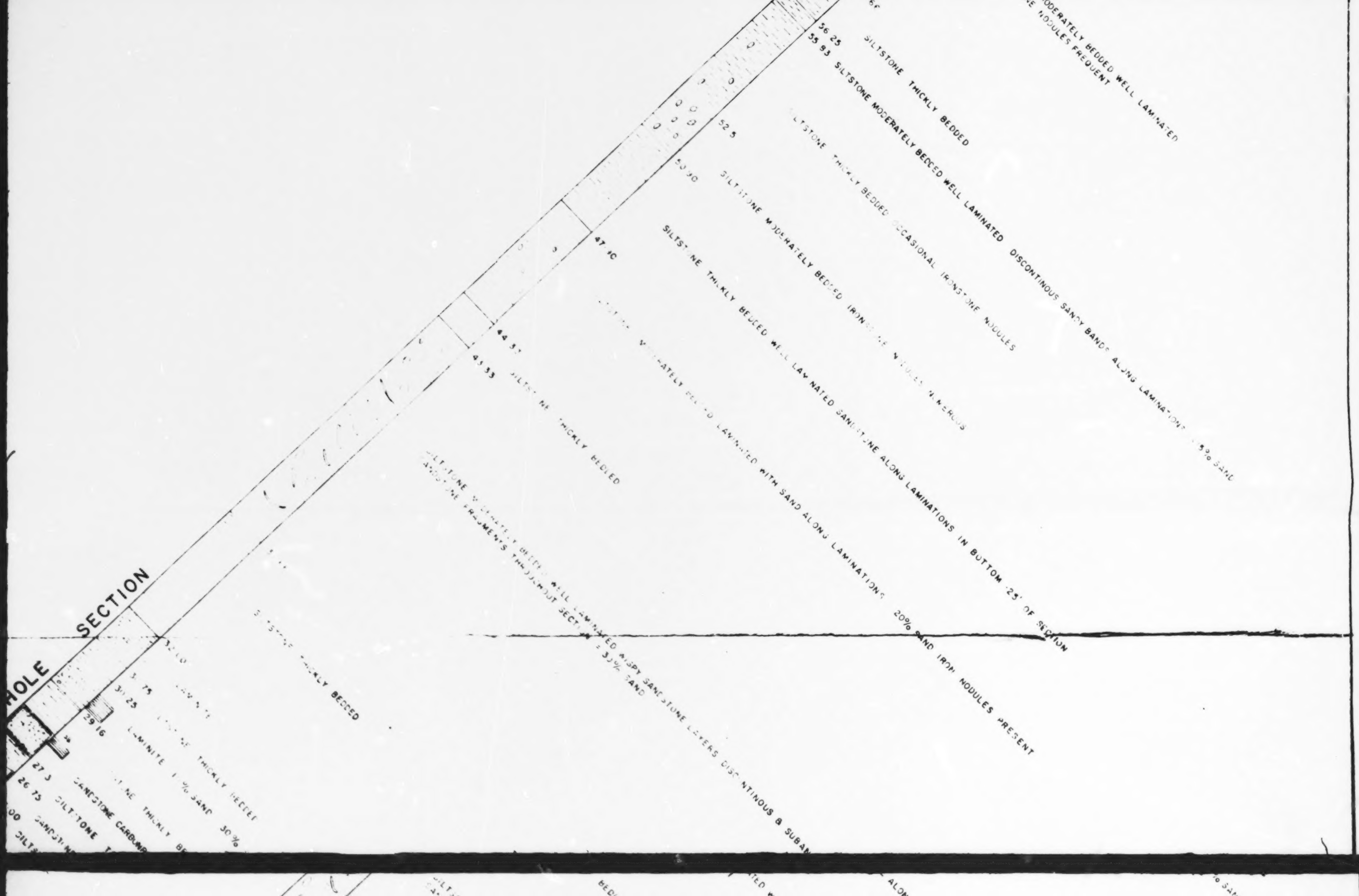
HOLE SECTION
56 25
55 93
52 5
50 90
47 40
44 33
43 33
29 16
27 3
26 75
MODERATELY BEDDED WELL LAMINATED
NE NODULES FREQUENT
SILTSTONE THICKLY BEDDED
SILTSTONE MODERATELY BEDDED WELL LAMINATED DISCONTINOUS SANDY BANDS ALONG LAMINATIONS 5% SAND
SILTSTONE THICKLY BEDDED OCCASIONAL IRONSTONE NODULES
SILTSTONE MODERATELY BEDDED IRONSTONE NODULES NUMEROUS
SILTSTONE THICKLY BEDDED WELL LAMINATED SANDSTONE ALONG LAMINATIONS IN BOTTOM 25' OF SECTION
MODERATELY BEDDED LAMINATED WITH SAND ALONG LAMINATIONS 20% SAND IRON NODULES PRESENT
SILTSTONE THICKLY BEDDED
SILTSTONE MODERATELY BEDDED WELL LAMINATED WISPY SANDSTONE LAYERS DISCONTINOUS & SUBAN
SANDSTONE FRAGMENTS THROUGHOUT SECTION 35% SAND
SILTSTONE THICKLY BEDDED
LAMINITE
SILTSTONE THICKLY BEDDED
LAMINITE % SAND 30%
SILTSTONE THICKLY BE
SANDSTONE CARBONA
SILTSTONE
SANDSTONE
SILTS

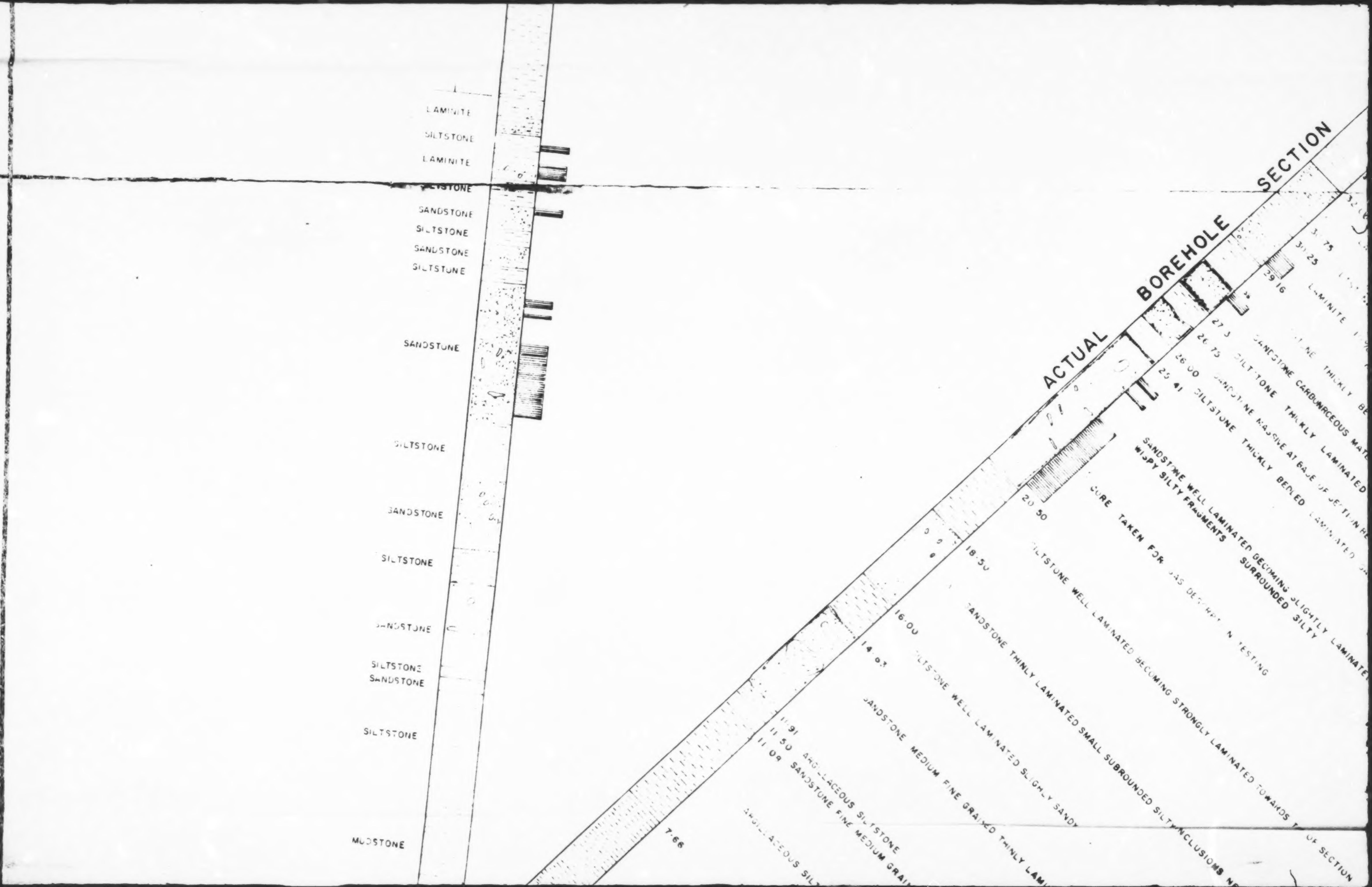
LAMINITE
SILTSTONE
LAMINITE
SILTSTONE
SANDSTONE
SILTSTONE
SANDSTONE
SILTSTONE
SANDSTONE
SILTSTONE
SANDSTONE
SILTSTONE
SANDSTONE
SILTSTONE
SANDSTONE
SILTSTONE
MUDSTONE
ACTUAL BOREHOLE SECTION
30.75
30.25
29.16
LAMINITE
THICKLY BE
27.3
SANDSTONE CARBONACEOUS MATE
26.75 SILTSTONE THICKLY LAMINATED
26.00 SANDSTONE MASSIVE AT BASE OF SECTION
25.41 SILTSTONE THICKLY BEDDED LAMINATED
SANDSTONE WELL LAMINATED BECOMING SLIGHTLY LAMINATE
WISPY SILTY FRAGMENTS SURROUNDED SILTY
20.50
CORE TAKEN FOR GAS DESORPTION TESTING
18.50
SILTSTONE WELL LAMINATED BECOMING STRONGLY LAMINATED TOWARDS TOP OF SECTION
16.00
SANDSTONE THINLY LAMINATED SMALL SUBROUNDED SILT INCLUSIONS
14.63
SILTSTONE WELL LAMINATED SLIGHTLY SANDY
SANDSTONE MEDIUM FINE GRAINED THINLY LAMI
11.91 ARGILLACEOUS SILTSTONE
11.50 SANDSTONE FINE MEDIUM GRAI
11.09
ARGILLACEOUS SIL
7.66

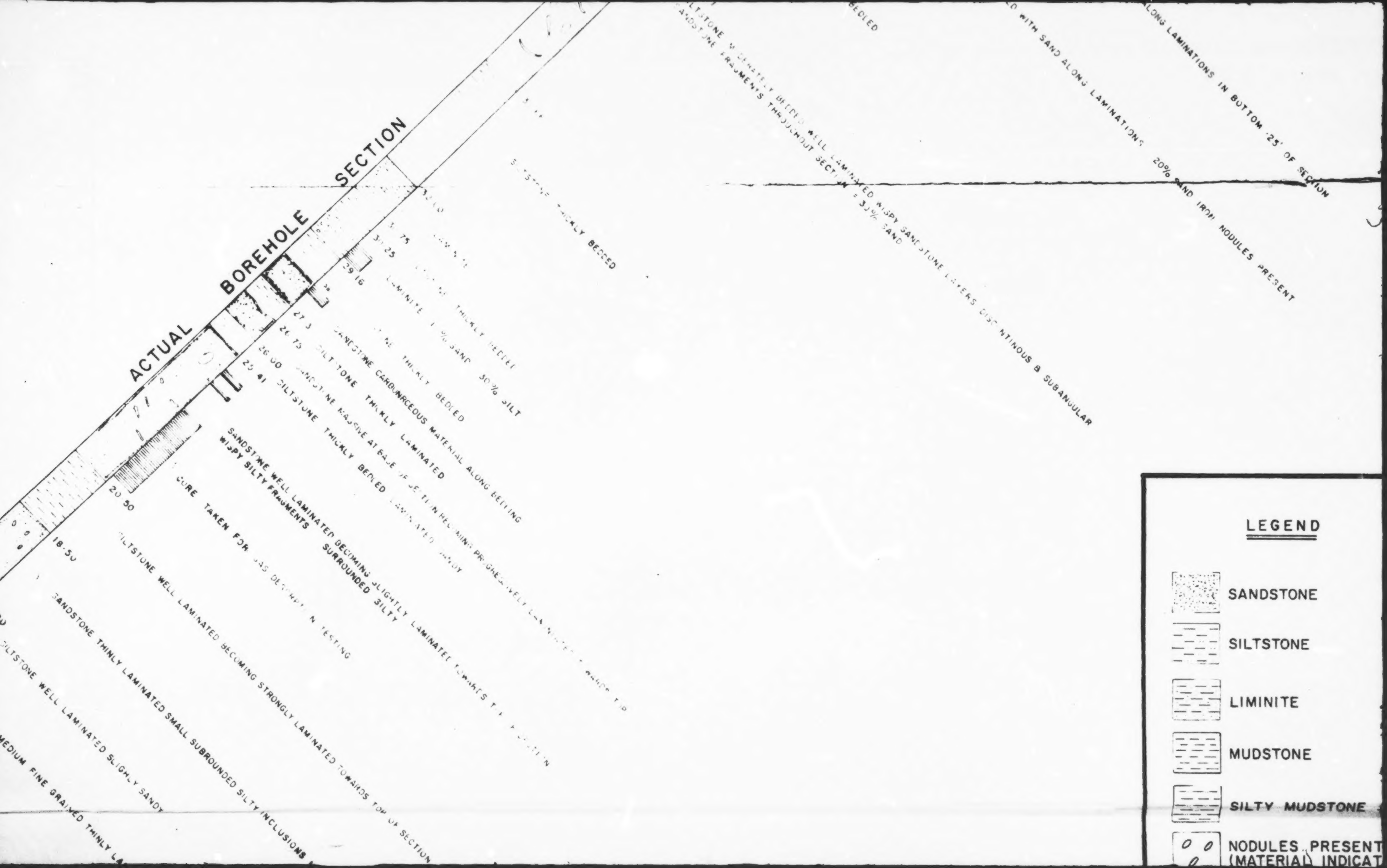
ACTUAL BOREHOLE SECTION
32.00
31.75
30.25
29.16
27.3
26.75
26.00
25.41
20.50
18.50
SILTSTONE THICKLY BEDDED
LAMINITE THICKLY BEDDED
LAMINITE 1% SAND 30% SILT
THICKLY BEDDED
SANDSTONE CARBONACEOUS MATERIAL ALONG BEDDING
SILTSTONE THICKLY LAMINATED
SANDSTONE MASSIVE AT BASE OF SECTION BECOMING PROGRESSIVELY LAMINATED TOWARDS TOP
SILTSTONE THICKLY BEDDED LAMINATED SANDY
SANDSTONE WELL LAMINATED BECOMING SLIGHTLY LAMINATED TOWARDS TOP OF SECTION
WISPY SILTY FRAGMENTS SURROUNDED SILTY
CORE TAKEN FOR GAS DESORPTION TESTING
SILTSTONE WELL LAMINATED BECOMING STRONGLY LAMINATED TOWARDS TOP OF SECTION
SANDSTONE THINLY LAMINATED SMALL SUBROUNDED SILTY INCLUSIONS
SILTSTONE WELL LAMINATED SLIGHLY SANDY
MEDIUM FINE GRAINED THINLY LA
SILTSTONE MODERATELY BEDDED WELL LAMINATED WISPY SANDSTONE LAYERS DISCONTINOUS & SUBANGULAR
SANDSTONE FRAGMENTS THROUGHOUT SECTION = 30% SAND
BEDDED
WITH SAND ALONG LAMINATIONS
20% SAND IRON NODULES PRESENT
ALONG LAMINATIONS IN BOTTOM 25' OF SECTION
LEGEND
SANDSTONE
SILTSTONE
LIMINITE
MUDSTONE
SILTY MUDSTONE
NODULES PRESENT
(MATERIAL) INDICAT

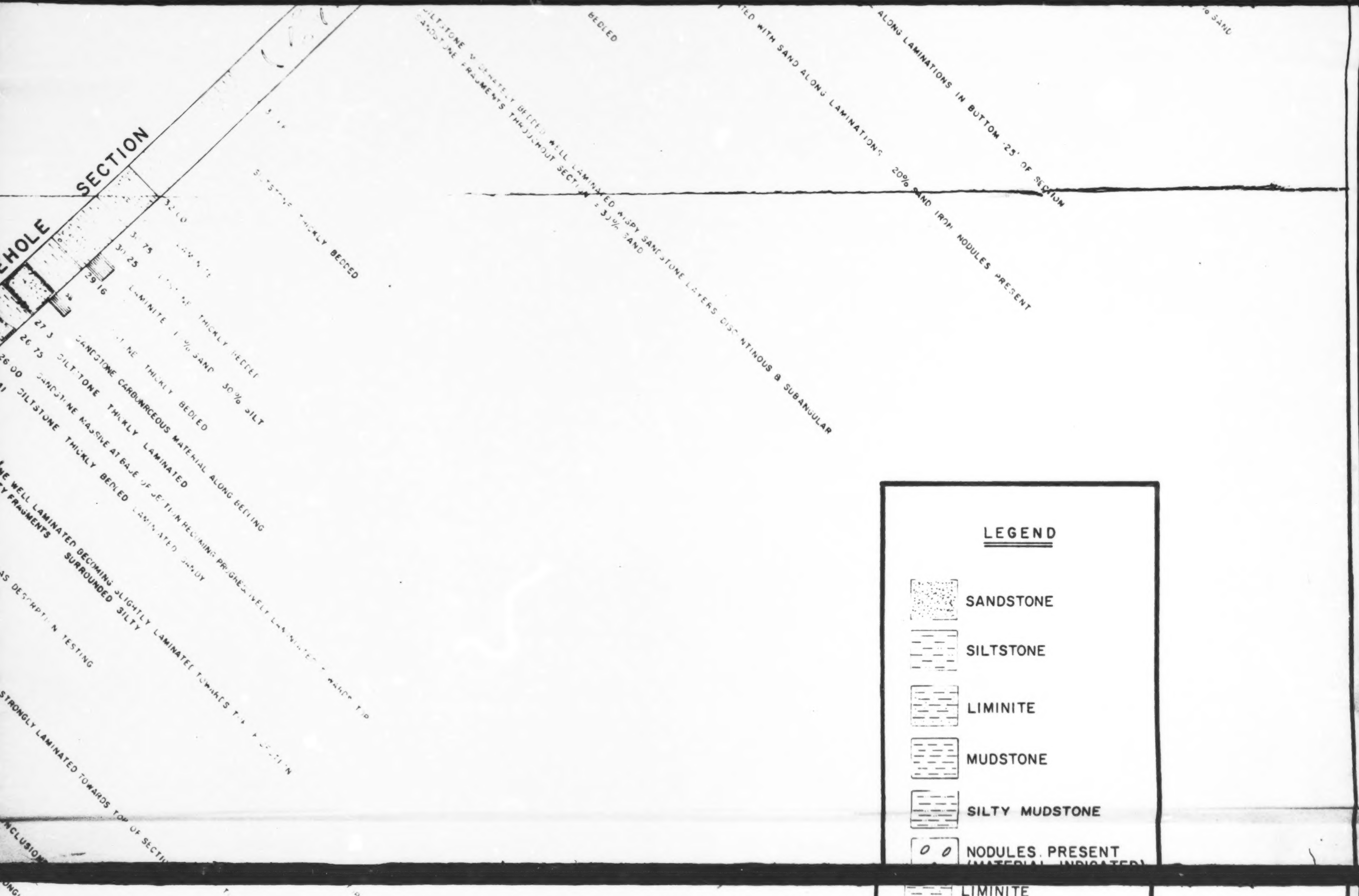
EHOLE SECTION
32.00
31.75
31.25
29.16
27.3
26.75
26.00
SILTSTONE THICKLY BEDDED
LAMINITE
LAMINITE THICKLY BEDDED
LAMINITE 70% SAND 30% SILT
STONE THICKLY BEDDED
SANDSTONE CARBONACEOUS MATERIAL ALONG BEDDING
SILTSTONE THICKLY LAMINATED
SANDSTONE MASSIVE AT BASE OF SECTION BECOMING PROGRESSIVELY LAMINATED TOWARDS TOP
SILTSTONE THICKLY BEDDED LAMINATED SANDY
NE WELL LAMINATED BECOMING SLIGHTLY LAMINATED TOWARDS TOP OF SECTION
Y FRAGMENTS SURROUNDED SILTY
AS DESCRIPTION TESTING
STRONGLY LAMINATED TOWARDS TOP OF SECTI
NCLUSION
SILTSTONE MODERATELY BEDDED WELL LAMINATED WISPY SANDSTONE LAYERS DISCONTINOUS & SUBANGULAR
SANDSTONE FRAGMENTS THROUGHOUT SECTION = 30% SAND
BEDDED
ATED WITH SAND ALONG LAMINATIONS
ALONG LAMINATIONS IN BOTTOM 25' OF SECTION
20% SAND IRON NODULES PRESENT
% SAND
LEGEND
SANDSTONE
SILTSTONE
LIMINITE
MUDSTONE
SILTY MUDSTONE
0 0 NODULES PRESENT (MATERIAL INDICATED)
LIMINITE

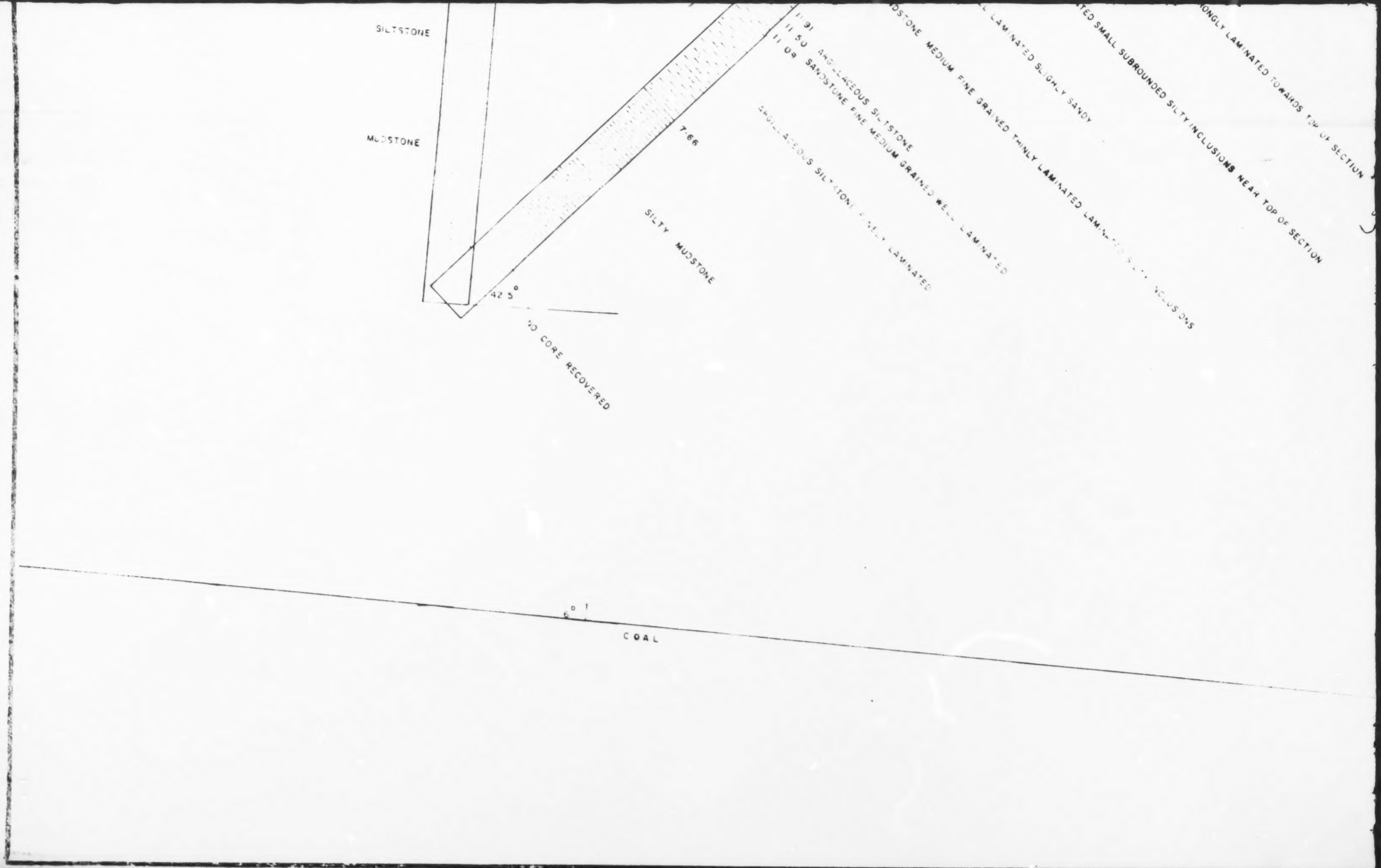
SILTSTONE
MUDSTONE
7·66
42 5°
NO CORE RECOVERED
SILTY MUDSTONE
11·91
11 50 ARGILLACEOUS SILTSTONE
11 08 SANDSTONE FINE MEDIUM GRAINED WELL LAMINATED
ARGILLACEOUS SILTSTONE FINELY LAMINATED
DSTONE MEDIUM FINE GRAINED THINLY LAMINATED LAMINATED SILTY INCLUSIONS
L LAMINATED SLIGHTLY SANDY
TED SMALL SUBROUNDED SILTY INCLUSIONS NEAR TOP OF SECTION
ONGLY LAMINATED TOWARDS TOP OF SECTION
6°
COAL

E MEDIUM FINE GRAINED THINLY LAMINATED LAMINATED SILTY INCLUSIONS
LAMINATED SLIGHLY SANDY
D SMALL SUBROUNDED SILTY INCLUSIONS NEAR TOP OF SECTION
NGLY LAMINATED TOWARDS TOP OF SECTION
E
RAINED WELL LAMINATED
NATED

▤	LIMINITE
▤	MUDSTONE
▤	SILTY MUDSTONE
○ ○ ○	NODULES PRESENT (MATERIAL INDICAT
⟋	CROSS - BEDDING
▤	SHALE
▦	LIMESTONE
┼	CALCAREOUS
▒	DISCING OF CO

ATTACHMENT

C. B. D. C. Cape

GEOL

BOREHOLE D-164 No 2
(ACTUAL SECTION PROJE

Scale	1"= 2'0"	Date	R
Drawn			
DRAFTED	W.C.C.		
Checked			Dv
Approved	CF		N

NGLY LAMINATED TOWARDS TOP OF SECTION

NCLUSIONS NEAR TOP OF SECTION

S

- ▤ LIMINITE
- ▤ MUDSTONE
- ▤ SILTY MUDSTONE
- 0 0 0 NODULES PRESENT (MATERIAL INDICATED)
- CROSS - BEDDING
- ▤ SHALE
- ▦ LIMESTONE
- ┴ ┴ CALCAREOUS
- ≡ DISCING OF CORE

ATTACHMENT No 6.

C. B. D. C.

Cape Breton Development Corporation

GEOLOGY

BOREHOLE D-164 No 26 COLLIERY
(ACTUAL SECTION PROJECTED TO TRUE THICKNESS

Scale	1"= 2'0"	Date	Ref Dwgs.	Sheet No. of
Drawn				
DRAFTED	W.C.C.			
Checked			Dwg No	-G-
Approved	CF			

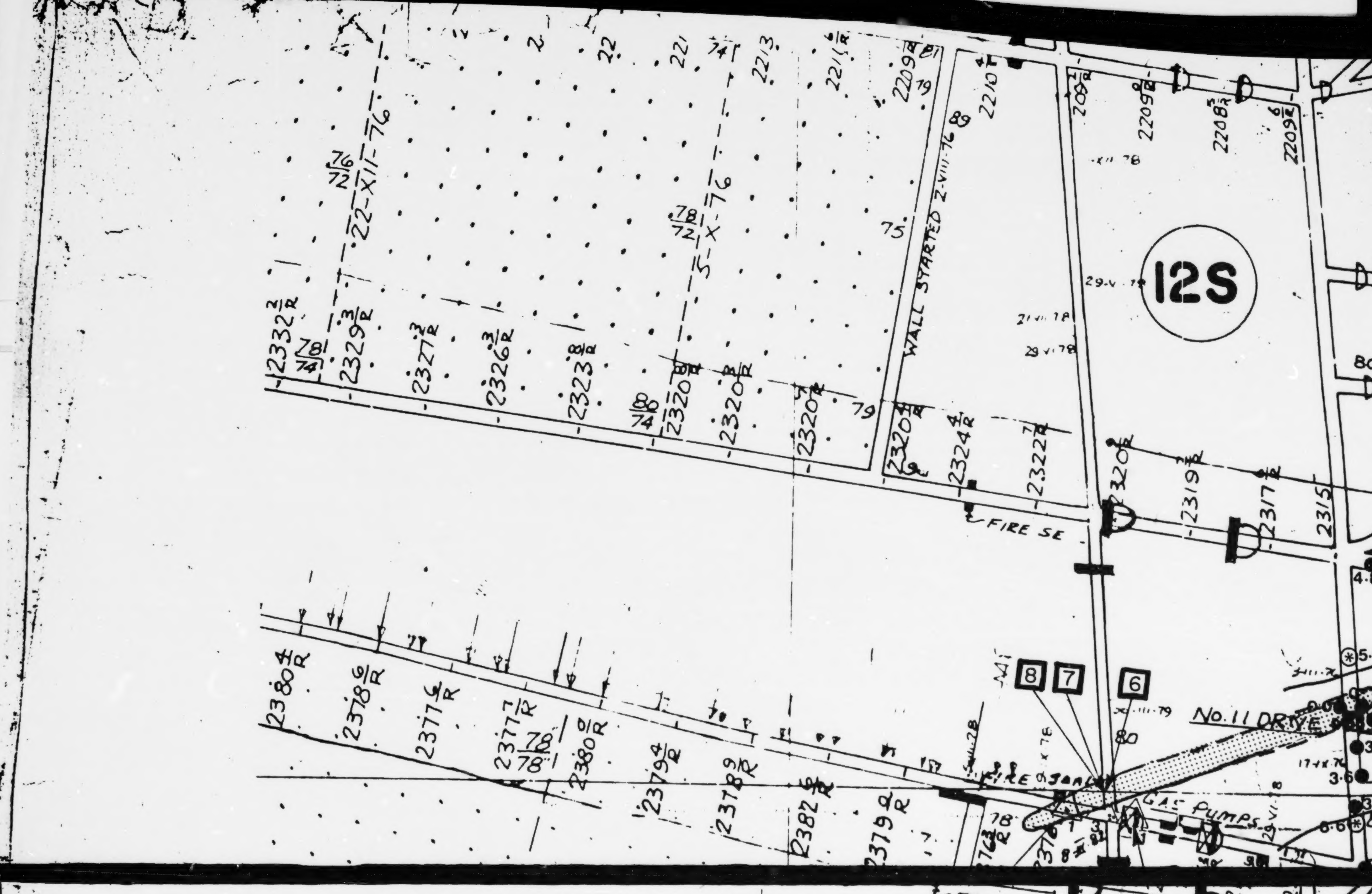
12S
22-XII-76
76/72
5-X-76
78/72
WALL STARTED 2-VIII-76
75
79
89
2332
78/74
2329
2327
2326
2323
80/74
2320
2320
2320
2320
2324
2322
2320
2319
2317
2315
2210
2209
2208
2209
29-V-78
21-VI-78
29-VI-78
FIRE SE
8
7
6
No.11 DRIVE
FIRE SEAL
GAS PUMPS
2380
2378
2377
2377
78/78
2380
2379
2378
2382
2379
80

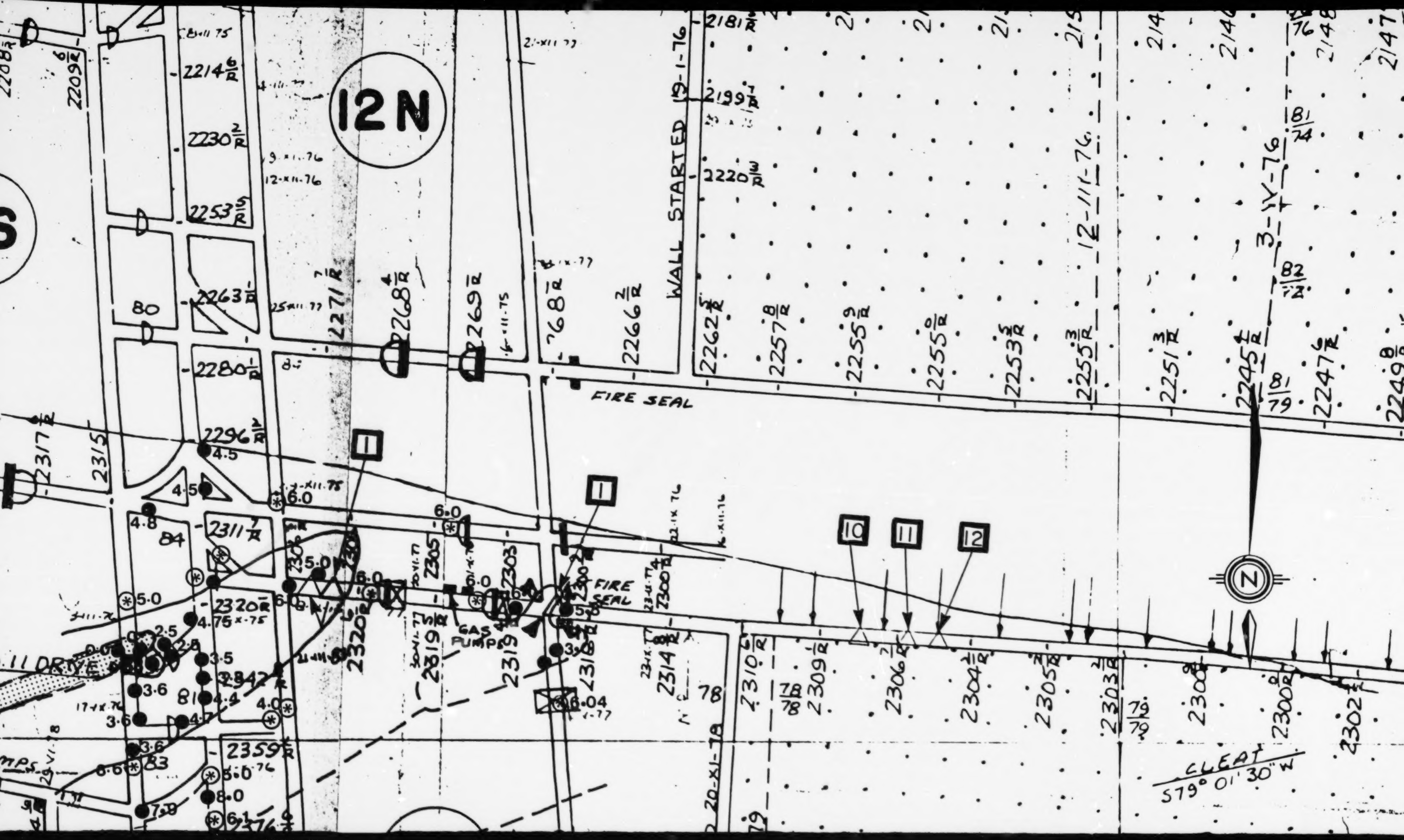
12N
WALL STARTED 19-1-76
12-III-76
3-IV-76
FIRE SEAL
FIRE SEAL
GAS PUMPS
CLEAT
S79° 01' 30" W
2181
2199
2220
2214
2230
2253
2263
2271
2268
2269
2266
2262
2257
2255
2253
2251
2245
2247
2249
2280
2296
2311
2315
2317
2320
2319
2314
2310
2309
2306
2304
2305
2303
2300
2302
2359
80
84
81
83
78
1
1
10
11
12
N
20-XI-78

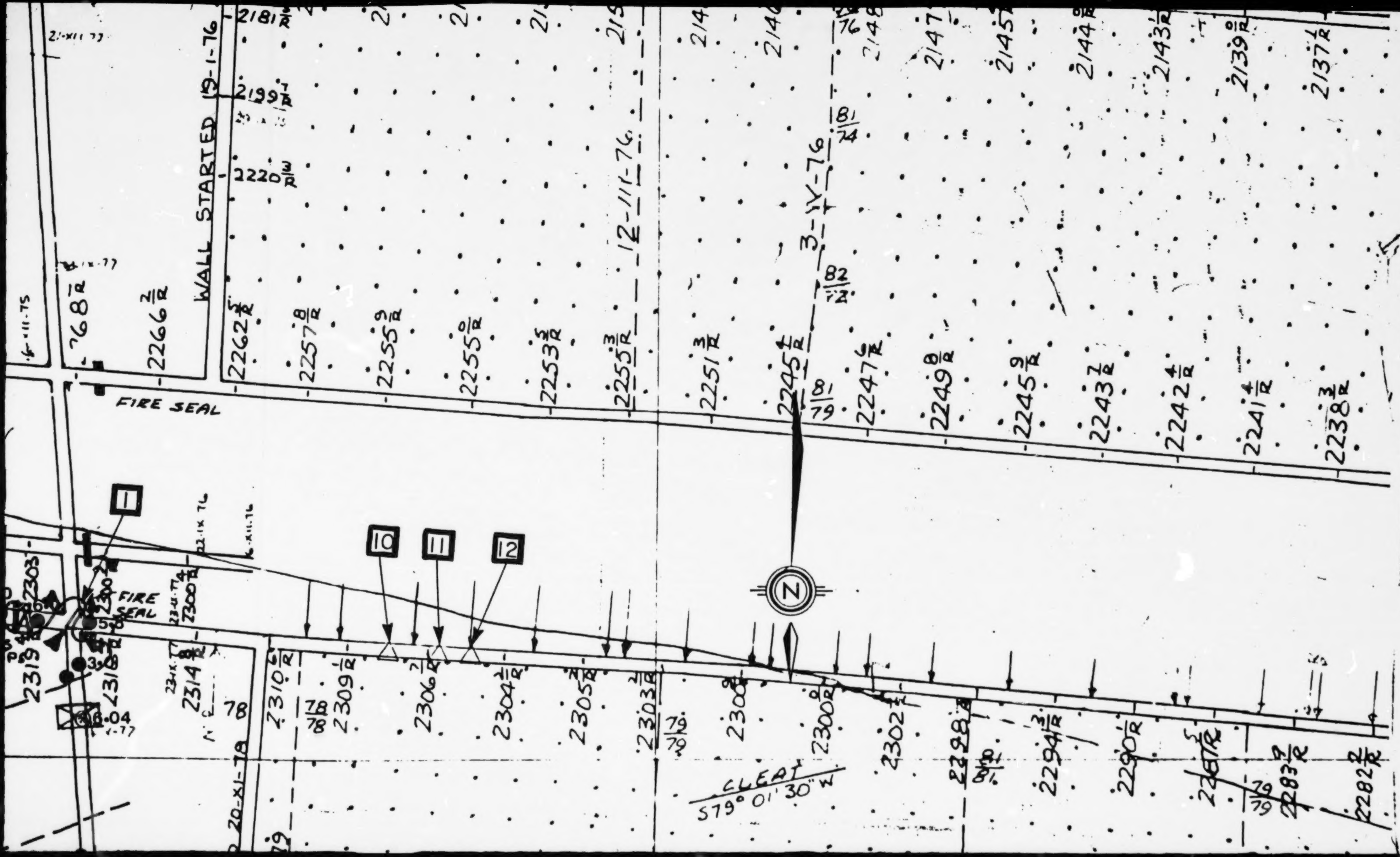

WALL STARTED 13-I-76
12-III-76
3-IV-76
FIRE SEAL
FIRE SEAL
CLEAT
S79° 01' 30" W
N
1
10
11
12
2181
2199
2220
2262
2257
2255
2255
2253
2255
2251
2245
2247
2249
2245
2243
2242
2241
2238
2147
2145
2144
2143
2139
2137
2266
768
2319
2318
2314
2310
2309
2306
2304
2305
2303
2300
2300
2302
2298
2294
2290
2287
2283
2282
2303
2300
20-XI-78
78
78/78
79/79
81/79
81/74
82/72
3.04

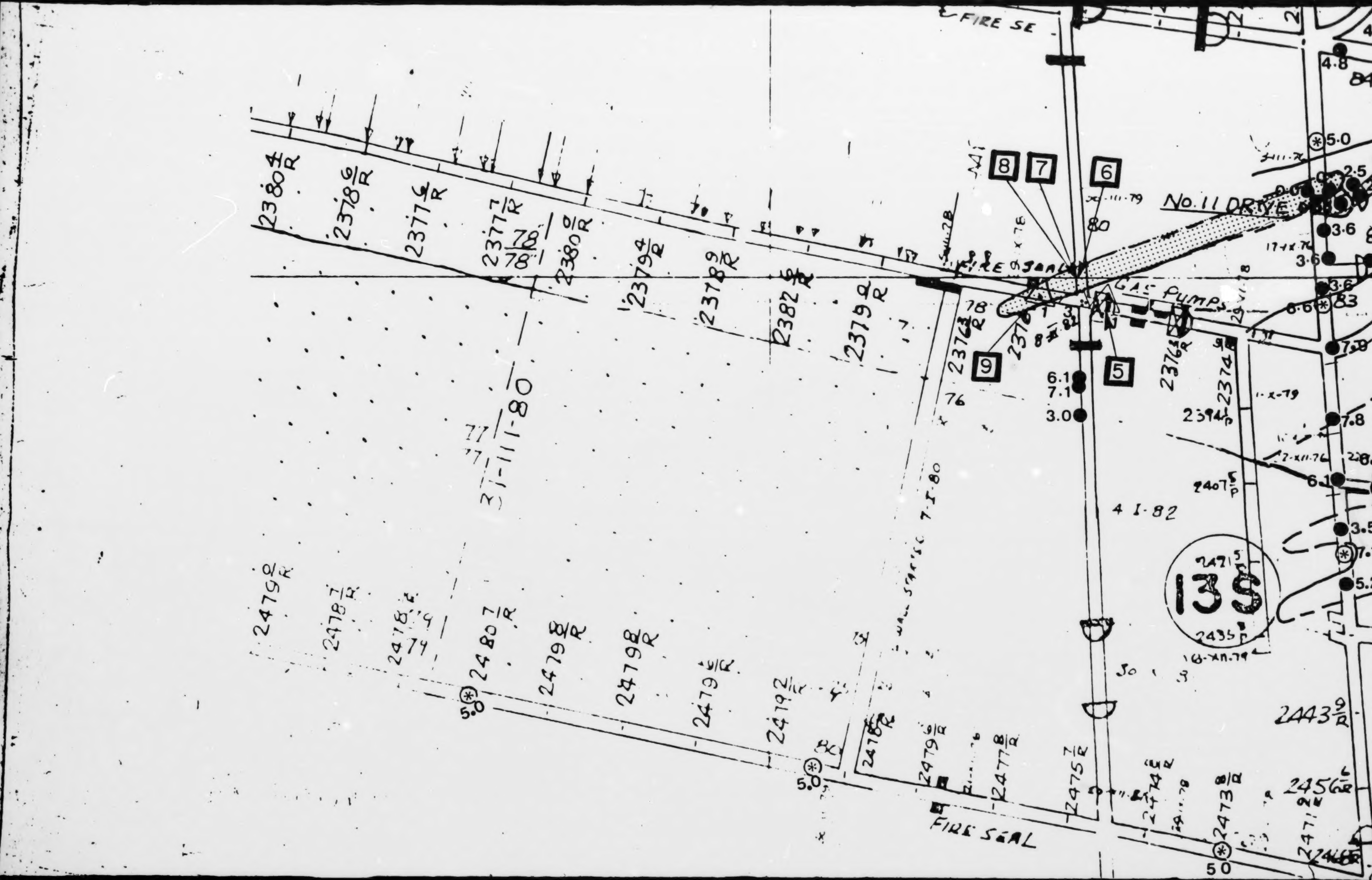
FIRE SE
No. 11 DRIVE
FIRE SEAL
GAS PUMPS
FIRE SEAL
8
7
6
9
5
135
2380 4/R
2378 6/R
2377 6/R
2377 7/R
78/78
2380 0/R
2379 4/R
2378 9/R
2382 6/R
2379 0/R
2376 2/R
2376
2376 5/R
2374
2394 1/P
2407 5/P
2471 5
2435 5
2443 9/R
2456 6/R
2479 0/R
2478 7/R
2478
2480 7/R
2479 8/R
2479 8/R
2479
2479 2/R
2478 6/R
2479 6/R
2477 8/R
2475 7/R
2473 8/R
5.0
5.0
5.0
5.0
4.8
2.5
3.6
3.6
3.6
6.6
83
7.8
7.8
2.8
6.1
3.5
7.1
3.0
4 I-82
21-III-80
7-I-80
18-XII-79
76
77
80

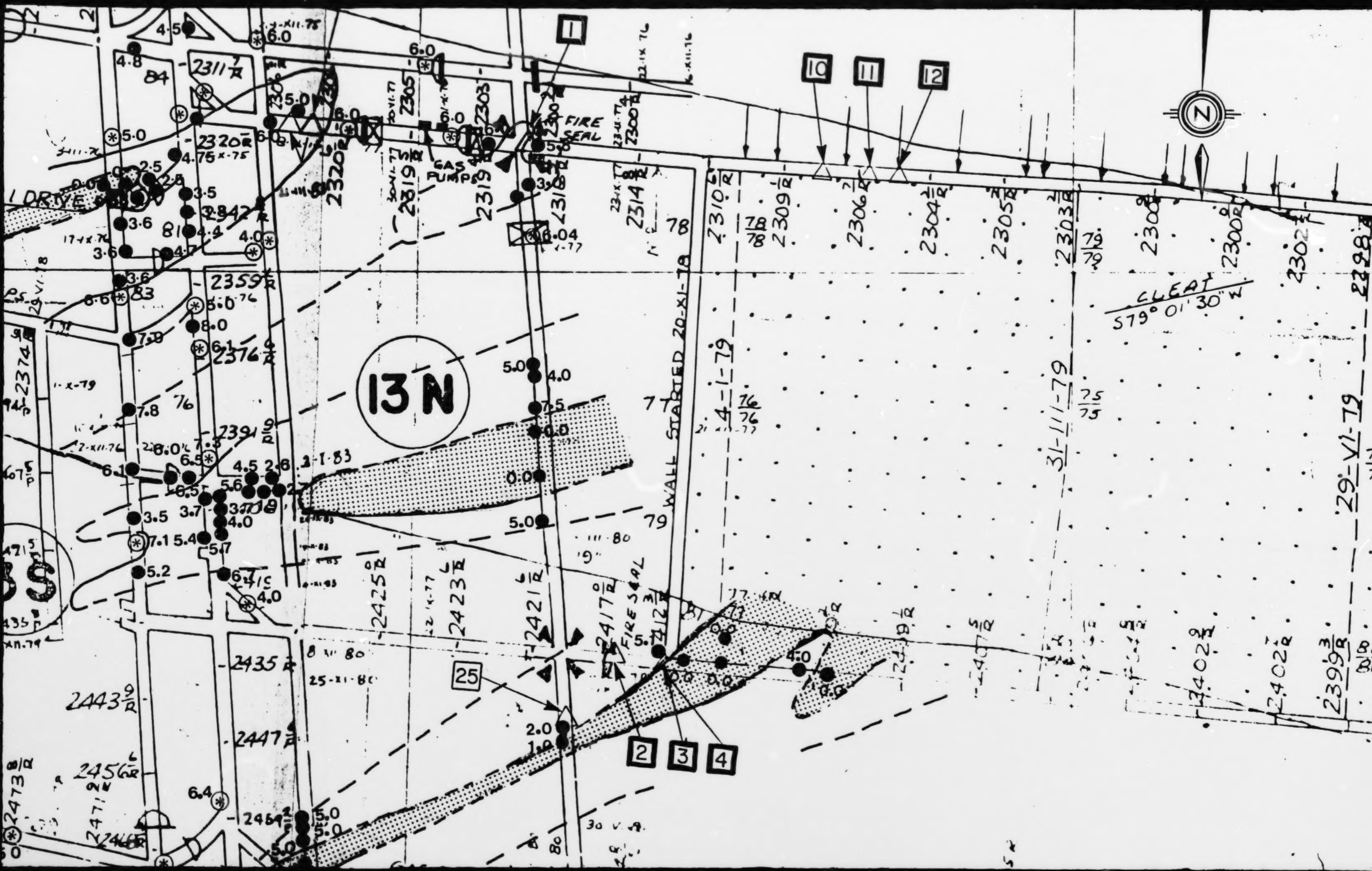

13N
N
1
10
11
12
25
2
3
4
FIRE SEAL
GAS PUMPS
WALL STARTED 20-XI-78
4-1-79
31-III-79
29-VI-79
CLEAT
S79° 01' 30" W
FIRE SEAL
2311
2320
2305
2303
2300
2319
2318
2314
2310
2309
2306
2304
2305
2303
2302
2300
2302
2298
2359
2376
2391
2374
2425
2423
2421
2417
2412
2435
2443
2447
2456
2461
2473
2471
2402
2402
2399
84
83
81
78
78
77
76
76
75
79
79
2-I-83

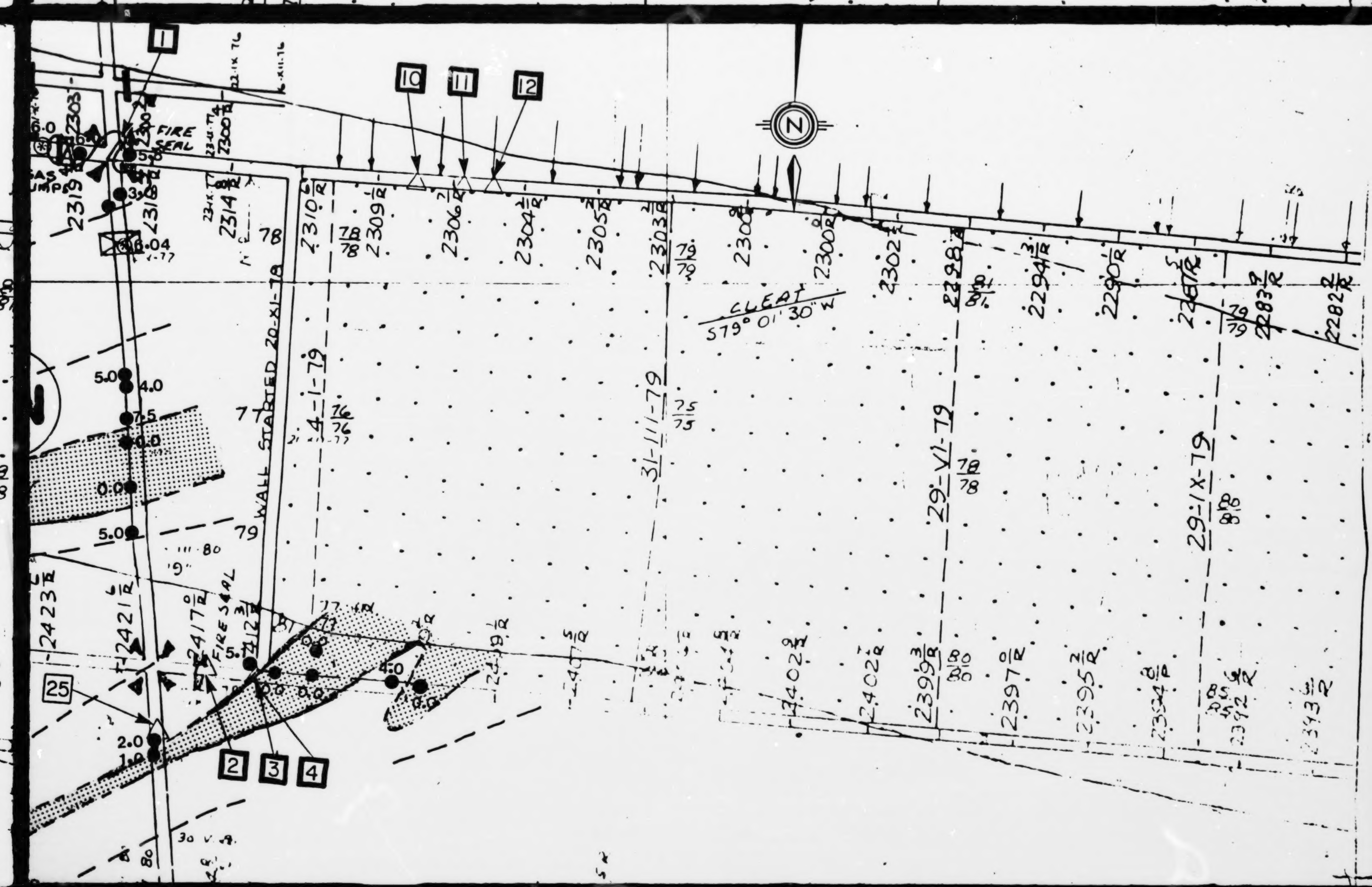
1
10
11
12
N
FIRE SEAL
GAS PUMPS
2319
2318
2314
2303
2300
2310
2309
2306
2304
2305
2303
2300
2302
2298
2294
2290
2287
2283
2282
78
78/78
79/79
80/81
79/79
CLEAT
S79° 01' 30" W
WALL STARTED 20-XI-78
4-1-79
31-III-79
29-VI-79
29-IX-79
77
76/76
75/75
78/78
80/80
79
5.0
4.0
7.5
0.0
0.0
5.0
6.04
6.0
5.0
3.0
111-80
"9"
FIRE SEAL
2423
2421
2417
2412
2402
2402
2399
2397
2395
2394
2392
2393
80/80
4.0
0.0
0.0
0.0
5.0
2.0
1.0
25
2
3
4
30 V.8.
80

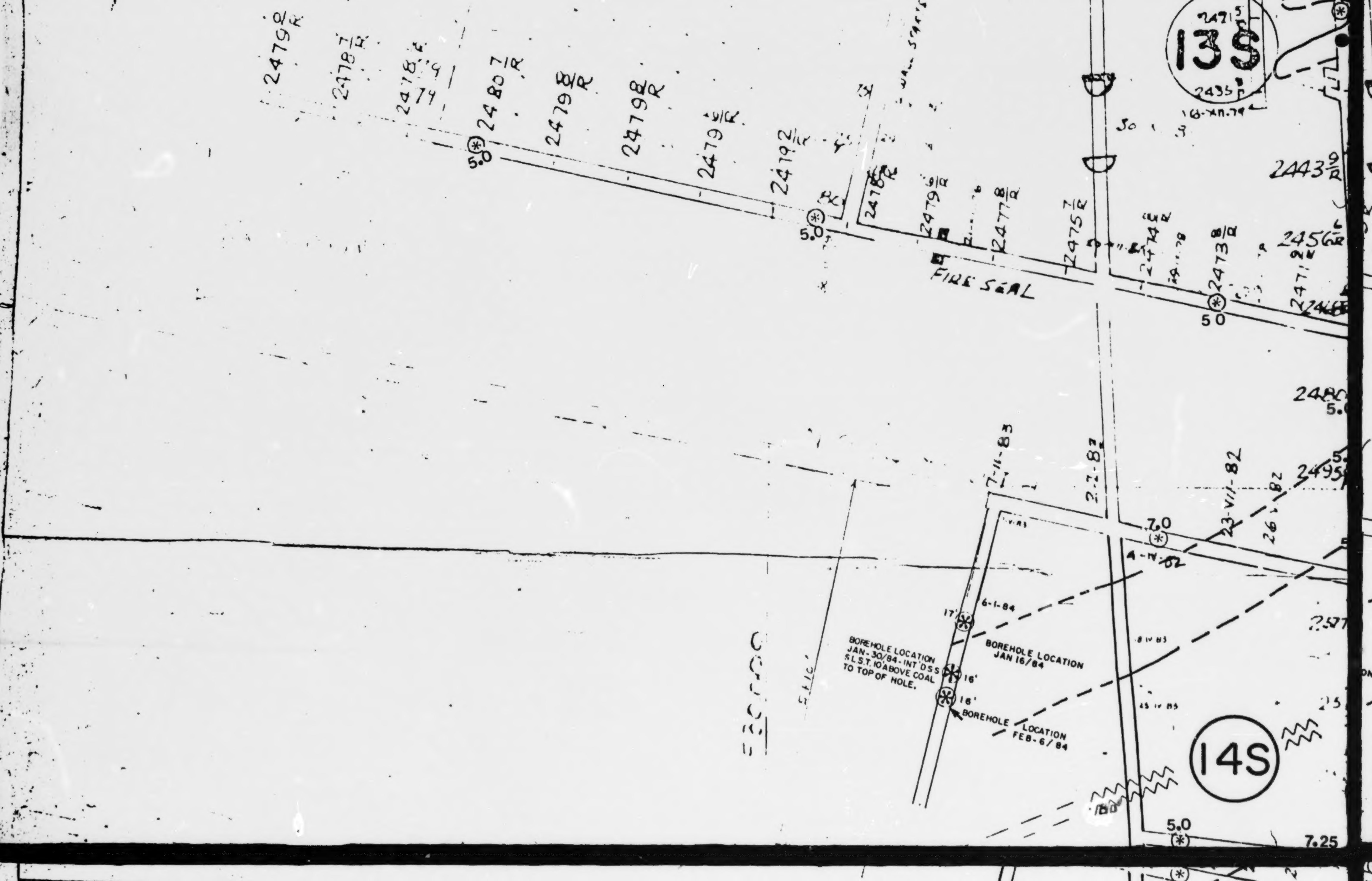
13S
2471
2435
16-XII-79
FIRE SEAL
5.0
5.0
50
2443 9/R
2456
2480
2495
7.0
4-IV-82
7-II-83
23-VII-82
6-1-84
17'
16'
16'
BOREHOLE LOCATION JAN-30/84-INT'D S.S. S.L.S.T. 10' ABOVE COAL TO TOP OF HOLE.
BOREHOLE LOCATION JAN 16/84
BOREHOLE LOCATION FEB-6/84
14S
5.0
7.25

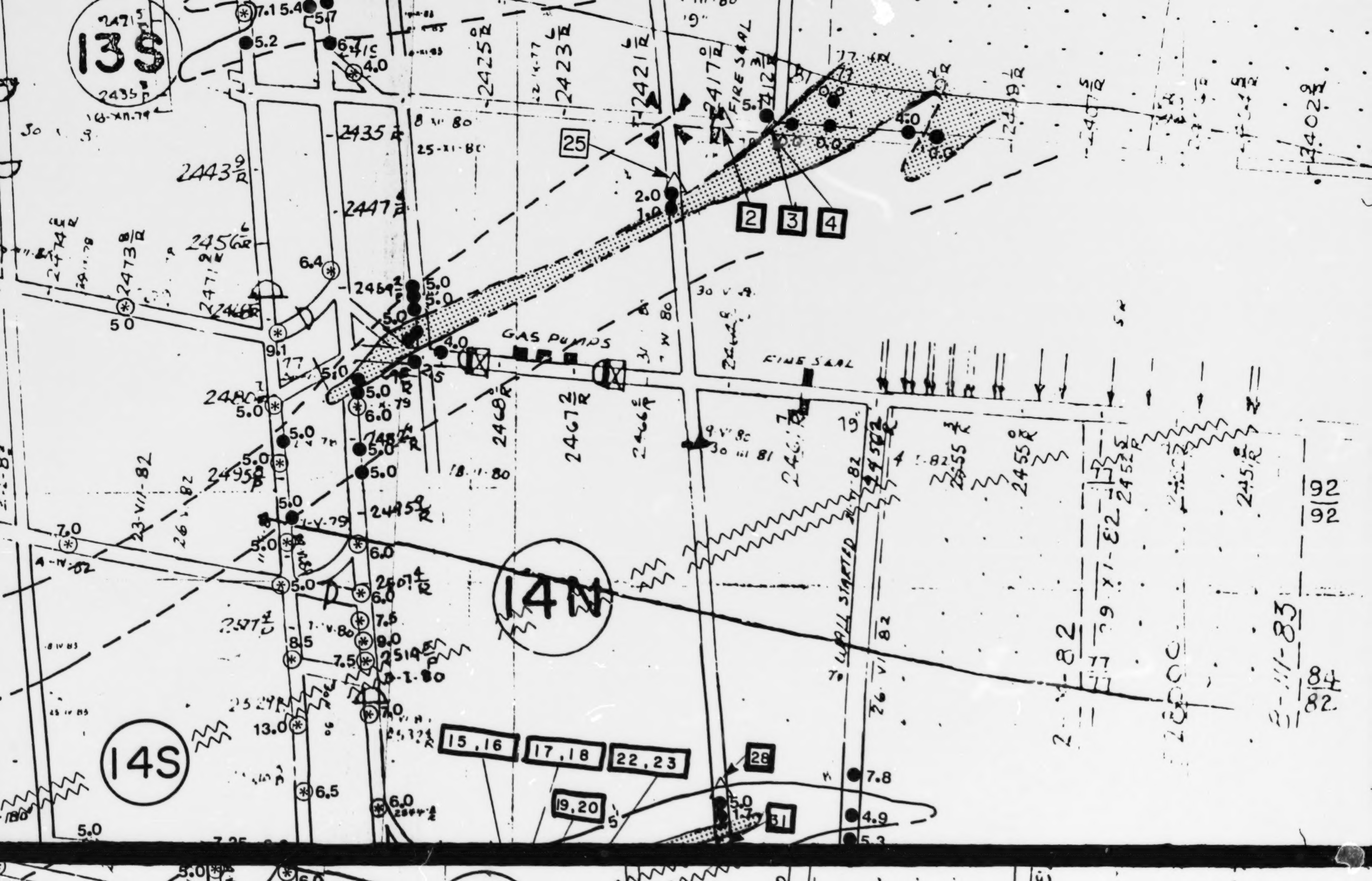
13S
14N
14S
GAS PUMPS
FIRE SEAL
FIRE SEAL
WALL STARTED
"9"
19"
25
2
3
4
15,16
17,18
22,23
19,20
28
31
2435
2443
2447
2456
2473
2469
2480
2495
2507
2514
2525
2425
2423
2421
2417
2468
2467
2455
2452
2402
7.1
5.4
5.7
5.2
4.0
6.4
9.1
5.0
6.0
7.0
7.5
7.6
8.5
9.0
13.0
6.5
2.0
1.0
0.0
7.8
4.9
5.3
1.7
92
92
84
82
8 XI 80
25-XI-80
30 V 80
30 III 81
18 I 80
23-VIII-82
4-IV-82
1-V-79
2-II-80
26 VI 82

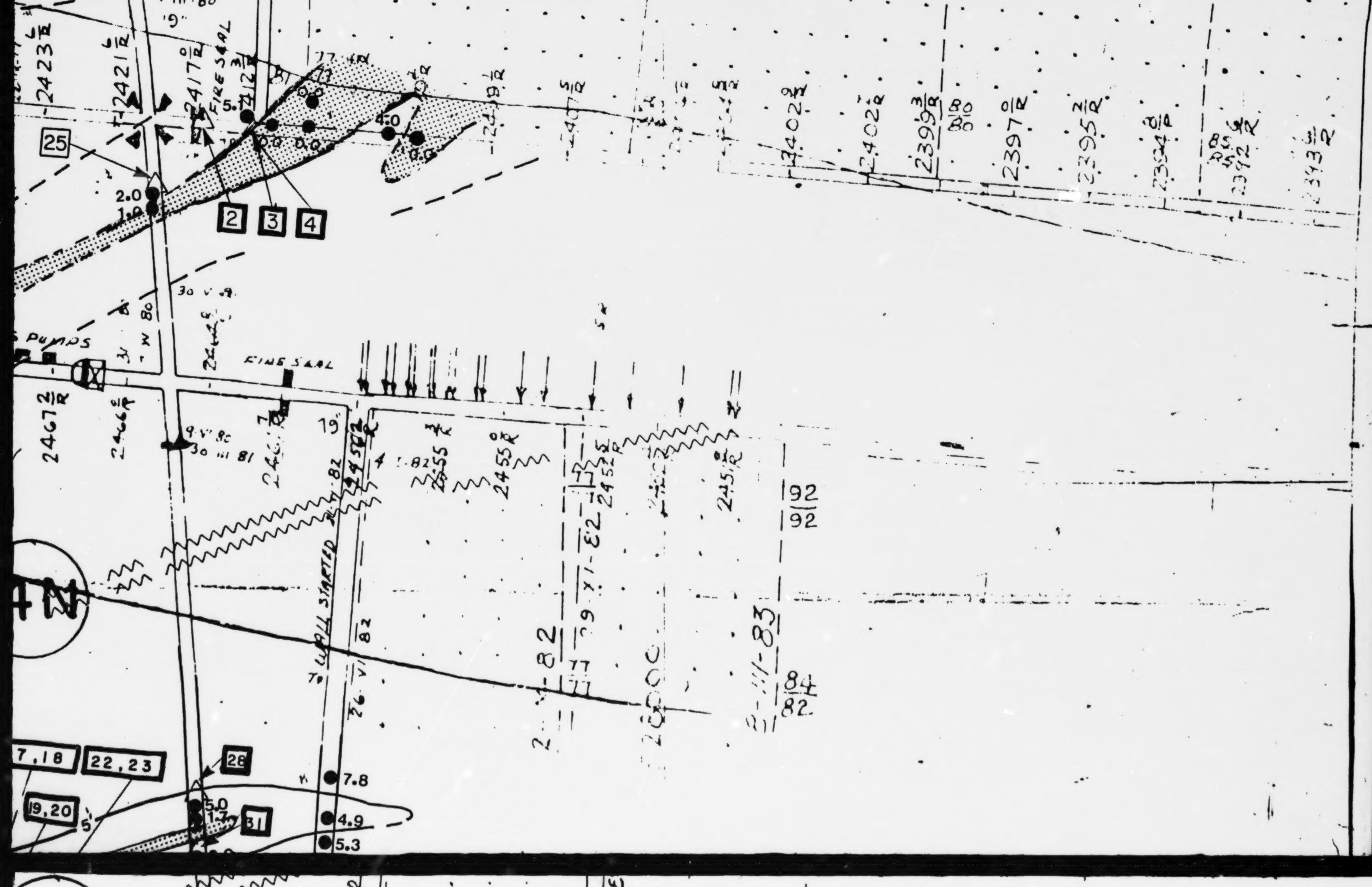2423
2421
2417
2412
FIRE SEAL
25
2.0
1.0
5.0
4.0
2
3
4
2402
2399
2397
2395
2393
30 V 81
PUMPS
FIRE SEAL
2467
2466
2450
2455
2452
2451
9 V 80
30 III 81
WALL STARTED
92
92
84
82
4N
7,18
22,23
19,20
28
31
7.8
4.9
5.3
5.0
1.7

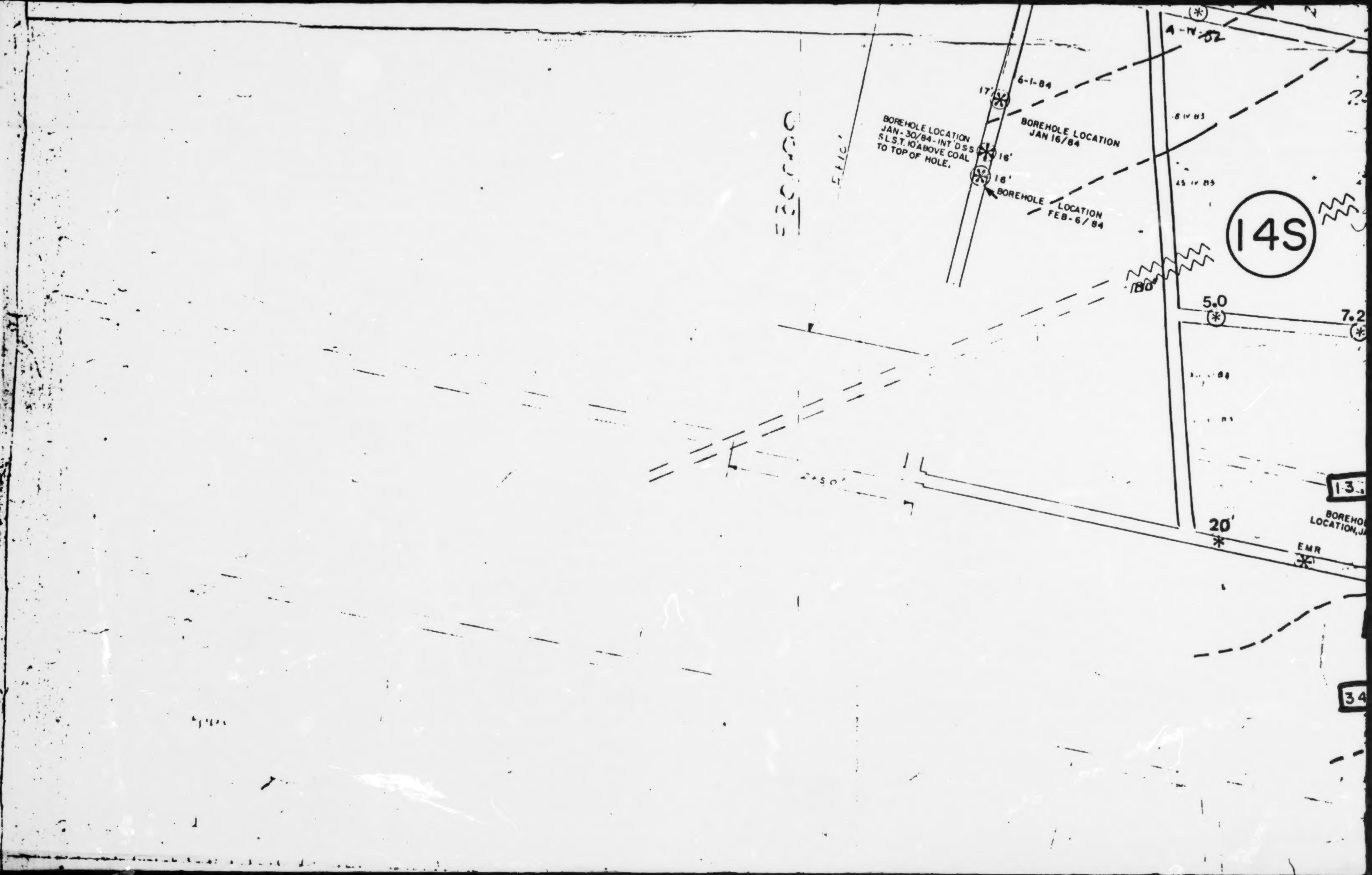
4-IV-82
6-1-84
17'
BOREHOLE LOCATION JAN-30/84-INT'DSS S.L.S.T. 10'ABOVE COAL TO TOP OF HOLE.
BOREHOLE LOCATION JAN 16/84
16'
16'
BOREHOLE LOCATION FEB-6/84
14S
180
5.0
7.2
13.
20'
BOREHOLE LOCATION, JA
EMR
34

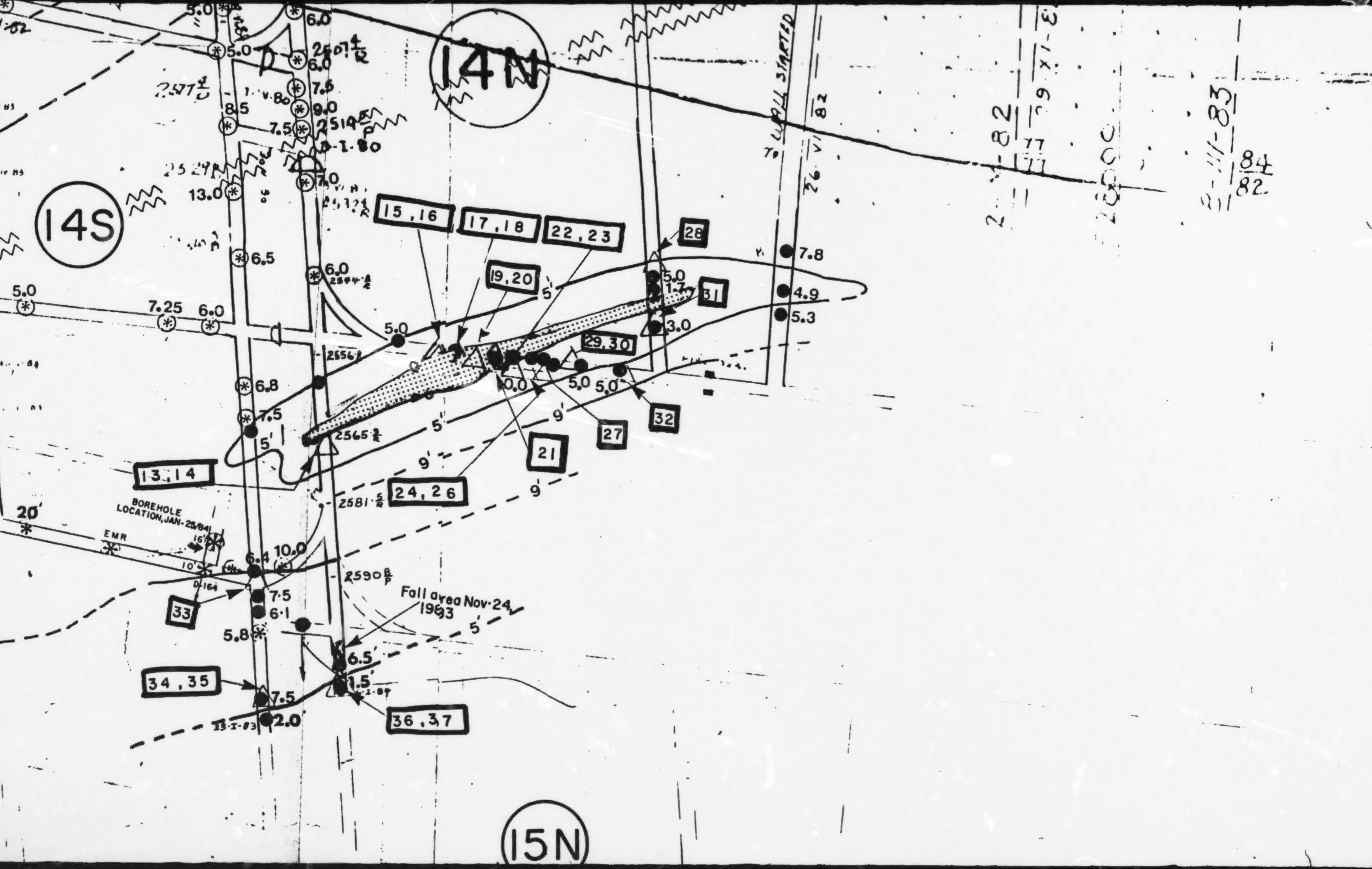

14N
14S
15N
15,16
17,18
22,23
19,20
28
31
29,30
13,14
24,26
21
27
32
33
34,35
36,37
BOREHOLE LOCATION, JAN-25/84
EMR
Fall area Nov·24, 1983
WALL STARTED
2507
2517
2514
2524
2556
2565
2581
2590
5.0
6.0
7.5
9.0
8.5
13.0
6.5
7.25
6.8
7.8
4.9
5.3
1.7
3.0
10.0
6.4
6.1
5.8
1.5
2.0
20'
5'
9'
84/82

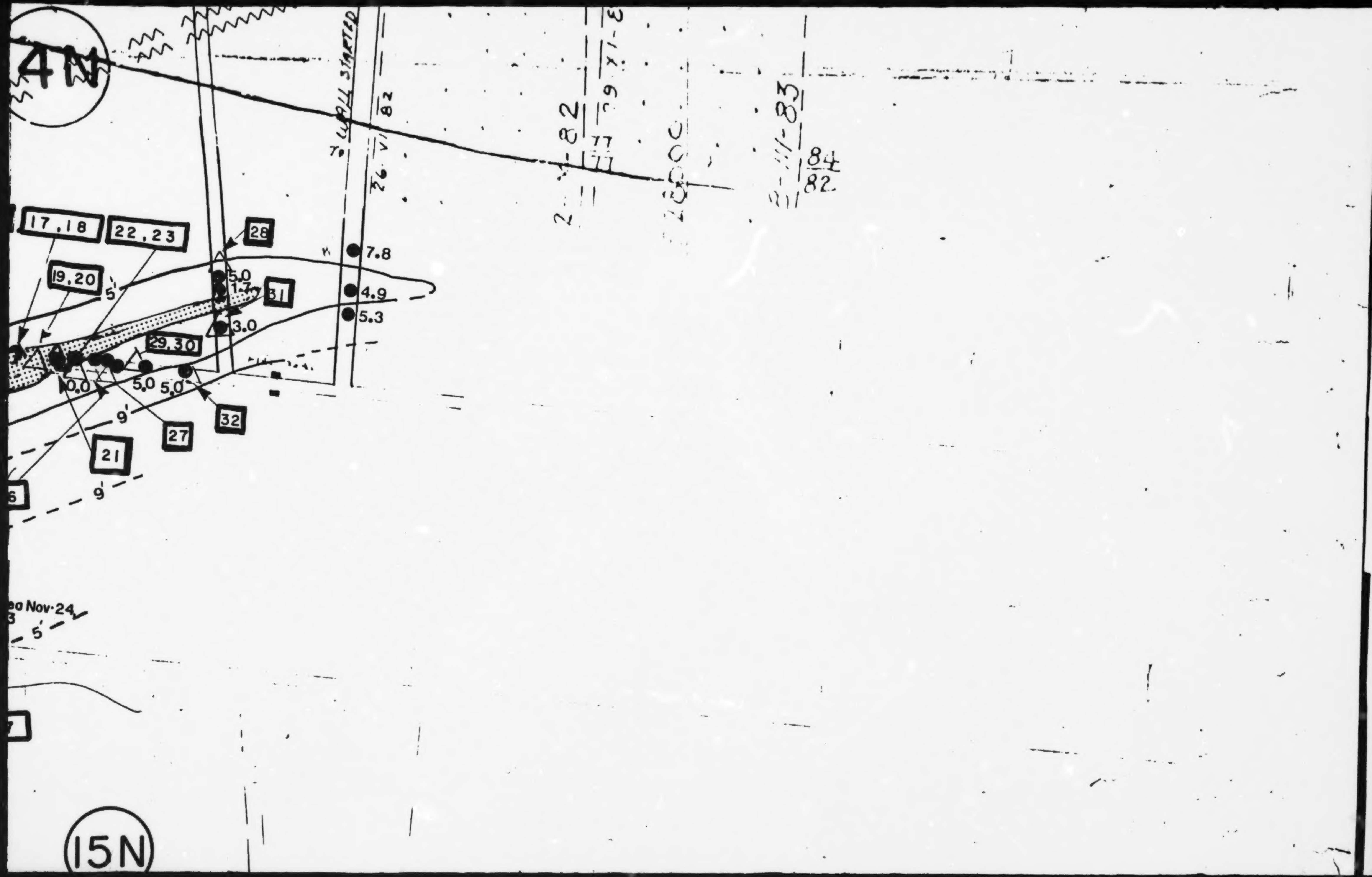
4N
WALL STARTED
VI 82
76
2-X-82
XI-E
77
11
2000
3-III-83
84
82
17,18
22,23
19,20
28
31
29,30
5.0
1.7
3.0
7.8
4.9
5.3
5'
0.0
5.0
5.0
9'
21
27
32
6
9'
ea Nov·24
3
5'
7
15N

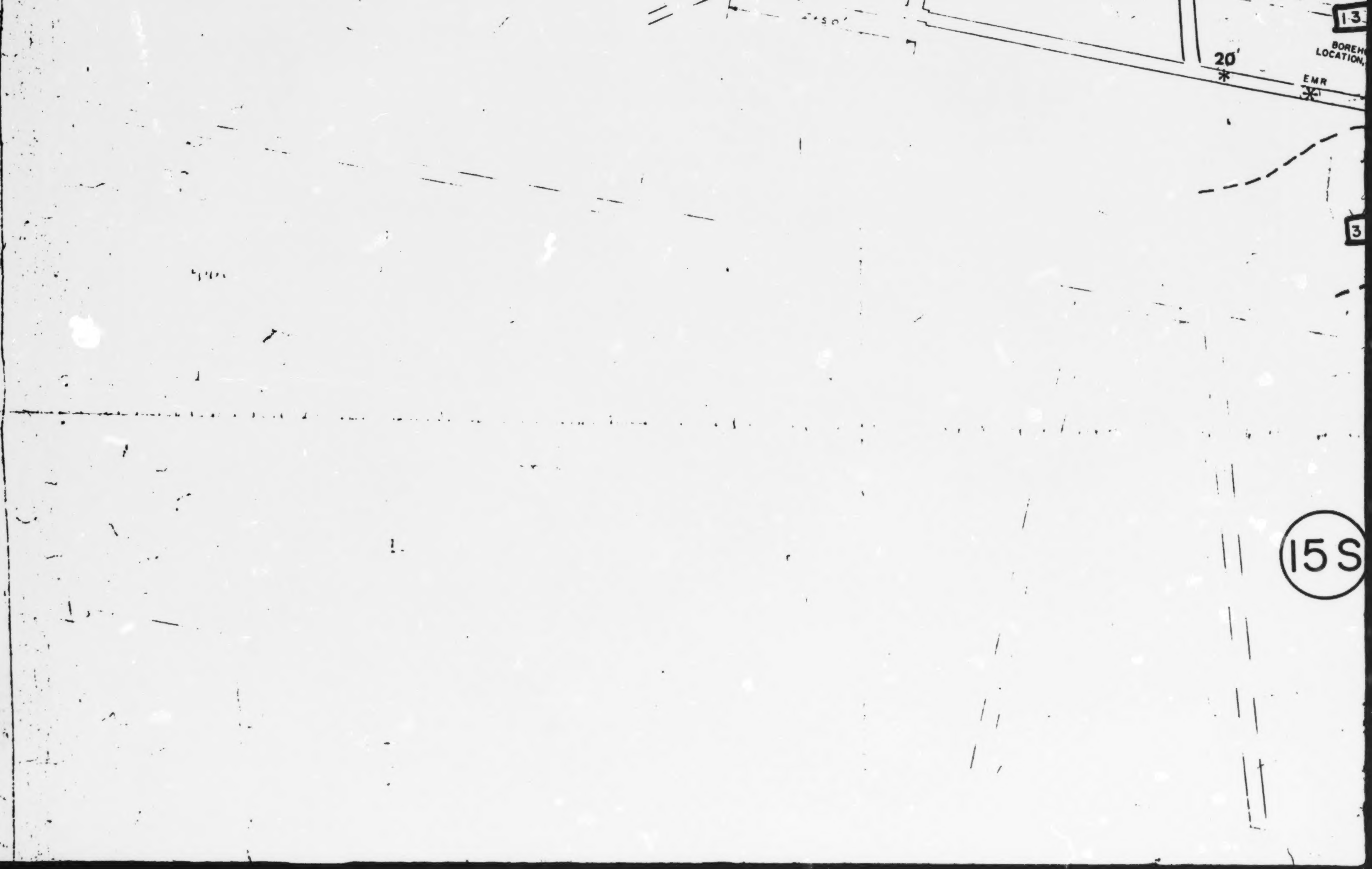
13
BOREH
LOCATION,
20'
EMR
3
15S

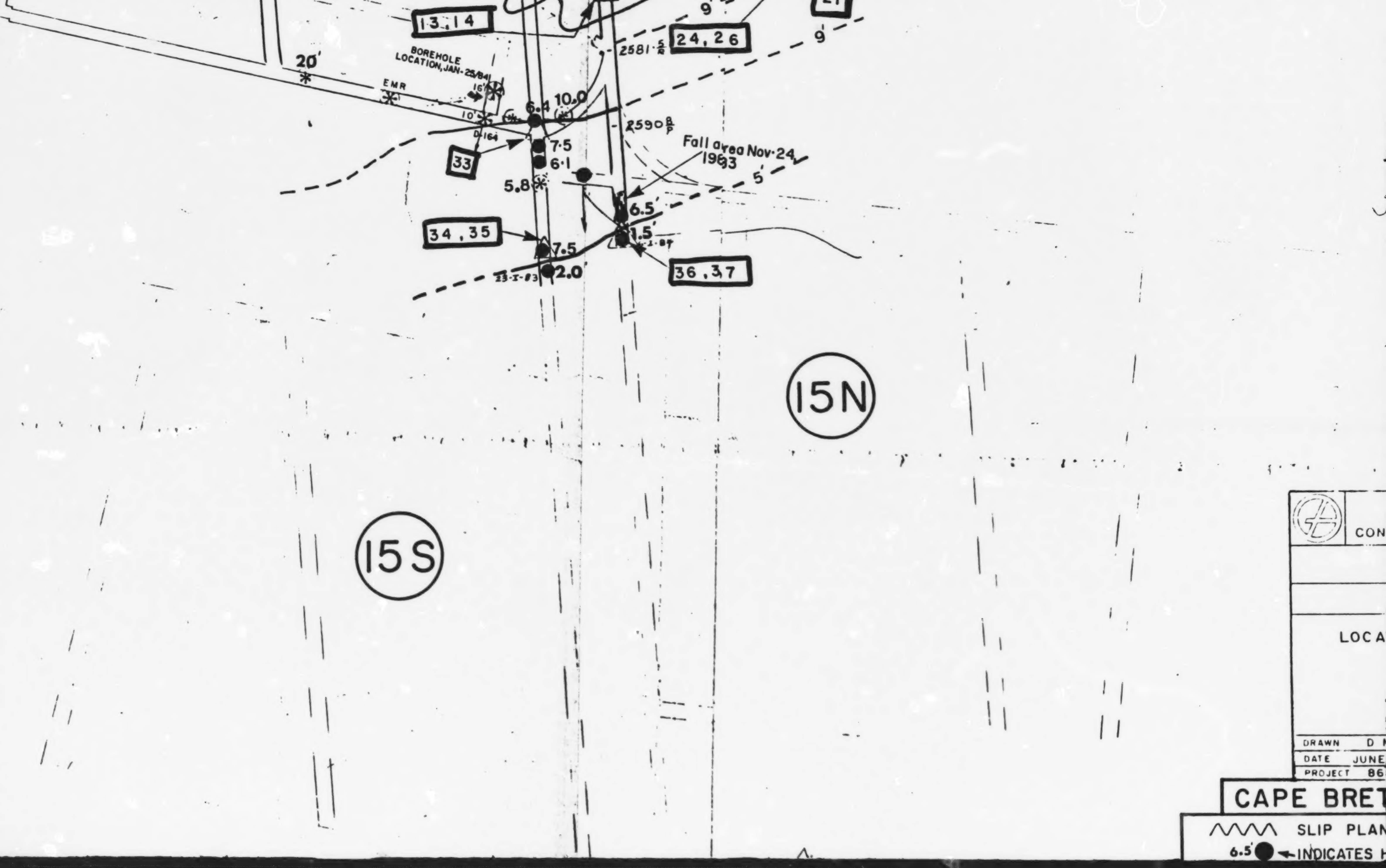
13,14
9
24,26
9
2581 S/R
BOREHOLE LOCATION, JAN-25/84
20'
EMR
16'
10'
D-164
6.4
10.0
2590 B/P
33
7.5
6.1
5.8
Fall area Nov·24, 1983
5'
6.5'
1.5'
34,35
7.5
2.0'
23-I-83
36,37
15N
15S
CON
LOCA
DRAWN D
DATE JUNE
PROJECT 86
CAPE BRET
SLIP PLAN
6.5 INDICATES H

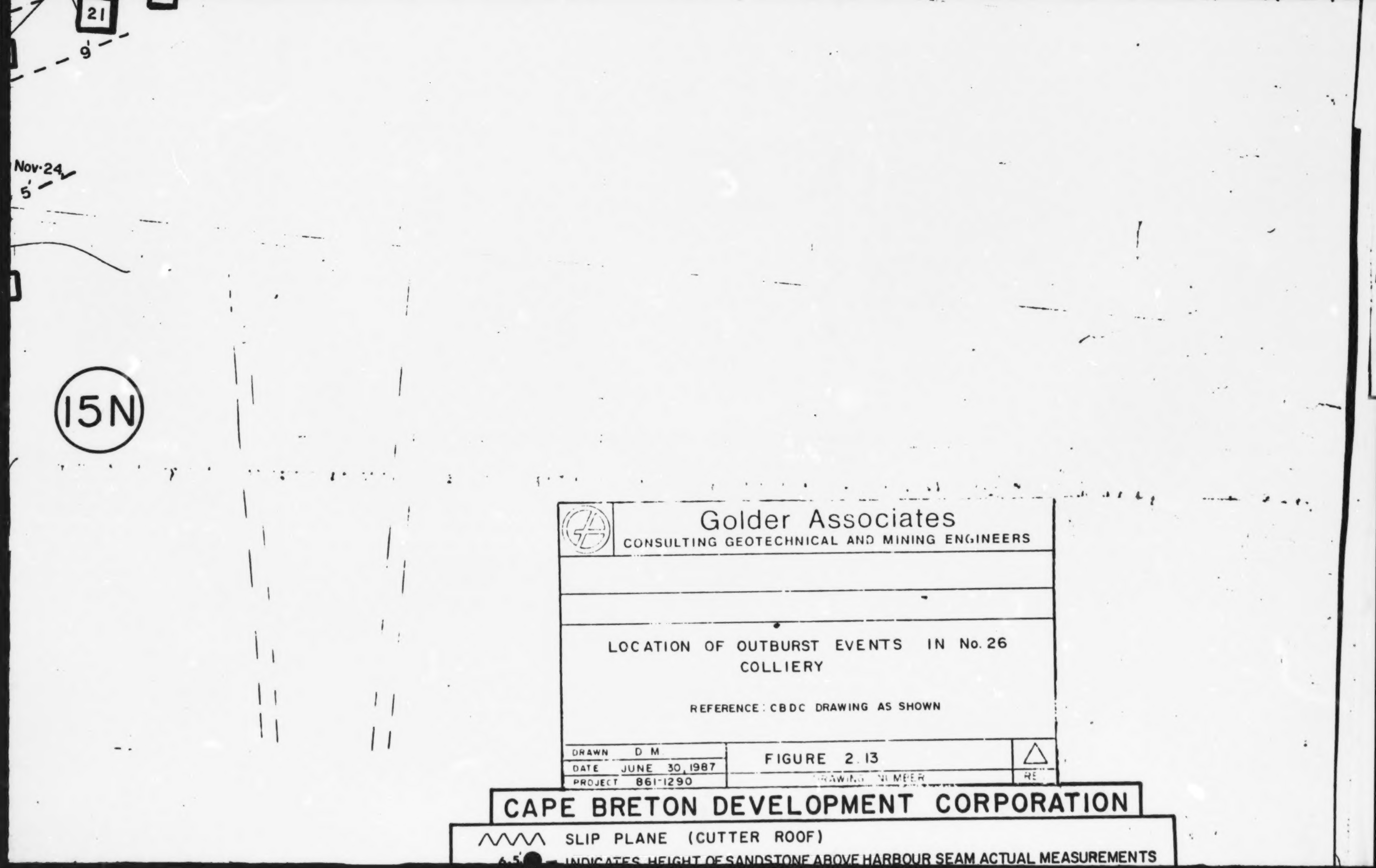

Golder Associates
CONSULTING GEOTECHNICAL AND MINING ENGINEERS

LOCATION OF OUTBURST EVENTS IN No. 26
COLLIERY

REFERENCE: CBDC DRAWING AS SHOWN

DRAWN	D M	FIGURE 2.13	△
DATE	JUNE 30, 1987		
PROJECT	861-1290	DRAWING NUMBER	REV

CAPE BRETON DEVELOPMENT CORPORATION

ʌʌʌʌ SLIP PLANE (CUTTER ROOF)

6.5● — INDICATES HEIGHT OF SANDSTONE ABOVE HARBOUR SEAM ACTUAL MEASUREMENTS

15S

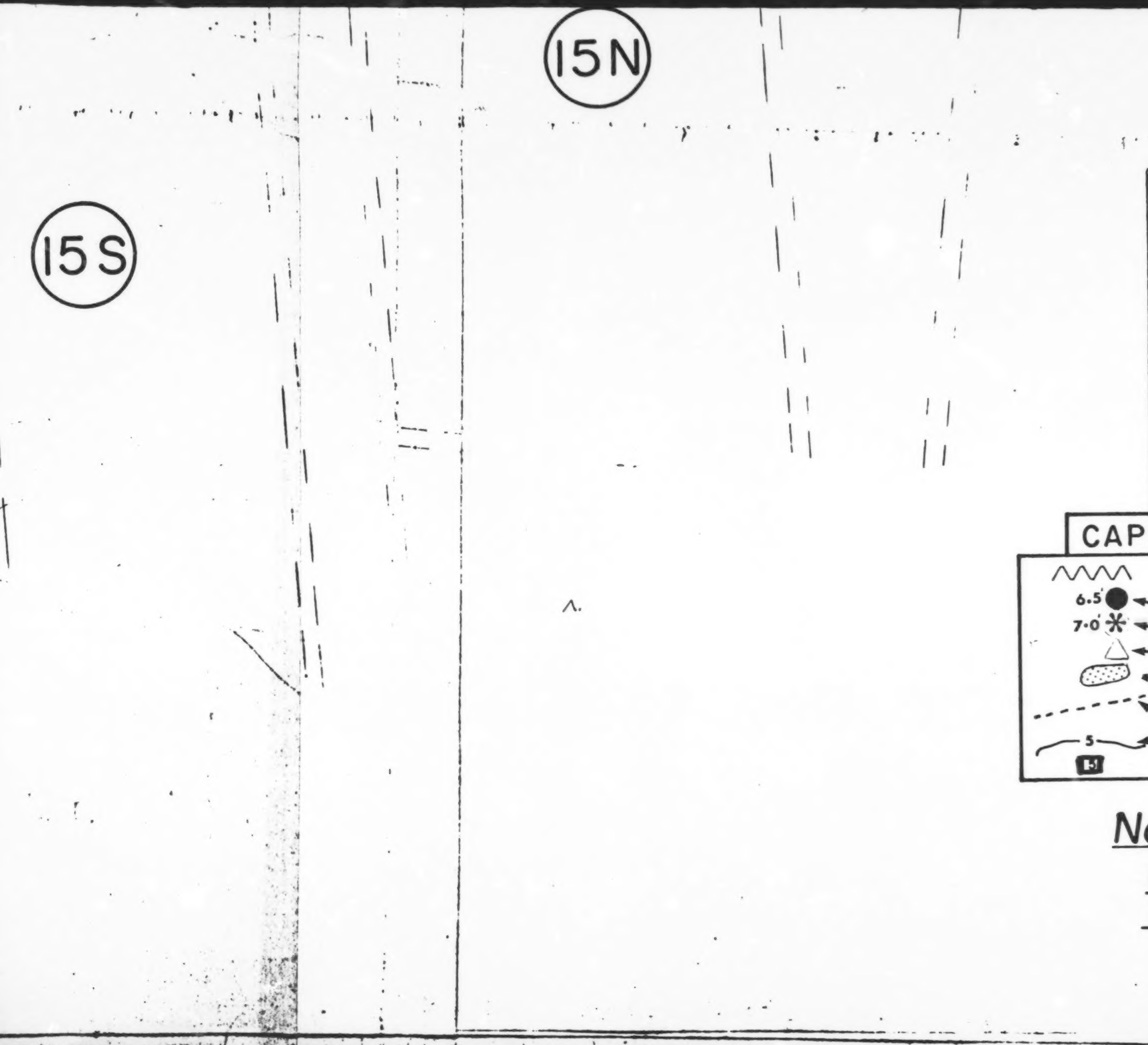

Golder Associates
CONSULTING GEOTECHNICAL AND MINING ENGI

LOCATION OF OUTBURST EVENTS IN No.
COLLIERY

REFERENCE: CBDC DRAWING AS SHOWN

DRAWN D M	FIGURE 2.13
DATE JUNE 30, 1987	DRAWING NUMBER
PROJECT 861-1290	

CAPE BRETON DEVELOPMENT COR

∧∧∧∧ SLIP PLANE (CUTTER ROOF)
6.5 ● ←INDICATES HEIGHT OF SANDSTONE ABOVE HARBOUR SEAM A
7.0 * ←INDICATES AN OBSERVATION POINT WITH NO SANDSTONE V
△ ←INDICATES PREVIOUS ROCK BURST OCCURENCES
▨ ←SANDSTONE IN CONTACT WITH OR INTRUDING COAL SEA
- - - - ←INDICATES AREAS SUSCEPTIBLE TO ROCK BURSTS
—5— ←INDICATES HEIGHT OF SANDSTONE ABOVE COAL
B-1 INDICATES OUTBURST NUMBER IN CHRONOLOGICAL ORDER

No. 26 COLLIERY - (GEO

GEOLOGY OF THE IMMEDIATE ROOF
THE DEEPS & DEVELOPMENT HEAD

SCALE - 1" = 100'

6.5 ● INDICATES HEIGHT OF SANDSTONE ABOVE HARBOUR SEAM ACTUAL MEASUREMENTS

(15N)

Golder Associates
CONSULTING GEOTECHNICAL AND MINING ENGINEERS

LOCATION OF OUTBURST EVENTS IN No. 26
COLLIERY

REFERENCE: CBDC DRAWING AS SHOWN

DRAWN D M	FIGURE 2.13	△
DATE JUNE 30, 1987		
PROJECT 861-1290	DRAWING NUMBER	REV.

CAPE BRETON DEVELOPMENT CORPORATION

LEGEND

∧∧∧∧	SLIP PLANE (CUTTER ROOF)
6.5 ●	INDICATES HEIGHT OF SANDSTONE ABOVE HARBOUR SEAM ACTUAL MEASUREMENTS
7·0 *	INDICATES AN OBSERVATION POINT WITH NO SANDSTONE VISIBILE TO HEIGHT SHOWN
△	INDICATES PREVIOUS ROCK BURST OCCURENCES
▨	SANDSTONE IN CONTACT WITH OR INTRUDING COAL SEAM
- - - -	INDICATES AREAS SUSCEPTIBLE TO ROCK BURSTS
~5~	INDICATES HEIGHT OF SANDSTONE ABOVE COAL
1-5	INDICATES OUTBURST NUMBER IN CHRONOLOGICAL ORDER

W.C.C.

No. 26 COLLIERY - (GEOLOGY)

GEOLOGY OF THE IMMEDIATE ROOF IN THE DEEPS & DEVELOPMENT HEADINGS.

SCALE - 1" = 100'